Functional characterisation of Tim17 and Tim23 proteins in *Arabidopsis thaliana*

Yan Wang

School of Biomedical, Biomolecular and Chemical Science and
the ARC Centre of Excellence for Plant Energy Biology

The University of Western Australia

This thesis is presented for the degree of Doctor Philosophy of the University of Western Astralia

October 2011

Coordinating supervisor: Prof. James Whelan
Co-supervisor: Assistant Research Prof. Murcha MW

Declaration

The research presented in this thesis is my own work unless otherwise stated. This work was carried out in the Australian Research Council Centre of Excellence in Plant Energy Biology at the University of Western Australia. The material presented in this thesis has not been submitted for any other degree.

Yan Wang

October 2011

To my grandmother and my beautiful aunty
Both who are in heaven

Acknowledgements

First and foremost I offer my sincerest gratitude to my supervisor Jim Whelan, who gave me the precious opportunity to work and be trained in his lab. His expertise, guidance and support ensured me to go ahead with my study throughout the past few years. Thank you for the untiring help during my difficult moments. I am indebted to him more than he knows.

My sincere gratitude also goes to Dr Monika Murcha, who is the backbone of this work. Her wide knowledge and extensive discussions around this work has been of great value to me. Thanks for your encouragement and valuable advice during those tough times and the stressful writing-up period. All the jokes and laughs, in the freezing cold room and on the protein import bench, will be kept in my memory. Also thanks to your babies' hugs.

I would also like to thank all the members of the Whelan lab. Special mentions must go to Chris for always being accessible and willing to help here and there, Owen for doing the Mass Spectrometry and teaching me how to run the BN gels, Reena and Estelle for the professional advice and encouragement and finally Sophia, for the daily lunch walk.

I owe deep gratitude to my parents. Sorry for the long distance and time apart. Thanks for your love and unconditional support. I could not have done this without you. Lastly, particular appreciations go to Di Yong, who is always there keeping me optimistic and pushing me to the final line. Thank you for brightening everything around me.

Abstract

Mitochondrial protein import is a multi-step process that requires the translocation of proteins across one or both mitochondrial membranes, that is achieved by multi-subunit proteins complexes called translocases. While the translocase of the outer membrane (TOM) has been extensively characterized in a variety of organisms, from *Saccharomyces cerevisiae* (single celled yeast) to plants and animals, the translocases of the inner membrane (TIM) have only been extensively characterized in yeast. The TIM17:23 complex is the main translocase in the inner membrane that mediates protein translocation through the inner membrane or lateral insertion into the inner membrane. The core components of this complex, Tim17 and Tim23, play an important role in the protein import pathway and are essential for cell viability in yeast. In Arabidopsis, three genes have been found to encode Tim17 and Tim23 proteins respectively, named as *Tim17-1*, *Tim17-2*, *Tim17-3*, *Tim23-1*, *Tim23-2* and *Tim23-3* (Murcha et al., 2007). It is unclear if the proteins encoded by these different genes have divergent functions.

In this project, functional analysis of Tim17 and Tim23 was investigated using T-DNA insertion homozygote lines, obtained for each gene. Apart from *Tim17-2*, for which a homozygous T-DNA insertion was lethal, inactivation of any single gene of the *Tim17* and *Tim23* families did not result in a growth defective phenotype. However, inactivation of any two genes from the *Tim23* family was lethal. Interestingly, one particular T-DNA insertion line, with an insertion located

upstream of the *Tim23-2* translational start site, displayed a severely retarded growth phenotype and a 2-fold over-expression of Tim23-2 protein was observed in this line. Thus, the mechanistic basis of this growth phenotype was further investigated.

tim23-2 mutant lines that resulted in an increase or decrease in Tim23 protein were further investigated. *In vitro* protein import assays revealed that the disruption or over-expression of Tim23-2 protein resulted in a decrease or increase in the general import pathway. The increased amounts of Tim23-2 also resulted in a change in protein abundances for some protein import components, such as Tom20-2, Tom20-4, Tim50 and Tim21. Surprisingly, complex I of the mitochondrial respiratory chain was severely reduced in abundance in the Tim23-2 over-expressed line; in addition, a novel complex, which was identified to be a mixture of different proteins from various inner membrane complexes, was observed. The connection between complex I and the TIM17:23 complex was further investigated, revealing that the imported radiolabelled Tim23-2 protein was assembled into both the TIM17:23 complex and complex I of the respiratory chain.

In order to verify the connection between complex I and Tim23, three mutant lines known to express reduced amounts of complex I via independent genetic manipulation were investigated. All three lines displayed an increase in the protein abundance of Tim23-2 and other mitochondrial import components. Furthermore, all three lines displayed increased import capability of both the general import pathway and the carrier import pathway.

This study showed that the amount of the TIM17:23 translocase was rate limiting for protein import into plant mitochondria. Additionally, it was uncovered that an increase in Tim23-2 resulted in a decrease in the amount of complex I, and that a decrease in complex I resulted in an increase in Tim23-2. This interaction between Tim23 and complex I provides a mechanism to link mitochondrial activity to mitochondrial biogenesis via the respiratory chain, as the amounts of these proteins are inter-linked.

Abbreviations

AAC	ADP/ATP carrier protein
ADP	adenosine diphosphate
ANT	adenine nucleotide transporter
AOX	alternative oxidase
APX	ascorbate peroxidase
At	*Arabidopsis thaliana*
ATP	adenosine triphosphate
ATP α	mitochondrial ATP synthase alpha subunit
ATP β	mitochondrial ATP synthase beta subunit
BCS	protein involved in cytochrome bc1 assembly
BN-PAGE	blue native polyacrylamide gel electrophoresis
Col-0	Columbia wild-type
COX	Cytochrome Oxidase
Cyt *c*	Cytochrome C
Cys	Cysteine
DMSO	Dimethyl sulfoxide
dNTP	deoxyribonucleotide triphosphate
DTT	Dithiothreitol
E. coli	*Escherichia coli*
EDTA	ethylenediaminetetraacetic acid
Erv1	essential for respiration and vegetative growth
FAD	Flavin adenine dinucleotide
F_Ad	F_Ad subunit of ATP Synthase
$FADH_2$	flavin adenine dinucleotide hydroquinone
GDP	guanosine diphosphate
GFP	Green fluoresence protein

GIP	general import pathway
GST	glutathione *S*-transferase
His	Histidine
HM	Homozygous
HSP	heat shock proteins
HT	Heterozygous
IMS	inter membrane space
IM	inner membrane
IPTG	isopropyl β-D-1-thiogalactopyranoside
kDa	kilo Dalton
MDHAR	monodehydroascorbate reductase
Mdm10	mitochondria distribution and morphology protein 10
MES	2-(*N*-morpholino)ethanesulfonic acid
MIA	mitochondrial import and assembly
MIC	Mixed inner membrane complex
MOPS	3-(N-morpholino)propanesulfonic acid
MPP	mitochondrial processing peptidase
MS	Mass spectrometry
NAD(P)H	nicotinamide adenine dinucleotide (phosphate)
NBD	N-terminal nucleotide binding domain
nm	Nanometer
mtHsp	mitochondrial heat shock protein
OD	Optical density
OEP	outer envelope protein
OM	outer membrane
OM64	mitochondrial outer membrane protein of 64 kDa
OXPHOS	Oxidative phosphorylation
PAM	presequence translocase associated import motor
PCR	polymerase chain reaction

PiC	phosphate translocator
PK	proteinase K
PMSF	phenylmethylsulfonyl fluoride
PPR	pentatricopeptide repeat-containing protein
PRAT	preprotein and amino acid transporter
PVDF	polyvinylidene Fluoride
PVP-40	polyvinylpyrollidone (MW 40000)
Redox	reduction/oxidation
rpm	revolutions per minute
RISP	Rieske iron sulphur cluster protein
SAM	sorting and assembly machinery
SAP	shrimp alkaline phosphatase
SBD	C-terminal substrate binding domain
SDS	sodium dodecyl sulfate
SW	Sterile water
TAE	tris, acetic acid and EDTA
T-DNA	transferred DNA
TE	tris-HCl / EDTA
TEMED	N', N', N', N'-tetramethylethylenediamine
TES	N-tris[hydroxymethyl]methyl-2-aminoethnesulfonic acid
TIM	translocase of the inner mitochondrial membrane
TOM	translocase of the outer mitochondrial membrane
TPR	tetratricopeptide repeat
UCP	uncoupling protein
UTR	untranslated region
VDAC	voltage dependent anion channel

Table of Contents

Chapter 1 Introduction

Chapter 1 Introduction

1.1 The function and structure of mitochondria

Mitochondria are essential organelles found in almost all eukaryotic organisms. Their primary function is energy production, through the process of oxidative phosphorylation to generate adenosine triphosphate (ATP) (Walker and Dickson, 2006). Mitochondria are also involved in many other cellular processes, such as fatty acid metabolism, amino acids metabolism, the synthesis of ascorbic acid and folate, iron-sulfur cluster biogenesis and photorespiration (Bauwe et al., 2010; Lill et al., 2006; Lill and Muhlenhoff, 2006; Lutz et al., 2001; Reisch and Elpeleg, 2007; Wang et al., 2009). Furthermore, a number of studies have shown that mitochondria play an important role in programmed cell death (Li and Xing, 2010; Petrussa et al., 2009; Qi et al., 2011; Wabnitz et al., 2010).

Mitochondria have two distinct membranes, the outer membrane (OM) and the inner membrane (IM), encapsulating the intermembrane space (IMS) and the matrix, respectively. The OM is only permeable to solutes of less than 10 kilo-Dalton (kDa) due to the presence of the integral voltage-dependent anion channel (VDAC) protein allowing metabolites such as ATP and adenosine diphosphate (ADP) to freely cross the OM (Kmita and Stobienia, 2006; Mannella, 1987). In contrast, the IM is a highly impermeable membrane where facilitated transport of solutes is mediated by a diverse family of metabolite transporters or “carrier proteins”, which mediate the exchange of

molecules through the IM (Laloi, 1999; Millar and Heazlewood, 2003). Similarly, the translocation of proteins to the inner membrane and matrix is also regulated by a variety of complexes on the inner membrane. The translocation of proteins and metabolites through the inner membrane must be tightly regulated to maintain the essential proton motive gradient, which powers oxidative phosphorylation.

1.2 The origin and evolution of mitochondria

The endosymbiotic hypothesis is generally accepted to explain the origin of mitochondria. The model suggests that mitochondria originated from a single bacterium being engulfed by a primitive host cell (Gray et al., 1999; Lang, 1999). Comparison of mitochondrial and bacterial genomes has indicated that the endosymbiont was likely related to a α-proteobacterium (Dolezal et al., 2006; Gray et al., 1999; Lang, 1999). A number of distinctive prokaryotic features are retained in the mitochondria found in eukaryote cells today, such as a circular DNA chromosome and the presence of Hsp60 and Hsp70 family of proteins derived from proteobacteria (Kurland and Andersson, 2000). With time, the majority of the genome from the endosymbiont was lost or transferred to the nucleus of the host cell (Karlberg et al., 2000), and only a small amount of information is still retained by mitochondria, thus establishing a semi-autonomous system (de Duve, 2007; Embley and Martin, 2006; Marienfeld, 1999). As a consequence, the majority of mitochondrial proteins are encoded in the nucleus and to achieve effective mitochondrial function,

mitochondrial proteins must be targeted, translocated and imported across the barrier of the mitochondrial membranes.

Over time, as the α-proteobacteria was converted into mitochondria, sophisticated mechanisms evolved to efficiently target and translocate proteins to and across the mitochondrial membranes. Two views of mitochondrial evolution are proposed; the “outside” view suggests that the process of mitochondrial evolution was driven by the host cell, where the host proteins were imposed on the ancestral endosymbiont in the early evolutionary stage (Alcock et al., 2010). However, most studies support the alternative “inside” view, that the endosymbiont plays an important role in establishing the import pathways (Cavalier-Smith, 2006; Clements et al., 2009; Herrmann, 2003). Due to the presence of similar translocase subunits in eukaryotic organisms, it has been suggested that mitochondria evolved from an ancestral proto-mitochondria (Dolezal et al., 2006). The pre-existing bacterial translocation apparatus provided the basic modules for the stepwise evolution of mitochondrial import machineries and the additional machines created *de novo* were added during the co-evolution of the host cell and endosymbiont (Alcock et al., 2010; Dolezal et al., 2006; Lithgow and Schneider, 2010; Rassow et al., 1999).

1.3 Protein import into mitochondria

1.3.1 Mitochondrial targeting signals

As previously described, most mitochondrial proteins are nuclear encoded, synthesized in the cytosol and thus need to be efficiently recognized by mitochondria prior to import. The precursor proteins usually contain targeting information that is necessary and sufficient to direct them to the mitochondria. Although diverse targeting information exists, two main groups have been identified (Dolezal et al., 2006; Neupert and Herrmann, 2007).

In many cases, the targeting peptide is located at the N-terminus of the proteins, also termed matrix-targeting sequences, presequences or prepeptides. They direct the protein into the mitochondrial matrix and are usually cleaved off by the mitochondrial-processing peptidase (MPP) upon translocation to the matrix. The average length of a presequence is 20-50 amino acids (Chacinska et al., 2002) and these presequences have the potential to form amphipathic α-helices, that contain one hydrophobic and one positively charged face (Abe et al., 2000; Chupin et al., 1996; Pfanner and Geissler, 2001). However, there is no consensus in the primary structure, which often differs considerably, even between closely related orthologs (Roise and Schatz, 1988). The general properties of these amphipathic helices are widely conserved across fungi, animals and plants. Statistical analysis of numerous presequences suggests two distinct domains, the N-terminal amphipathic domain containing a high proportion of positively charged and hydroxylated residues (Hartl and Neupert,

1989) and a less structured carboxy-terminal domain thought to be involved in recognizing presequence cleavage (Glaser et al., 1998). The N-terminal amphiphilic helix has a likely role in receptor recognition, as the α-helix can interact with residues of the translocase of the outer membrane (TOM) promoting receptor binding and preventing any mistargeting (Abe et al., 2000). The acid chain hypothesis suggests that positive residues in the presequence successively interact with a sequence of binding sites on the import components, allowing the translocation of the precursor from the outer membrane receptors to the inner membrane (Honlinger et al., 1995; Meisinger et al., 2001). Recently, more characteristics have been identified to be involved in receptor interaction, such as hydrophobic interactions (Abe et al., 2000; Gordon et al., 2001) and the α-helical conformation (Abe et al., 2000). The studies reported that the cytosolic domain of Tom20 forms an α-helical structure with a groove and the amphiphilic helical structure of the presequence with hydrophobic leucines aligned on one side could interact with the hydrophobic patch in the Tom20 groove.

Whilst the majority of proteins destined to the mitochondrial matrix contain N-terminal presequences, many precursors that are to be translocated to the outer and inner membrane contain internal signals instead. Precursors of outer membrane proteins all have internal signals, such as Tom22 and Tom70 (Hase et al., 1984; Lithgow et al., 1994). In the inner membrane, carrier proteins involved in metabolite transport and import components such as Tim17 and Tim23 also contain internal signals (Brix et al., 1999; Kaldi et al., 1998; Pfanner

et al., 1987a; Pfanner et al., 1987b; Pfanner and Neupert, 1987). Although the characteristics of internal signals remain largely elusive, studies on the ADP/ATP carrier protein (AAC1), have proposed that carrier proteins consist of three similar modules linked by extramembrane loops, where each module is comprised of two transmembrane regions connected by an extramembrane loop that is exposed to the matrix (Palmieri et al., 1996; Saraste and Walker, 1982; Wiedemann et al., 2001). Binding studies of mitochondrial phosphate carrier proteins and the import receptors Tom20 and Tom70 indicate multiple receptor-binding regions throughout the carrier proteins (Brix et al., 1999; Brix et al., 2000). Both Tom20 and Tom70 bind to the charged extramembrane loops, whereas Tom70 also binds to the transmembrane regions (Brix et al., 1999; Brix et al., 2000). It has been reported that each of the three modules of the ADP/ATP carrier protein contains targeting information that binds to the Tom70 import receptor and allows import to occur (Wiedemann et al., 2001). It has also been shown that the purified Tim9/10 chaperone complex, which ferries carrier proteins to the inner membrane through the intermembrane space, binds most strongly to the central module (Curran et al., 2002). Therefore, from these studies, it appears that multiple internal signal modules within the protein contribute to several binding sites along the import process.

1.3.2 Translocase of the outer membrane

The import and sorting of mitochondrial proteins are mediated by membrane-protein complexes called translocases in the outer and inner

membrane and soluble factors in the cytosol, intermembrane space (IMS) and matrix (Endo and Yamano, 2009; Koehler, 2004; Neupert and Herrmann, 2007).

Whilst the import machinery has been extensively characterized in lower eukaryotic models such as *Saccharomyces cerevisiae* and *Neurospora crassa* (Figure 1.1), due to the relative ease of various genetic approaches, the characterization of plant mitochondrial import apparatus has been more complex due to the involvement of a larger number of genes encoding protein import components. The import components in plant mitochondria will be discussed in section 1.6.

1.3.2.1 The TOM complex

The TOM complex (translocase of the outer membrane) is the major translocase of the outer membrane responsible for the recognition and translocation of all nuclear-encoded mitochondrial proteins into the mitochondria. The TOM complex consists of the general insertion pore (GIP) and several receptors loosely attached to it. Precursors are recognized on the mitochondrial surface by receptor proteins Tom70, Tom20 and Tom22, then transferred to the translocation channel fomed by Tom40 (Mokranjac and Neupert, 2009). Tom20 and Tom70 are the primary receptors, both proteins are anchored into the outer membrane with a single N-terminal transmembrane domain, leaving the receptor domain exposed in the cytosol (Chan et al., 2006; Harkness et al., 1994; Iwahashi et al., 1997; Wu and Sha, 2006). Tom22 serves as an additional receptor of the complex and has a central role in maintaining

the integrity of the TOM complex (Kiebler et al., 1993; Mayer et al., 1995; Meisinger et al., 2001).

The three receptors, Tom20, Tom70 and Tom22 are characterized by their specificities to different precursor proteins, however, some overlap in protein recognition has been shown (Brix et al., 1997; Yamano et al., 2008). Precursor proteins containing a cleavable presequence are recognized by Tom20. Tom20 recognizes hydrophobic residues within the presequences, while the α-helical structure of the presequence can bind to the hydrophobic groove of Tom20 (Abe et al., 2000; Muto et al., 2001; Saitoh et al., 2007). Recently, Tom20 has been identified to have two distinct binding elements and play a dual role in protein import into mitochondria (Yamamoto et al., 2011). The N-terminal element is essential for recognition of the targeting signal of the presequence, while the C-terminal tethers the presequence to the TOM40 complex to increase import efficiency (Yamamoto et al., 2011). Another receptor protein is Tom70. It is a single N-terminal transmembrane anchored protein with a soluble cytosolic region comprised of 11 tetratricopeptide repeat (TPR) motifs (Chan et al., 2006) and has the ability to recognize the internal targeting signals (Wiedemann et al., 2001). However, Tom70 is also involved in the import of presequence-containing precursor proteins (Yamamoto et al., 2009). Instead of recognizing the presequence, it has been shown that Tom70 plays a role in maintaining the solubility of the presequence-containing precursor to efficiently transfer it to the downstream import machineries (Yamamoto et al., 2009).

Following precursor binding to either Tom20 or Tom70, proteins are then

transferred to Tom22, a protein containing three domains: an N-terminal *cis* domain exposed to the cytosol, a transmembrane domain and a C-terminal *trans* domain in the intermembrane space. The negatively charged region of the *cis* cytosolic domain transiently interacts with positive residues of the presequence directing the precursor to the Tom40 channel (Kiebler et al., 1993; Mayer et al., 1995). This interaction has been shown to be a transitional binding site for cleavable presequences (Moczko et al., 1997), but shows poor bindings of preproteins with internal targeting signals *in vitro* (Brix et al., 1997; Brix et al., 1999). The cytosolic domain of Tom22 functions as a receptor in cooperation with Tom20 and these two receptors have been identified to be involved in the same step or sequential steps of targeting signal recognition (Yamano et al., 2008)

Tom40, the central component of TOM complex, is a β-barrel protein that forms the translocation channel in the outer membrane (Becker et al., 2005; Hill et al., 1998). The translocation channel consists of 3 pores, each individually formed by Tom40 (Ahting et al., 1999; Kunkele et al., 1998a; Kunkele et al., 1998b; Model et al., 2002). Apart from working as a protein-conducting channel, Tom40 is also able to bind with non-native proteins to prevent their aggregation before translocating through the outermembrane (Esaki et al., 2003; Voos, 2003). Precursor proteins are sorted to various sub-mitochondrial compartments upon crossing the outer membrane. Tom40 has been reported to play an active role in sorting imported proteins, in that a single point mutation in Tom40 has been observed to selectively affect the ability of the TOM

complex to discriminate precursors destined for different import pathways (Gabriel et al., 2003).

Three small proteins, Tom5, Tom6 and Tom7, are single-pass transmembrane integral proteins that are closely associated with Tom40 and Tom22. Tom5 assists with the insertion of presequences into the Tom40 pore, with its small negatively charged cytosolic domains interacting with the larger receptors (Dietmeier et al., 1997; Model et al., 2001; Schmitt et al., 2005; Wiedemann et al., 2003). Tom6 appears to be in close contact with Tom22 and has been identified to assist in the assembly of the TOM complex (Dekker et al., 1998; Kassenbrock et al., 1993). In contrast, Tom7 has been reported to be involved in the disassembly of the complex, enabling the exchange of TOM subunits within the mature TOM complex (Model et al., 2001; Rapaport et al., 2001). Tom6 and Tom7 may also have a role in the import pathway as both proteins have been shown to be involved in the import of porin, an outer membrane non-cleavable protein (Krimmer et al., 2001).

Two different mechanisms have been proposed for the translocation of proteins through the TOM complex. The binding chain hypothesis, which suggests that presequence-carrying preproteins are translocated as loosely folded linear polypeptide chains, sequentially binding to a series of binding sites: such as from Tom20 and Tom22, then with the help of Tom5 and Tom40, and are eventually passed to Tom7 and the intermembrane space domain of Tom22 (Chacinska et al., 2005; Esaki et al., 2003; Esaki et al., 2004; Kanamori et al., 1999; Komiya et al., 1998). In the other proposed mechanism, the precursors

are not translocated as a linear chain but traverse the outer membrane in a loop formation with both termini still on the cytosolic surface while a middle portion reaches the intermembrane space (Wiedemann et al., 2001).

1.3.3 The sorting and assembly machinery (SAM complex)

The precursors of β-barrel proteins in the outer membrane are synthesized in the cytosol, targeted to the TOM complex and translocated through the Tom40 channel into the intermembrane space, incidentally Tom40, a β-barrel protein itself is targeted this way (Model et al., 2001; Rapaport and Neupert, 1999; Wiedemann et al., 2004). The Tim9-Tim10 and Tim8-Tim13 chaperone complexes in the intermembrane space bind to the precursor proteins (Hoppins and Nargang, 2004; Wiedemann et al., 2004) and guide them to the sorting and assembly machinery (SAM) complex (Gentle et al., 2004; Kutik et al., 2008; Paschen et al., 2003; Wiedemann et al., 2003).

The SAM complex located in the outer membrane consists of three subunits: the peripheral membrane proteins Sam35 and Sam37 on the cytosolic side of the outer membrane and the β-barrel subunit Sam50 (Gentle et al., 2004; Ishikawa et al., 2004; Kozjak et al., 2003; Paschen et al., 2003). Sam50 is the core subunit forming the channel of the SAM complex (Kutik et al., 2008). It contains N-terminal polypeptide transport-associated (POTRA) domains which can bind to precursor proteins and also promote precursors to release from the SAM complex (Stroud et al., 2011). Sam35 is a partner of Sam50. The topology of Sam35 has not yet been fully determined, though one

study suggests that Sam35 is embedded in a hydrophilic environment between Sam50 molecules and binds to the β signal arriving in the SAM complex (Chan and Lithgow, 2008). Sam37, the third subunit of the core SAM complex, promotes the release of precursors from the SAM complex into the lipid phase of the outer membrane (Chan and Lithgow, 2008).

1.3.4 The translocase of the inner membrane (TIM)

For proteins that continue their journey beyond the outer membrane, the import of precursor proteins diverges into two different pathways: the general import pathway and the carrier import pathway, each involving different proteins and complexes. There are two receptor and translocation complexes in the inner membrane: the TIM17:23 complex responsible for the recognition and translocation of precursors following the general import pathway to the matrix, and the TIM22 complex responsible for transport of precursor proteins through the carrier import pathway to the inner membrane (Neupert, 1997).

1.3.5 The TIM17:23 complex

1.3.5.1 Subunit composition of the TIM17:23 complex

TIM17:23 complex is the central translocase of the inner membrane. The components of the TIM17:23 complex can be divided into a membrane-embedded part and the import motor. The membrane-embedded part is responsible for the recognition and initial membrane-potential-dependent translocation of the proteins across the inner membrane. The import motor is

required for the ATP-dependent translocation into the matrix. The membrane part of the TIM17:23 complex comprises Tim50, Tim23 and Tim17. The import motor consists of Tim14, Tim16, Tim44, Mge1 and mtHsp70.

Upon emergence from the TOM channel, the first point of contact is Tim50, a protein anchored in the inner membrane with a single transmembrane domain and a large C-terminal domain exposed to the intermembrane space (Geissler et al., 2002; Mokranjac et al., 2003a; Yamamoto et al., 2002). It works as a receptor subunit of the TIM17:23 complex, which recognizes the preproteins as soon as they emerge at the outlet of the TOM complex (Mokranjac et al., 2003a; Mokranjac et al., 2009b; Witzigmann et al., 2002). The C-terminal domain was shown to interact with the intermembrane space domain of Tim23 (Mokranjac et al., 2009b; Tamura et al., 2009b). This association is required for the transfer of preproteins from the TOM complex to the TIM17:23 complex (Tamura et al., 2009b). It is also found that the intermembrane space domain of Tim50 induces the oligomerization and closure of the Tim23 channel in the absence of presequence (Meinecke et al., 2006). The presequence triggers the dissociation of the Tim23 dimer and activates the channel for translocation (Meinecke et al., 2006). Thus, Tim50 plays a role in maintaining the permeability of mitochondria (Meinecke et al., 2006) and not surprisingly, Tim50 is also an essential protein in yeast (Mokranjac et al., 2003a).

Tim23 is one of the core components of the TIM17:23 complex. The C-terminus is anchored in the inner membrane with four transmembrane

helices which form the translocation channel (Truscott et al., 2001). The first 20 amino acid residues of the N-terminal are inserted into the outer membrane, however the functional significance of this association is still debated (Chacinska et al., 2009; Chacinska et al., 2003). Several independent research groups have reported that the association between Tim23 protein and the outer membrane is dynamic and dependant on the translocation activity of the TIM17:23 complex (Donzeau et al., 2000; Popov-Celeketic et al., 2008). The intermembrane space (IMS) domain of Tim23, which interacts with Tim50 serves as a further presequence receptor of the TIM17:23 complex and is also involved in the membrane potential-dependent dimerization of Tim23 (Bauer et al., 1996; Geissler et al., 2001; Yamamoto et al., 2002).

Like Tim23, Tim17 is also predicted to span the inner membrane with four transmembrane helices (Ryan et al., 1994). The C-terminal region of Tim23, anchored in the inner membrane, interacts with Tim17 forming the channel of the TIM17:23 complex (Berthold et al., 1995; Dekker et al., 1997; Ryan et al., 1998). Tim17 and Tim23 share significant homology with each other, both containing four transmembrane domains, however, they are not functionally interchangeable (Ryan et al., 1998). Tim17 has very short segments facing the IMS space. The N-terminal segments contain conserved negative charges, which are important for protein import and gating of the translocation channel (Chacinska et al., 2005; Martinez-Caballero et al., 2007; Meier et al., 2005; Milisav et al., 2001). Though the exact function of Tim17 is still unclear, it is possible that Tim17 forms part of the translocation channel of the TIM17:23

complex. However, it is also likely that only Tim23 is the major pore for translocation and Tim17 is involved in the stabilization of the actual translocation channel (Alder et al., 2008).

Tim21 is a non-essential and peripheral subunit of the TIM17:23 complex associating with the core complex (Chacinska et al., 2005). It is anchored to the inner membrane by the single transmembrane segment, exposing the N-terminal domain to the matrix and the C-terminal domain to the IMS (Mokranjac et al., 2005a). Tim21 competes with presequences for binding to Tom22 and thus contributes to the transient connection between the translocases of the outer and inner membrane (Chacinska et al., 2005). The binding of Tim21 to Tom22 results in the release of the preprotein and promotes its further transfer to the Tim23 channel (Albrecht et al., 2006).

Tim44 is a matrix protein peripherally attached to the inner membrane (Maarse et al., 1992; Moro et al., 1999; Scherer et al., 1992). It consists of two domains. The N-terminal domain, attached to the Tim17-Tim23 core (Weiss et al., 1999) and the C-terminal domain, which interacts with mtHsp70 and J complex recruiting both the chaperone and the regulatory factors required to drive the translocation channel (D'Silva et al., 2008; Kozany et al., 2004; Mokranjac et al., 2003a; Schiller et al., 2008). Tim44 is presumed as a subunit coordinating the Tim17-Tim23 core and the import motor, however, the mechanism of this interaction is complex and still uncertain.

MtHsp70 is the ATP-hydrolyzing subunit of the TIM17:23 complex which functions as the “power station” of the translocation channel (Kang et al., 1990;

Voos and Rottgers, 2002). MtHsp70 consists of an N-terminal nucleotide binding domain (NBD) and a C-terminal substrate binding domain (SBD) (Bukau et al., 2006). The SBD binds to substrates with low affinity when ATP is bound to the NBD (Bukau et al., 2006). After hydrolyzation of ATP to ADP in the NBD, the bound substrate is locked in the SBD. The ATPase cycle of mtHsp70 is used to mediate the vectorial movement of the preprotein into mitochondria (Ungermann et al., 1994).

The reaction cycle of mtHsp70 requires assistance of several additional proteins such as Tim14, Tim16, Mge1 and Hep1 (Laloraya et al., 1994; Rowley et al., 1994; Sichting et al., 2005). Tim14, which is recruited to Tim44 by its homologous partner protein Tim16, stimulates the ATPase activity of mtHsp70 (Mokranjac et al., 2003b; Mokranjac et al., 2005b; Moro et al., 1999). Mge1 and Hep1, both of which are soluble proteins in the matrix, facilitate the motor function of mtHsp70, although they are not integral subunits of the TIM17:23 complex (Bolliger et al., 1994; Laloraya et al., 1994; Nakai et al., 1994). Mge1 promotes the ADP to ATP exchange through mtHsp70, by binding to mtHsp70 to distort the nucleotide-binding site (Liu et al., 2003; Moro and Muga, 2006; Strub et al., 2000). Hep1 also binds to the nucleotide-free mtHsp70, however, its main role is to maintain the solubility of aggregate-prone mtHsp70 in the matrix (Momose et al., 2007; Sichting et al., 2005).

1.3.5.2 Two models of the TIM17:23 complex

The TIM17:23 complex functions in both translocation and insertion modes with two different forms (Chacinska et al., 2005). One form, termed

$TIM23^{SORT}$, contains Tim23, Tim17, Tim50 and Tim21. It is involved in the early stage of preprotein transfer from TOM to the TIM17:23 complex and the lateral release of preproteins containing an innermembrane-sorting signal into the inner membrane. The other form, termed TIM23-PAM, functions in the translocation of preproteins into the matrix. This form is associated with the presequence translocase-associated import motor (PAM complex), but lacks Tim21 (Chacinska et al., 2005; Chacinska et al., 2010). The PAM complex contains several essential subunits, mtHsp70, Tim44, Mge1, Tim14, and Tim16 (Frazier et al., 2004; Li et al., 2004; van der Laan et al., 2005).

1.3.5.3 Cooperation of the TIM17:23 complex with the TOM complex

As described above, the TOM complex can form a dynamic association with the TIM17:23 complex, thus, forming a TOM-TIM supercomplex while the cleavable precursor proteins translocate from the outer membrane to the inner membrane (Chacinska et al., 2010). Several proteins, such as Tom22, Tim23 and Tim50, have exposed domains in the intermembrane space, which transiently connect the TOM and TIM17:23 complexes via protein translocation (Geissler et al., 2002; Mokranjac et al., 2009b; Tamura et al., 2009b; Yamamoto et al., 2002). Previous studies investigating the topology of Tim23 have revealed that Tim23 is anchored to the inner membrane via four transmembrane helices at C-terminus (Donzeau et al., 2000). The N-terminal part residing in the IMS is accessible to protease treatment in intact mitochondria, and has the ability to draw TOM complex and TIM17:23 complex into proximity of one another (Donzeau et al., 2000).

The structure of Tim50 also provides another important insight for understanding the cooperation of the two translocases. It is the first subunit of the TIM17:23 machinery that contacts polypeptide segments following their passage through the TOM channel (Geissler et al., 2002; Mokranjac et al., 2003a; Yamamoto et al., 2002). Experiments showed that the generation of the TOM-TIM supercomplex, as determined by BN-PAGE, was blocked in Tim50-depleted mitochondria, while the mobility of independent TOM and TIM23 complexes on BN-PAGE was unaffected (Chacinska et al., 2003). The interaction of the IMS-exposed domain of Tom22 with Tim50 has also been demonstrated using site specific crosslinking *in vivo* (Chacinska et al., 2005; Mokranjac et al., 2009b; Tamura et al., 2009b). This indicates that Tim50 is important for the generation of the TOM-TIM supercomplex and most likely has a role in maintaining its stability.

The third component that has been implicated in the cooperation with the TOM complex is Tim21. It binds to the intermembrane-space tail of Tom22 and plays a role in the direct but transient connection between the translocases of the outer and inner membranes (Albrecht et al., 2006). It competes with presequences for binding to Tom22. Thus, the binding of Tim21 to Tom22 results in the release of the preprotein and promotes its further transfer towards the Tim23 channel (Albrecht et al., 2006). It suggests that Tim21 does not bind preprotein but rather plays a regulatory role in preprotein transfer (Albrecht et al., 2006; Kozany et al., 2004; Mokranjac et al., 2005a; Tamura et al., 2009b).

1.3.5.4 Coupling of TIM23 to the respiratory chains

Tim21 is also involved in the interaction of the $TIM23^{sort}$ complex with the respiratory chain complexes. Tim21 alternates between binding Tom22 and a supercomplex of the respiratory chain that contains two proton-pumping complexes; cytochrome bc_1-complex (complex III) and cytochrome oxidase (complex IV) (van der Laan et al., 2006a). The exact function of this interaction has not yet been identified, though current results suggest that the coupling of the TIM17:23 complex with the proton-pumping complexes makes an efficient use of the electrochemical proton gradient for preprotein translocation (Dienhart and Stuart, 2008; Wiedemann et al., 2007).

1.3.6 The TIM22 complex

The TIM22 complex inserts precursors of the carrier protein family into the inner membrane (Kaldi et al., 1998). The central component is Tim22, a homolog to both Tim17 and Tim23. It is inserted into the inner membrane with four transmembrane helices, which likely form a channel for insertion of polypepetide substrates (Kovermann et al., 2002). Tim22 is essential for cell viability in yeast and can be cross-linked to translocated precursors (Davis and Davis, 2002; Sirrenberg et al., 1996). Several additional proteins, Tim54, Tim18, Tim12 , Tim 9, Tim10, Tim8 and Tim13 are associated with Tim22, though these components do not form part of the core channel.

Tim54 is another important component of TIM22 complex with the C-terminal domain exposed to the intermembrane space (Kerscher et al., 1997).

It is not essential for cell viability but disruption of Tim54 has been known to result in a reduced rate of import (Kovermann et al., 2002). Tim54 does not associate with Tim22, but rather has a role in the stability of the Tim22 channel (Hwang et al., 2007; Wagner et al., 2008)

Tim18 was also identified as a component of TIM22 complex. It is an integral inner membrane protein with the C-terminal domain exposed in the intermembrane space (Kerscher et al., 2000; Koehler et al., 2000). Though the exact function of Tim18 has not yet been elucidated, several studies have suggested that it functions in the assembly and stabilization of TIM22 complex as the depletion of Tim18 results in a decrease in the assembly of Tim54 into the TIM22 complex and further affects the rate of carrier import pathway (Koehler et al., 2000; Wagner et al., 2008)

Tim12 is essential for cell viability in yeast (Jarosch et al., 1996). It is peripherally attached to the inner mitochondrial membrane and associated with the TIM22 complex (Baud et al., 2007; Lionaki et al., 2008). It is thought to recruit Tim9-Tim10 to form a Tim12-core complex then integrate with the TIM22 complex (Gebert et al., 2008; Lionaki et al., 2008; Sirrenberg et al., 1998).

The Tim9-Tim10 complex and Tim8-Tim13 complex are located in the intermembrane space and play a chaperone-like role in the TIM22 import pathway, that mediates the insertion of proteins to the inner membrane (Hasson et al., 2010; Ivanova et al., 2008). It has been observed that the Tim9-Tim10 complex and Tim8-Tim13 complex could bind to specific sites on Tim23 protein, keeping Tim23 in the proper orientation for delivery and integration into the

inner membrane through the TIM22 complex (Davis et al., 2007). The import of these intermembrane space proteins is achieved via the mitochondrial intermembrane space assembly machinery Mia40-Erv1 (Chacinska et al., 2004; Hell, 2008), both of which are essential proteins in yeast (Chacinska et al., 2004; Lisowsky, 1994). The Mia40-Erv1 complex is a dedicated disulfide relay system, which introduce disulfide bonds into the cysteine-rich proteins and drive the import of these proteins into the IMS of mitochondria of by an oxidative folding mechanism (Endo et al., 2010; Hell, 2008).

1.4 Plant mitochondrial import apparatus

The majority of research into the process of protein import into mitochondria has utilised *S. cerevisiae* as the model system and initial studies suggested that the process of protein import is conserved across various phylogenetic lineages. With the availability of T-DNA insertion knock-out lines, the sequencing of the *Arabidopsis thaliana* genome and advances in proteomics, more detailed studies in plant mitochondria have revealed substantial differences. Plant mitochondrial import is a more complex system, with developmental regulation (Linke and Borner, 2005; Murcha et al., 1999) and effects of plant stress (Lam et al., 2001; Taylor and Millar, 2007; Vacca et al., 2004; Yao et al., 2004). Furthermore, the existence of an additional organelle, the chloroplast, adds to the complexity of mitochondrial biogenesis in plants.

The plant outer membrane TOM complex differs in three aspects compared to the yeast TOM complex. Firstly, no biochemical or genetic

evidence exists for the presence of a Tom70-like protein in plants (Werhahn et al., 2001). Secondly, Tom22, which acts as a convergence point for precursor proteins before they enter the Tom40 channel, appears to be absent in plants (Macasev et al., 2004). It has been identified that Tom22 in yeast is replaced by a much smaller protein of 9 kDa in plants, Tom9 (Jansch et al., 1998a, b). It lacks the “receptor” domain of Tom22 yet still maintains the same function (Jansch et al., 1998a, b; Macasev et al., 2004). Thirdly, even when components appear to share function between organisms, they can be unrelated at a sequence level. For example, Tom20 from plants is not orthologous to yeast or mammalian Tom20, it displays low significant sequence similarity and has significant structural differences (Herald et al., 2003). Plant Tom20 belongs to the tetratricopeptide repeat (TPR) superfamily, but it is unusual in that it contains insertions lengthening the helices of each TPR motif (Perry et al., 2006). Also the structural elements of plant Tom20s are in reverse order whereas the plant Tom20 is C-terminally anchored (Perry et al., 2006). These examples suggest that distinct evolutionary pathways in yeast, plants and animals have resulted in unrelated proteins which fulfill similar functions.

In Arabidopsis, Tom20 is encoded by four paralogous genes, one of which shows transcription expression at very low levels, with no detectable protein (Lister et al., 2007). These genes encode 3 functionally redundant proteins all involved in mitochondrial import. Single knockouts of each of the *Tom20* genes did not result in a change in import ability (Lister et al., 2007). However, different isoforms display some precursor recognition specificity as simultaneous

inactivation of two of the three *Tom20* genes changed the rate of import for dual targeted proteins and proteins imported through the general import pathway. Inactivation of all three *Tom20* genes resulted in severely reduced rates of import for some precursors. It is important to note that the triple *Tom20* knock-out plants were still viable, therefore, suggesting additional receptors may also have a role to play (Lister et al., 2007).

Unlike the TOM components, the TIM complexes are highly conserved in all organisms and direct evolutionary lineages can be traced (Carrie et al., 2010b; Papatheodorou et al., 2007). The core subunit of the TIM complexes, Tim17, Tim22 and Tim23 are highly conserved in yeast and plants, with one notable difference with respect to Tim17. In Arabidopsis, Tim17 contains a significant extension at the C-terminus which is not present in fungi and mammals, and genome sequence information indicates this extension is present in Tim17 in other plant species (Murcha et al., 2003). Interestingly, the Arabidopsis orthologs can only complement yeast mutants when this extension has been removed. (Murcha et al., 2003). Furthermore, it is worth noting that the yeast Tim23 N-terminal extension shown to link the inner and outer membranes (Donzeau et al., 2000) does not appear to be present in the plant Tim23 isoforms (Murcha et al., 2003). In addition, a unique aspect of plant import components is that many import components are encoded by small multigene families (Carrie et al., 2010a). For example, the Tim17, Tim23 and Tim22 are actually members of the Preprotein and Amino Acid Transporters family (PRAT) (Murcha et al., 2007), which will be described in section 1.6.

Another unique aspect of the protein import pathway in plants is the mitochondrial processing peptidase (MPP). In yeast, it is a general peptidase recognizing and processing the N-terminal targeting presequence from precursor proteins after protein import into mitochondria (Glaser et al., 1998; Neupert, 1997; Schatz, 1996). It contains two structurally related components, α-MPP and β-MPP, both located in the matrix (Braun and Schmitz, 1997). However, in plants, MPP is integrated into the cytochrome bc_1 complex. The core proteins of the cytochrome bc_1 complex in plants are identical to the MPP subunits and the MPP activity resides in the inner membrane (Braun et al., 1992; Emmermann et al., 1993). As a result, the plant cytochorome bc_1 complex is bifunctional, involved in both in electron transport and in the general proteolytic processing of mitochondrial precursor proteins (Glaser and Dessi, 1999; Glaser et al., 1994). However, studies revealed that the protein processing and electron transfer are two independent events in plants, as the inhibition of processing activity has not been seen to correlate with the inhibition of electron transport (Eriksson et al., 1996). However, other studies showed that inhibition of protein processing do reduce the rate of protein import into plant mitochondria (Tanudji et al., 1999; Whelan et al., 1996)

1.5 Respiratory chain complexes

The current work presented in this thesis will focus on the mitochondrial inner membrane protein import components Tim17 and Tim23. As previously mentioned, the TIM17:23 complex has found to be associated with respiratory

chain complex III and can also form a supercomplex with complex IV (Dienhart and Stuart, 2008; van der Laan et al., 2006) (section 1.3.5.4). Additionally, one of the respiratory chain complex I subunits, encoded by At2g42210, has been identified as a member of the Preprotein and Amino acids Transporter family, along with Tim17 and Tim23 (Meyer et al., 2008b; Murcha et al., 2007). Thus, complex I and complex III will be described in detail in the following sections specifically, in regard to their interactions with the protein import apparatus.

1.5.1 ATP synthesis

As a “power station”, one of the most important functions that takes place in mitochondria is the synthesis of ATP via the process of oxidative phosphorylation. Reduced compounds, nicotinamide adenine dinucleotide (NADH) and flavin adenine dinucleotide hydroquinone ($FADH_2$), within the mitochondrial matrix, or the intermembrane space, are oxidized to generate a proton gradient that is used to synthesise ATP from ADP and inorganic phosphate (Pi).

The respiratory chain consists of a series of multi-subunit protein complexes located in the inner mitochondrial membrane termed complex I (NADH dehydrogenase), complex II (succinate dehydrogenase), complex III (cytochrome bc_1) and complex IV (cytochrome c oxidase) (Acin-Perez et al., 2008; Boekema and Braun, 2007). The flow of electrons through these complexes is coupled to the pumping of hydrogen ions out of the matrix into the intermembrane space, thereby establishing an electrochemical gradient over

the inner membrane (Mitchell, 1961). Ultimately, the donated electrons reduce oxygen to form water. The flow of hydrogen ions back into the matrix through complex V (ATP synthesis complex) provides the energy to catalyse the synthesis of ATP from ADP and Pi (Klingenberg, 2008).

Besides the classical oxidoreductase complexes of the respiratory chain, plant mitochondria also possess an alternative non-phosphorylating bypass respiratory pathway, which is mediated by NAD(P)H dehydrogenases and the alternative oxidase (AOX) (Clifton et al., 2006; Smith et al., 2011). The enzymes in this pathway do not translocate protons out of matrix. As a result, they do not contribute to the generation of the electrochemical gradient over the inner membrane, uncoupling electron transport from ATP synthesis (Juszczuk and Rychter, 2003; Liu, 1999; Vanlerberghe and McIntosh, 1997). The non-phosphorylating respiratory pathway has been proposed to play an important role during environmental stresses and in the interaction between chloroplasts and mitochondria (Affourtit et al., 2001; Noctor et al., 2007; Noguchi and Yoshida, 2008).

1.5.2 Complex I

The mitochondrial respiratory chain consists of five multi-subunit complexes embedded in the inner mitochondrial membrane. Complex I is the largest complex of the mitochondrial oxidative phosphorylation (OXPHOS) system and provides the major entry point for electrons into the electron transfer chain of the inner mitochondrial membrane (Lazarou et al., 2009;

Remacle et al., 2008; Zickermann et al., 2009).

1.5.2.1 The subunits of complex I

Bacterial complex I is composed of a basic core of 14 structural subunits with a molecular mass of 550 kDa. During evolution, the homologues of the core subunits were retained as part of mitochondrial complex I in eukaryotes, while a number of non-core subunits were acquired, thus increasing the molecular mass to 900-1000 kDa. In bovine heart mitochondria, complex I comprises of 45 subunits (Fearnley et al., 2007; Hirst, 2005), while in plants, there are at least 42 subunits in *Arabidopsis thaliana* and *Oryza sativa* (Heazlewood et al., 2003a; Klodmann et al., 2010b; Meyer et al., 2008b; Pineau et al., 2008). All mitochondrial complex I share 33 subunits in common, including the 14 core subunits (Cardol et al., 2005). The remaining subunits are specific to only a few lineages (Videira and Duarte, 2002). The role of non-core subunits is not yet fully understood though it is generally assumed that they are required for assembly of the complex and/or regulation of complex I activity (Angell et al., 2000; Lu and Cao, 2008; Vogel et al., 2004; Zhang et al., 2003). In contrast to most eukaryotes, yeast contains only three small type II NADH dehydrogenases instead of complex I (De Vries et al., 1992; Luttik et al., 1998).

1.5.2.2 The structure of complex I

Similar to that present in bacteria, eukaryotic complex I displays a typical L-shaped structure with a hydrophilic arm exposed to the matrix and a hydrophobic arm embedded in the mitochondrial inner membrane (Djafarzadeh et al., 2000; Grigorieff, 1998; Guenebaut et al., 1997; Hofhaus et al., 1991).

Some subunits of complex I have been found to be phosphorylated (Palmisano et al., 2007; Sardanelli et al., 1995; Schilling et al., 2005; Schulenberg et al., 2003). Though the significance of this post-translational modification is not clear, one hypothesis is that phosphorylation can regulate the activity of complex I (Bellomo et al., 2006; Palmisano et al., 2007; Papa, 2002; Piccoli et al., 2006), as this process was also found to have a biological role in regulating complex IV and V (Reinders et al., 2007).

1.5.2.3 The role of complex I in plant

A number of studies on plant complex I subunit mutants shows that complex I plays an important role in energy production and metabolism (Pla et al., 1995). One interesting mutant is CMSII in *N. sylvestris*, which lacks the NAD7 subunit of complex I (Pla et al., 1995). The mutant plants showed that the growth was retarded compared with the wild type, the activity of complex I was lower, photosynthesis was reduced and the expression of many stress-related genes was modified (Dutilleul et al., 2003; Sabar et al., 2000). Another interesting mutant is *ndufs4* in Arabidopsis, which lacks the complex I of the respiratory chain and also shows retarded growth phenotype (Meyer et al., 2009). The mutant resulted in a wide change of the nuclear transcriptome changes related to growth and photosynthetic function (Meyer et al., 2009).

1.5.3 Complex III

1.5.3.1 The composition of complex III

Complex III is the central component of the mitochondrial OXPHOS

system (Berry et al., 2000; Hunte et al., 2000). It consists of cytochromes *b* and c_1, the Rieske iron–sulfur protein (RISP), two core proteins, and five low-molecular mass subunits, assembling as a homodimer (Hunte et al., 2008; Smith et al., 2004; Zara et al., 2009a). The major part of complex III is exposed to the mitochondrial matrix, while a portion of the complex is embedded in the inner membrane and a small part protrudes into the mitochondrial intermembrane space (Hunte et al., 2000; Iwata, 1998).

The Rieske iron–sulfur protein (RISP) is one of the catalytic subunits of the complex, functionally cooperating with cytochromes *b* and c_1 in the transfer of electrons (Fisher et al., 2004; Gurung et al., 2005; Rajagukguk et al., 2007). Besides functioning as a component for the redox activity, it also appears to have an important role in building up the mature dimeric complex III, as its transmembrane domain interacts with one monomer and the intermembrane domain interacts with the other monomer of the complex (Conte and Zara, 2011).

The constituents of plant complex III are quite similar to those of complex III in nonplant species. However, there is a striking feature that the general mitochondrial processing peptidase (MPP) is integrated into the complex III (Glaser and Dessi, 1999). As a result, the complex III in plants is bifunctional, playing roles both in electron transport and in the general proteolytic processing of mitochondrial precursor proteins (Glaser and Dessi, 1999).

1.5.3.2 The assembly of complex III

The assembly process of complex III is quite intricate, as it is an inner

membrane dimeric complex and each monomer has at least 10 subunits. All of the subunits, except one (cytochrome *b*), are encoded by the nuclear DNA and have to be imported from the cytosol to the mitochondria. Cytochrome *b* is encoded by mitochondrial DNA (Acin-Perez et al., 2004; Halbreich et al., 1980).

Although the assembly pathway of complex III is not fully elucidated, several studies have suggested that the assembly pathway requires the participation of several bc_1 subcomplexes, including the central core of the bc_1 complex, the two core proteins associated with each other and the RISP protein associated with subunit 9 (Crivellone et al., 1988; Zara et al., 2007, 2009a, b). In yeast, Bcs1p protein has been identified to be a chaperone involved in the assembly of RISP into the cytochrome bc_1 complex (Cruciat et al., 1999; Nobrega et al., 1992). Deletion of the Bcs1p protein resulted in the formation of a functionally inactive bc_1 core structure and it could be rescued by the expression of Bcs1p in the mutant strain (Conte et al., 2011).

Several studies have reported that the assembly state of complex III could affect the function of complex I (Suthammarak et al., 2010). Previous studies have identified that the failure to assemble a functional complex III due to the mutation in *cytochrome b* gene, results in a dramatic loss of complex I activity (Acin-Perez et al., 2004). Conversely, the assembly state of complex III is not significantly affected by the loss of complex I (Acin-Perez et al., 2004), although a partial reduction of complex III activity has been observed with the total loss of complex I in the *ndufs4* mutant (Budde et al., 2000; Meyer et al., 2009).

1.5.4 Respiratory chain supercomplexes

Apart from complex II (succinate dehydrogenase), all the respiratory chain complexes are able to associate with each other to form the supercomplexes (Dudkina et al., 2005; Eubel et al., 2004; Schagger, 2002). Several supercomplexes have been identified in yeast through the solubilization of mitochondrial membranes using Triton or digitonin followed by blue-native PAGE (BN-PAGE). The dimeric ATP synthase, the dimeric form of complex III, and the direct association of complex III with complex IV have all been observed (Arnold et al., 1998; Cruciat et al., 2000; Schagger, 2002; Stuart, 2008).

In higher plants, the dimeric form of ATP synthase, supercomplexes of complex I+III_2, III+IV and I+III+IV have all been identified (Eubel et al., 2004; Eubel et al., 2003; Krause et al., 2004). The dimeric complex III was found to associate with the membrane arm of complex I within the inner membrane to form the supercomplex I+III_2 with a molecular mass of 1.5 MDa (Dudkina et al., 2005). Compared to the supercomplex I+III_2 in mammalian, this supercomplex has been shown to be more abundant and stable in Arabidopsis (Dudkina et al., 2005; Schagger and Pfeiffer, 2000).

The functional significance of supercomplexes is still unclear. They have been proposed to play roles in enhancing the electron transfer rates, stabilizing the protein complexes, increasing the insertion capacity of the inner membrane (Arnold et al., 1998; Schagger and Pfeiffer, 2000; Perez et al., 2004) and maintaining the cristae structure of the inner membrane (Stuart, 2008; Vonck and Schafer, 2009). In plants, supercomplexes are also proposed to play a role

in regulating alternative respiration (Eubel et al., 2003; (Eubel et al., 2004)).

1.6 The plant PRAT proteins

In yeast, the preprotein and amino acids transporter (PRAT) family is defined by the similarities in the sequences and functions of Tim17, Tim22 and Tim23, and an outer envelope protein (OEP) of 16 kDa from *Pisum sativum* (pea), termed OEP16 and the Liv H permease from bacteria. They are thought to have evolved from a single prokaryotic amino acid transporter. All of these comprise four hydrophobic segments, connected by three short hydrophilic loops, with a characteristic motif: $[G/A]X_2[F/Y\}X_{10}RX_3DX_6[G/A/S]GX_3G$, where X is any amino acid (Rassow et al., 1999).

In Arabidopsis, 17 loci encode 16 proteins of the PRAT family. It is a large increase in family size in comparison to yeast. The predicted proteins in Arabidopsis, range in size from 133 to 261 amino acids. The four transmembrane regions used to define this family were only predicted for 5 of the 17 proteins in the Aramemnon database (Murcha et al., 2007). The PRAT domain was present in 7 of the 17 predicted Arabidopsis proteins, whereas 4 contained a degenerate PRAT domain (Murcha et al., 2007). Of all 17 members: 11 were determined to be mitochondrial, 5 chloroplastic, and one protein dual-targeted to both locations (Murcha et al., 2007). The mitochondrial PRAT proteins group into three subfamilies, Tim23, Tim17 and Tim22. Three proteins, encoded by At3g25120, At5g24650 and At3g49560, could not group with the

subfamilies and the function is unknown (Figure 1.2).

1.6.1 Tim23

In Arabidopsis, three genes encode Tim23, termed Tim23-1, Tim23-2 and Tim23-3, with an amino acid identity of 23%, 21% and 18%, respectively when compared to yeast Tim23 (Murcha et al., 2007). In contrast to yeast, the 34 N-terminal amino acids of Tim23, which are necessary for binding to Tim50 in yeast are missing in all plant isoforms. However, the extended C-terminus of plant Tim17-2 may compensate for the loss of the N-terminal extension in Tim23 (Murcha et al., 2007). The *in vitro* uptake assay has indicated that all three Tim23 proteins are located in the mitochondrial inner membrane (Murcha et al., 2007). *Tim23-2* is expressed ubiquitously in all tissues and represents the most highly expressed *Tim23* (Murcha et al., 2003). *Tim23-1* transcript is detected in late seed development as well as in pollen grains, whereas *Tim23-3* is only very weakly expressed with transcript abundance at least 10 times lower than that observed for *Tim23-1* and *Tim23-2* (Murcha et al., 2003).

1.6.2 Tim17

The three Tim17 isoforms in Arabidopsis have amino acid identity of 31%, 29% and 33%, respectively, when compared to that of yeast (Murcha et al., 2003). Tim17-1 and Tim17-2 have an extended C-terminus with 58 and 80 additional amino acids respectively, whereas Tim17-3 protein sequence terminates at the fourth predicted α-helix (Murcha et al., 2003). The *in vitro*

uptake assay defined that all three Tim17 proteins are located in the mitochondria (Murcha et al., 2007).

At the transcript level, Arabidopsis *Tim17-2* is expressed in all tissue types tested (Murcha et al., 2003). *Tim17-3* is also expressed ubiquitously as well but at a much lower level, whereas *Tim17-1* transcripts are generally low, peaking in cotyledons, cauline, senescent leaves and seeds (Murcha et al., 2003). The C-terminal region of the Tim17-2 links the outer and the inner membrane of mitochondria, thereby substituting for the lack of the plant Tim23 N-terminus. Blockage of the C-terminus of Tim17-2 with a specific antibody resulted in inhibition of the general import pathway, thus, Tim17-2 is essential for preprotein translocation via the general import pathway (Murcha et al., 2005a).

1.6.3 Tim22

The identity of Tim22 in Arabidopsis could not be clearly defined by sequence analysis alone, as Tim22 of yeast branches with three proteins encoded by At1g18320, At3g10110 and At2g42210 (Murcha et al., 2007). Although not located in duplicated segments of chromosomes, At1g18320 and At3g10110 encode predicted proteins with 100% identity. The proteins encoded by At1g18320 or At3g10110 have been shown to complement a yeast mutant for Tim22 (Murcha et al., 2007). Thus, At1g18320 and At3g10110 may represent the Tim22 isoforms in Arabidopsis. The protein encoded by At2g42210, has been identified as a subunit of complex I (Meyer et al., 2008b).

1.6.4 PRAT proteins of unknown function

Through phylogenetic analysis, three PRAT proteins encoded by At5g24650, At3g49560 and At3g25120 could not be grouped with any yeast homolog (Figure 1.2) and so far, have not been assigned a possible function. The proteins encoded by At5g24650 and At3g49560 share 83% sequence identity with each other. The *in vitro* uptake assays and *in vivo* GFP targeting showed that the protein encoded by At3g49560 was localized to the chloroplast and the protein encoded by At5g24650 may be dual targeted to the chloroplast and mitochondria (Mucha et al., 2007). It indicated that the minor difference in amino acid sequence could result in the different subcellular targeting. The protein encoded by At3g25120 has been defined as located in the mitochondrial inner by *in vitro* uptake assay, but to date no function has been assigned to this protein (Mucha et al., 2007).

1.7 Project aims

The endosymbiotic event that gave rise to plastids is thought to have occurred approximately one billion years ago (Gray et al., 1999; Lang, 1999) and has resulted in the divergence of many functions between plant and other cell types. In particular, plant mitochondria display many unique features, including large genomes that have comparatively very low rates of mutation compared to animals, extenisve *cis* and *trans* splicing of transcripts, extensive processing and editing of primary transcripts. Biochemically, plants also display many unique features, including the presence of the respiratory chain by-passes that are activated when electron transport through the cytochrome pathway is blocked. Thus, as noted in section1.4, it is not unexpected that the plant mitochondrial protein import apparatus differs significantly from other higher eukaryotes.

While some aspects of the protein import apparatus in plants can be considered well studied, such as the preprotein processing by MPP, presequence degradation by presequence protease (PreP) and the composition of the TOM complex, the translocases of the inner membrane are not well understood in terms of function compared to their yeast counterparts. The focus of the work presented in this thesis is to carry out further detailed studies on the TIM17:23 complex of plant (Arabidopsis) mitochondria.

Thus, the primary aims of this study were to:

1) Identify the T-DNA insertion knock-out lines for each gene of Arabidopsis *Tim17* and *Tim23* family, to determine if inactivation of any one gene

resulted in altered growth phenotypes or viability.

2) Investigate if depletion of Tim17 or Tim23 protein levels can affect the rate of protein import.
3) Identify the proteins associated with Tim17 and Tim23, and determine the composition of the TIM17:23 complex in Arabidopsis.

The expected outcomes of these investigations would be to determine if the gene families that encode Tim17 and Tim23 display functional redundancy, as has been observed with similar studies analysing the Tom20 receptor of the TOM complex, which shows considerable functional redundancy. Furthermore, characterization of Tim17 and Tim23 from Arabidopsis, and the interacting proteins, would provide insight into if this complex has any different function in plants compared to yeast. Note, given the relatively high level of amino acid sequence identity between Tim17 and Tim23 from plants and yeast, it was not investigated or expected that the basic mechanism of the translocase would differ, i.e. a voltage gated twin pore translocase, rather its regulation and specific role may differ given the one billion years of evolution between the last common ancestor of plants and yeast.

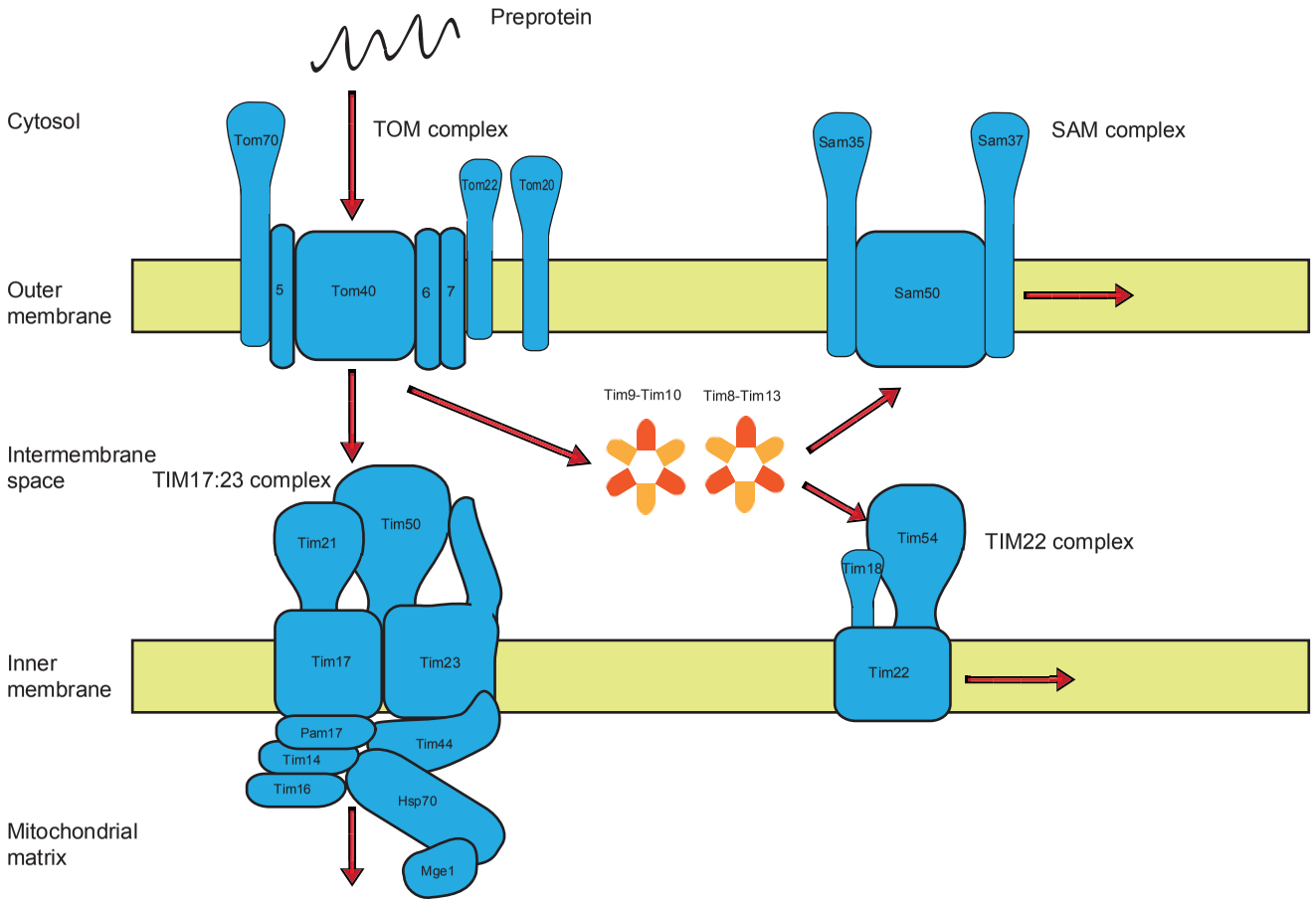

Figure 1.1. Model of the protein import apparatus in yeast mitochondria. Proteins synthesized in the cytosol are imported into mitochondria through the TOM complex. After translocating through the outer membrane, the import pathway diverges. Proteins destined to the matrix are transported through the inner membrane by the TIM17:23 complex. The β-barrel proteins destined for the outer membrane are imported by the Tim9-Tim10 and Tim8-Tim13 complexes in the inter membrane space and the SAM complex in the outer membrane, while proteins destined for the inner membrane are transported through the TIM22 complex.

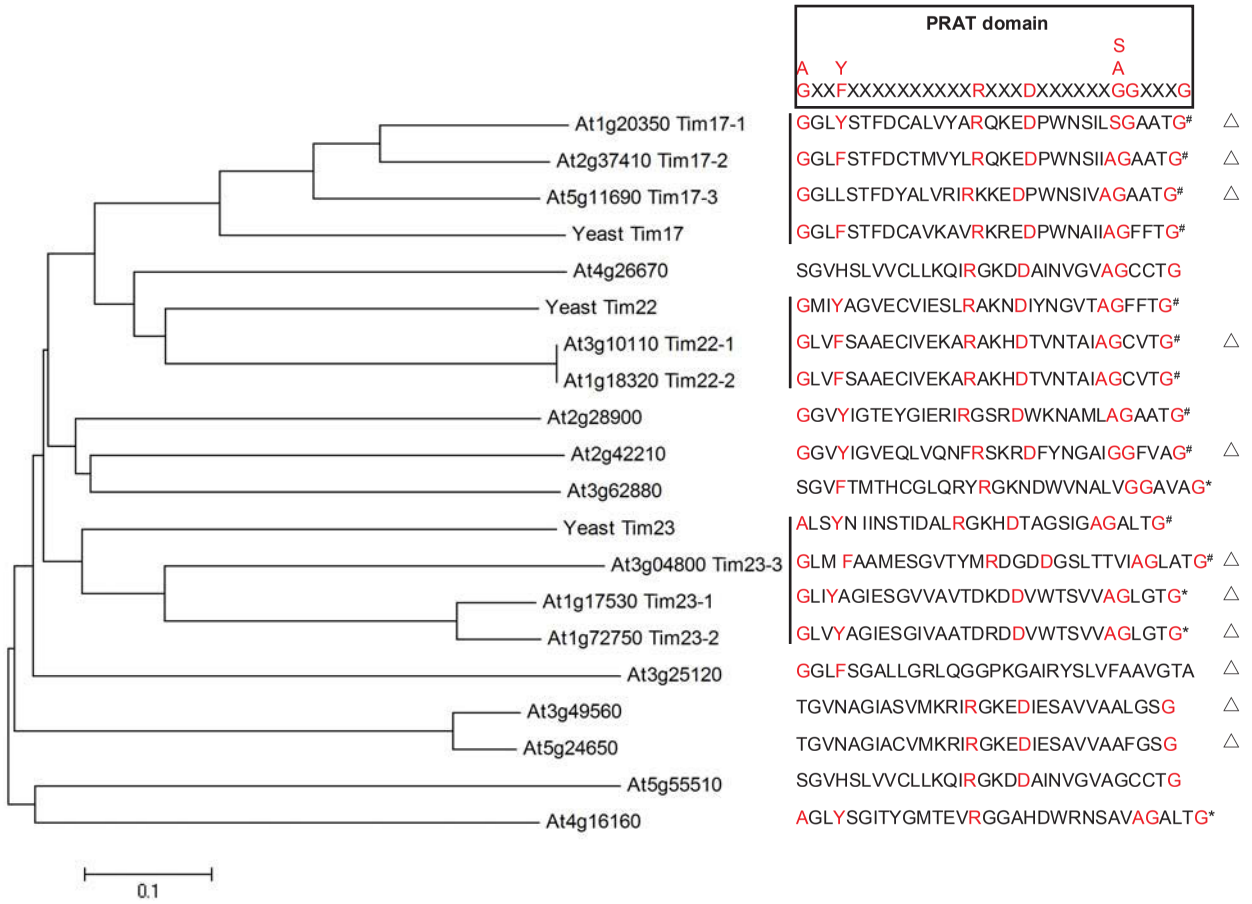

Figure 1.2. Phylogenetic analysis and the PRAT domain in PRAT family proteins. Neighbor joining tree of the Arabidopsis PRAT protein family with yeast TIM17, 22 and 23. Three proteins are grouped with yeast Tim17, Tim23 and Tim22 respectively. The sequence containing PRAT domain is listed alongside each protein. The PRAT domain is indicated above the sequences, where X indicates any amino acid and the consensus amino aicds are indicated in red. Seven of the 17 Arabidopsis PRAT proteins contain the complete PRAT domian (indicated by #), while four proteins contain a degenerated PRAT domain with one additional amino acid spacing or with one of the consensus amino acids missing (indicated by *). Of all 17 members, 11 were determined to be mitochondrial proteins (indicated by △). Abbreviations, PRAT: preprotein and amino acid transporter.

Chapter 2
Materials and methods

Chapter 2 Materials and methods

2.1 Materials

2.1.1 Plant growth

Arabidopsis thaliana cv. Columbia was used in this study. All plants were grown at 22 ^{o}C under long-day conditions (16 h of 100 µE m^{-2} s^{-1} light, 8 h dark). For T-DNA insertion line genotyping: The Arabidopsis seeds were planted on a soil mix consisting of grade 2 vermiculite, perlite P5, coco peat, black peat dolomite lime and complete fertilizer. Stratification was carried out for 2 days in the dark at 4 ^{o}C. The plants were watered 3 times a week, allowing for the water to dry out between watering.

For mitochondrial isolation: The Arabidopsis seeds were sterilized in 70% (v/v) ethanol and 5% (v/v) bleach with 0.1% (v/v) Tween-20. The plants were grown for 14 days on an orbital shaker at 80 revolutions per minute (rpm) in 80 ml of sterile liquid growth media (0.5 x Murashige and Skoog media, 0.5 x Gamborgs B5 salts, 3% (w/v) sucrose, 50 µg/ml cefotaxime, 2 mM 2-(*N*-morpholino)ethanesulfonic acid (MES), adjusted to pH 5.7 with KOH).

2.1.2 T-DNA insertion lines

The T-DNA insertion lines (SALK_030470, SALK_107963, GABI_689C11, SALK_143656, SALK_129386, SAIL_1151_B01, SALK_092885, SALK_091528, GABI_561E03, SALK_048425, SALK_125567) were obtained from the ABRC seed stock centre and GABI-Kat.

2.1.3 Bacterial growth media

LB media: 10 g/L Bacto™ tryptone, 10 g/L NaCl, 5 g/L Bacto™ yeast extract, sterilised by autoclaving. Agar plates were prepared by the addition of 15 g/L agar, prior to autoclaving.

SOC media: 20 g/L Bacto™ tryptone, 5 g/L Bacto™ yeast extract, 10 mM NaCl, 2.5 mM KCl, 20 mM glucose and 20 mM Mg^{2+}.

2.1.4 Bacterial strains

DH5α: F^- *sup*E44 Δ*lac*U169 *(*Φ80*lacZ*ΔM15*) hsd*R17 *rec*A1 *gyr*A96 *thi*-1 *rel*A1

BL21(DE3): *E. coli B* F^- *dcm omp T hsdS*($r_B^- m_B^-$) *gal λ(DE3)*

2.1.5 Sterile distilled water

Sterile distilled water (SDW) refers to the use of double deionised water filtered through the Millipore Milli-Q plus® ultra pure water system (Millipore, Sydney, Australia) and autoclaved.

2.2 General gene cloning

2.2.1 PCR

Polymerase chain reaction (PCR) was carried out on either genomic DNA or complementary DNA (cDNA), and 30 pmol each of forward and reverse primers. The reaction was assembled on ice using the Expand™ High Fidelity PCR system (Roche, Sydney, Australia). The amplification profile consisted of 94 °C for 5 minutes (min), followed by 35 cycles of 94 °C for 30 seconds (sec), 55

^{o}C for 30 sec and 72 ^{o}C for 1 min, 72 ^{o}C for 10 min followed by cooling to 14 ^{o}C. The products were separated by agarose gel electrophoresis (section 2.6.1) and visualised under a UV transilluminator. The DNA was either purified through gel extraction or purified using QIAquick PCR Purification Kit (Qiagen, Sydney, Australia) for cloning. All procedures were carried out according to the manufacture's instruction.

2.2.2 Restriction enzyme digestion

Restriction enzyme digestion was carried out using 10 units of enzyme per 500 ng of DNA in a total volume of 20 µl, incubated for 2 h under specific temperature and buffer conditions for each enzyme. Digested DNA products were seperated by agarose gel electrophoresis (section 2.6.1) and visualised under a UV transilluminator.

2.2.3 DNA shrimp alkaline phosphatase treatment

Digested plasmid DNA was treated with shrimp alkaline phosphatase (SAP, Roche, Sydney, Australia) to prevent plasmid re-ligation by de-phosphorylating the 5' phosphate of DNA. Restriction digests were terminated by heating the sample to 65 ^{o}C for 15 min. One µl of SAP and 1.5 µl of 10 x buffer was added to a 15 µl reaction volume. The reaction was further incubated at 37 ^{o}C for 1 h.

2.2.4 T4 DNA ligation

The reaction consisting of 8 µl DNA, 1 µl 10 x ligation buffer and 1 µl T4

DNA ligase (Roche, Sydney, Australia), was assembled on ice and incubated overnight at 14 ^{o}C. Ligations were then transformed to chemically competent bacterial cells as outlines (section 2.2.6).

2.2.5 Preparation of chemically competent cells

Chemically competent DH5α cells were prepared in the laboratory as followed. DH5α cells were spread onto a LB agar plate. The plate was incubated overnight at 37 ^{o}C. The following morning a 100 ml conical flask of sterilized LB media was inoculated with 5-6 colonies and incubated at 37 ^{o}C at 225 rpm. The optical density was checked every hour until it reached 0.4 at 600 nm. All subsequent steps were performed at 4 ^{o}C with chilled solutions. The cells were transferred into 2 pre-cooled 50 ml tubes and were incubated on ice for 10 min. The 2 tubes were centrifuged at 2 000 x g for 10 min, the supernatant was removed and the bacterial pellet was resuspended in 5 ml of 0.1 M $CaCl_2$. The tubes were incubated on ice for a further 10 min and then centrifuged at 2 000 x g for 10 min. The supernatant was removed and the bacterial pellet was resuspended in 1 ml of 0.1 M $CaCl_2$ with 20% (v/v) glycerol and incubated for a further 10 min. One hundred µl aliquots of bacteria were snap frozen in 1.5 ml microcentrifuge tubes with liquid nitrogen and stored at – 80 ^{o}C until required.

2.2.6 Bacterial transformation

Plasmids were transformed into chemically competent DH5α cells using a heat shock approach. Plasmid DNA was added into competent cells in 1:10

volume ratios. Usually 200 ng of DNA was incubated with 50-100 µl freshly thawed competent cells on ice for 30 min and heat shocked at 42 ^{o}C for 45 sec. The cells were placed on ice for a further 2 min and 500 µl of SOC media was added before shaking at 200 rpm for 1 h at 37 ^{o}C. Fifty µl of cells were plated on LB agar plates containing the appropriate antibiotic, either Kanamycin or Ampicillin at a final concentration of 50 µg/ml.

2.2.7 Plasmid mini preparations

A single colony of bacteria was inoculated into 2 ml of LB media containing the appropriate antibiotic and grown overnight at 37 ^{o}C, shaking at 200 rpm. The culture was centrifuged for 1 min at 15 000 x g and the plasmid DNA was isolated using High Pure Plasmid Isolation Kit (Roche, Sydney, Australia). All procedures were carried out according to the manufacturer's instructions.

2.2.8 Plasmid midi preparations

A single colony of bacterial was inoculated into 50 ml of LB media containing the appropriate antibiotic and grown overnight at 37 ^{o}C, shaking at 200 rpm. The culture was pelleted in a 50 ml oakridge tube (Nalgene, New York, USA) by centrifugation for 15 min at 5 000 x g. Plasmid was isolated using the QIAGEN Plasmid Midiprep Kit (QIAGEN, Clifton Hill, Australia) according to the manufacture's instructions.

2.2.9 Ethanol DNA precipitation

Precipitation of DNA was carried out by adding 0.1 volume of 3 M sodium acetate, pH 5.2, and 2 volume of 100% ethanol into the DNA sample and incubated at – 20 ^{o}C for 30 min. The DNA was centrifuged for 20 min at 20 000 x g, washed once in 200 µl of 70% (v/v) ethanol and centrifuged for 5 min at 20 000 x g. The DNA pellet was air dried at room temperature and resuspended in 30 µl SDW.

2.2.10 Isopropanol DNA precipitation

Isopropanol precipitation was carried out using the same protocol as for ethanol precipitations except one volume of isopropanol was used in place of two volumes of ethanol. Isopropanol precipitation was used when DNA fragments less than 100 base pairs (bp) were to be excluded from the precipitation.

2.3 Screening *Arabidopsis thaliana* T-DNA insertion lines

2.3.1 Selecting T-DNA insertion lines and designing primers

Two T-DNA insertion lines were selected for each gene based on the location of the T-DNA insertion within the gene of interest. For genes that did not have any insertion within the coding regions, lines were selected with insertions either in the promoter, 5’ untranslated region (UTR) or 3’UTR. Primer pairs for genotype screening were designed specifically for each T-DNA insertion line

using the T-DNA primer design program (Salk Institute Genomic Analysis Laboratory, http://signal.salk.edu/tdnaprimers.2.html). The primers were designed approximately 400 bp upstream and downstream of the T-DNA insertion. Two sets of primers were designed, one to amplify the gene of interest and the other to amplify the T-DNA insertion sequence within the gene of interest.

2.3.2 Genomic DNA isolation

The Arabidopsis genomic DNA was isolated from young leaf tissue. Two or three small leaves were collected and snap frozen in a 1.5 ml microcentrifuge tube using liquid nitrogen. Two hundred µl of extraction buffer (Appendix I, 1) was added and the sample was crushed with one tungsten bead using Retsch MM301 Ball Mill (Retsch, Hann, Germany) at maximum speed for 2 min. After centrifugation for 2 min at 20 000 x g, 170 µl of supernatant was transferred to a fresh microcentrifuge tube, taking care to avoid transferring of the green pellet. One hundred and seventy µl of isopropanol was added and incubated for 5 min at room temperature. The DNA was pelleted by centrifugation for 5 min at 20 000 x g at room temperature, and the supernatant was removed. The pellet was air dried at room temperature and resuspended with 100 µl SDW and stored at – 20 ^{o}C until required.

2.3.3 PCR screening

The genotype of the plant was determined by PCR using the RED

Extract-N-Amp^{TM} Plant PCR Kit (Sigma Aldrich, Sydney, Australia) according to the manufacturer's instructions. Two PCR reactions were performed for each plant. The first reaction containing the right border primer (RP) and left border primer (LP) was to amplify the gene of interest. The second reaction to amplify the T-DNA insertion sequence was performed using the RP primer and the SALK_LB or SAIL_LB or GABI_LB primer, depending on the type of T-DNA insertion line. The PCR reactions were performed in a 96 well plate (Sigma Aldrich, Sydney, Australia). A typical PCR reaction was performed as outlined in section 2.2.1 and the products were visualized by agarose gel electrophoresis (section 2.6.1).

2.3.4 Crossing Arabidopsis plants

For reducing the possibility of self-fertilization, the female parents must be used before the anthers shed pollen onto the stigma and the male parents which are visible to shed pollen are chosen. The flowers and siliques which are above or below the flower selected for crossing were removed. For the selected female parent plants, the sepals, petals and anthers are removed but the carpels are left intact. Anthers removed from the male parent plants were brushed against the stigmatic surface of the exposed carpels of the female plants. Siliques were collected after 2 or 3 weeks and dried at room temperature for 2 weeks.

2.4 Mitochondrial preparation

2.4.1 Mitochondrial isolation

Approximately 100 g (fresh weight) of 14-day old seedlings from water culture pots were used to isolate mitochondria. All steps were carried out at 4 ºC. Tissue was harvested and homogenized in 300 ml of grinding buffer (Appendix I, 2.1) and filtered through 4 layers of micracloth. The filtrate was poured into 50 ml polycarbonate centrifuge tubes and centrifuged for 5 min at 2 500 x g. The supernatant was centrifuged for 20 min at 17 400 x g and the pellet was gently resuspended in 1 x wash buffer (Appendix I, 2.2) and the two centrifugation steps were repeated. The pellet was gently resuspended in a small amount of 1 x wash buffer and layered onto a PVP Percoll gradient as outlined below.

The PVP percoll gradient was assembled using a gradient former model 385 (Bio-Rad, Sydney, Australia) consisting of a 4.4% (w/v) PVP heavy gradient solution (Appendix I, 2.3) and a light gradient solution (Appendix I, 2.4). The gradient was overlayed with the crude mitochondrial fraction and centrifuged at 40 000 x g for 40 min with no brakes, resulting in the separation of mitochondria from chloroplasts and thylakoids. The mitochondrial fraction was washed twice in 40 ml of 1 x wash buffer by centrifugation at 31 000 x g for 15 min with slow brake. The mitochondria was resuspended in 500 µl of 1 x wash buffer and kept on ice to use immediately in the import assay or stored at – 80 ^{o}C.

2.4.2 Protein assay

Protein assay was used to determine the final protein amount following the mitochondrial isolation procedure. Five hundred µl of Coomassie Protein Assay Reagent (Pierce®, Rockford, Illinois, USA) was added to 1 µl of isolated mitochondria diluted in 499 µl of SDW. The samples were mixed and the absorbance was measured at 595 nm UVmini-1240 spectrophotometer (Shimadzu, Kyoto, Japan). The concentration of protein was determined by comparison to a standard curve generated by the measurement of bovine serum albumin of known concentrations.

2.5 *In vitro* protein import assay

2.5.1 [^{35}S]-methionine labeled precursor protein translation

The TNT® Coupled Transcription/Translation Rabbit Reticulocyte system (Promega, Melbourne, Australia) was used for translation of [^{35}S]-methionine precursor proteins. The reaction master mix (Appendix I, 3) consisting of reticulocyte lysate, RNA polymerase, amino acids, buffer, RNase inhibitor and [^{35}S]-radiolabelled methionine (>1000 Ci/mmol at 10 mCi/ml; Amersham Pharmacia Biotech, Sydney, Australia), was assembled on ice into an microcentrifuge tube containing 0.2-0.4 µg of plasmid DNA. The reaction was incubated at 30 ^{o}C for 2 h and stored at – 80 ^{o}C until use.

2.5.2 Import of precursor protein into mitochondria

In vitro import assays were carried out as described by (Whelan et al., 1996). An import reaction consists of 50 µl mitochondria (250 µg) and 450 µl of import master mix (Appendix I, 4.1). The mitochondria were incubated on ice for 3 min, after which 10 µl of radiolabelled precursor protein was added and incubated at 26 ^{o}C at 300 rpm using an Eppendorf thermomixer comfort (Eppendorf, Hamburg, Germany).

For time-course analysis, one hundred µl of the import reaction was removed at 5, 10, 15 and 20 min time points. Three µg of proteinase K (PK) was added to the aliquot and incubated on ice for 30 min. Proteolysis was inhibited by the addition of 1 µl of 100 mM phenylmethylsulfonyl fluoride (PMSF). Mitochondria were re-isolated by centrifugation at 20 000 X g for 3 min at 4 ^{o}C, the mitochondrial pellet was resuspended in sample buffer (Appendix I, 4.2), and resolved by sodium dodecyl sulfate (SDS) -PAGE analysis (section 2.6.2). The gel was Coomassie stained, dried, and exposed to a BAS TR2040 phosphoimaging plate (Fuji, Tokyo, Japan) for at least 24 h. The exposed plate was visualized using the BAS 2500 Bio-Imaging Analyser (Fuji, Tokyo, Japan). The imported radiolabelled protein was quantitated at each time point and normalized to the highest time point measurement in the wild type for replicate experiments.

2.5.3 Quantification of import

The Bio-Rad Quantity one® 1-D Anaylsis Software (Bio-Rad, Sydney,

Australia) was used for the quantification of the imported radiolabelled proteins. The intensity of the radiolabelled protein was determined by measuring the pixel density per mm^2 of protein band minus the pixel density of the background. The background was measured in an area close to the band of interest. The pixel density was normalized to the highest level in Col-0 set to a value of 1. Standard error was calculated using the Microsoft Excel software.

2.6 Gel electrophoresis

2.6.1 Agarose gel electrophoresis

One percent (w/v) agarose gel was prepared by heating agarose powder in 1 x TAE buffer (Appendix I, 5.1) into which 1 mg/L of ethidium bromide was added. Gels were assembled into a Bio-Rad gel tank (Bio-Rad, Sydney, Australia) containing 1 x TAE buffer and samples were prepared in 5 x loading buffer (Appendix I, 5.2). DNA was visualized by placing the gel above a UV transilluminator 2000 (Bio-Rad, Sydney, Australia).

2.6.2 SDS-PAGE

Polyacrylamide gels were assembled with a 14% (w/v) acrylamide separating component and a 4% (w/v) acrylamide stacking component. The Bio-Rad PROTEAN II ^{TM} system (Bio-Rad, Sydney, Australia) was used to assemble the gel. The separating gel was composed of 14% (w/v) acrylamide and 0.1% (w/v) SDS with the separating buffer (Appendix I, 6.1). The solution was degassed for 5 min before the addition of 0.05% (w/v) ammonium

persulphate (AMPS) and 0.05% (v/v) N', N', N',N'- tetramethylethylenediamine (TEMED). After the seperating gel was set, the stacking buffer (Appendix I, 6.2) with 4% (w/v) acrylamide, 0.1% (w/v) SDS, 0.05% (w/v) ammonium persulphate (AMPS) and 0.05% (v/v) TEMED was prepared and poured.

Before loading on the gel, protein samples were resuspended in 2 x sample buffer and boiled for 4 min. The samples were resolved in running buffer (Appendix I, 6.3) for 4.5 h at 20 mA per gel with voltage limited to 200 V. Gels that were not for western blot analysis were stained in the Coomassie staining buffer (Appendix I, 6.4) for 3 h followed by destaining in destainig buffer (Appendix I, 6.5) for 2 h. Gels containing radiolabelled protein were dried under a vacuum drier for 2 h at 80 ^{o}C using the Bio-Rad Gel Dryer model 583 (Bio-Rad, Sydney, Australia). Gels were wrapped in a plastic film and exposed to a BAS TR2040 phosphoimaging plate for at least 24 h and scanned using the BAS 2500 Bio Imaging Analyser (Fuji, Tokyo, Japan).

2.6.3 Blue Native PAGE

Blue Native (BN) PAGE was performed according to (Jansch et al., 1996). Mitochondrial proteins (250 µg) were solubilized with 1% w/v digitonin in solubilization buffer (Appendix I, 7.1) and incubated for 20 min on ice. The samples were centrifuged for 10 min at 20 000 x g, and 0.2% v/v Serva Blue G (Appendix I, 7.2) was added to the supernatant. The samples were loaded onto a 4.5% (w/v) to 16% (w/v) gradient gel (Appendix I, 7.3). Gels were assembled using the Bio-Rad PROTEAN II protein gel electrophoresis system (Bio-Rad,

Sydney, Australia), which allows casting of acrylamide gradient gels from the bottom minimizing disturbances during gradient preparation. The preparation of the gradient component was carried out at 4 ^{o}C to delay premature acrylamide polymerization. After the polymerization of the gradient gel, the 4% (w/v) acrylamide stacking gel (Appendix I, 7.4) was overlayed.

Before sample loading and electrophoresis, the gel was pre-incubated in a gel rig with the Cathode buffer (Appendix I, 7.5) and the Anode buffer (Appendix I, 7.6) for 30 min at 4 ^{o}C. Gel electrophoresis is started at a constant voltage 100 V for 45 min, with current limited 6 to 8 mA, and continued at constant current 15mA for 10 to 15 h, with voltage limited to 500 V.

For BN-PAGE gels that were to be transferred to PVDF membrane, the normal Cathode buffer was changed with a Cathode buffer that excludes the Coomassie dye, half way throughout the electrophoresis. This was carried out to minimize the amount of Coomassie dye in the protein samples.

Gels containing radiolabelled proteins were incubated in the fixing buffer (Appendix I, 7.7) for 1 h and dried under a vacuum drier as previously mentioned (section 2.6.2).

2.7 Western blot

2.7.1 Blotting

Proteins separated by SDS-PAGE were transferred to the 0.45 μm nitrocellulose membrane. Ten pieces of Whatman filter paper, one piece of membrane and the gel were equilibrated in transfer buffer (Appendix I, 8.1) for

10 min, assembled and transferred for 1 h at 0.8 mA per cm^2 using a Milliblot graphite electroblotter (Millipore, Bedford, USA). After transferring, the membrane was stained in Ponceau-S solution (Appendix I, 8.2) for 1 min. Transferred proteins were visualised and the locations of the molecular weight markers were marked with a pencil. The membrane destained with TBS-Tween (Appendix I, 8.3) was directly used for immuno-detection, or dried between four sheets of Whatman paper and stored at 4 ^{o}C.

Proteins separated by BN-PAGE were transferred to a 0.45 µm Polyvinylidene Fluoride (PVDF) membrane using the Bio-Rad TransBlot Cell system (Bio-Rad, Sydney, Australia). Two pieces of Whatman filter paper, one piece of membrane and the gel were equilibrated in transfer buffer for 10 min and assembled as blotting sandwich. The unit was run in transfer buffer at 50 mA for 11 h at 4 ^{o}C, after which the membranes were detected as outlined in section 2.7.2.

2.7.2 Immuno-detection

For a standard membrane of 11 cm x 16 cm, 50 ml of BM chemiluminescence Blocking substrate (Roche, Sydney, Australia), that was diluted 1 in 10 with TBS-Tween, was used to incubate the membrane for 1 h. The membrane was rinsed with TBS-Tween and incubated with primary antibody diluted in 20 ml TBS-Tween for 1 h on a gentle rocker. Following the primary antibody incubation, the membrane was briefly rinsed twice with TBS-Tween, followed by one 15 min wash and two 5 min washes in

TBS-Tween. Secondary antibody, that was diluted 1 in 10 000 with 20 ml TBS-Tween, was placed on the membrane and incubated for 1 h on a gentle rocker. Detection was carried out via a chemiluminescence substrate (BM chemiluminescence kit). The membrane was placed onto a plastic sheet protector and layered with 6 ml of substrate solution [1% (v/v) starting solution B in substrate solution A]. Procedures were carried out according to the manufacturer's instructions. The membrane was covered with a plastic sheet and incubated for 4 min, ensuring no air bubbles were trapped underneath. Excess solution was removed and the membrane was wrapped in a plastic wrap for visualization using the ImageQuant RT ECL Imager (GE Healthcare, Sydney, Australia) according to the manufacturer's instructions.

2.7.3 Quantification of protein abundance

The Bio-Rad Quantity one® 1-D Anaylsis Software (Bio-Rad, Sydney, Australia) was used for the quantification of the protein abudance. The intensity of the immuno-detected protein was determined by measuring the pixel density per mm^2 of protein band minus the pixel density of the background. The background was measured in an area close to the band of interest. The pixel density was normalized to the level in Col-0 to a value of 1. Standard error and Student's *t* test was calculated using the Microsoft Excel software.

2.8 Complex I activity staining in Blue Native PAGE gels

The assay was performed according to (Zerbetto et al., 1997). The 1D BN

PAGE gel was washed with 2 M Tris-Cl (pH 7.4) twice for 10 min, then incubated in the complex I activity staining solution (Appendix I, 9.1) from 10 min to 1 h until the stained respiratory chain complexes were clearly visible. The reaction was stopped by transferring the gel into fixing solution (Appendix I, 9.2).

2.9 Protein electro elution from Blue Native PAGE gels

This experiment was carried out by Owen Duncan, a colleague also in the Whelan laboratory. The complex of interest was excised from Blue Native PAGE gels and proteins were extracted by electroelution. Gel slices were minced by passing back and forth between two syringes and were added to the H shaped eluter vessel of the ECU-040 Electro-Eluter (CBS scientific, California, USA). Proteins were eluted according to the technique detailed previously by (Hunkapiller et al., 1983).

2.10 Protein expression and purification

2.10.1 Gateway® cloning

In order to clone the cDNA of interest for recombinant bacterial expression, the Gateway® cloning (Invitrogen, Sydney, Australia) approach was used. The cDNA region of interest was amplified with primers that were flanked with AttB1 and AttB2 sites. Genes of interest were cloned into the Gateway pDEST17 vector (Invitrogen, Sydney, Australia) containing a 6 x histidine tag at the N terminus. Clones were confirmed by restriction enzyme digestion and DNA

sequencing (section 2.12).

2.10.2 Large scale protein expression

The Gateway clone was transformed into *E.coli* BL21 (DE3) cells. A single colony of cells was inoculated in 50 ml LB media and incubated at 37 ºC for overnight at 250 rpm. The following morning, the 50 ml cells were transferred to 500 ml LB and grown until the optical density reached approximately 0.6 at 600 nm. Protein expression was induced with the addition of Isopropyl β-D-1-thiogalactopyranoside (IPTG) to a final concentration of 10 mM. The culture was further incubated at the same condition for 3 h. The culture was poured into 250 ml Nalgene centrifuge tubes (Selby-Biolab, Sydney, Australia) and centrifuged at 8 000 x g at 4 ^{o}C for 10 min using Beckman coulter Avanti J-301 centrifuge and JLA 10.5 rotor (Beckman, Sydney, Australia). The pellet was resuspended in 10 ml of lysis buffer (Appendix I, 10.1) and sonicated 3 times for 10 s at a setting of 4 using the Vibra Cell (Sonics, Newtown, USA). The lysate was stored at – 80 ^{o}C.

2.10.3 Protein purification

The sonicated lysate was cleared by centrifugation at 16 000 x g for 20 min at 4 ^{o}C. The supernatant was filtered through a 0.45 µm filter and the clarified lysate was transferred to a 50 ml tube and loaded into the Profinia Protein Purification System (Bio-Rad, Sydney, Australia). The Denaturing IMAC program was chosen to purify the protein. The buffers were made up according

to the manufacturer's instructions (Appendix I, 10.2-10.7)

2.10.4 Protein electro elution from SDS-PAGE gels

The protein sample was separated by SDS-PAGE, stained in colloidal Coomassie (Appendix I, 11) for 1 h and destained with SDW. The band of interest was cut out from the gel and the protein was purified from the gel slices using the Model 422 Electro-Eluter (Bio-Rad, Sydney, Australia).

2.10.5 Acetone/TCA protein precipitation

Protein was mixed with 10 volumes of cold 10% (v/v) TCA in acetone, vortexed and incubated at – 20 ^{o}C for at least 3 h. The sample was centrifuged at 15 000 x g for 10 min and the supernatant was removed to a clean tube. The same volume of cold acetone was added, vortexed and the sample was further incubated at – 20 ^{o}C for 10 min. Following centrifugation at 15 000 x g for 5 min, the protein pellet was air dried and stored at – 80 ^{o}C until required.

2.11 Antibody production

Purified recombinant protein was sent to IMVS (Adelaide, Australia) for injection into rabbits. Four aliquots of 1 mg protein were sent for four injections. The antigen was injected every three weeks with Freund's Adjuvant. A test sample was bled out and tested after the third injection. The final bleed was achieved following the fourth injection.

2.12 DNA sequencing

The DNA samples were sent to Macrogen (Seoul, Korea) for sequencing. The samples were prepared at 10 ng/100 bases with at least 10 pmol of primer in SDW.

2.13 Mass spectrometry analysis

Mass spectrometry analysis was carried out by Owen Duncan, a colleague in the Whelan laboratory, using the ESI MS/MS system. The protein samples were cut from the gels and destained twice with destaining buffer (Appendix I, 12.1) for 45 min. Samples were then dehydrated on a block heater for 30 min at 50 ^{o}C, rehydrated with 15 µl of digestion solution (Appendix I, 12.2) and incubated overnight at 37 ^{o}C. Peptides were extracted by treating with 15 µl of acetonitrile, shaking vigorously for 15 min. The liquid was removed and 15 µl of extraction buffer (Appendix I, 12.3) was added to the gel plugs shaking for another 15 min. After the extraction step was repeated twice, the washes were pooled and dried. Samples were resuspended with resuspension buffer (Appendix I, 12.4) and were loaded onto the mass spectrometer.

Chapter 3
Isolation of Tim17/Tim23 knock-out lines

Chapter 3 Isolation of Tim17/Tim23 knock-out lines

3.1 Introduction

In Arabidopsis, 3 paralogues were identified to yeast *Tim17* and yeast *Tim23*. The *Tim17* paralogues are named as *Tim17-1*, *Tim17-2* and *Tim17-3* (At1g20350, At2g37410 and At5g11690). The *Tim23* paralogues are named as *Tim23-1*, *Tim23-2* and *Tim23-3* (At1g17530, At1g72750 and At3g04800) (Murcha et al., 2003). All the genes were defined as mitochondrial proteins through a combination of *in vitro* mitochondrial uptake assays and green fluorescent protein (GFP) tagging analysis (Murcha et al., 2007). Sequence alignments showed that three putative isoforms to yeast Tim23 protein possessed 35% similarity to yeast (Murcha et al., 2003). They are quite similar to each other, with Tim23-2 displaying 83% protein sequence identity to Tim23-1 and 50% protein sequence identity to Tim23-3 (Murcha et al., 2007).

The expression profile of all isoforms has been previously investigated throughout development (Murcha et al., 2007). It revealed that *Tim17-1* and *Tim17-2* were expressed in a similar pattern as *Tim23-1* and *Tim23-2*, increasing steadily throughout development from 6 to 24 days, with the highest levels at the stage of tissue senescence (Murcha et al., 2007). *Tim17-3* and *Tim23-3* were expressed in a different pattern, which peaked early in development and declined after 6 days (Murcha et al., 2007). Of all these genes, *Tim17-2*, *Tim23-1* and *Tim23-2* were the highest expressed genes and the resultant proteins from these genes were shown to constitute the majority of the

TIM17:23 translocase (Murcha et al., 2007).

The aims of this chapter were to:

1) Isolate two T-DNA insertion homozygous knock-out lines for each *Tim17* and *Tim23* gene.
2) Analyze the growth phenotype of the T-DNA insertion knock-out plants, compared to wild type plants.
3) Express and purify recombinant proteins for the production of antibodies specific for each isoform and confirm the T-DNA insertion knock-out plants by immuno-detection.

3.2 Results

3.2.1 Establishing and verifying T-DNA insertion lines

In order to characterize the role of the three isoforms encoding Tim23 or Tim17 in Arabidopsis, attempts to over-express tagged or un-tagged Tim17 (At1g20350 Tim17-1; At2g37410 Tim17-2; At5g11690 Tim17-3) and Tim23 (At1g17530 Tim23-1; At1g72750 Tim23-2; At3g04800 Tim23-3) proteins in Arabidopsis were carried out (Murcha, unpublished results). However, no over-expressed protein could be detected in the transgenic plants. Therefore, to characterize the role of the three isoforms, two T-DNA insertion lines for each of the genes were obtained.

For each line, at least 30 plants were screened to identify homozygotes. Two PCR reactions are required for the correct genotyping of a T-DNA insertion plant (Stepanova and Alonso, 2006). The first contains gene specific primers

termed LP and RP to amplify gene specific sequence, and the second uses the gene specific RP primer and the T-DNA insertion sequence LB primer to confirm T-DNA insertion (the primer sequences are attached in Appendix II). Only when there is a correctly sized PCR product in the second PCR reaction, the T-DNA insertion in the proposed location is confirmed and the homozygous plant is identified. A T-DNA insertion prevents the amplification of a PCR product using gene specific LP and RP primers due to its large size. A Columbia wild type (Col-0) Arabidopsis plant was used in the screening as a control for each set of primers.

3.2.1.1 Tim17

Two SALK T-DNA insertion knock-out lines were selected and screened for *Tim17-1* (At1g20350), SALK_091528 with an insertion in the 5'UTR region and SALK_092885 with an insertion in the middle of the gene. For SALK_091528, homozygous (HM) plants were confirmed with a PCR product of the correct size (530 bp) using primer set 2. A PCR product of 1108 bp was confirmed using primer set 1 in the wild type (Col-0) control reaction. For SALK_092885, homozygous (HM) plants were confirmed with a PCR product of 683 bp using primer set 4. A PCR product of 1042 bp was confirmed using primer set 3 in the wild type (Col-0) control reaction (Figure 3.1.1). Thus it was concluded that the insertion inactivation of Tim17-1 was not lethal as homozygous plants could be obtained.

For *Tim17-2* (At2g37410), GABI_561E03 was the only line available with a T-DNA insertion within the coding region. A PCR product of 1030 bp with

primer set 1 and a PCR product of 785 bp with primer set 2 were obtained for all plants screened (Figure 3.1.2), indicating they were all heterozygous (HT) plants. Further genotyping the offspring of self-pollinated plants resulted only in heterozygous plants. It was concluded from this that Tim17-2 was essential for viability.

For *Tim17-3* (At5g11690), two homozygous SALK T-DNA insertion lines were identified, SALK_048425 and SALK_125567, both with a T-DNA insertion located at the 3' UTR region of the gene. Homozygous plants were confirmed with a PCR product of 750 bp with the set 2 and set 4 primers. In the Col-0 reaction, a PCR product of 1100 bp was obtained with the set 1 and 3 primers (Figure 3.1.3). As the insertions were located in the 3' UTR, it is not possible to determine if *Tim17-3* is an essential gene.

3.2.1.2 Tim23

Two T-DNA insertion lines were selected and confirmed for *Tim23-1* (At1g17530). Both lines contain a T-DNA insertion in the 3' UTR region. For SALK_030470, the homozygous plant was confirmed with a PCR product of 650 bp using the set 2 primer and a PCR product of 1027 bp using set 1 primer was only evident in the wild type. For SALK_107963, the homozygous plant was confirmed with a PCR product of 600 bp using the set 4 primer and a PCR product of 1019 bp using primer set 3 was only observed in the wild type (Figure 3.1.4). Again as the insertions were located in the 3' UTR it is not possible to conclude if the function of Tim23-1 is essential.

For *Tim23-2* (At1g72750), two homozygous T-DNA insertion lines were

confirmed. The homozygous GABI_689C11 plant with an insertion located downstream of the translational start site was confirmed with a PCR product of 700 bp using set 2 primer and the PCR product of 1012 bp was only observed in the wild type. For SALK_143656 with an insertion located upstream of the translational start site, the homozygote was confirmed using set 4 primer exhibiting a PCR product of 704 bp and the product of 1239 bp was obtained in the wild type (Figure 3.1.5). From this, it appears that Tim23-2 function is not essential for viability.

Two homozygous T-DNA insertion lines (SALK_129386 and SAIL_1151_B01) were obtained for *Tim23-3* (At3g04800), both with T-DNA insertions located at the end of the coding region. For SALK_129386, the homozygote was confirmed with a PCR product of 580 bp using set 2 primer. The Col-0 control reaction resulted in a PCR product of 1001 bp with set 1 primer. For SAIL_1151_B01, the homozygous plant was identified with a PCR product of 650 bp using set 4 primer and a PCR product of 1020 bp was obtained in the Col-0 plant (Figure 3.1.6). While these results suggest that the function of Tim23-2 is not essential, the location of the insertions near the C-terminal of the protein may mean that function is not fully abolished.

3.2.2 Phenotype analysis

All identified homozygous lines were further investigated for any growth phenotypic difference compared to the wild type. Plants were planted in individual pots and grown in the soil in a 16/8 h day/night cycle at 22 ^{o}C. The

phenotype was monitored twice weekly for any phenotypic differences from germination to 6 weeks old, and pictures were taken at 2 weeks, 4 weeks and 6 weeks old (Figure 3.2). Most of the plants didn't display any obvious phenotypic abnormality, with the exception of SALK_143656, the T-DNA insertion line of *Tim23-2*. The SALK_143656 line showed a 2 week developmental delay and the plants showed wrinkly rosette leaves (Figure 3.2). Mapping and sequencing of the T-DNA insertion in both lines revealed that while one line (GABI_689C11) represented an insertion in the gene at position 43 bp 3' of the translational start site (Figure 3.3A), the insertion for the other line (SALK_143656) was in fact located at 135 bp 5' of the translational start site (Figure 3.3B). To determine the effect of both insertions on the abundance of Tim23-2 protein, specific antibodies against each Tim23 proteins were raised.

3.2.3 Production and testing of Tim23 protein

3.2.3.1 Expression of antigen

All three Tim23 proteins have high sequence identity, especially Tim23-1 and Tim23-2, which display 83% protein identity (Figure 3.4A), and thus a specific antibody seems unlikely for Tim23-1 and Tim23-2. Tim23-2 and Tim23-3 exhibit 50% identity and thus regions that share the least protein sequence similarity were chosen. For each protein, two regions of interest were amplified by PCR from a confirmed cDNA clone using specifically designed primers (Figure 3.4B and C). The sequences of these primers are listed in Appendix III.

For Tim23-2 antibody, the amino acid regions 2-31 and 104-143 (Figure 3.4B, indicated in bold) were cloned by two sets of primers ATTB1/ B1_Reverse and B2_Forward/ATTB2 (Figure 3.4B). The B1_Reverse and B2_Forward primers are amplified with the restriction site of EcoR1 to ligate two PCR products together prior to cloning into a protein expression vector. For Tim23-3 antibody, the amino acid regions 6-32 and 65-132 (Figure 3.4C, indicated in bold) were amplified by two sets of primers ATTB1'/ B1_Reverse' and B2_Forward'/ATTB2' (Figure 3.4C) and cloned as above.

The recombination vectors were transformed into competent BL21 (DE3) cells and expression was induced to purify sufficient amounts of protein. Purification of the protein was carried out with the Profinia Protein Purification System (Bio-Rad, Sydney, Australia). Fractions obtained from a 2 L batch of cell culture were resolved by SDS-PAGE. Lane 1 and 3 are the fractions before purification, Lane 2 and 4 are fractions purified from the Profinia Protein Purification System (Figure 3.5A). The molecular weights of the purified proteins are 13 kDa and 16 kDa, which are the predicted size of the Tim23-2 recombinant protein and Tim23-3 recombinant protein (Figure 3.5A). The purified fractions were electro-eluted from SDS-PAGE gels to ensure no contaminating proteins in the antigen samples, which were then inoculated into rabbits for polyclonal antibody production.

3.2.3.2 Testing the specificity of the antibody

To test the specificity of antibodies produced, all the PRAT gene family members were expressed in a cell-free system, resolved by SDS-PAGE and

immuno-detected with Tim23-2 and Tim23-3 antiserum at a 1:2000 dilution.

For the Tim23-2 antibody, there was no cross reaction against the recombinantly expressed proteins of Tim17-1 (Figure 3.5B, Lane 1), Tim17-2 (Figure 3.5B, Lane 2), Tim17-3 (Figure 3.5B, Lane 3), Tim23-3 (Figure 3.5B, Lane 6), At3g25120 (Figure 3.5B, Lane 7), Tim22 (Figure 3.5B, Lane 8), At3g49560 (Figure 3.5B, Lane 9) and At5g24650 (Figure 3.5B, Lane 10). However, a band with an apparent molecular weight of 20 kDa in both Tim23-1 (Figure 3.5B, Lane 4) and Tim23-2 (Figure 3.5B, Lane 5) was detected, which is in agreement with the known size of Tim23-1 and Tim23-2 (Murcha et al., 2007). The Tim23-2 antibody cross- reacted with a band of an apparent molecular weight of 20 kDa against Col-0 mitochondria (Figure 3.5B, Lane 11). As expected, it was not possible to distinguish between Tim23-1 and Tim23-2 using the Tim23-2 antibody alone, due to the high sequence identity between the proteins. Thus, the Tim23-2 antibody did not cross-react with any other expressed PRAT proteins except for Tim23-1 and Tim23-2.

For the Tim23-3 antibody, no band was detected against recombinantly expressed Tim17-1 (Figure 3.5B, Lane 1), Tim17-2 (Figure 3.5B, Lane 2), Tim17-3 (Figure 3.5B, Lane 3), At3g25120 (Figure 3.5B, Lane 7), Tim22 (Figure 3.5B, Lane 8), At3g49560 (Figure 3.5B, Lane 9) and At5g24650 (Figure 3.5B, Lane 10). A band with the apparent molecular weight of 20 kDa was detected against expressed Tim23-1 (Figure 3.5B, Lane 4) and Tim23-3 (Figure 3.5B, Lane 6). Thus, the Tim23-3 antibody did not cross-react against any other recombinantly expressed PRAT proteins other then Tim23-1 and Tim23-3,

although weak cross reactivity was observed against Tim23-2 (Figure 3.5B, Lane 5). The Tim23-3 did not cross-react with any endogenous protein from the Col-0 mitochondria tested (Figure 3.5B, Lane 11), which is consistent with the fact that transcript abundance for this isoform was very low compared to *Tim23-1* and *Tim23-2*.

3.2.4 Confirming the protein knock-out mutants

The Tim23 T-DNA insertion lines were further investigated by immuno-detection using antibodies against Tim23-2 and Tim23-3. The seeds of the confirmed T-DNA insertion homozygote lines were bulked and mitochondria were isolated from water culture plants. The samples were resolved by SDS-PAGE and probed with each specific antibody.

Mitochondria isolated from the SALK_143656 line exhibited an increase in the abundance of Tim23-2 when probed with the Tim23-2 antibody, the protein band with the apparent moleluar weight of 20 kDa (Figure 3.6A, Lane 2). In contrast, immuno-detection against mitochondria isolated from the T-DNA insertion line GABI_689C11, where the T-DNA is located in position 43 bp of the gene, did not cross-react with any protein with the molecular weight of 20 kDa (Figure 3.6A, Lane 3). However, due to the long time exposure, a smaller protein of approximately 18 kDa was detected (see attached manuscript, Figure 1C). It was probably a truncated version of Tim23-2 protein.

As the Tim23-2 antibody is specific against both the recombinant Tim23-1 and Tim23-2 (Figure 3.5B, Lane 4 and 5), it was not possible to distinguish

between endogenous Tim23-1 and Tim23-2 in isolated mitochondria using the Tim23-2 antibody alone. Immuno-detection with the Tim23-3 antibody, which was shown to detect both recombinant Tim23-1 and Tim23-3 proteins but not Tim23-2 (Figure 3.5B, Lane 4, 5 and 6), did not detect any signal in mitochondria isolated from Col-0 plants (Figure 3.6A, Lane 4), SALK_143656 (Figure 3.6A, Lane 5) or GABI_689C11 plants (Figure 3.6A, Lane 6). This suggests that both Tim23-1 and Tim23-3 are not present in mitochondria or not present at amounts detectable under the conditions tested in this study. So the 20 kDa band detected by Tim23-2 antibody (Figure 3.6A, Lane 1 and 2) presents Tim23-2 protein alone. Thus, it can be concluded that SALK_143656 is a Tim23-2 over-expressor line and GABI_689C11 is a Tim23-2 knock-out line, which will be referred as *tim23* OE and *tim23* KO respectively.

In order to further investigate the induced level of Tim23-2 protein in SALK_143656 line, a series dilution (10 µg, 20 µg and 40 µg) of mitochondria from Col-0 (wild type) and SALK_143656 lines were immuno-detected using the Tim23-2 antibody. The amount of Tim23-2 protein was quantitated and normalized against the amount of Tim23-2 protein in 40 µg wild type mitochondria from triple biological replicate experiments. The results showed that with 10 µg mitochondria, the average relative abundance ratio of Tim23-2 protein was 0.08 in Col-0 and 0.18 in SALK_143656, which was 2.25 fold higher in SALK_143656 than Col-0 (Figure 3.6B). With 20µg mitochondria, the average relative abundance ratio of Tim23-2 protein was 0.34 in Col-0 and 0.64 in SALK_143656, which was 1.88 fold higher in SALK_143656 than Col-0

(Figure 3.6B). With 40μg mitochondria, the average relative abundance ratio of Tim23-2 protein was 1.00 in Col-0 and 1.70 in SALK_143656, which was 1.70 fold higher in SALK_143656 than Col-0 (Figure 3.6B). These data indicated that the level of Tim23-2 protein in SALK_143656 line was consistently about 2 fold higher than Col-0. The Student's *t* test analysis indicated that SALK_143656 line had a significantly higher amount of Tim23-2 protein than wild type, with a *p* value < 0.05 (Figure 3.6B). As a loading control, the series dilution (10 μg, 20 μg and 40 μg) of mitochondria from Col-0 and SALK_143656 lines were also immuno-detected using the antibody against Porin, an outer membrane β-barrel protein. The result showed that the amount of Porin did not change significantly between SALK_143656 line and Col-0 (Figure 3.6C). It confirmed that SALK_143656 was a Tim23-2 over-expresseor line.

As Tim23-1 and Tim23-3 could not be detected in isolated plant mitochondria (Figure 3.6A, Lane 4-6), it was unclear if the T-DNA insertion lines could be verified at a protein level, i.e. it is possible that T-DNA insertions do not result in loss of protein. In order to investigate the function of *Tim23-1* and *Tim23-3* genes, single homozygous plants were crossed with the confirmed Tim23-2 knock-out line to make double knock-out lines. The *Tim23-2* KO line (GABI_689C11) was crossed with *Tim23-1* lines (SALK_030470, SALK_107963) and *Tim23-3* lines (SALK_129386, SAIL_1151_B01) respectively. After genotyping a sufficient number of progeny plants, no double homozygous knock-out lines could be obtained. Several double heterozygous plants were confirmed by genotyping and their seeds were further investigated.

For SALK_107963/ GABI_689C11 double heterozygous plant and SALK_129386/ GABI_689C11 double heterozygous plants, all siliques showed aborted ovules/embryos at a ratio of 1/4 (Figure 3.7). This suggests that the Tim23-1 protein and Tim23-3 protein were disrupted in their respective SALK_107963 and SALK_129386 lines, as a double knock-out plant of *tim23-2* with *tim23-1* or *tim23-3* is lethal.

Screening T-DNA insertion lines of *Tim17-2*, failed to identify homozygous mutant plants, instead only heterozygous plants could be identified. The siliques from the GABI_561E03 heterozygous plant were investigated and small, undeveloped seeds were observed in 1/4 of the seed pod (Figure 3.7). Analysis of the seed from self-fertilized heterozygous plants consistently resulted in 1/4 of the seed appearing early embryonically lethal. This is consistent with a lethal phenotype due to the absence of a functional gene, indicating that this protein is essential in plants as it is in yeast (Maarse et al., 1994).

3.3 Discussion

3.3.1 Protein expression

The major obstacle in the production of antibodies against Tim23 proteins is the high protein sequence similarity of the three Arabidopsis members. In order to obtain a specific antibody, a region that does not share any sequence similarity must be chosen. However, any unique sequence region was less than 50 amino acids that would have resulted in a 5 kDa recombinant protein, and

thus, not optimal for antigen protein expression. The strategy we took to solve this problem was to ligate two unique regions together producing a recombinant protein at least 10 kDa. Although specificity was obtained for Tim23-2 and Tim23-3, some cross-reactivity exists with Tim23-1 for both antibodies.

No signal was detected in mitochondria isolated from the wild type, or any of the T-DNA lines tested using the Tim23-3 antibody. This is most likely due to very little or no expression of the protein. Quantitative real-time PCR analysis shows that *Tim23-3* is the lowest expressed gene of the *Tim23* family (Lister et al., 2004; Murcha et al., 2003). However, as the double knock-out of *tim23-2* and *tim23-3* was lethal, compared to the single *tim23-2* knock-out, it indicates that *Tim23-3* is expressed either at a level too low to be detected with antibodies, or that expression is cell or developmental specific.

3.3.2 Viability of T-DNA insertion lines

In order to determine if Tim17 and Tim23 proteins were essential for plant viability or if any phenotypic changes could be observed upon disruption of the proteins, a genetic approach was undertaken to genotype T-DNA insertion homozygous lines. For the majority of the T-DNA insertion lines, a line with an insertion at the start or within the coding region was selected. Surprisingly, most of the plants did not display any obvious abnormal phenotype. This may be explained by a number of different reasons, such as the T-DNA insertion resulted in the expression of a truncated protein which may still be functional, or the T-DNA insertion resulted in the loss of a functional protein which may be

complemented due to the overlapping functions of the isoforms.

For GABI_561E03, which has a T-DNA insertion in the centre of the coding region of *Tim17-2*, no homozygous plants could be identified. It has been backcrossed with both wild type plants and heterozygous plants and the heterozygous progeny is consistently embryonically lethal. This confirms that the lethality of this line is not the result of an additional insertion within another region of the genome, suggesting that Tim17-2 is an essential protein required for the plant viability. It has been previously demonstrated that the C-terminus of Tim17-2 plays a role in protein import, either by binding precursor proteins on the outer membrane or by interacting with components that bind them and assisting in the transfer to the TIM17:23 complex on the inner membrane (Murcha et al., 2005a). In addition, *Tim17-2* is the most highly expressed gene from the three Tim17 genes (Murcha et al., 2003), suggesting that it plays an major role in the import pathway and thus a embryonically lethal phenotype was expected within a knock-out line, as it is also an essential gene in yeast (Maarse et al., 1994).

The normal growth phenotype of *Tim17-1* and *Tim17-3* knock-out lines suggests that these genes may not have a functional role in mitochondria at least under the standard growing conditions. The non-essential *Tim17* genes may have a specialized function or may be required in specialized conditions, such as during plant stress. It has been proposed that *Tim17* may have a role to prevent mitochondrial DNA loss in yeast and humans (Iacovino et al., 2009), which could be the unique function of *Tim17-1* and *Tim17-3* in plants.

One knock-out line was identified for each *Tim23* genes SALK_107963 (*Tim23-1*), GABI_689C11 (*Tim23-2*) and SALK_129386 (*Tim23-3*). However, no severe phenotypic abnormalities were observed in any of the insertion mutants. The three Tim23 proteins have high percentage similarity to each other, with Tim23-1 having 92% and 70% protein sequence similarity to Tim23-2 and Tim23-3 respectively (Murcha et al., 2007). Moreover, the expression pattern of the *Tim23* genes is quite similar during development and in different tissues (Murcha et al., 2003). It is possible that knocking out one gene could be completely compensated for by one another. The inability to get Tim23-2/Tim23-1 double knock-out plant and Tim23-2/Tim23-3 double knock-out plant demonstrates that Tim23-1 and Tim23-3 must play a role in compensating for the Tim23-2 protein, although they are not detectable in mitochondria using western blot analysis.

Although none of these knock-out mutants displays any phenotypic changes, one Tim23-2 line (SALK_143656) with an insertion upstream of coding region resulted in the over-expression of Tim23-2 and interestingly this line exhibited a significantly delayed growth phenotype. It suggests that the expression level of Tim23-2 is critical for the function of mitochondria. As Tim23 is a vital component in yeast, the over-expression of Tim23-2 may affect the protein translocases and thus effect mitochondrial function which in turn affects plant growth and development.

As *Tim17* and *Tim23* are essential genes in yeast, it is not unexpected that a similar situation was observed in Arabidopsis (Dekker et al., 1993;

Maarse et al., 1994). Notably, for Arabidopsis, there is additional complexity, in that for *Tim23,* some redundancy is observed; while for *Tim17*, *Tim17-2* is the only essential gene and neither *Tim17-1* nor *Tim17-3* can compensate for its loss at a functional level. In the case of *Tim23-2*, one T-DNA line (SALK_143656) displayed retarded growth compared to wild type (Col-0), whilst another T-DNA line (GABI_689C11) displayed a normal growth phenotype. Thus, both T-DNA lines for *Tim23-2* were further investigated.

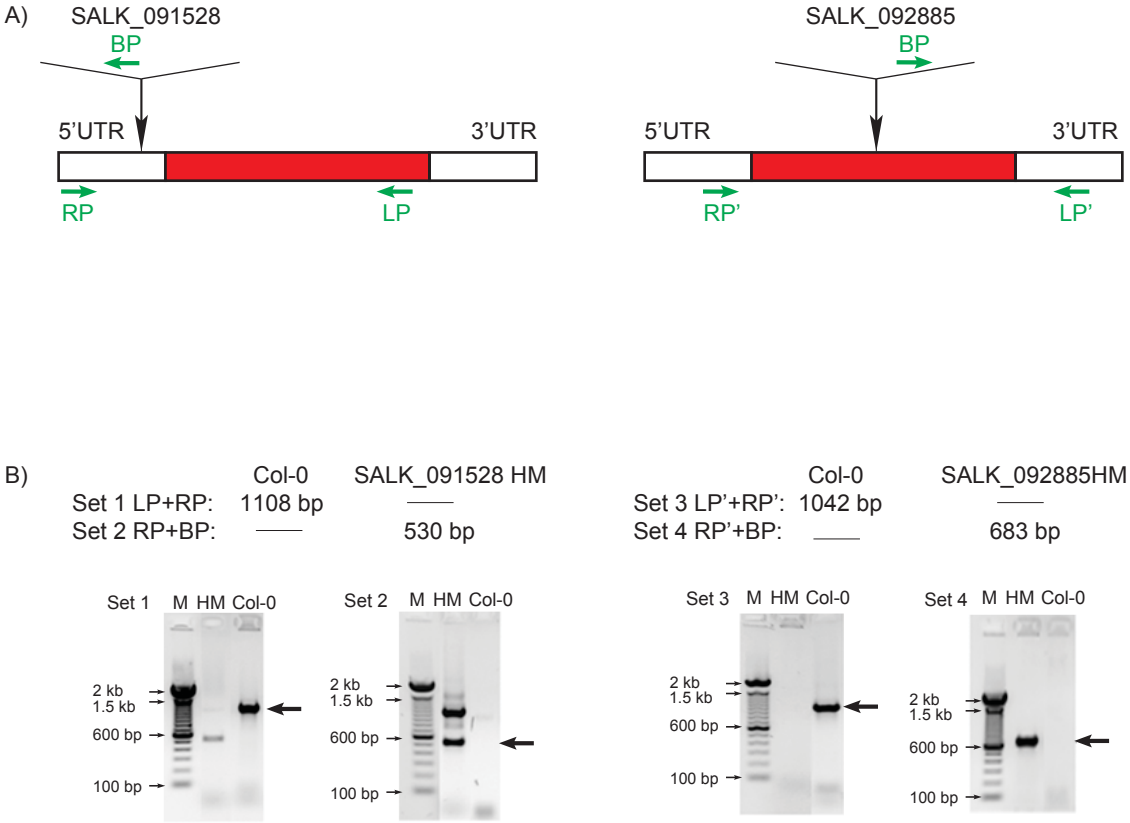

Figure 3.1.1. TIM17-1 T-DNA insertion line screening by PCR. Two T-DNA insertion lines were screened SALK_091528 and SALK_092885. A) The encoding region was indicated in red. The T-DNA insert location is indicated by the arrow. The primers for the two screening reactions were indicated in green. B) The PCR products from two screening reactions were indicated by the arrow. First PCR reaction (Set 1 and Set 3) uses LP/RP and LP'/RP' primers to amplify gene specific sequence. Second PCR reaction (Set 2 and Set 4) uses RP/BP and RP'/BP primers to confirm T-DNA insertion. Abbreviations, M: marker, HM: homozygous, Col-0: wild type, UTR: untranslated region, LP: gene specific left primer, RP: gene specific right primer, BP: T-DNA left border primer.

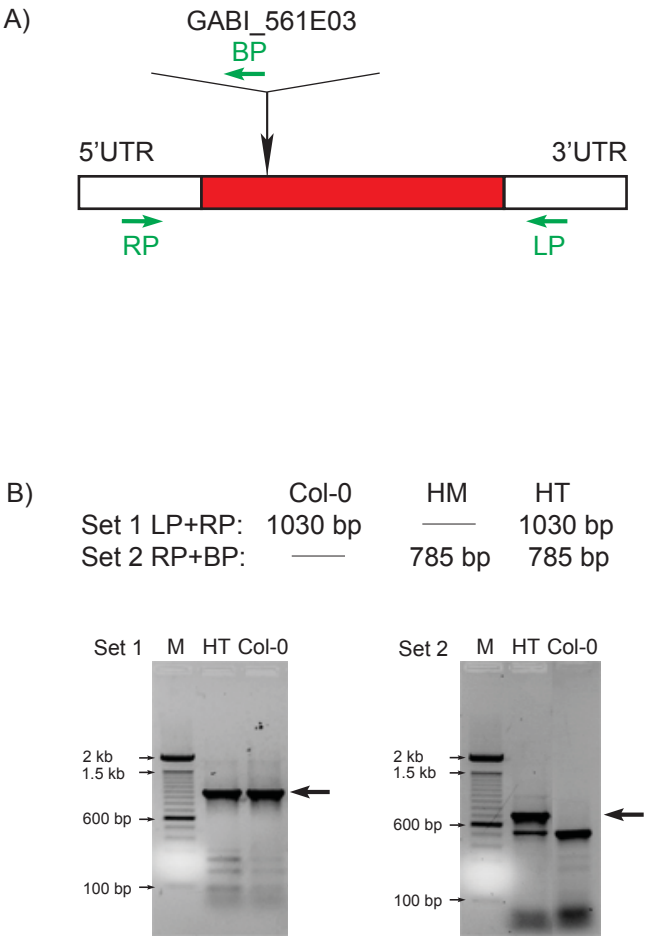

Figure 3.1.2. TIM17-2 T-DNA insertion line screening by PCR. One Tim17-2 T-DNA insertion lines was screened GABI_561E03. A) The encoding region was indicated in red. The T-DNA insert location is indicated by the arrow. The primers for the two screening reactions were indicated in green. B) The PCR products from two screening reactions were indicated by the arrow. First PCR reaction (Set 1) uses LP/RP primers to amplify gene specific sequence. Second PCR reaction (Set 2) uses RP/BP primers to confirm T-DNA insertion. Abbreviations, M: marker, HM: homozygous, HT: heterzygous, Col-0: wild type, UTR: untranslated region, LP: gene specific left primer, RP: gene specific right primer, BP: T-DNA left border primer.

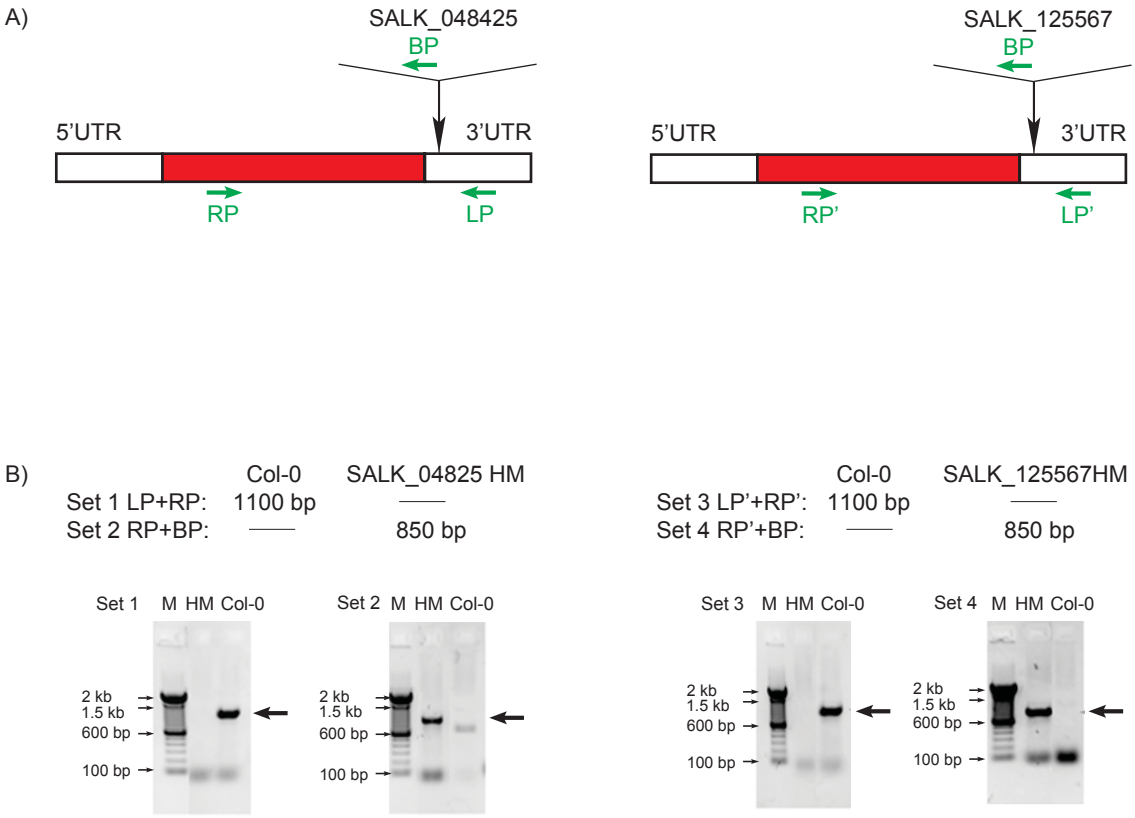

Figure 3.1.3. TIM17-3 T-DNA insertion line screening by PCR. Two T-DNA insertion lines were screened SALK_048425 and SALK_125567. A) The encoding region was indicated in red. The T-DNA insert location is indicated by the arrow. The primers for the two screening reactions were indicated in green. B) The PCR products from two screening reactions were indicated by the arrow. First PCR reaction (Set 1 and Set 3) uses LP/RP and LP'/RP' primers to amplify gene specific sequence. Second PCR reaction (Set 2 and Set 4) uses RP/BP and RP'/BP primers to confirm T-DNA insertion. Abbreviations, M: marker, HM: homozygous, Col-0: wild type, UTR: untranslated region, LP: gene specific left primer, RP: gene specific right primer, BP: T-DNA left border primer.

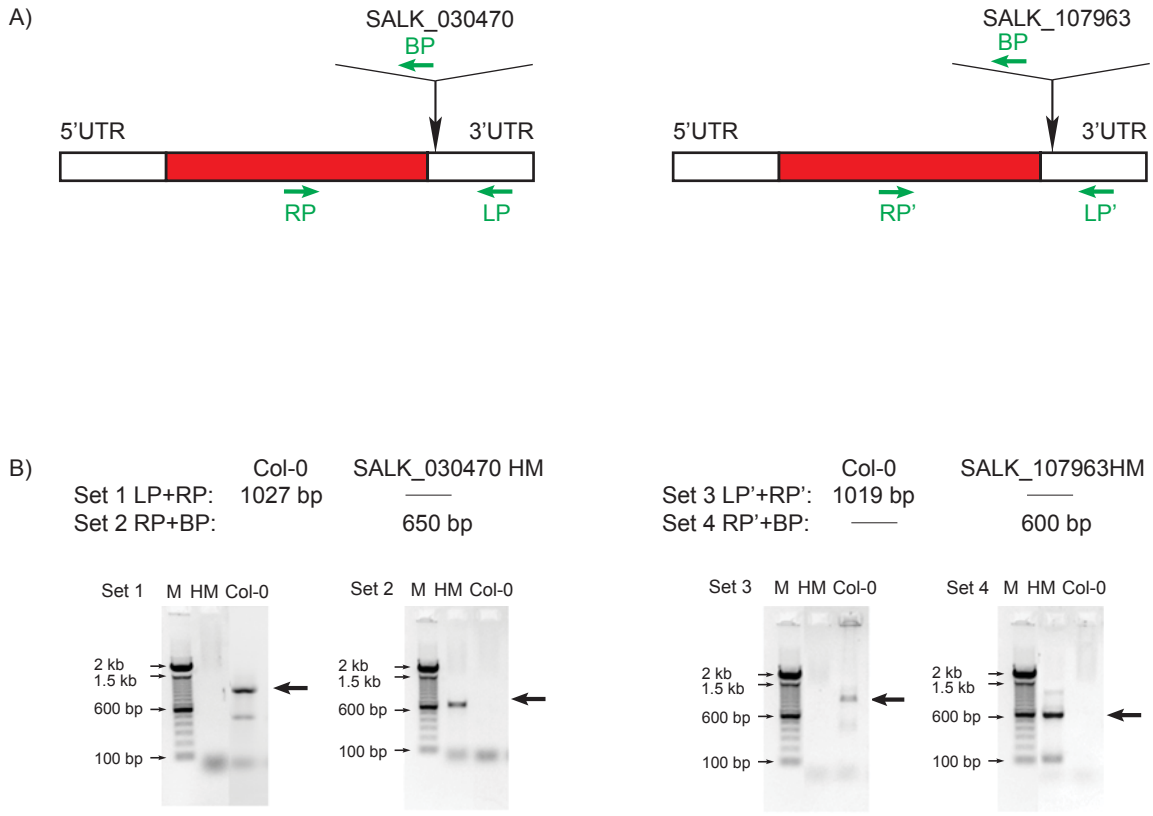

Figure 3.1.4. TIM23-1 T-DNA insertion line screening by PCR. Two T-DNA insertion lines were screened SALK_030470 and SALK_107963. A) The encoding region was indicated in red. The T-DNA insert location is indicated by the arrow. The primers for the two screening reactions were indicated in green. B) The PCR products from two screening reactions were indicated by the arrow. First PCR reaction (Set 1 and Set 3) uses LP/RP and LP'/RP' primers to amplify gene specific sequence. Second PCR reaction (Set 2 and Set 4) uses RP/BP and RP'/BP primers to confirm T-DNA insertion. Abbreviations, M: marker, HM: homozygous, Col-0: wild type, UTR: untranslated region, LP: gene specific left primer, RP: gene specific right primer, BP: T-DNA left border primer.

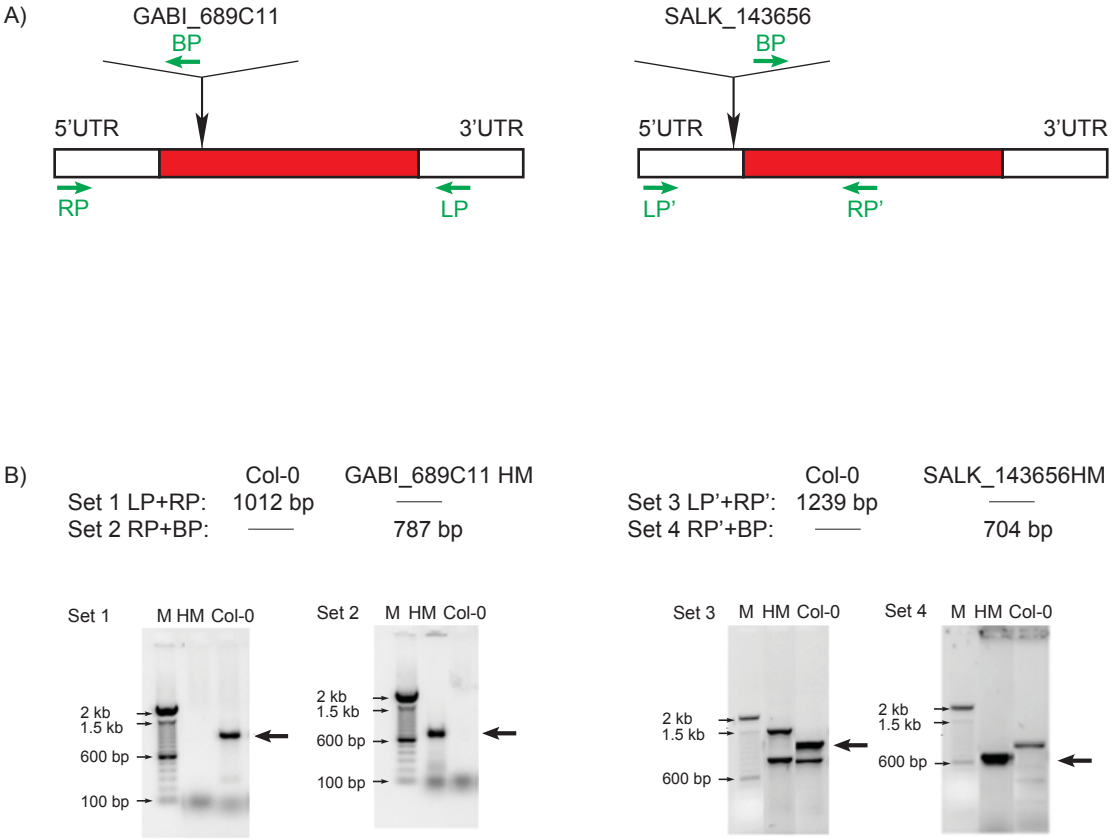

Figure 3.1.5. TIM23-2 T-DNA insertion line screening by PCR. Two T-DNA insertion lines were screened GABI_689C11 and SALK_143656. A) The encoding region was indicated in red. The T-DNA insert location is indicated by the arrow. The primers for the two screening reactions were indicated in green. B) The PCR products from two screening reactions were indicated by the arrow. First PCR reaction (Set 1 and Set 3) uses LP/RP and LP'/RP' primers to amplify gene specific sequence. Second PCR reaction (Set 2 and Set 4) uses RP/BP and RP'/BP primers to confirm T-DNA insertion. Abbreviations, M: marker, HM: homozygous, Col-0: wild type, UTR: untranslated region, LP: gene specific left primer, RP: gene specific right primer, BP: T-DNA left border primer.

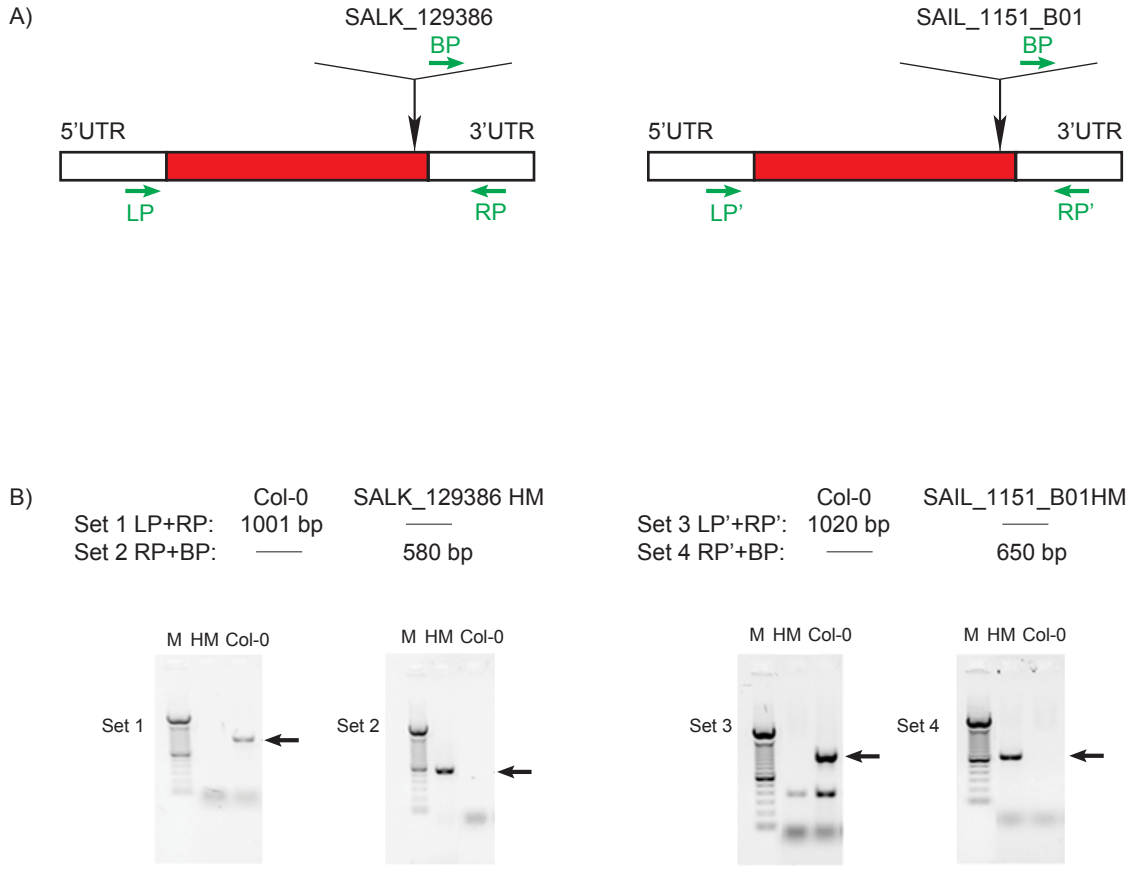

Figure 3.1.6. TIM23-3 T-DNA insertion line screening by PCR. Two T-DNA insertion lines were screened SALK_129386 and SAIL_1151_B01. A) The encoding region was indicated in red. The T-DNA insert location is indicated by the arrow. The primers for the two screening reactions were indicated in green. B) The PCR products from two screening reactions were indicated by the arrow. First PCR reaction (Set 1 and Set 3) uses LP/RP and LP'/RP' primers to amplify gene specific sequence. Second PCR reaction (Set 2 and Set 4) uses RP/BP and RP'/BP primers to confirm T-DNA insertion. Abbreviations, M: marker, HM: homozygous, Col-0: wild type, UTR: untranslated region, LP: gene specific left primer, RP: gene specific right primer, BP: T-DNA left border primer.

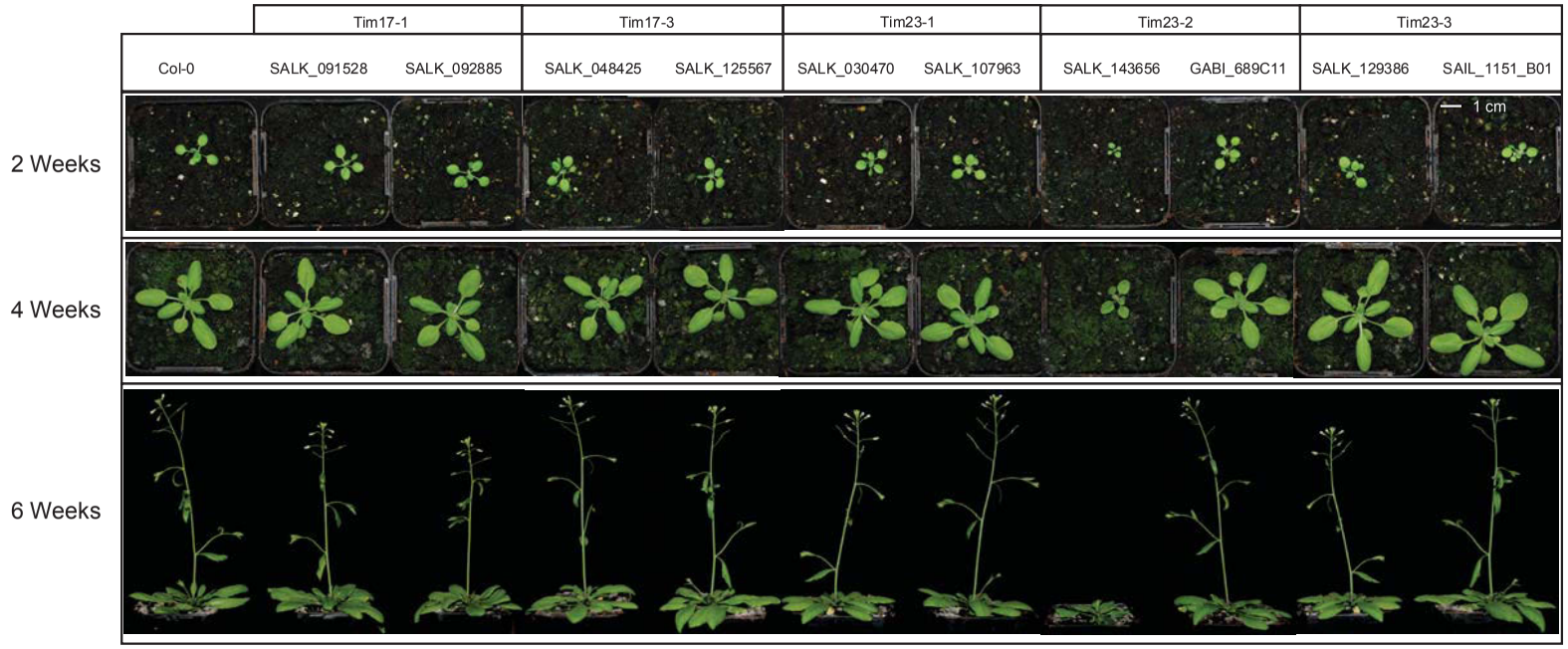

Figure 3.2. The growth phenotype of T-DNA inserted homozygote lines of Tim17 and Tim23 gene family. The T-DNA insertion homozygote plants and the wild type (Col-0) were grown in a 16 h photoperiod. 2 week, 4 week and 6 week growth profile did not show any difference between wild type and the T-DNA inserted homozygote lines, except SALK_143656 which displays a retarded growth phenotype.

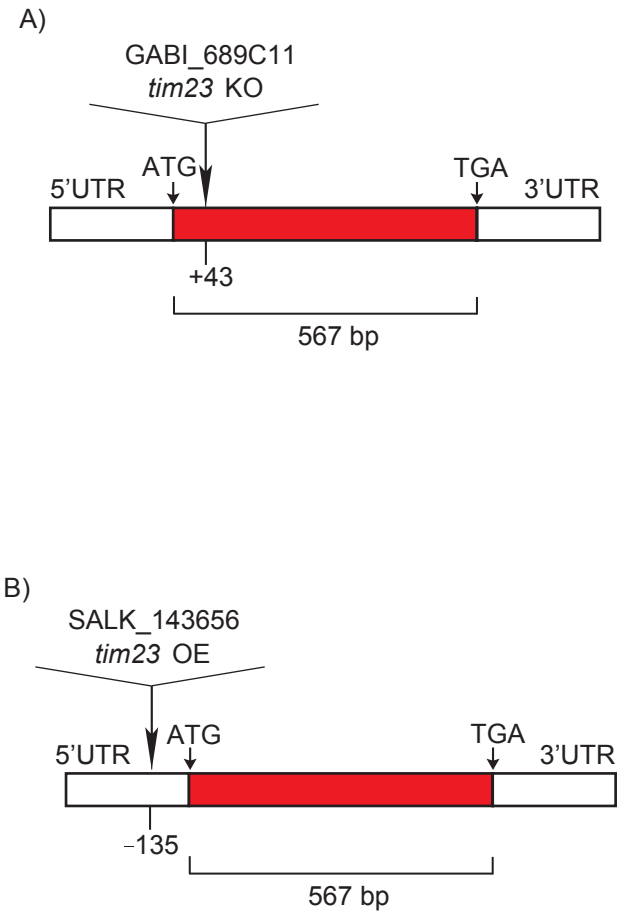

Figure 3.3. The T-DNA location in GABI_689C11 and SALK_143656 lines. The coding sequence of Tim23-2 gene is 567 bp. The translation start site and the end of the encoding region was indicated by the start codon (ATG) and the stop codon (TGA). A) For *tim23* KO line (GABI_689C11), the T-DNA is inserted at 43 bp 3' of the translational start site. B) For *tim23* OE line (SALK_143656), the T-DNA is located 135 bp 5' of the translational start site. Abbreviations, KO: knockout, OE: overexpressor, UTR: untranslated region, bp: base pair.

A)

```
TIM23-1,  MA--INRSSDHESDENTRLYHPYQNYQVPI-KSQYLYKLP  37
TIM23-2,  MA--ANNRSDHGSDENTRLYNPYQNYEVPINKSQYLYKLP  38
TIM23-3,  MADPMNHSTGHQQQQKYRQYNPYQQVNLPYRK---LYELP  37

TIM23-1,  TSPEFLFTEESLKQRRSWGENLTFYTGTGYLAGSVAGASA  77
TIM23-2,  TSPEFLFTEEALRQRRSWGENLTFYTGTAYLGGSVAGASV  78
TIM23-3,  TSPEFLFEEEATKKRLTWGENLTFFTGWGYCTGSVLGAFK  77

TIM23-1,  GIFSGIKSFENGDTTKLKINRILNSSGQAGRTWGNRVGIV 117
TIM23-2,  GVITGVKSFESGDTTKLKINRILNSSGQTGRTWGNRIGII 118
TIM23-3,  GTIAGMRAAERGESLKIRTNRILNSGGLVARRGGNCLGSV 117

TIM23-1,  GLIYAGIESGVVAVTDKDD-VWTSVVAGLGTGAVFRAARG 156
TIM23-2,  GLVYAGIESGIVAATDRDD-VWTSVVAGLGTGAVCRAARG 157
TIM23-3,  GLMFAAMESGVTYMRDGDDGSLTTVIAGLATGVLYRAASG 157

TIM23-1,  VRSAAVAGAFGGIAAGAVVAGKQVFKRYAHI          187
TIM23-2,  VRSAAVAGALGGLAAGAVVAGKQIVKRYVPI          188
TIM23-3,  PRSAVVAGAVGGVAALAAVAGRRIVKRFVPI          188
```

B) The gateway cloning for Tim23-2 antibody

ATTB1 → B1_Reverse ←

M**AANNRSDHG SDENTRLYNP YQNYEVPINK SQ**YLYKLPTS PEFLFTEEAL

RQRRSWGENL TFYTGTAYLG GSVAGASVGV ITGVKSFESG DTTKLKINRI

B2_Forward → ATTB2 ←

LN**SSGQTGRT WGNRIGIIGL VYAGIESGIV AATDRDDVWT SVV**AGLGTGA

VCRAARGVRS AAVAGALGGL AAGAVVAGKQ IVKRYVPI

C) The gateway cloning for Tim23-3 antibody

ATTB1' → B1_Reverse' ←

MADPM**NHSTG HQQQQKYRQY NPYQQVNLPY RK**LYELPTSP EFLFEEEATK

B2_Forward' →

KRLTWGENLT FFTG**WGYCTG SVLGAFKGTI AGMRAAERGE SLKIRTNRIL**

ATTB2' ←

NSGGLVARRG GNCLGSVGLM FAAMESGVTY MRDGDDGSLT TVIAGLATGV

LYRAASGPRS AVVAGAVGGV AALAAVAGRR IVKRFVPI

Figure 3.4. The protein sequences selected for Tim23 antibody production. A) The multi sequence alignment of Tim23-1, Tim23-2 and Tim23-3 protein shows that Tim23-2 protein is 83% identical with Tim23-1 and they both display about 50% identical with Tim23-3. B) and C) The protein regions cloned for antibody production are indicated in bold.

A) Protein expression and purification

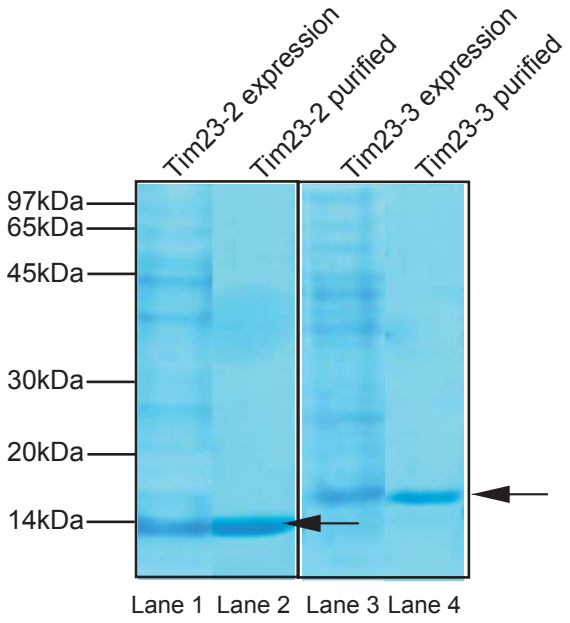

B) Determining antibody specificity

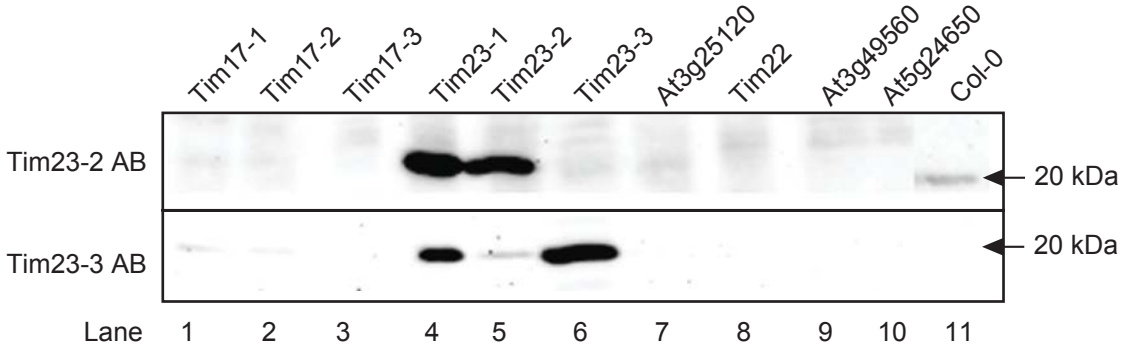

Figure 3.5. Production of Tim23 antibody. A) The recombinant proteins were over-expressed (Lane 1 and 3) and purified (Lane 2 and 4). The antigen for Tim23-2 antibody is 13kDa and the one for Tim23-3 antibody is 16 kDa as the arrow indicated. B) The specificiy of antisera raised against Tim23-2 and Tim23-3 was tested against full length recombinant proteins of Tim17-1, Tim17-2, Tim17-3, Tim23-1, Tim23-2, Tim23-3, At3g25120, Tim22-1, At3g49560, At5g24650 and mitochondria from wild-type plants (Col-0). Abbreviations, AB: antibody.

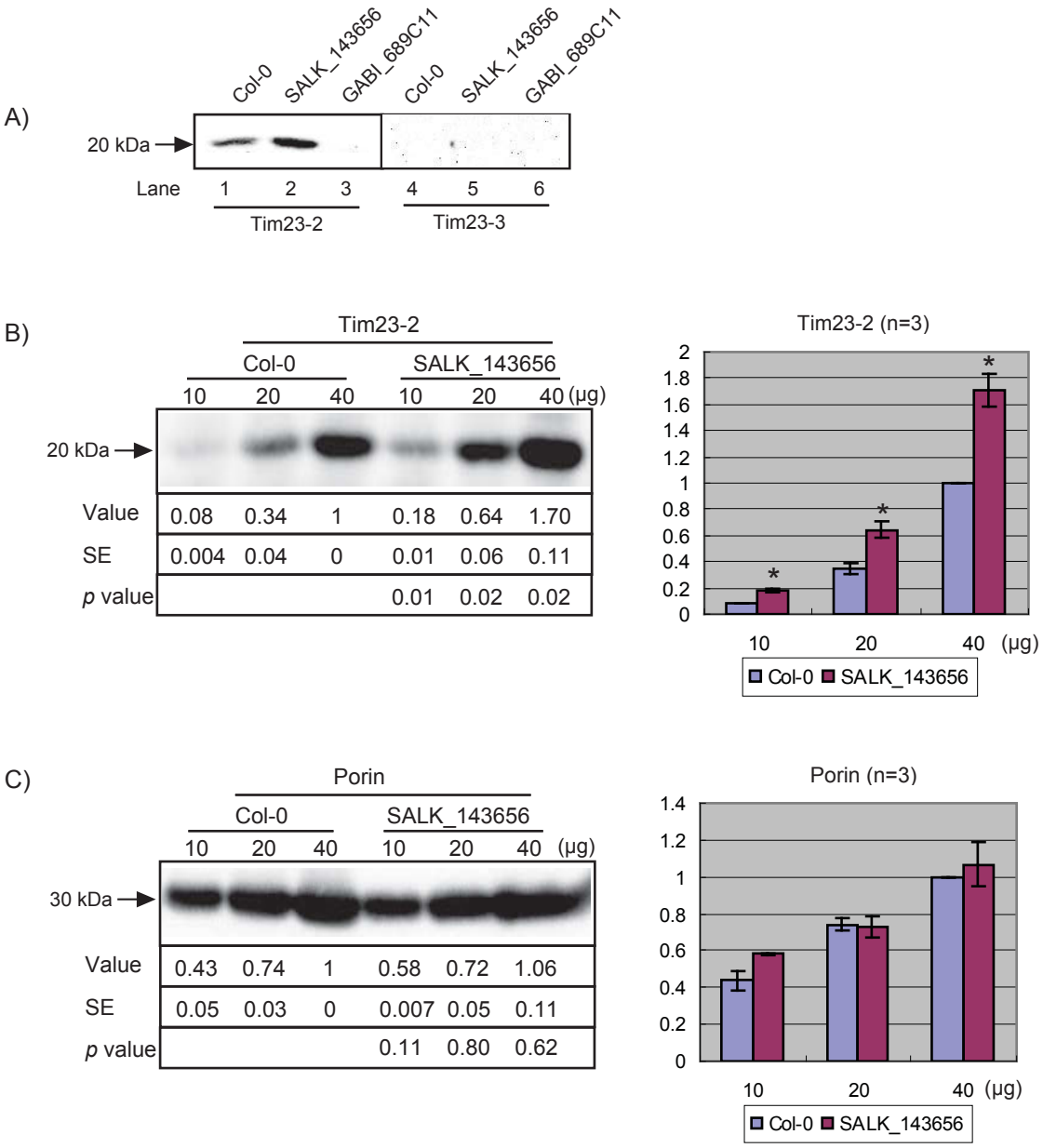

Figure 3.6. Immuno-detection of Tim23-2 mutant lines. A) The mitochondria isolated from Col-0, SALK_143656 and GABI_689C11 were immunodetected by Tim23-2 and Tim23-3 antibodies. B) A series dilution (10 µg, 20 µg and 40 µg) of mitochondria from Col-0 and SALK_143656 were immuno-detected with Tim23-2 antibody. Values below the image represent the average relative abundance ratios of Tim23-2 protein, compared to the amount of Tim23-2 in 40 µg Col-0 mitochondria, for replicate experiments (n=3± SE). The standard error (SE) is indicated under each value. SALK_143656 has a significantly higher amount of Tim23-2 protein than Col-0, with a *p* value < 0.05 (*) using Student's *t* test. C) The same analysis as B) was carried out with Porin antibody. Abbreviations, Col-0: wild type, kDa: kilodalton, SE: Standard Error, HT: hetrozygote, DBHT: double hetrozygote.

Figure 3.7 Aborted seeds were observed in Tim23 crossed plants and Tim17-2 heterozygous plants. The *Tim23-2* knock out line GABI_689C11 was crossed with Tim23-1 T-DNA lines (SALK_030470, SALK_107963) and Tim23-3 T-DNA lines (SALK_129386, SAIL_1151_B01) respectively. The aborted seeds were observed in the siliques from GABI_689C11 and SALK_107963 double heterozygous plants (Tim23-2/Tim23-1 DBHT), GABI_689C11 and SALK_129386 double heterozygous plants (Tim23-2/Tim23-3 DBHT), as the red arrow indicated. The aborted seeds were also observed in Tim17-2 heterozygous plants (Tim17-2 HT). Abbreviations, Col-0: wild type, DBHT: double heterozygote, HT: heterozygote.

Chapter 4
Characterization of Tim23-2 protein in Arabidopsis

Chapter 4 Characterization of Tim23-2 protein in Arabidopsis

4.1 Introduction

Tim23 is a central component of the TIM17:23 complex which is responsible for the import of protein via the general import pathway, directing preproteins into the matrix and for some proteins reinserted from the matrix into the inner membrane (Mokranjac and Neupert, 2010). Tim23 has been extensively characterized in yeast (Truscott et al., 2001). It contains four transmembrane helices and is anchored in the inner membrane and participates in the formation of the translocation channel (Truscott et al., 2001). The first 34 N-terminal amino acids located in the intermembrane space has been shown to interact with Tim50 and functions as a receptor of TIM17:23 complex (Bauer et al., 1996). The first 20 N-terminal amino acid residues are inserted in the outer membrane as they are accessible to the protease in intact mitochondria (Donzeau et al., 2000). This association with the outer membrane is actively remodeled during the translocation of preproteins into mitochondria (Popov-Celeketic et al., 2008).

In the last decade, studies have revealed the higher order structure of multi-subunit protein complexes in the mitochondrial inner membrane, in particular the identification of respiratory chain super complexes (Dudkina et al., 2010; Stuart, 2008; Wittig and Schagger, 2009). In the case of the protein import complexes, the TIM17:23 complex has been reported to be associated

with both the TOM complex and respiratory chain complexes, in addition to the presequence assisted motor complex (PAM) (Schmidt et al., 2010). Tim21, Tim23 and Tim50 play a role in facilitating the interactions with the outer membrane TOM complex to form a dynamic TOM-TIM super complex (van der Laan et al., 2006a). Furthermore, current evidence indicates that Tim21 mediates the interaction between the TIM17:23 and complex III in yeast and an increase in the level of the TIM17:23 translocase associated with the cytochrome bc_1-COX supercomplex was observed in the absence of the F_1F_0-ATP synthase subunits (Saddar et al., 2008).

In Arabidopsis, three isoforms *Tim23-1*, *Tim23-2* and *Tim23-3* all share high protein sequence identity, especially *Tim23-1* and *Tim23-2*, which are located in duplicated regions of the Arabidopsis genome, displaying 83% protein identity (Murcha et al., 2007). Compared with yeast Tim23 protein, Arabidopsis Tim23 proteins are 34 and 35 amino acids shorter and the three isoforms do not appear to contain the N-terminal region which is shown to be inserted in the outer membrane in yeast and required for the subsequent transfer of preproteins from TOM complex to the inner membrane (Murcha et al., 2003). The functional complementation of the yeast deletion strain was only achieved by a chimeric Arabidopsis *Tim23-2* gene, which contained the PRAT domain and didn't require the yeast N-terminal region (Murcha et al., 2003). It suggests that although structurally different, Arabidopsis and yeast Tim23 have functional similarity. The study by Murcha et al. 2003 has shown that Tim23-2 is likely to be the main component of the TIM17:23 translocase, as it is most

highly expressed during development and is expressed ubiquitously in all tissues tested whilst the lowest expressed isoform is *Tim23-3*, with RNA levels 10 times lower than that of *Tim23-1* and *Tim23-2* (Murcha et al., 2003).

The previous chapter identified that the SALK_143656 line was a Tim23-2 over-expressed line, which displayed a delayed growth phenotype and was termed as *tim23* OE. Additionally, the GABI_689C11 line which had no apparent altered phenotype and appears to be a knock-out line of Tim23-2 is termed as the *tim23* KO. The two lines were further investigated to determine the role of Tim23-2 in the protein import pathway.

The aims of this chapter were to:

1) Investigate the role of Tim23-2 protein in the protein import pathway in mitochondria.
2) Identify the proteins associated with Tim23-2.

4.2 Results

4.2.1 Analysis of protein import into mitochondria isolated from Tim23-2 mutant plants

In order to investigate if protein import was affected in the *tim23* KO and *tim23* OE plants, *in vitro* import of radiolabelled mitochondrial precursor proteins into mitochondria isolated from WT, *tim23* KO and *tim23* OE plants was carried out (Figure 4.1). A range of precursor proteins representing different protein import pathways were selected. Two proteins that contain N-terminal cleavable targeting signals and are imported via the general import pathway were selected, the alternative oxidase (AOX) (Whelan et al., 1995) and the F_Ad subunit of ATP synthase (F_Ad) (Dessi et al., 1996; Smith et al., 1994). Monodehydroascorbate reductase (MDHAR) identified to be a dual-targeted protein (Chew et al., 2003a; Chew et al., 2003b) was also chosen. Protein import via the carrier import pathway was also tested, using the adenine nucleotide translocator (ANT) and the phosphate carrier (PiC) (Murcha et al., 2005a; Murcha et al., 2005c). Import assays were carried out from 5, 10, 15 to 20 min and the aliquots from each time point were treated with Proteinase K (PK). The pixel density of the mature processed radiolabelled protein band was quantitated and normalized to the highest point observed in wild type.

The precursor (p) of AOX containing an N-terminal presequence was processed upon import into mitochondria producing a PK protected mature protein of 32 kDa indicated by *. The amount of mature AOX gradually

increased from 5 to 20 min (Figure 4.1A, I). Compared with the wild type, the amount of imported AOX was nearly 2-fold higher in the *tim23* OE mitochondria while the import decreased about 40% in the *tim23* KO (Figure 4.1B, I).

The import of F_Ad into the mitochondria also resulted in a PK protected mature form of 21 kDa indicated by * (Figure 4.1A, II). The amount of import was 1.4 times greater in the *tim23* OE than the wild type after 20 min while the amount of import into the *tim23* KO line decreased about 40% compared to the wild type (Figure 4.1B, II).

The dual-targeted protein, MDHAR, was also processed upon import to a protein with an apparent molecular weight of 47 kDa. The amount of mature protein increased from 5 to 20 min (Figure 4.1A, III). Similarly to AOX and F_Ad, the import was greater in the *tim23* OE line and significantly reduced in the *tim23* KO at all time points tested when compared to the wild type (Figure 4.1A & B, III).

ANT is a carrier protein that is imported into the inner membrane through the carrier import pathway (Lister et al., 2002). Import of the ANT into isolated mitochondria, resulted in the production of a 30 kDa band that was resistant to protease treatment (Figure 4.1A, IV). The mature protein accumulated over time (Figure 4.1A, IV), however, the amount of the imported ANT did not change between Col-0, *tim23* OE and KO lines at all time points tested. Similarly, another carrier import pathway protein, PiC, was also tested. A mature protein of 34 kDa was produced upon import into the mitochondria. The mature protein accumulated from 5 to 20 min (Figure 4.1A, V), and as with ANT,

no difference in the amount of the imported PiC was observed between lines (Figure 4.1B, V).

Over all, the amount of protein import for ANT and PiC did not differ in either the *tim23* KO mutants or the *tim23* OE mutants when compared to wild type. However, the amount of imported AOX, F_Ad and MDHAR was higher in mitochondria isolated from *tim23* OE and much less in the *tim23* KO.

4.2.2 The change of protein abundance with inactivation or induction of Tim23-2 protein

The abundance of mitochondrial PRAT proteins, respiratory chain components, various mitochondrial protein import components and the stress response proteins was investigated to gain insight into the effects of disruption or induction of the Tim23-2 protein.

Immuno-detection of the mitochondrial PRAT proteins showed that Tim17-2 increased by 42% in the *tim23* OE line and decreased 52% in the KO line (Figure 4.2A). A protein encoded by At3g10110 or At1g18320, which have 100% protein sequence identity and have been shown to be able to complement a yeast *tim22* deletion mutant (Murcha et al., 2007), was at least 200% higher in the *tim23* OE line (Figure 4.2A). In contrast, a PRAT protein of unknown function, which was encoded by At3g25120, decreased by 45% in the *tim23* OE line and increased by 50% in *tim23* KO line (Figure 4.2A). Additionally, the PRAT protein of unknown function, encoded by At5g24650, did not change either in the *tim23* OE or *tim23* KO line. Finally, At2g42210, a

gene that encodes a PRAT family member and also previously has been identified as a subunit of complex I in two independent studies (Klodmann and Braun, 2010; Klodmann et al., 2010b; Meyer et al., 2008a, b), was shown to decrease dramatically in the *tim23* KO line and slightly increased in the *tim23* OE line (Figure 4.2A).

In the case of a variety of other respiratory chain components, the most notable effect was a > 80% reduction of Ndufs4 in the *tim23* OE line (Figure 4.2B). This is a complex I subunit proposed to be present in the peripheral portion of complex I (Klodmann and Braun, 2010; Klodmann et al., 2010a, b). Interestingly, Nad9, another complex I component, that is encoded by the mitochondrial genome, did not show any significant change in the *tim23* OE or the *tim23* KO lines, compared to the wild type (Figure 4.2B). Immuno-detection against the α subunit of ATP synthase (ATP α) showed 300% higher abundance in the *tim23* OE than in the wild type, while no change was observed in *tim23* KO line (Figure 4.2B). The β-subunit of the ATP synthase complex (ATP β) did not change either in the *tim23* OE or the *tim23* KO. The Rieske FeS protein (RISP) of the cytochrome bc_1 complex increased slightly in the *tim23* OE line by 25% and decreased to 65% in the *tim23* KO line (Figure 4.2B). COXII did not show any obvious change either in the *tim23* OE or in the *tim23* KO line (Figure 4.2B).

Immuno-detection using antibodies raised against a range of import components was also carried out in both lines. No obvious change was observed in the abundance of Porin, Sam50, Tom40, Mia40 and Erv1 either in

tim23 OE or *tim23* KO lines (Figure 4.2C). The abundance of Metaxin increased about 30% in both the *tim23* OE and *tim23* KO lines (Figure 4.2C). The abundance of Tom20-2 was at least 200% higher in the *tim23* OE line than the wild type and decreased 50% in the *tim23* KO (Figure 4.2C). Similarly, Tom20-4 was induced at least 200% in the *tim23* OE line compared to the wild type and no significant change was observed in *tim23* KO (Figure 4.2C). Tom20-3 only increased 44% in the *tim23* OE and did not change in the *tim23* KO (Figure 4.2C). Tim50, a component of the TIM17:23 complex, increased 40% in the *tim23* OE line and levels remained unchanged in the *tim23* KO line (Figure 4.2C). Tim21, another component of the TIM17:23 complex, increased 65% in the *tim23* OE line and did not change obviously in the KO line (Figure 4.2C). Tim44, the import motor of the TIM17:23 complex increased about 24% in the *tim23* OE line and did not change in the *tim23* KO line (Figure 4.2C). Tim9, an import component of the intermembrane space, increased about 60% in the *tim23* OE mutant and did not change in the KO (Figure 4.2C).

The Alternative Oxidase (AOX), a marker of stress-induced mitochondrial retrograde signalling, increased about 500% in both *tim23* KO and *tim23* OE lines (Figure 4.2D). Whilst the abundance of Prohibitin did not change in the mutant lines compared with the wild type (Figure 4.2D).

4.2.3 Over-expression of Tim23 results in a reduction of complex I

Western blot analysis suggested that the over-expression of the Tim23-2

protein resulted in many changes in the abundance of import components and surprisingly, changes to the abundance of respiratory chain components, such as the 80% reduction of Ndufs4 in the *tim23* OE line. The respiratory chain complexes were further investigated from wild type, *tim23* OE and *tim23* KO lines by BN-PAGE analysis. The Coomassie stained gel showed that there was a difference in the pattern of bands observed for the *tim23* OE mitochondria and the mitochondria from wild type and *tim23* KO. Mitochondria from wild type plants contained the characteristic pattern of respiratory chain complexes, with both monomeric complex I and the supercomplex I and III (Figure 4.3, Lane 1). Interestingly, the monomeric complex I appeared totally absent in the *tim23* OE line, while the supercomplex I and III was reduced in intensity (Figure 4.3, Lane 2). Mitochondria isolated from *tim23* KO plants showed similar bands to mitochondria from the wild type plants, except that the monomeric complex I appeared slightly more diffused (Figure 4.3, Lane 3). Activity staining for complex I confirmed the dramatic reduction of complex I in the *tim23* OE line although it is notable that some activity is still present, especially in the band of the supercomplex I and III (Figure 4.3, Lane 5). The activity staining of mitochondria isolated from *tim23* KO line did not alter significantly when compared to the wild type (Figure 4.3, Lane 6).

The BN-PAGE gels were also transferred to PVDF membrane and immuno-detected with antibodies raised against components of complex I, III, IV and V of the respiratory chain. Immuno-detection against Ndufs4 and Nad9 confirmed the positions of complex I and supercomplex I and III (Figure 4.3,

Lanes 7 and 10, indicated by the star). The reduction of Ndufs4 was again observed in the *tim23* OE line (Figure 4.3, Lane 8) and a similar reduction was observed with the immuno-detection against Nad9 (Figure 4.3, Lane 11). The abundance of neither subunit changed in the *tim23* KO line (Figure 4.3, Lane 9 and 12). Immuno-detection against the α subunit of ATP synthase (Figure 4.3, Lanes 13-15) appeared to be induced in the *tim23* OE line (Figure 4.3, Lane 14) and no change was observed in the *tim23* KO line (Figure 4.3, Lane 15,). However, the amount of Rieske Iron Sulphur Protein (RISP, a subunit of complex III) and Cytochrome Oxidase II (COX II, a subunit of complex IV) were unaltered either in the *tim23* OE or the *tim23* KO when compared to wild type (Figure 4.3, Lane 16-21).

4.2.4 A novel complex was observed in the *tim23* OE line

Whilst a reduction of complex I and the supercomplex of I and III was observed in the *tim23* OE line, an additional complex band was identified in the *tim23-2* OE line. This additional band exhibited a molecular mass higher than complex I but lower than the supercomplex of I and III, as indicated by the arrow (Figure 4.3, Lane 2).

This additional band was excised from the gel, purified, resolved by SDS-PAGE and the individual constituents were identified by mass spectrometry (MS). The constituents of this complex contained a number of proteins from complex I (At2g42210, At4g16450 and At5g63510), complex III (At3g52730, At4g32470 and At1g51980), complex V (AtMg01190 and

At5g08670). Several other membrane proteins such as prohibitin (At1g03680 and At5g40770) and unknown proteins (At2g33220) (Figure 4.4A) were identified and as such this additional complex band will be referred to as the Mixed Inner membrane Complex (MIC).

In order to confirm the identity of the constituents of the MIC complex, the radiolabelled import of a number of proteins, which were identified to be in the MIC by MS, was carried out and the products were analysed by BN-PAGE. This has previously been carried out for a number of studies investigating the assembly of multisubunit protein complexes in mitochondria (Carrie et al., 2010a). The 14 kDa subunit of cytochrome C reductase encoded by At4g32470, the α-subunit of the mitochondrial processing peptidase (Mpp α) encoded by At1g51980 and two complex I subunits of unknown function encoded by At1g47260 and At2g42210 were translated with rediolabelled methionine *in vitro* system and imported into mitochondria from *tim23* OE plants, the incorporation of the radiolabelled proteins into the MIC of the *tim23* OE line could be observed by resolving the mitochondria on BN-PAGE after *in vitro* protein import and autoradiography of the dried gel (Figure 4.4B, Lane 2, 4, 6 and 8). The incorporation of Mpp α and cytochrome c into the supercomplex I and III was observed in wild type mitochondria (Figure 4.4B, Lane 1 and 3) as indicated by the radioactive band at the expected positions. The protein encoded by At1g47260 was assembled into both complexes I and the supercomplex of I and III (Figure 4.4B, Lane 5) in wild type mitochondria. The protein encoded by At2g42210, a known complex I subunit was only seen to

assemble into the monomeric form of complex I (Figure 4.4B, Lane 7).

The assembly of these four respiratory chain components, MPP α (At1g51980), cytochrome c (At4g32470), and the subunits of complex I encoded by At1g47260 and At2g42210, were monitored over time (Figure 4.4C). It was evident that the assembly of radiolabelled cytochrome C reductase into complex III occurred in 5 min of the import reaction, and the intensity of labeling increased throughout time. Incorporation into the supercomplex I and III was evident after 10 min which similarly increased in intensity (Figure 4.4C I). This suggests that the cytochrome C reductase can be traced from initial assembly into complex III to incorporation into the supercomplex of complex I and III. Incorporation of cytochrome C reductase into complex III was also evident in mitochondria isolated from *tim23* OE (Fig 2.4C I). Though only very weak incorporation was evident into the supercomplex of I and III. Instead the assembly of cytochrome C reductase was observed into the MIC complex (indicated by the arrow) which was seen to accumalate over the time course tested (Figure 4.4C, I).

The Mpp α subunit was also assembled into complex III and the supercomplex of complexes I and III in wild type mitochondria and similarly, the amount of labeling increased over time from 5 to 60 min (Figure 4.4C II), Incorporation of Mpp α into mitochondria was only visualized into complex III and the MIC in the *tim23* OE line.

The protein encoded by At1g47260, a subunit of complex I, was shown to assemble into complex I and the supercomplex of I and III in the wild type

mitochondria. The assembly into complex I was seen to decrease after 30 min and the assembly into supercomplex I and III was shown to increase (Figure 4.4C, III). In *tim23* OE, the assembly into complex I was only observed weakly at 10 and 30 min whilst the accumulation into the MIC complex was evident at 60 and 90 min (Figure 4.4C, III). Another subunit of complex I encoded by At2g42210 was also shown to assemble into complex I in wild type mitochondria though this labeling was only evident at 15 and 30 mins (Figure 4.4C, IV). Incorporation of this protein in the MIC of *tim23* OE was only observed following 120 min of import (Figure 4.4C, IV).

It was evident that the MIC complex is not a complex I assembly intermediate but rather it is a mixture of different protein from various inner membrane complexes.

4.2.5 The assembly of Tim23-2 into TIM17:23 complex and complex I in Arabidopsis

The subunits of the TIM17:23 complex have been extensively described in yeast. It is widely accepted that the complex exists in multiple forms and on BN-PAGE the complex can be grouped into two populations: a small complex ranged at 100 -140 kDa and the larger form ranged at 150-300 kDa (Chacinska et al., 2005; Saddar et al., 2008; van der Laan et al., 2006a). In plants, the TIM17:23 complex is identified on a gel with the size of 110 kDa and 150 kDa (Klodmann et al., 2011).

In order to determine the complexes that Tim23-2 is associated with in

Arabidopsis, radiolabelled Tim23-2 precursor was imported into the mitochondria isolated from wild type plants. Following the import reaction, mitochondria was reisolated at four time points (5, 10, 20 and 40 min) and solubilized in 1% (w/v) digitonin. The samples were resolved by BN-PAGE and visualized by autoradiography.

Incorporation of radiolabelled Tim23-2 protein into the TIM17:23 complex was observed in two distinct forms with the molecular mass of 100 kDa and 200 kDa (Figure 4.5A, I), which is close with the size of TIM17:23 complex observed in previous studies (Chacinska et al., 2005; Saddar et al., 2008; van der Laan et al., 2006a). Notably Tim23-2 was also found to be incorporated into complex III and into complex I as indicated with the arrow. This incorporation into complex I was shown to accumulate over time from 5 to 40 min (Figure 4.5A, I) and thus is thought to be a real interaction and not a result of non specific binding. Note that the labeling of the complex V band is a result of incorporation of radiolabelled methionine into ATP subunits that are mitochondrially encoded in Arabidopsis (α subunit and subunit 9 of ATP synthase complex). These are the most prominent bands labeled upon in organelle translation in Arabidopsis mitochondria and thus radiolabelled complex V is evident with *in vitro* import and analysis by BN-PAGE for a variety of precursor proteins. Thus Tim23 is not concluded to be imported into complex V.

The assembly of radiolabelled Tim17-2 was also investigated. The precursor was found to be accumulated in two complexes same as Tim23-2, sized at ~100 kDa and ~200 kDa. However, it is important to note that no

incorporation into complex III and complex I was observed (Figure 4.5A, II).

To confirm the location of complex I, import of complex I subunits encoded by At2g42210 and At1g47260 was also carried out. At2g42210 displayed accumulating incorporation into complex I from 5 to 40 min, indicated with the arrow. Incorporation into a complex band of ~400 kDa was also evident which may represent an assembly intermediate (Figure 4.5A, III). The complex I subunit encoded by At1g47620 was strongly incorporated into complex I at 5 min, the intensity of which decreased through out time (Figure 4.5A, IV). It was seen that the amount of accumulation of radiolabelled protein shifted to the supercomplex I and III at 20 and 40 min, indicated by the * (Figure 4.5A, IV).

The Arabidopsis Tim44 (At2g20510) and Tim50 (At1g55900) were similarly tested and confirmed as components of TIM17:23 complex. The BN-PAGE revealed that both precursors were assembled into the smaller complex with the molecular weight of ~100 kDa as indicated by the ● (Figure 4.5B, Lane 3 and 4). The assembly of Tim44 and Tim50 is consistent with the observation assembly of Tim23-2 and Tim17-2, also incorporated into the band of ~100 kDa (Figure 4.5B, Lane 1 and 2).

The composition of the Tim17:23 complex and the migration by BN-PAGE was also tested using antibodies specific for Tim23-2, Tim17-2 and Tim50. Immuno-detection of wild type mitochondria, using Tim23-2 antibody, detected two complex bands of ~100 kDa and ~200 kDa. Whilst several other bands cross reacted with the antibody, Tim23-2 protein was also detected at the position of complex I which was indicated by the arrow (Figure 4.5B, Lane 5),

which was consistent with the bands detected on BN-PAGE following protein import. Antibodies against Tim17-2 and Tim50 cross reacted with a complex band of ~200 kDa indicated by the ●, although the smaller complex of ~100 kDa was not detected (Figure 4.5B, Lane 6 and 7). Similarly to the detection with Tim23-2 antibody, antibodies against Tim17-2 and Tim50 cross reacted with several other complex bands, though no detection of complex I was evident.

Taken all the results together, we conclude that Tim23-2, Tim17-2, Tim50 and Tim44 co-exist in the same mitochondrial protein complexes with the size of ~100 kDa and ~200 kDa. Furthermore, Tim23-2 alone can interact and be incorporated into complex I which was observed both by protein import and western blot following BN-PAGE.

4.2.6 The assembly of Tim23-2 into complex I is reduced in *tim23* OE line

Tim23-2 has been shown to be incorporated into two complexes of ~100 kDa and ~200 kDa and also incorporated into complex I (Figure 4.5A, I). A similar assay was also carried out into the *tim23* KO and *tim23* OE mitochondria. The assembly of radiolabelled Tim23-2 precursor into mitochondria from *tim23* OE plants showed that as in wild type the protein assembled into complexes of ~100 kDa and ~200 kDa (Figure 4.6 A). The assembly state was not much altered compared with wild type. In the *tim23* KO mitochondria, the assembly of Tim23-2 into the complexes sized at ~100 kDa and ~200 kDa was much

reduced. The association of Tim23-2 into complex I was evident in both the wild type and *tim23* KO line but much reduced in the *tim23* OE (Figure 4.6A, Lanes 1 and 3).

In the case of Tim17-2, the assembly efficiency into the complex of ~100kDa was increased in the *tim23* OE mitochondria compared to wild type, though assembly into the larger form was reduced (Figure 4.6A, Lane 5). The assembly into TIM17:23 complex was much less in the *tim23* KO mitochondria compared to wild type (Figure 4.6A, Lane 6 vs Lane 4). No incorporation into complex I was observed in either of the wild type or the mutant lines.

Western blot analysis revealed that the amount of Tim23 protein associated with complex I was dramatically reduced in the *tim23* OE compared with the wild type (Figure 4.6B, Lane 2 vs Lane 1). In *tim23* KO line, Tim23 protein was not detected either in complex I or TIM17:23 complex (Figure 4.6B, Lane 3). The amount of Tim17-2 protein assembled into TIM17:23 complex was not altered in *tim23* mutant lines compared to the wild type (Figure 4.6B, Lanes 4-6). In agreement with the results of the *in vitro* import, the antibody of Tim17-2 did not cross react with any complex that was related to complex I (Figure 4.6B, Lane 4-6).

On the basis of these results, it was concluded that the biogenesis of complex I was affected by the over-expression of Tim23 protein and due to the lack of this complex in the *tim23* OE line the incorporation of Tim23 into complex I was not evident.

4.3 Discussion

4.3.1 Tim23-2 protein plays a role in the general protein import pathway

In yeast, Tim23 is a core component of the general import pathway via the TIM17:23 complex, for either matrix-located proteins or membrane proteins re-inserted from the matrix into the inner membrane (Pudelski et al., 2010). The studies performed in this chapter demonstrate that the import of general import pathway precursors was partially reduced in the *tim23* KO mitochondria and up-regulated in the *tim23* OE mitochondria. Furthermore, no changes were observed with the import of carrier proteins, confirming that Tim23-2 is involved in the general import pathway in plants. The changes in protein abundance detected in the mutants revealed that the abundance of Tim17-2, which is another essential component of TIM17:23 complex, was also reduced in response to the deletion of Tim23-2 and similarly increased with the over-expression of Tim23-2. In addition, the amount of Tim50, Tim44 and Tim21, also involved in the Tim17:23 complex, increased in response to the up-regulation of Tim23-2. No other significant changes in other components of the mitochondrial protein import apparatus were observed, except Tom20-2 and Tom20-4, which were also down-regulated in the *tim23* KO and up-regulated in the *tim23* OE lines. However, the changes in Tom20 isoforms alone are unlikely to account for the observed changes in the protein import pathway, as inactivation of two of three Tom20 protein isoforms in Arabidopsis

does not greatly affect the general import pathway (Lister et al., 2007).

Interestingly, whilst there was no increase in the carrier import pathway, immuno-detection of Tim9 and Tim22 (At3g10110/At1g18320) was seen to increase in the *tim23-2* OE line. These increases may be a result of increased transcription or translation and their abundance did not affect the rate of the carrier import pathway.

4.3.2 The Tim23 multiple gene family

Although the import pathway via the TIM17:23 complex was compromised, the *tim23* KO plants were viable and there was no deleterious phenotype associated with the deletion of Tim23-2. The reason for this could be the partial complementation of Tim23-1 and Tim23-3 proteins for Tim23-2 protein. Especially for Tim23-1, it displays 83% protein identity with Tim23-2 and they are located in duplicated regions of the Arabidopsis genome. However, the Tim23-1 and Tim23-3 proteins could not be detected in wild type mitochondria or the *tim23* KO line, possibly because of the low protein expression levels below the limits of detection.

However, the *tim23* KO plant is still under stress, as the induction of AOX was observed in the *tim23* line. *In vitro* protein import assays revealed that the uptake of AOX was induced in the *tim23* OE line but down in the *tim23* KO line. It suggested that the increased abundance of AOX in both *tim23* KO and OE lines was not a consequence of the alteration of protein import rate, but rather the outcome of a precise retrograde signaling pathway. It indicates that Tim23-2

protein plays an important role in the Tim23 gene family, as mitochondria would be stressed either knocking out or inducing the protein. We assumed that Tim23-1, Tim23-2 and Tim23-3 were functionally redundant proteins. Tim23-1 and Tim23-3 could only partially complement for the function of Tim23-2, as the protein import via TIM17:23 complex was still defective in the *tim23* KO line. This was evidenced by crossing the *tim23* KO plants with the Tim23-1 knock-out plants and the Tim23-3 knock-out plants, which showed that no double knock-outs were viable, suggesting that Tim23-1 and Tim23-3 could complement the *tim23* KO line (Figure 3.7).

4.3.3 Tim23-2 protein is not essential for the stability of TIM17:23 complex

Although in *tim23* KO mitochondria, the assembly of Tim23-2 and Tim17-2 into TIM17:23 complex was reduced (Figure 4.6A, Lane 3 and 6), the mobility of TIM17:23 complex and the amount of Tim17-2 in TIM17:23 complex were unchanged (Figure 4.6B, Lane 6). It indicates that TIM17:23 complex is stable with the deletion of Tim23-2 protein, however the efficiency of Tim17:23 complex function is impaired. It could because of the partial complementation of Tim23-1 or Tim23-3 protein for Tim23-2 protein or other unknown protein import components, which could replace the role of Tim23-2 protein. In reverse, it also explains the reduction of general import pathway via the TIM17:23 complex.

4.3.4 The connection between complex I and Tim23

TIM17:23 complex has been found to associate with a variety of other protein complexes in yeast. It forms a dynamic TOM-TIM super complex with the TOM complex (Geissler et al., 2002; Mokranjac et al., 2009a, b; Tamura et al., 2009a, b; Yamamoto et al., 2002), TIM17:23-PAM super complex (Chacinska et al., 2005; Chacinska et al., 2010) and the TIM17:23^{sort} supercomplex with complex III (van der Laan et al., 2006b). However, as yeast lack complex I, no interaction with complex I is possible (Melo et al., 2004a, b).

In this study, we identified that there is an interaction between complex I of the respiratory chain and the mitochondrial import component Tim23-2 in Arabidopsis. Although the deletion of Tim23-2 protein in the *tim23* KO line has little or no affect on the abundance of complex I or the super complex I+III, the over-expression of Tim23-2 at a protein level resulted in a dramatic reduction in complex I activity and a decrease in the protein level of complex I subunits. A direct interaction between complex I and Tim23-2 protein was also observed, in that radiolabelled imported Tim23-2 was incorporated into complex I and could also be detected in complex I using a Tim23-2 antibody.

This interaction between Tim23-2 and complex I has a significant effect on respiratory chain activity, as it appears that altering the amount of Tim23-2 results in a dramatic decrease in complex I. However, while this represents an exciting finding, it comes from a single genetic background, an over-expression of Tim23-2 due to a fortuitous insertion in the 5' UTR. This mutant cannot be

complemented, to confirm a direct molecular link. Also, while biochemically, we demonstrated that Tim23-2 could be assembled into complex I and that Tim23-2 could be detected in complex I with antibodies, it cannot be ruled out that the reduction in complex I is due to another alteration in this genetic background. Thus, further studies in independent genetic backgrounds were pursued to confirm the link between Tim23-2 and complex I.

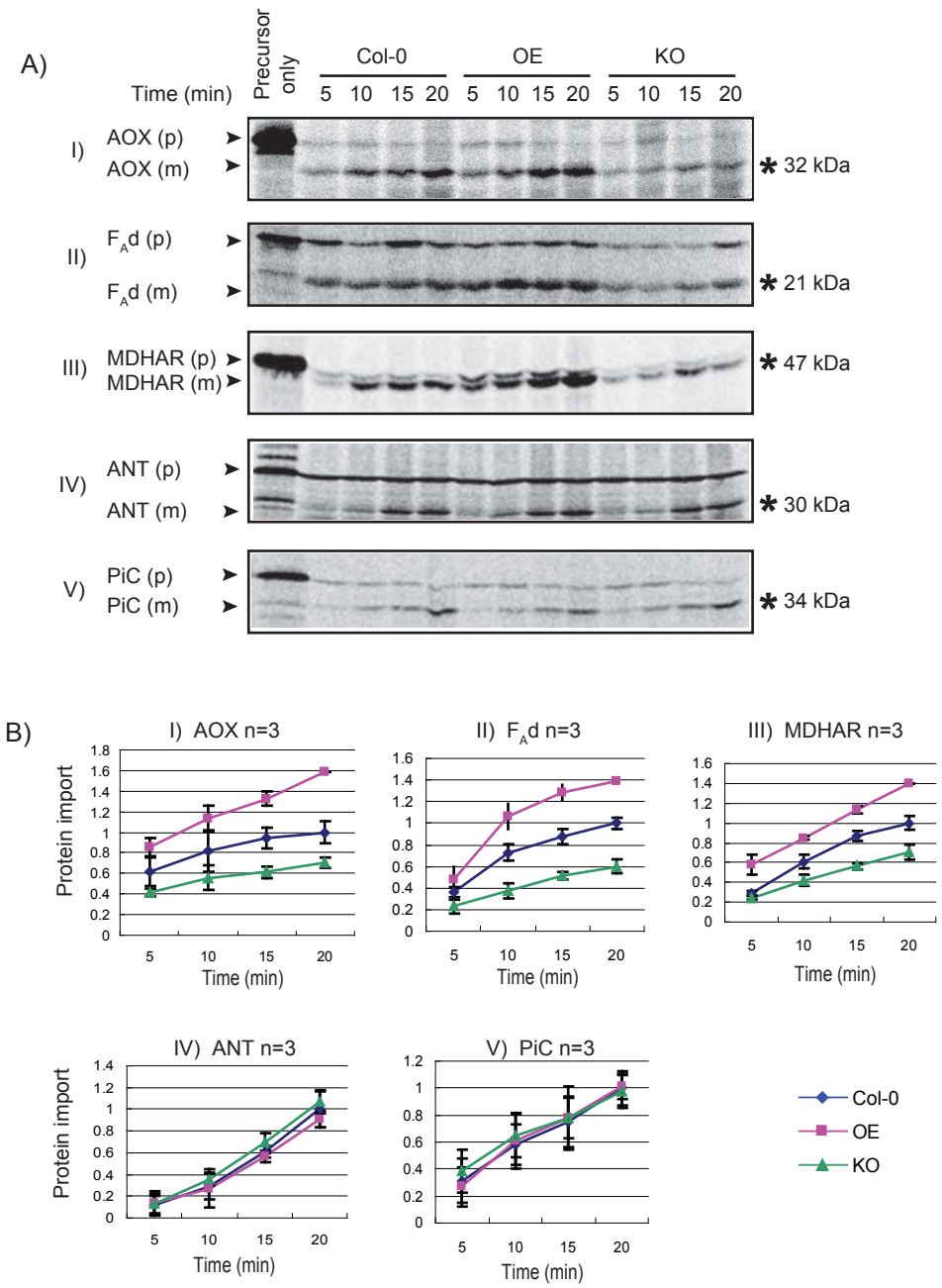

Figure 4.1. Analysis of protein import into mitochondria isolated from Tim23-2 mutant plants. A) [^{35}S]-labelled precursor proteins AOX, F_Ad, MDHAR, ANT, PiC were incubated with mitochondrial isolated from Col-0 (wild type), OE (*tim23* OE line) and KO (*tim23* KO line) under conditions that support protein import. Aliquots were removed at 5, 10, 15 and 20 min and treated with PK. B) The PK protected mature radiolabelled protein (indicated by the asterisk) was quantitated at each time point and normalised to the highest time point of the wild type for replicate experiments (n ≥ 3 ± SE). Abrreviations, PK: Proteinase K, AOX: Alternative Oxidase, F_Ad: FAd subunit of ATP synthase, MDHAR: monodehydroascorbate reductase, ANT: adenine nucleotide translocator, PiC: phosphate carrier, OE: over-expressor, KO: knock out, kDa: kilodalton, p: precursor protein, m: mature protein.

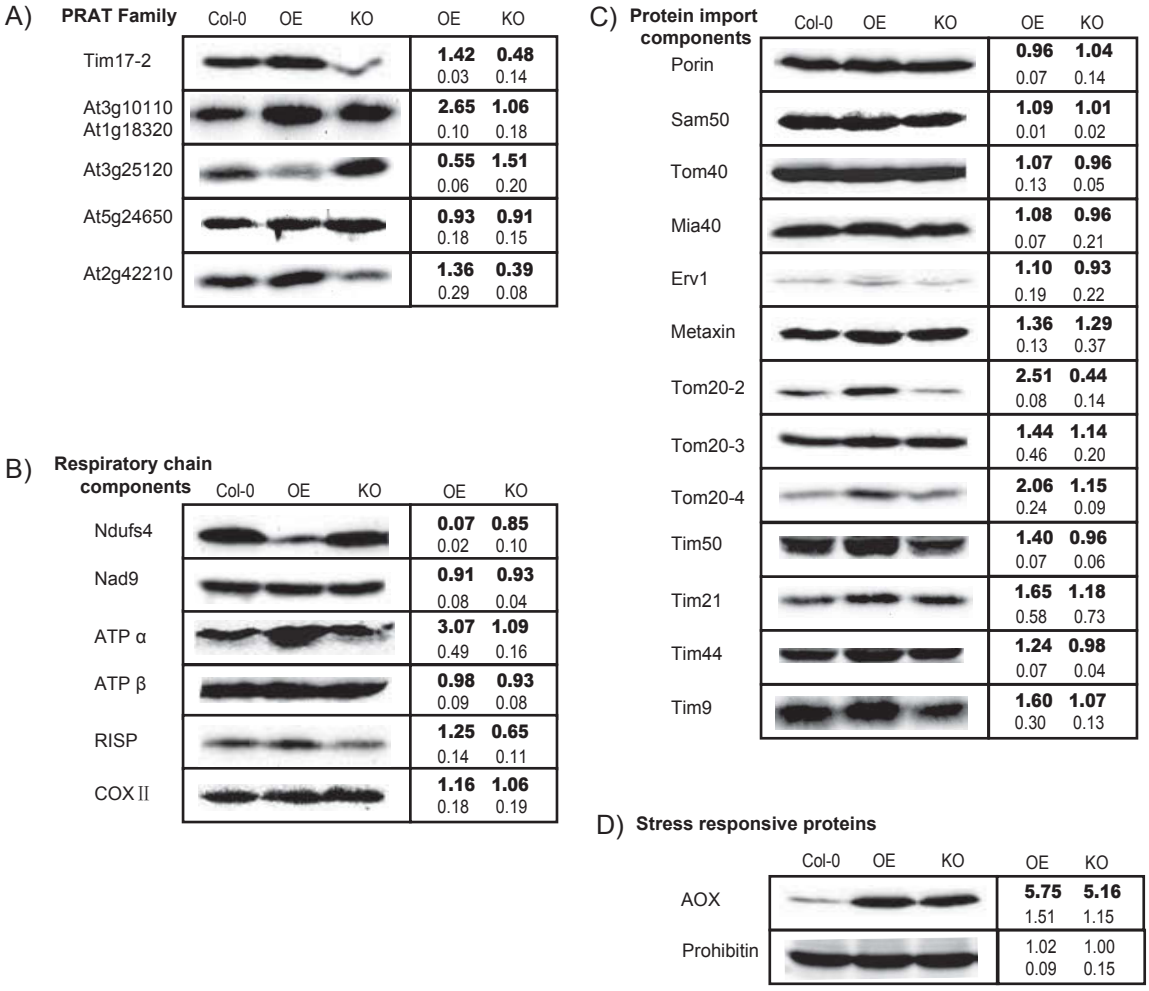

Figure 4.2. The abundance of a variety of proteins as determined by western blot analysis of mitochondria isolated from Col-0 (wild type), OE (*tim23* OE line), KO (*tim23* KO line). A) Immunodetection with antibodies raised against various proteins that belong to the mitochondrial Preprotein and amino acid transporters (PRAT) family, B) various respiratory chain proteins, C) mitochondrial protein import apparatus and D) mitochondrial Alternative oxidase (AOX) and prohibitin. Values alongside the image represent the average relative abundance ratios of proteins present in the two mutants, respectively, compared to Col-0 mitochondria (n ≥ 3 ± SE). Standard errors are indicated below. Abbreviations, PRAT: preprotein and amino acids transporter, Col-0: wild type, OE: over-expressor, KO: knock out.

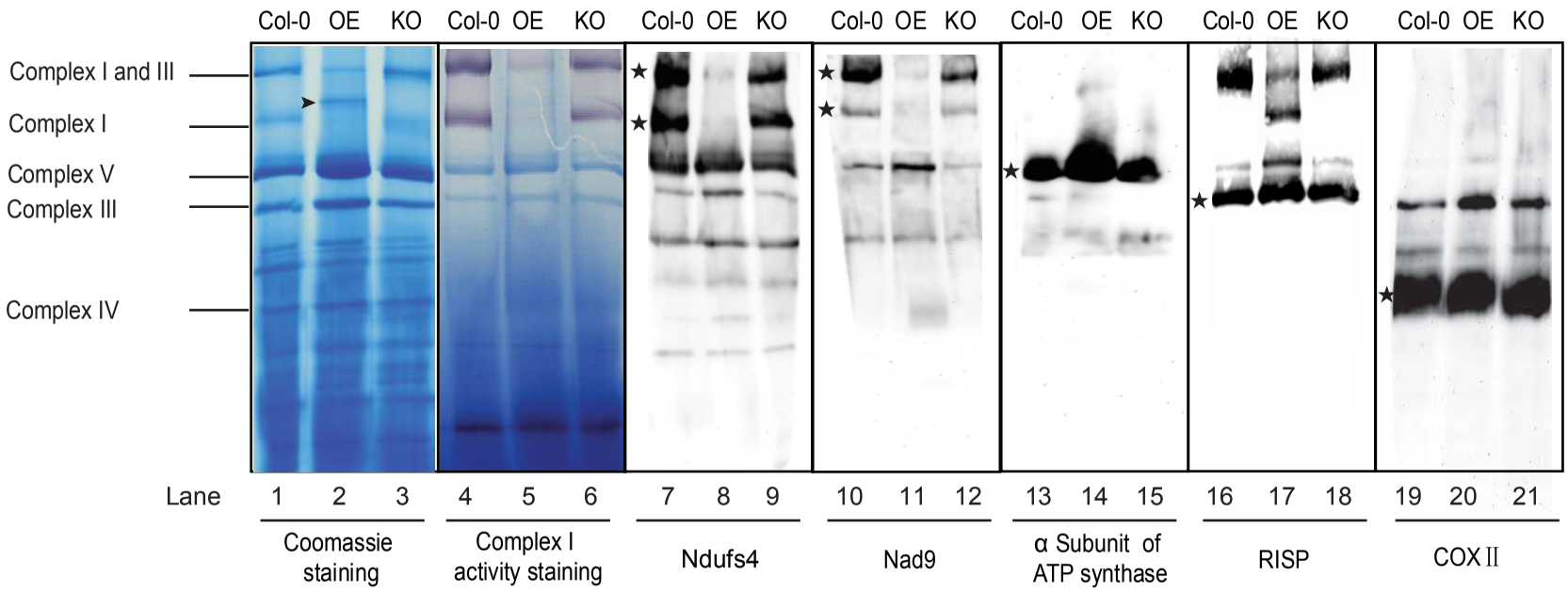

Figure 4.3. Complex I is reduced in *tim23* OE (Tim23 overexpressor). Mitochondria was isolated from Col-0 (wild-type), OE (Tim23 overexpressor) and KO (Tim23 knock out) lines and resolved by one-dimensional BN-PAGE, stained with Coomassie and analysed for complex I activity. The mitochondria was immunodetected with antibodies against Ndufs4 and Nad9 (complex I subunits), α subunit of ATP synthase (complex V subunit), Rieske iron-sulfur protein (RISP) (complex III subunit) and COXII (complex IV subunit). The bands corresponding to the super complex I and III, complex I, complex V, complex III and complex IV are indicated. The additional band observed in the OE was indicated by the arrow. The corresponding band of each respiratory chain complex subunit was indicated by ★.

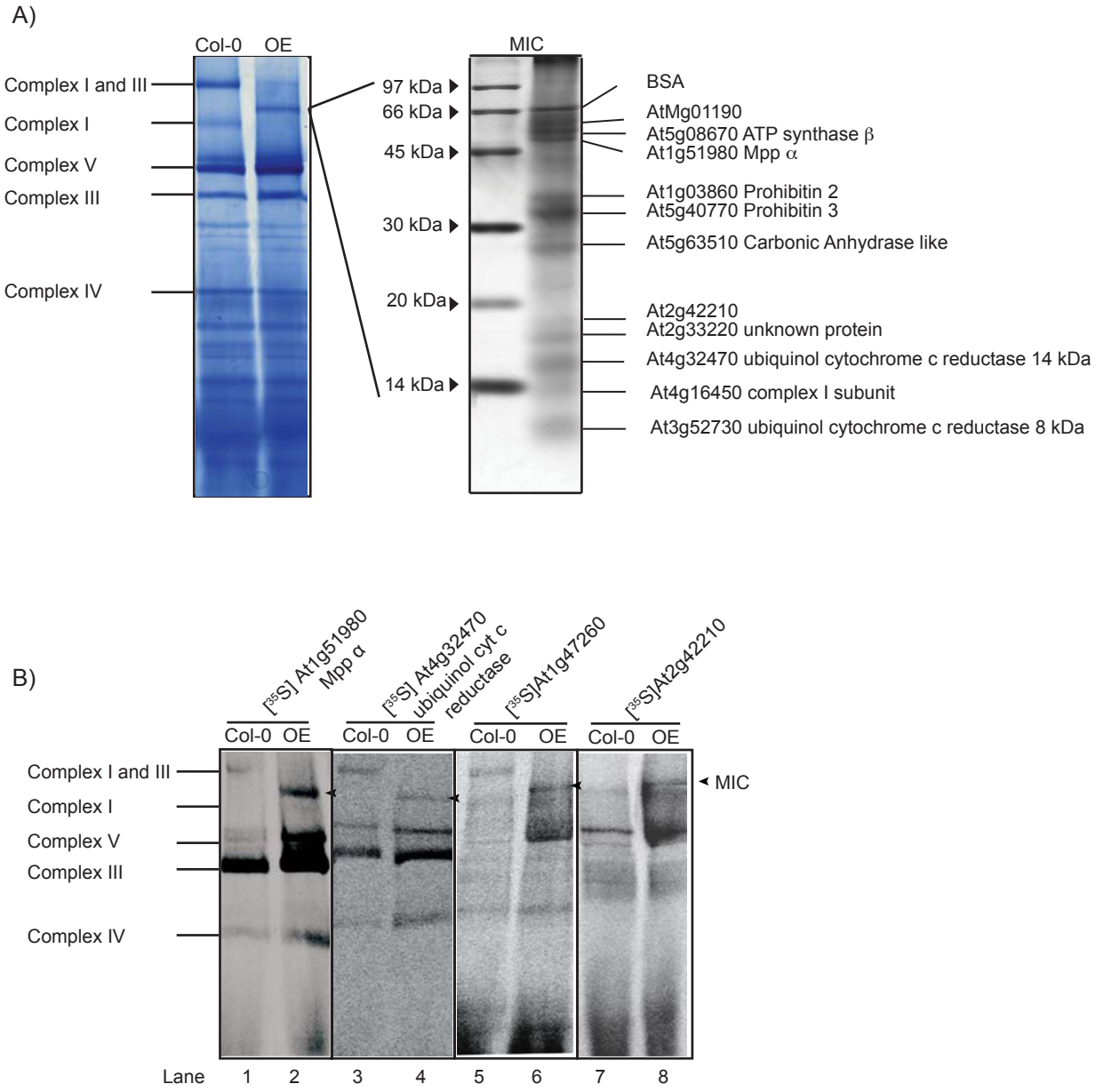

Figure 4.4. Identification of the Mixed Inner membrane Complex (MIC) in the OE (Tim23 over-expressor) line. A) Mitochondria isolated from the *tim23* OE was resolved by one dimensional BN-PAGE and stained with Coomassie. The MIC was excised from the gel and proteins identified by ESI MS/MS. The identifying peptide matches are listed corresponding to the protein bands that reside in the mixed intermediate complex (MIC). B) The radiolabelled At1g51980 (Mpp α), At4g32470 (ubiquinone cytochrome c reductase), At1g47260 and At2g42210 were imported into mitochondria isolated from Col-0 (wild-type) and OE plants and analyzed by one dimensional BN-PAGE. The gels were Coomassie stained, dried and exposed to phosphor-imaging plates. The positions of the respiratory complexes are indicated. The position of the MIC complex is indicated with the arrow.

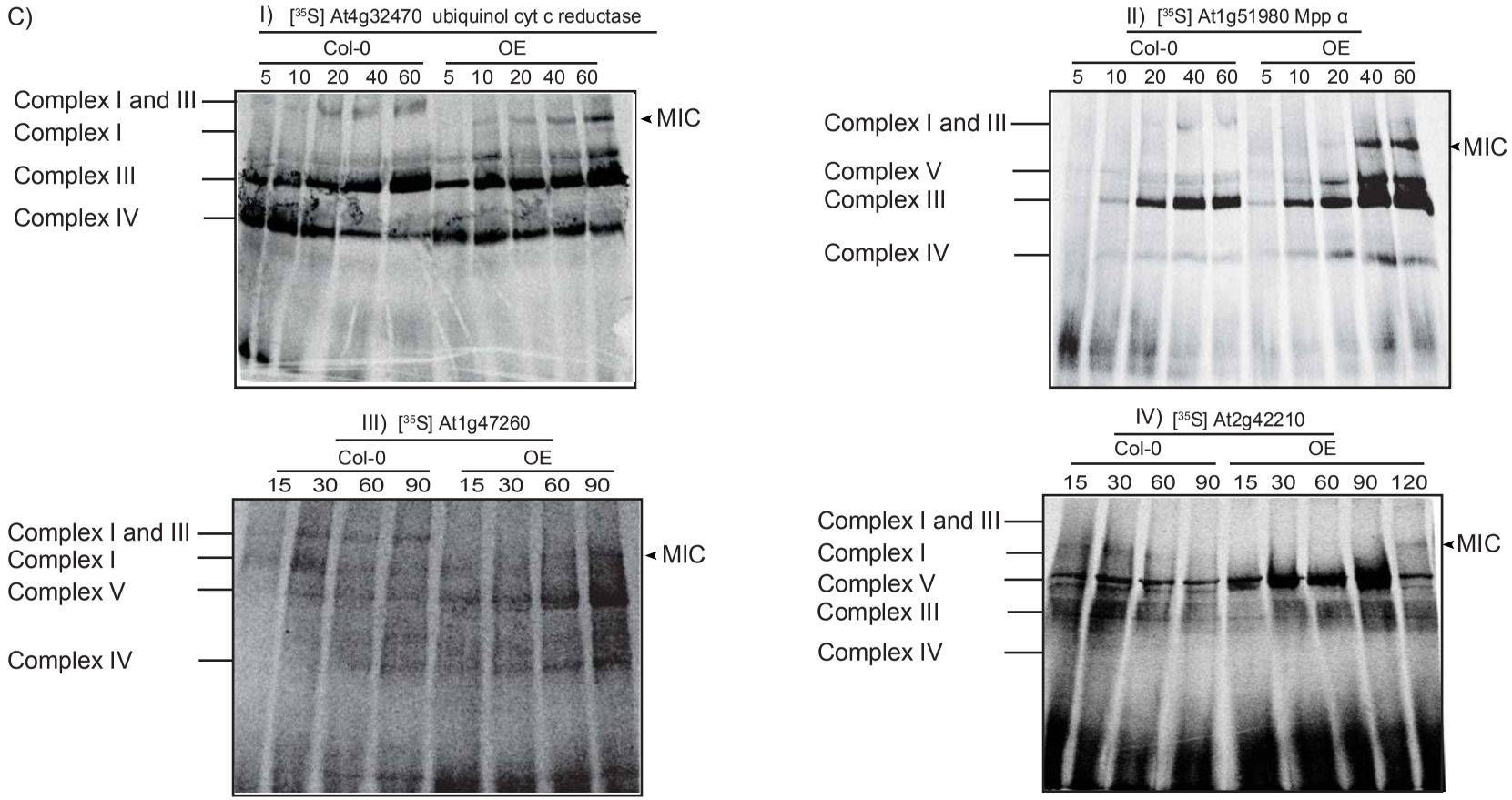

Figure 4.4. C) Time course analysis of protein import into mitochondria isolated from Col-0 (wild-type) and OE (Tim23 over-expressor) lines was carried out using the radiolabelled proteins, At4g32470 (ubiquinone cytochrome c reductase), At1g51980 (Mpp α), At1g47260 and At2g42210 . The aliquots were removed at various time points (min). The locations of respiratory chain complexes are indicated and the assembly of the radiolabelled protein into the MIC was indicated by the arrow. Abbreviations, OE: overexpressor, MIC: mixed inner membrane complex.

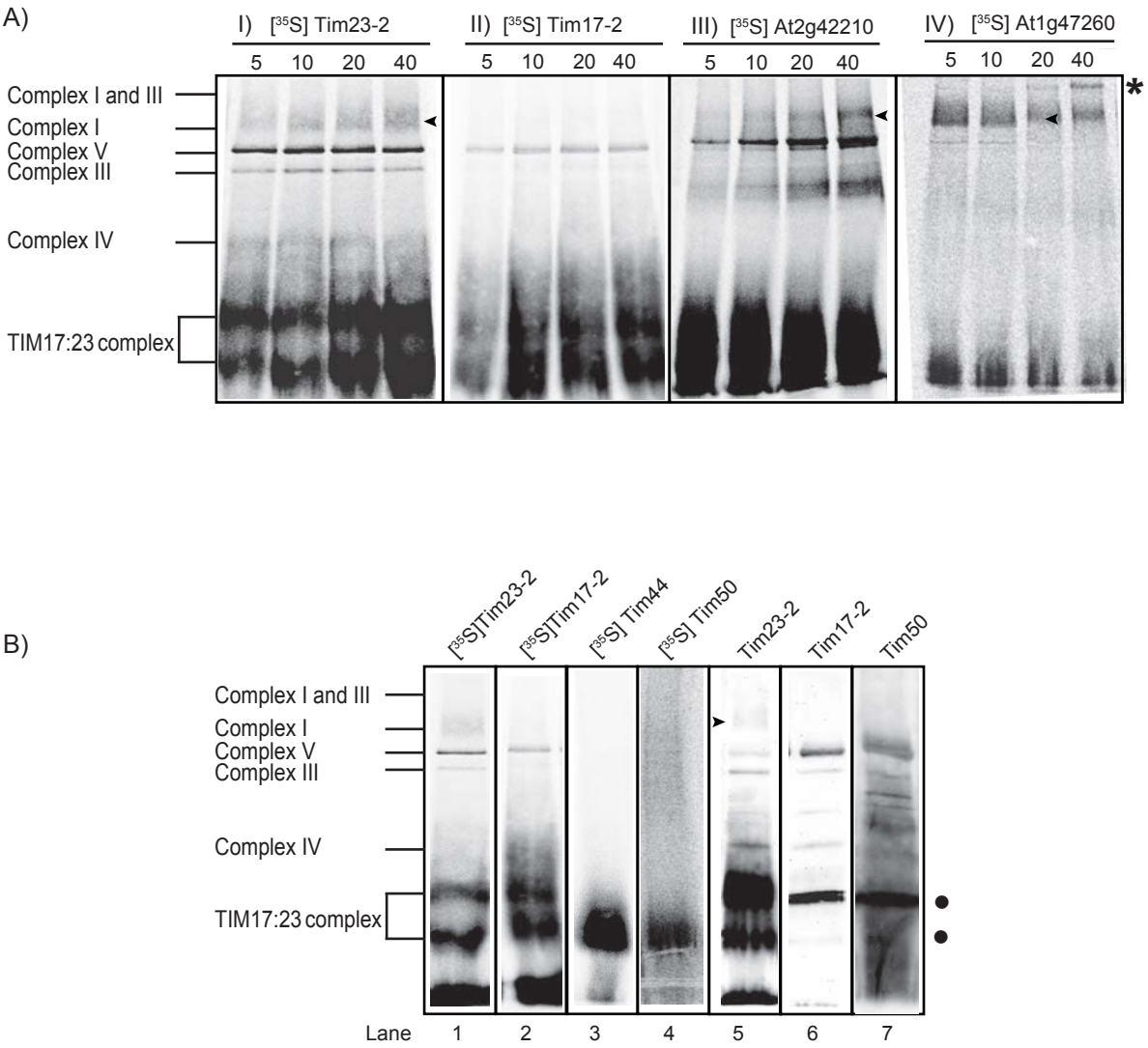

Figure 4.5. Identification of Tim23-2 assembled into TIM17:23 complex and complex I. A) The radiolabelled Tim23-2, Tim17-2, At2g42210 and At1g47260 proteins were imported into mitochondria isolated from Col-0 (wild-type). Impoort was stopped at 5, 10, 20, 40 min. After the import assay, mitochondrial proteins were resolved by one-dimensional BN-PAGE. The gels were Coomassie stained, dried and exposed to phosphor-imaging plates. The assembly of radiolabelled proteins into complex I was indicated with the arrow. The shift of At1g47260 from complex I to supercomplex I and III was indicated by the *. B) The radiolabelled Tim23-2, Tim17-2, Tim44 and Tim50 proteins were imported into wild-type mitochondria. The protein samples were resolved by BN-PAGE (Lane 1 to 4). Mitochondria isolated from Col-0 was also resolved by one dimensional BN-PAGE and immunodetected by the antibodies raised against Tim23-2, Tim17-2, Tim50 (Lane 5 to 7). The incorporation of Tim23-2 with complex I was indicated by the arrow. The assemly of Tim50 and Tim44 into Tim17:23 complex was indicated by the ●. The positions of the respiratory complexes and TIM17:23 complex are indicated.

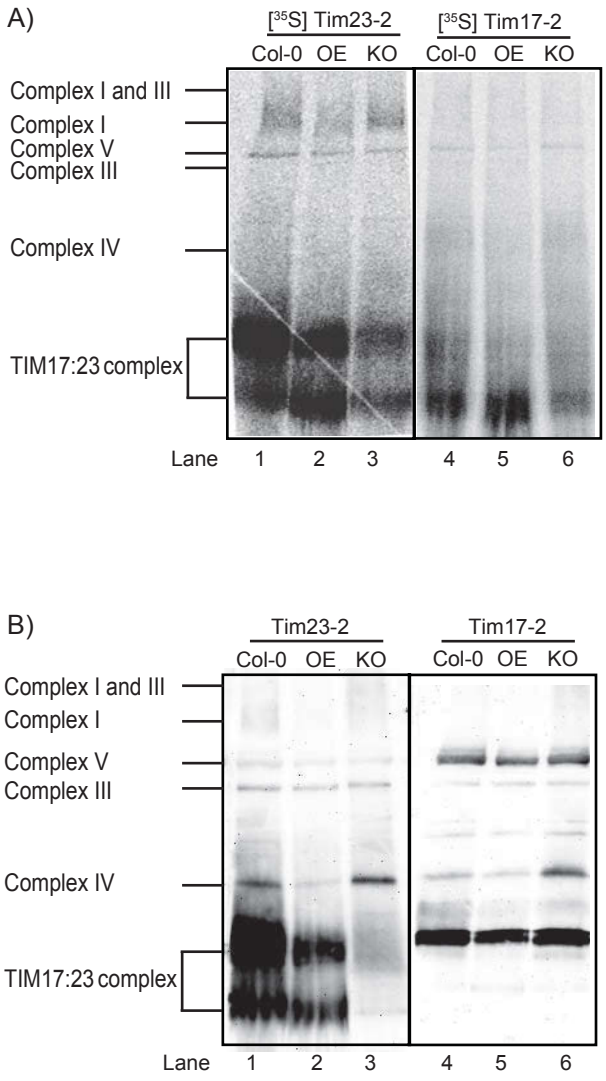

Figure 4.6. The assembly of Tim23-2 into complex I is reduced in the *tim23* OE line. A) The radiolabelled Tim23-2 and Tim17-2 proteins were imported into the mitochondria isolated from the wild type (Col-0), *tim23* OE and *tim23* KO. The protein samples were treated with digitonin and resolved by BN-PAGE. B) The mitochondria isolated from the wild type (Col-0), *tim23* OE and *tim23* KO plants was seprated by BN-PAGE, transferred to PVDF membrane and immunodetected with Tim23-2 and Tim17-2 antibodies. The location of respiratory chain complexes and TIM17:23 complex was indicated. Abbreviations, Col-0: wild type, OE: Tim23 overexpressed line, KO: Tim23 knock-out line.

Chapter 5

Characterizing the connection between the complex I and Tim23-2

Chapter 5 Characterizing the connection between the complex I and Tim23-2

5.1 Introduction

In order to verify the connection between Tim23 and complex I described in the previous chapter, three independent T-DNA insertion mutants (*rug3*, *rpoTmp* and *ndufs4*) all exhibiting a reduction of complex I were further characterized (Kuhn et al., 2011; Kuhn et al., 2009; Meyer et al., 2009). The level of Tim23-2 protein, various other mitochondrial proteins and their import capacity were investigated.

The *rug3* mutant line has a specific defect in splicing the mitochondrial *nad2* gene in Arabidopsis and as a result fails to assemble complex I. BN-PAGE and complex I activity staining revealed an obvious reduction in complex I levels. In contrast, the abundance of complex III and complex V (F_0F_1 ATP synthase) in *rug3* was unaltered (Kuhn et al., 2011). The *rug3* plants were developmentally delayed and displayed mildly curled rosette leaves when grown in a long-day photoperiod (Kuhn et al., 2011).

The RPOTmp is a T3/T7 phage-type RNA polymerase, imported into both mitochondria and plastids (Kuhn et al., 2009). A previous study revealed major differences in transcription abundances between wild type and *rpoTmp* plants. Furthermore, in *rpoTmp* plants, the decreased transcription levels of a subset of

mitochondrial genes were correlated with reduced abundances of respiratory chain complexes I and IV. Immuno-detection following blue-native PAGE analysis showed that complex I and complex IV are barely detectable in mutant mitochondria, while complex III and complex V appeared slightly more abundant than in the wild type (Kuhn et al., 2009). The electron transport capacities of complex I and complex IV in the mutant mitochondria were 85% reduced compared to the wild type (Kuhn et al., 2009).

The NADH dehydrogenase [ubiquinone] fragment S subunit 4 (Ndufs4) is a 18-kDa subunit of complex I. It has been shown that *ndufs4* mutant plants lack complex I activity and the capacity of electron transport chain was impaired (Meyer et al., 2009). However, the respiratory rate was not significantly modified in the *ndufs4* plants (Meyer et al., 2009). The study revealed that the loss of Ndufs4 did not lead to retrograde signals affecting the expression of nucleus-encoded complex I components or other respiratory chain components (Meyer et al., 2009). The plants were much smaller than wild type plants and showed a delay in all developmental stages of growth (Meyer et al., 2009).

The aims of this chapter were to:

1) Analyze the abundance of Tim17 and Tim23 proteins in the complex I mutants and characterize the import capacity of these complex I mutants, to investigate if an independent reduction of complex I results in similar characteristics observed with the *tim23* OE.

2) Characterize the protein profiles of a variety of mitochondrial proteins of the complex I mutant plants and compare to that observed in the *Tim23* OE line.

5.2 Results

5.2.1 The protein levels of Tim17-2 and Tim23-2 were increased in complex I mutants

In order to get a closer insight into the link between Tim23-2 and complex I, the abundance of Tim23-2 and Tim17-2 proteins in all three complex I mutant lines was investigated. Mitochondria were isolated from two-week old water culture tissues of *rug3*, *rpoTmp*, *ndufs4* mutant lines and the wild type plants respectively. Thirty μg of mitochondrial proteins of each line were transferred to a membrane and immuno-detected using Tim23-2 and Tim17-2 antibodies. The results revealed that Tim23-2 protein was greatly induced in *rug3* (Figure 5.1A, Lane 4), *ndufs4* (Figure 5.1A, Lane 5) and *rpoTmp* (Figure 5.1A, Lane 6) compared to wild type (Figure 5.1A, Lane 1). This is consistent with the observation in the *tim23* OE line (Figure 5.1A, Lane 3). No Tim23-2 protein was detected in the *tim23* KO line and the abundance of Tim17-2 was greatly reduced in the *tim23* KO line (Figure 5.1B, Lane 2). Furthermore, the level of Tim17-2 was dramatically increased in *rug3* (Figure 5.1B, Lane 4), *ndufs4* (Figure 5.1B, Lane 5) and *rpoTmp* (Figure 5.1B, Lane 6) mutants which is in agreement with the observation in the *tim23* OE line (Figure 5.1B, Lane 3).

The growth phenotype was also investigated, where the plants were planted into individual pots and grown in a 16/8 h day/night cycle at 22 ^{o}C. Compared with the wild type, the growth of all three complex I mutant lines were delayed in all developmental stages (Figure 5.1C), which is similar to the growth phenotype of *tim23* OE plants (Figure 3.2). The root growth was also much slower compared with the wild type (Figure 5.1D).

5.2.2 *In vitro* protein import was increased in complex I mutants

As the abundance of Tim23-2 and Tim17-2 proteins increased in the complex I mutants, it was of great interest to investigate if their import capacity was also affected. *In vitro* protein import assays of several precursor proteins was carried out with mitochondria isolated from *rug3, rpoTmp, ndufs4* mutants and wild type plants. The precursor proteins, represent the general import pathway (AOX, F_Ad), the dual-targeted protein (MDHAR) and the carrier import pathway (ANT and PiC), were tested. Aliquots were removed at each time point and treated with PK. The PK protected mature protein was quantitated and normalized to the highest time point observed in the wild type. Experiments were repeated on individual mitochondrial preperations at least three times for each precursor protein and the standard mean and standard error are indicated.

In the case of AOX, the amount of mature 32 kDa protein gradually

increased from 5 min to 20 min (Figure 5.2A, I). Compared with the wild type mitochondria, the amount of import into *rug3* mitochondria was at least 2-fold higher (Figure 5.2B, I). The precursor of F_Ad forms a 21 kDa PK protected mature protein following import. The import amount was steadily increasing from 5 min to 20 min (Figure 5.2A, II) and compared with the wild type mitochondria, the amount of import was 2-fold higher in *rug3* mitochondria (Figure 5.2B, II). The dual targeted protein, MDHAR, processed to a 47 kDa protein, increased throughout the timecourse in both lines. (Figure 5.2A, III). The amount of import into *rug3* mitochondria was at least 5-fold higher than the wild type (Figure 5.2B, III).

For the carrier import pathway protein, ANT was processed to a 30 kDa protein upon import into the mitochondria. The amount of import steadily increased throughout the time course (Figure 5.2A, IV). Within the first 15 min, the import amount was not obviously different between the wild type and *rug3* mitochondria (Figure 5.2A, IV). However, the import of ANT into the *rug3* mutant was dramatically increased at 20 min, exhibiting a 4-fold higher amount of import than wild type (Figure 5.2B, IV). The other carrier import pathway protein, PiC, was processed to a 34 kDa mature protein upon import. The amount of mature protein increased throughout the time course (Figure 5.2A, V) and the amount of import into *rug3* mutant mitochondria was 3 fold higher than that observed in wild type (Figure 5.2B, V).

The import of AOX, MDHAR and PiC was also investigated in the *rpoTmp*

and *ndufs4* mutants with the time course of 3 min, 6 min and 12 min. The amount of imported AOX protein accumulated during the time course both in the *rpoTmp* and *ndufs4* mutant lines (Figure 5.3A, I). Compared with wild type, the amount of import of AOX into *ndufs4* and *rpoTmp* was about 2.5-fold and 1.5-fold higher respectively (Figure 5.3B, I). In the case of MDHAR, accumulation of the mature protein from 3 min to 12 min (Figure 5.3A, II) was about 2.5-fold higher in *ndufs4* mutant and 1.5-fold higher in *rpoTmp* mutant compared with the wild type (Figure 5.3B, II). The amount of import of PiC similarly increased from 3 min to 12 min and was about 2.5-fold and 1.5-fold higher in *ndufs4* and *rpoTmp* mutants than the wild type mitochondria (Figure 5.3B, III).

Overall, the import capacity of the general import pathway, the import of a dual-targeted protein and the carrier import pathway were all increased in the *rug3*, *rpoTmp* and *ndufs4* complex I mutant plants.

5.2.3 Protein abundance of *rug3* and *ndufs4* mutant mitochondria

In order to further investigate the changes in protein abundance relating to the changes observed in the import ability, mitochondria were isolated from Col-0, *rug3* and *ndufs4* plants and probed with a series of antibodies against mitochondrial PRAT proteins, protein import components and the respiratory chain components.

In the case of mitochondrial PRAT proteins, it has been identified in section 5.2.1 that the amount of Tim23-2 and Tim17-2 was induced in *rug3* and *ndufs4* mutants compared to wild type (Figure 5.1). Furthermore, the PRAT protein of unknown function encoded by At3g25120 decreased by 50% and Tim22 (encoded by At1g18320/At3g10110) was increased nearly 2.5-fold in both *rug3* and *ndufs4* mutants (Figure 5.4A). Notably, the PRAT protein encoded by At2g42210, which has been identified as a subunit of complex I, was decreased about 70% in *rug3* and *ndufs4* plants (Figure 5.4A).

Analysis of a variety of protein import components revealed that the abundance of the outer membrane proteins Porin, Tom40 and Sam50 did not change between the wild type and the mutants (Figure 5.4B). However, an increase in Tom20 proteins was observed, especially Tom20-2 and Tom20-4, which increased obviously in the *rug3* and *ndufs4* lines (Figure 5.4B). In the case of import components of the inner membrane, there was a increase in the amount of Tim21 with about 40 % and 70% respectively in the *rug3* and *ndufs4* lines (Figure 5.4B), whilst Tim44 was increased about 30-40% (Figure 5.4B). The abundance of Tim50 increased about 30-50% in the *rug3* and *ndufs4* lines and the amount of Tim9 was increased 60% (Figure 5.4B).

In the case of respiratory chain components, the complex I protein Ndufs4 was strongly reduced to 28% in the *rug3* line and not detected at all in the *ndufs4* mutant line (Figure 5.4 C). The abundance of complex I Nad9 was also obviously reduced both in *rug3* and *ndufs4* mutant lines to 60% compared with

wild type mitochondria (Figure 5.4C). The abundance other respiratory chain components such as the α-subunit of ATP synthase was dramatically increased 2-fold in both lines, in contrast the β-subunit of the ATP synthase was slightly reduced in *rug3* and *ndufs4* mutant lines (Figure 5.4C). The Rieske FeS protein of the cytochrome bc_1 complex slightly increased about 20-50% in *rug3* and *ndufs4* (Figure 5.4C) and the level of COX II showed 50% lower than the wild type (Figure 5.4C).

All the data indicates that there is a similar change in the protein profile between the *rug3*, *ndufs4* and the *tim23* OE, suggesting that there may be a direct correlation between the levels of Tim23-2 and complex I.

5.3 Discussion

To verify the observation that an increase in Tim23-2 resulted in a reduction of complex I in the *tim23* OE line, a number of independent mutants that exhibit over 80% reduction in complex I activity were investigated, including the *rug3* mutant (Kühn et al., 2011), the *rpoTmp* mutant (Kuhn et al., 2009) and the *ndufs4* mutant (Meyer et al., 2009). All three mutants displayed much slower plant growth, similar to the phenotype of the *tim23* OE line. In addition, all three mutants displayed an increase in Tim23-2 and Tim17-2, and thus supported the hypothesis that there is a link between the abundance of complex I and Tim23-2. Additionally, the protein abundance of other PRAT proteins and import components showed similar profiles between *tim23* OE, *rug3* and *ndufs4* mutant lines all showing similar increases in the Tom20s,

Tim50, Tim44, Tim21 and Tim9, whilst the PRAT protein of unknown function encoded by At3g25120 was reduced. However, the complex I subunit encoded by At2g42210 is dramatically reduced in the *rug3* and *ndufs4* mutants, which was not observed in the *tim23* OE line. Considering that the protein encoded by At2g42210 is present in the MIC complex (Figure 5.4A), the fact that the three complex I mutants do not contain the MIC complex can explain this disparity.

The up-regulation of various import components, correlate with the increased protein import ability in the complex I mutants, similar to that observed in the *tim23* OE line. However, the carrier import pathway did not change in the *tim23* OE line but was clearly up-regulated in the complex I mutants. The previous studies characterizing these complex I mutants, revealed that the transcripts of intermembrane space chaperones Tim9, Tim8, Tim10 and Tim13, which are all involved in the carrier import pathway, were significantly up-regulated in *rug3* and *ndufs4* knock-out lines (Kuhn et al., 2011). It is possible that these components of the carrier import pathway are not up-regulated in the *tim23* OE line and thus an induction of the carrier import pathway was not observed.

The protein abundance of respiratory chain components showed that COX II was slightly reduced in *rug3* and *ndufs4* mutants, while a minor induction of RISP was observed. It indicates that the protein level of other respiratory chain complexes is not significantly affected by the dysfunction of complex I, which is consistent with the previous study on *rug3* and *ndufs4* (Kuhn et al., 2011; Meyer et al., 2009). With respect to the *rug3* mutant, a minor reduction of complex IV

electron transport capacity was observed, though the accumulation of complex IV, III and V was largely unaffected and the capacity of alternative pathway was overall not affected (Kuhn et al., 2011). With regards to the *ndufs4* mutant, the data showed that the changes observed were limited to complex I and the capacity of alternative pathway was not altered (Meyer et al., 2009). The reasoning that has been proposed is that the mutant plants can survive without complex I because of the presence of the alternative pathway, compensating for the loss of complex I by maintaining the oxidation of matrix NADH (Juszczuk et al., 2011; Sabar et al., 2000).

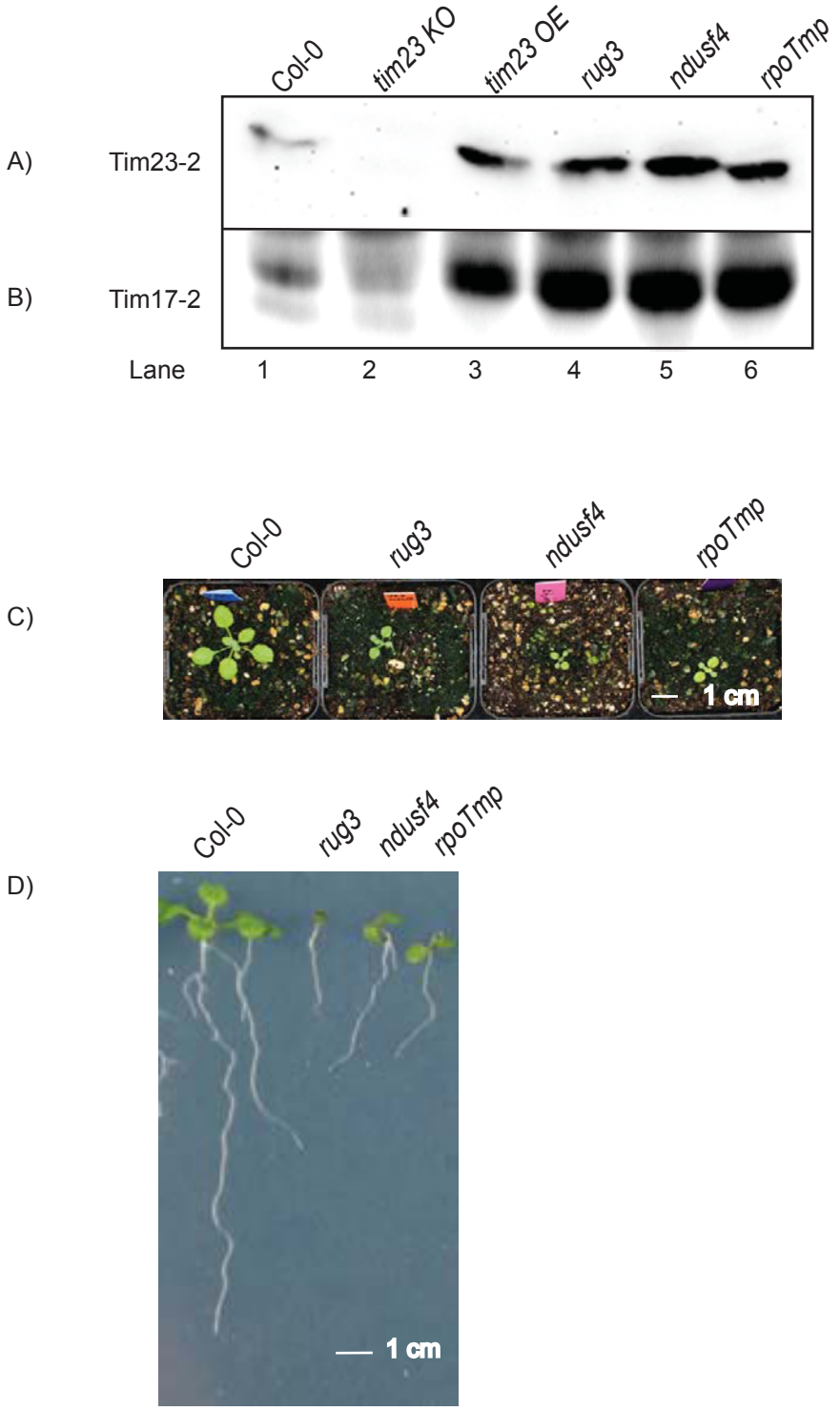

Figure 5.1. The abundance of Tim23 and Tim17 proteins in complex I mutant lines. Mitochondria isolated from the wild type (Col-0), *tim23* KO, *tim23* OE, *rug3* , *rpoTmp* and *ndufs4* mutant lines were immunodetected with A) Tim23-2 antibody and B) Tim17-2 antibody. C) The growth of *rug3* , *rpoTmp* and *ndufs4* mutant lines was delayed compared with wild type. D) The root growth of *rug3* , *rpoTmp* and *ndufs4* mutant lines was delayed compared with wild type. Abbreviations, KO: knock out, OE: overexpressor.

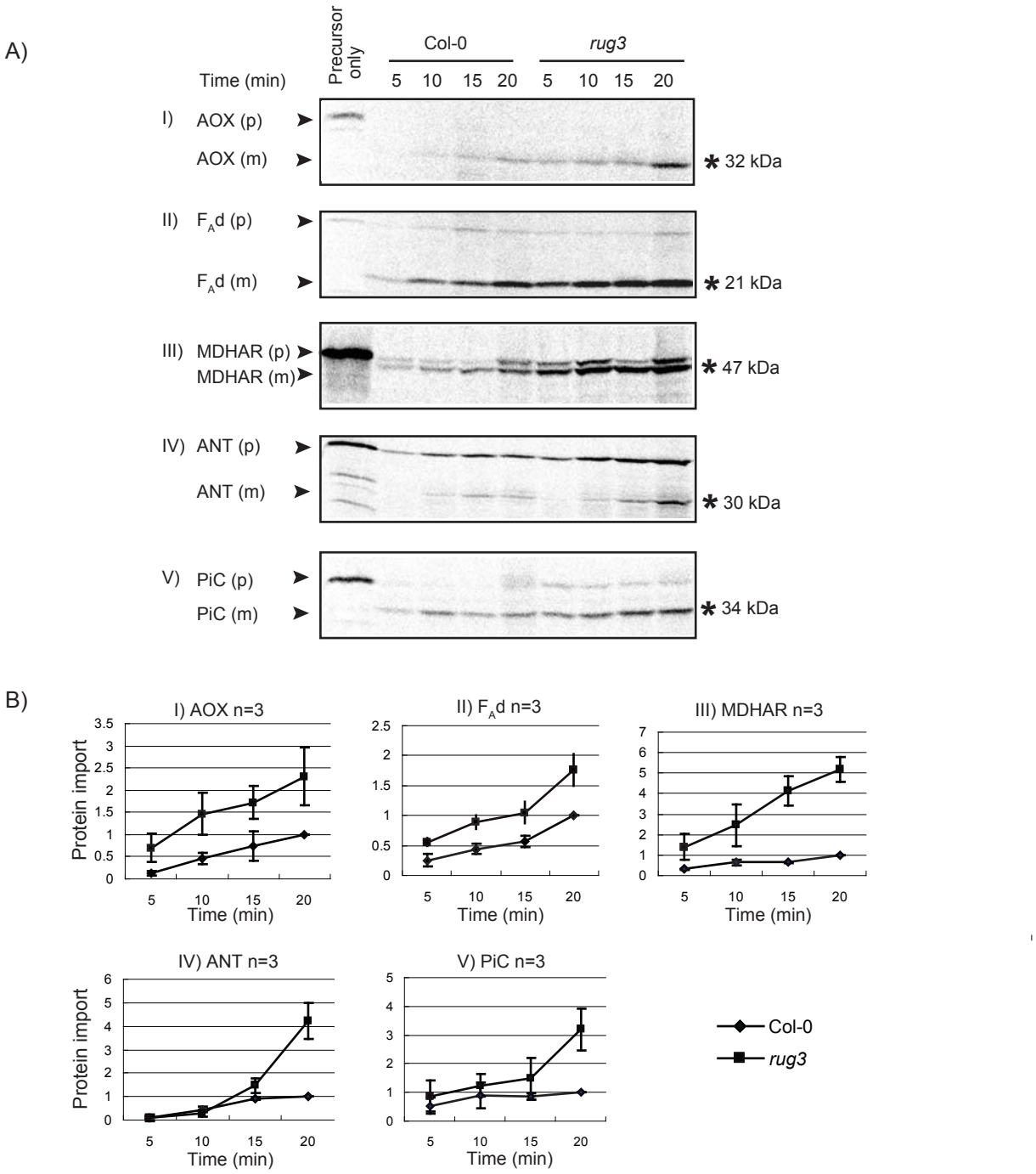

Figure 5.2. The amount of protein import is upregulated in the *rug3* mutant line. A) [^{35}S]-labelled precursor proteins AOX, F_Ad, MDHAR, ANT, PiC were incubated with mitochondrial isolated from wild-type (Col-0) and *rug3* plants under conditions that support protein import. Aliquots were removed at 5, 10, 15 and 20 min and treated with PK. B) The PK protected mature radiolabelled protein was quantitated at each time point and normalised to the highest time point of the wild type for replicate experiments (n ≥ 3 ± SE). Abrreviations, PK: Proteinase K, AOX: Alternative Oxidase, F_Ad: FAd subunit of ATP synthase, MDHAR: monodehydroascorbate reductase, ANT: adenine nucleotide translocator, PiC: phosphate carrier, kDa: kilodalton. The molecular weights of the mature processed bands are indicated by the asterisk.

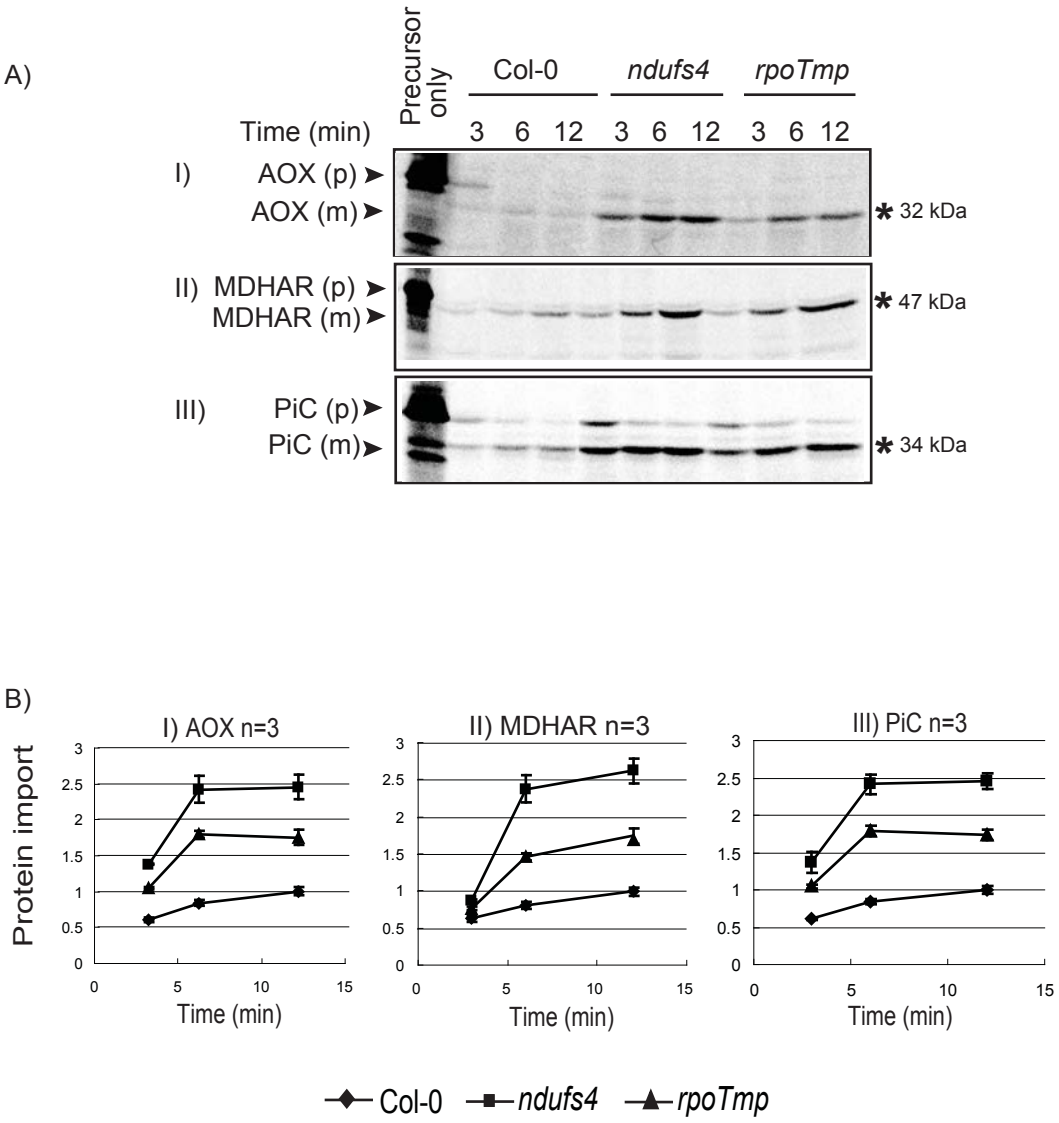

Figure 5.3. The amount of protein import is induced in the *rpoTmp* and *ndufs4* mutant lines. A) [^{35}S]-labelled precursor proteins AOX, MDHAR and PiC were incubated with mitochondrial isolated from wild-type (Col-0), *rpoTmp and ndufs4* plants under conditions that support protein import. Aliquots were removed at 3, 6 and 12 min and treated with PK. B) The PK protected mature radiolabelled protein was quantitated at each time point and normalised to the highest time point of the wild type for replicate experiments (n ≥ 3 ± SE). Abrreviations, PK: Proteinase K, AOX: Alternative Oxidase, MDHAR: monodehydroascorbate reductase, PiC: phosphate carrier, kDa: kilodalton. The molecular weights of the mature processed bands are indicated.

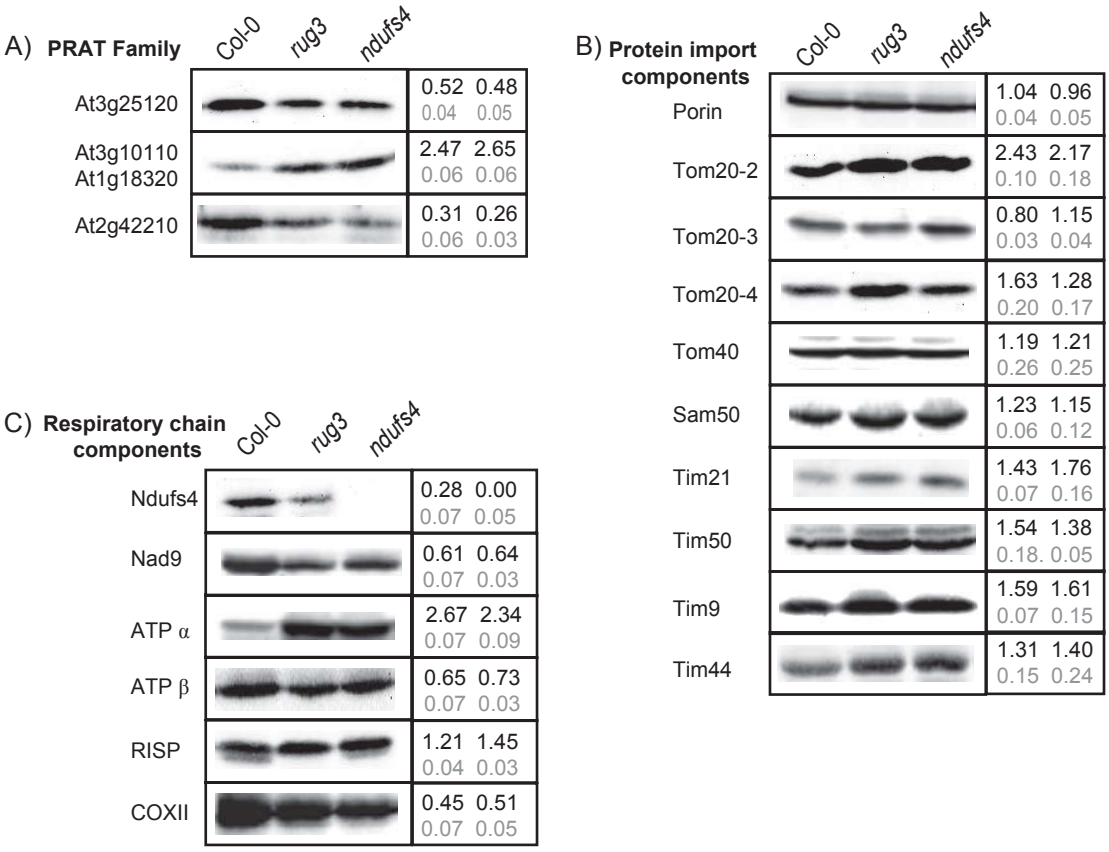

Figure 5.4. Immunodetection of mitochondria isolated from Col-0 (wild-type), *rug3* **and** *ndufs4* **lines.** A) Immunodetection with antibodies raised against various proteins that belong to the mitochondrial Preprotein and amino acid transporters (PRAT) family. B) Immunodetection was also carried out with antibodies raised against various respiratory chain proteins. C) Immunodetection with antibodies raised against various import components. Values represent the average relative abundance ratios of proteins present in the two mutants, compared to Col-0 mitochondria (n ≥ 3 ± SE). Standard errors are indicated below.

Chapter 6

General discussion

Chapter 6 General discussion

6.1 Plant Mitochondria – Similarities and Differences

It is widely accepted that a single endosymbiotic event gave rise to mitochondria in all eukaryotic cells. However, since this event occurred, there has been diversification of mitochondria in various lineages in the 1 to 2 billion years. This is most evident with hydrogenosomes and mitosomes, present in trichomonads and microsporidia respectively (Lithgow and Schneider, 2010; van der Giezen et al., 1997; Waller et al., 2009). In more familiar eukaryotic lineages, such as fungi, animals and plants, mitochondria are also different. Plant mitochondria are known to be different with their animal and fungal counterparts in terms of genome size and mutation rate, as well as the extensive modification of mRNA (Michaud et al., 2010). Biochemically, plant mitochondria are the site of ascorbate and folate synthesis (Smith et al., 2007), and display many other noticeable biochemical features such as the presence of a branched respiratory chain (Rasmusson et al., 2004; Vanlerberghe et al., 1997; Vercesi, 2001). Thus, it is not surprising that plant mitochondria also display many unique features in terms of protein import.

The TOM complex is the best studied protein complex with respect to protein import. It is first characterized from potato and later Arabidopsis (Jansch et al., 1998b; Werhahn et al., 2001). Previous studies have revealed that plant

Tom20(s) are not orthologous to animal or fungal counterparts, and the similarities in size and binding of precursors represent convergent evolution (Carrie et al., 2010b; Perry et al., 2006; Perry et al., 2008; Werhahn et al., 2001). Other noticeable features of the protein import apparatus of plant mitochondria include the integration of MPP into the cytochrome bc_1 complex (Braun et al., 1992; Emmermann et al., 1993; Glaser and Dessi, 1999), the presence of an outer membrane receptor OM64 (Carrie et al., 2010b; Lister et al., 2007), and finally, protein import into plant mitochondria appears to be regulated in a developmental manner (Wood et al., 1996). As a single celled organism, yeast has been widely used as an elegant and informative model to study the mechanism of protein import. In comparison to yeast, protein import in multi-cellular organisms, that display tissue and developmental regulation, is likely to be different in that it is regulated. However, to date, little is known about the regulation of protein import in multi-cellular organisms.

There are few studies investigating the TIM complexes on the mitochondrial inner membrane of plant mitochondria (Murcha et al., 2007; Murcha et al., 2004, 2005a; Murcha et al., 2003; Murcha et al., 2005b). However, studies carried out to date have revealed novel features on Tim17 from plants. Additionally, given the fact that there is a large increase in PRAT gene family in plant mitochondria (Murcha et al., 2007), this project undertook the task to investigate the function of the various Tim17 and Tim23 isoforms in Arabidopsis. It was found that Tim17-2 is an essential protein for viability, and neither of the other two Tim17 proteins, Tim17-1 or Tim17-3, can functionally

replace Tim17-2. Probably, they are not expressed in an appropriate manner that would allow them to compensate Tim17-2. Previous studies in our laboratory have been unsuccessful at expressing any of the Tim17 isoforms under strong constitutive promoters in order to test for functional redundancy. Probably, the strong expression of Tim17 was toxic to the plants. Thus, native promoters need to be employed for this analysis. However, this requires the native promoter to be characterized prior to further studies being carried out. Initial investigations with Tim17-1 promoter in our laboratory indicate that it is a quite weak promoter, given that the expression of a reporter gene driven by the Tim17-1 promoter can be barely detected when transiently transformed into Arabidopsis suspension cells. Thus, the expression of Tim17-1, under the control of the Tim17-2 promoter would be required to determine if the former can functionally complement the latter.

In the case of Tim23, it can be concluded that there is functional redundancy between these proteins, as an inactivation of any single Tim23 gene did not result in any defective phenotype, whereas the inactivation of any two Tim23 proteins did result in a lethal phenotype. Given that Tim23-2 was the most abundant isoform as determined by western blot analysis, and the findings from the knock-out analysis, this suggests that the Tim23 isoforms are functionally redundant, but the expression levels of the other two isoforms, Tim23-1 and Tim23-3, are low.

Finally, from the studies carried out in this thesis, the other conclusion that can be reached is that the amount of the TIM17:23 translocase appears to be a

rate limiting step in protein import into plant mitochondria, as a reduction in the amount of this translocase resulted in a reduction in the rate of protein import, without any apparent growth phenotypic affect. This finding is not surprising given that the TOM complex is more abundant than the TIM17:23 complex. For instance, on 2D gel analysis of plant mitochondria, Tom40 is routinely identified, while Tim17 or Tim23 are identified in significantly less amounts (Heazlewood et al., 2003b; Millar et al., 2001). However, the TIM17:23 complex is clearly identified on a gel, with the size of 110 kDa and 150 kDa (Klodmann et al., 2011). In the experiments carried out in this thesis, the TIM17:23 complex was observed with the size of ~ 100 kDa and ~ 200 kDa. The minor change could be due to the gradient of the BN gel and different protein marker used in the experiments.

6.2 Complex I and TIM17:23

An unexpected outcome of the studies carried out in this thesis was that a direct molecular link between the complex of the mitochondrial respiratory chain (complex I) and a mitochondrial protein import component (Tim23) in Arabidopsis was uncovered. The approximate two-fold over-expression of Tim23, resulting from the T-DNA insertion in the 5' UTR of the gene resulted in a retarded growth phenotype; and the investigation of the cause revealed that the amount of complex I was severely reduced in the *tim23* OE line. The retarded growth phenotype, that was resulted from the reduction in complex I, has been previously characterized for several complex I mutants in both

Arabidopsis and tobacco (Dutilleul et al., 2003; Sabar et al., 2000).

The association of Tim23 with complex I has not been reported previously. It is worth noting that yeast (*Saccharomyces cerevisiae*) lack complex I, and instead can oxidise NADP using Type II NADH dehydrogenases (Buschges et al., 1994; De Vries et al., 1992; Lemaire and Dujardin, 2008; Luttik et al., 1998; Rigoulet et al., 2004). The association of Tim23 with complex I in Arabidopsis is likely to be both dynamic and non-stoichiometric. Firstly, Tim23 is present in much lower amounts compared to complex I. Secondly, most of Tim23 protein appears to be in the TIM17:23 translocase and only a portion of the imported Tim23 appears to assemble into complex I, but yet this is consistently detected. While the actual details of the association have not yet been fully elucidated, it has shown that this association is at least in part mediated by a subunit of complex I encoded by At2g42210 (Meyer et al., 2008b), which is also a member of the PRAT family (Murcha et al., 2007). Thus, given that Tim23 and Tim17 exist as oligomers in the mitochondrial inner membrane, a plausible explanation for the association between Tim23 and complex I is that Tim23 may associate with complex I via interaction with the protein encoded by At2g42210. Further study could be carried out on At2g42210 knock-out or over-expressed mutant lines, to investigate if the change of At2g42210 protein abundance would affect the abundance of Tim23-2 protein, if the assembly of complex I would be affected, or the mutants display the same growth phenotype as *tim23-2* OE.

Besides the association of Tim23 with complex I, it appears that over-expression of Tim23 also results in the destabilization of complex I. Thus,

Tim23 is not an assembly or stability factor, rather it appears to be an instability factor. This is supported by the finding that a reduction in the amount of Tim23 protein, in the *tim23* KO line, has little effect on complex I protein abundance. It was also confirmed in reverse by the fact that a reduction in complex I protein abundance resulted in an increase in Tim23 protein abundance, and the associated changes in protein abundance of other components of the mitochondrial protein import apparatus. Therefore, while the amount of complex I and Tim23 are linked in terms of increasing Tim23, a reduction in Tim23 abundance was not seen to result in an increase in complex I.

It was also observed that the increase in Tim23 in the *tim23* OE line was accompanied by an increase in mitochondrial biogenesis, as evidenced by an increase in the transcript abundance of mitochondrial encoded genes, mitochondrial translation and in transcript abundance of nuclear genes encoding mitochondrial proteins (see attached manuscript). This was also observed with the complex I mutants, but was not as widespread as seen in the *tim23* OE line.

6.3 Regulation of mitochondrial biogenesis

The relationship between complex I, the site of NADH oxidation, and Tim23, which appears to be rate limiting for protein import, provides a direct link between mitochondrial activity and mitochondrial biogenesis. A model explaining the coordination of mitochondrial activity with mitochondrial biogenesis is outlined in Figure 6.1. The TIM17:23 complex exists as a modular

complex of TIM17:23^{sort} and TIM17:23-PAM complex (Schmidt et al., 2010). Based on the evidence presented in the current work, a model for the novel interaction of Tim23 with complex I is proposed. Over-expression of Tim23 results in an increase in the amount of TIM17:23^{sort}, which is consistent with the observed increase in Tim50 and Tim21. The increase in the amount of TIM17:23^{sort} also results in an instability of complex I or an inability to assemble complex I, due to the interaction of Tim23 with complex I subunits. The interaction between Tim23 and complex I is possibly via the complex I protein At2g42210, which is also a member of PRAT family (Murcha et al., 2007). The analysis of the import of complex I subunits in the *tim23 OE* line suggests that the complex I subunits are unable to assemble into complex I, while the assembly other complexes is not affected. This model is also consistent with the presence of the MIC complex in the *tim23* OE line. As there is an increase in abundance of the transcripts encoding complex I and several other respiratory chain components, the increase in TIM17:23^{sort} results in them being imported and laterally inserted into the membrane. The reason that the MIC complex is not observed in the *rug3* line is simply that there is no up-regulation of transcript abundance for these proteins in the *rug3* line as observed in the *tim23* OE line, and thus the MIC complex does not accumulate.

While the nature of the signal or the trigger generated via the interaction between Tim23 and complex I to potentially regulate mitochondrial biogenesis is unknown, it is intriguing to speculate that it may be linked to the REDOX state in the intermembrane space. In addition to acting as an NAD(P)H oxidase in

mitochondria, complex I in plants is also the site for the synthesis of ascorbate, as the enzyme galactono-γ-lactone dehydrogenase (GLDH), which catalyzes the last step of ascorbate biosynthesis, is identified to be one of complex I subunits (Klodmann and Braun, 2011; Pineau et al., 2008). Furthermore, cytochrome c acts as an electron acceptor for ascorbate synthesis, linking ascorbate synthesis to complex I and complex IV (Figure 6.2) (Jang and Han, 2006). The presence of the disulphide relay system in the mitochondrial intermembrane space (Deponte and Hell, 2009) could act as a REDOX signalling system as it has been shown that a decrease in complex I results in an increase in ascorbate (Foyer and Noctor, 2011). Thus, these findings can link the activity of the mitochondrial respiratory chain and organelle biogenesis, resulting in a redox generated trigger to regulate gene expression. Notably, it is consistent with the fact that the Mia40-Erv1 disulfide relay system in plant mitochondria differs that in yeast, with Mia40 shown not to be an essential protein (Carrie et al., 2010a).

It is worth noting that an interaction of the TIM17:23 complex with respiratory chain complexes has been previously reported in yeast, where Tim21 mediates an interaction with the cytochrome bc_1 complex (van der Laan et al., 2006a). Although the physiological consequences of this interaction are not known, in Arabidopsis the Tim17:23 complex is also seen to interact with the cytochrome bc_1 complex via Tim21 (Dr Monika Murcha – personal communication). As complex I and complex III form a supercomplex in Arabidopsis (Dudkina et al., 2005Dudkina et al., 2005), it appears that subunits

of the TIM17:23 translocase may play a role in the formation of this supercomplex. However, Tim23 could only be readily be detected in complex I, never observed to be associated with the supercomplex I and III in this study.

It is also worth to note that the TIM17:23 translocase may not be the only inner membrane translocase associated with complex I. Analysis of the Arabidopsis 2D proteome identified that At1g18320 and At3g10110 migrated with complex I (Klodmann et al., 2011). This raises the possibility that the TIM22 translocase may also be associated with complex I, as At1g18320 and At3g10110 have previously been shown to complement a yeast Tim22 mutant and putatively been identified as Arabidopsis Tim22. Noting that the carrier import pathway was up-regulated in the complex I mutants, but not in *tim23* OE line, it is consistent with the proposal that the TIM22 complex, which is responsible for the carrier import pathway, may also be associated with complex I in plant mitochondria.

Conclusions

Overall, this study revealed a novel interaction between the TIM17:23 translocase and complex I of the respiratory chain that may serve as an elegant system to coordinate mitochondrial activity and biogenesis in Arabidopsis.

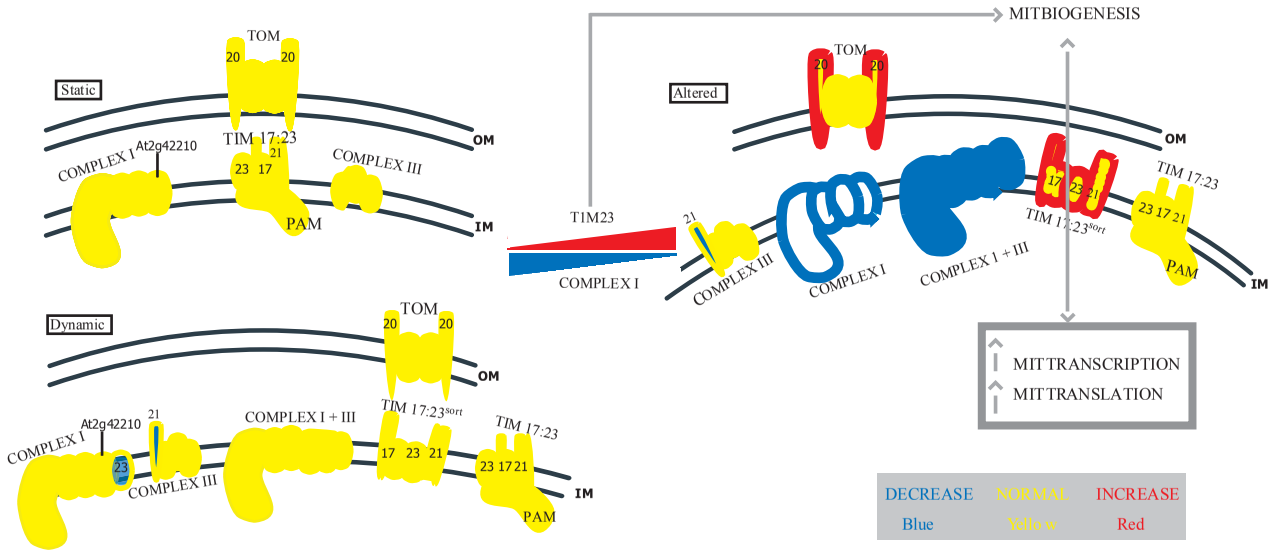

Figure 6.1. A model for the proposed interaction of TIM23 complex with complex I in mitochondria from Arabidopsis. The static model represents the complexes which have been identified so far. The dynamic model represents the interactions of the complexes with Tim23 and Tim21. As most of the Tim23 and Tim21 are present in the TIM17:23 complex and the respiratory chain complexes are more abundant than TIM17:23 complex, the incorporation of Tim23 into complex I and Tim21 into complex III (indicated in blue) is not in stoichiometric levels. Tim21 and Tim23 are not present in supercomplex I and III. The other PRAT protein, encoded by At2g42210, present in complex I is not present in supercomplex I and III either. The right panel shows that the overexpression of Tim23 results in an increase in the amount Tom20 and Tim17:23^{sort} complex (indicated in red). The monomeric complex I and supercomplex I and III are reduced (indicated in blue). Furhermore, there are global changes in the transcriptome appearing to require mitochondrial transcription and translation. Abbreviations, OM: outer membrane, IM: inner membrane.

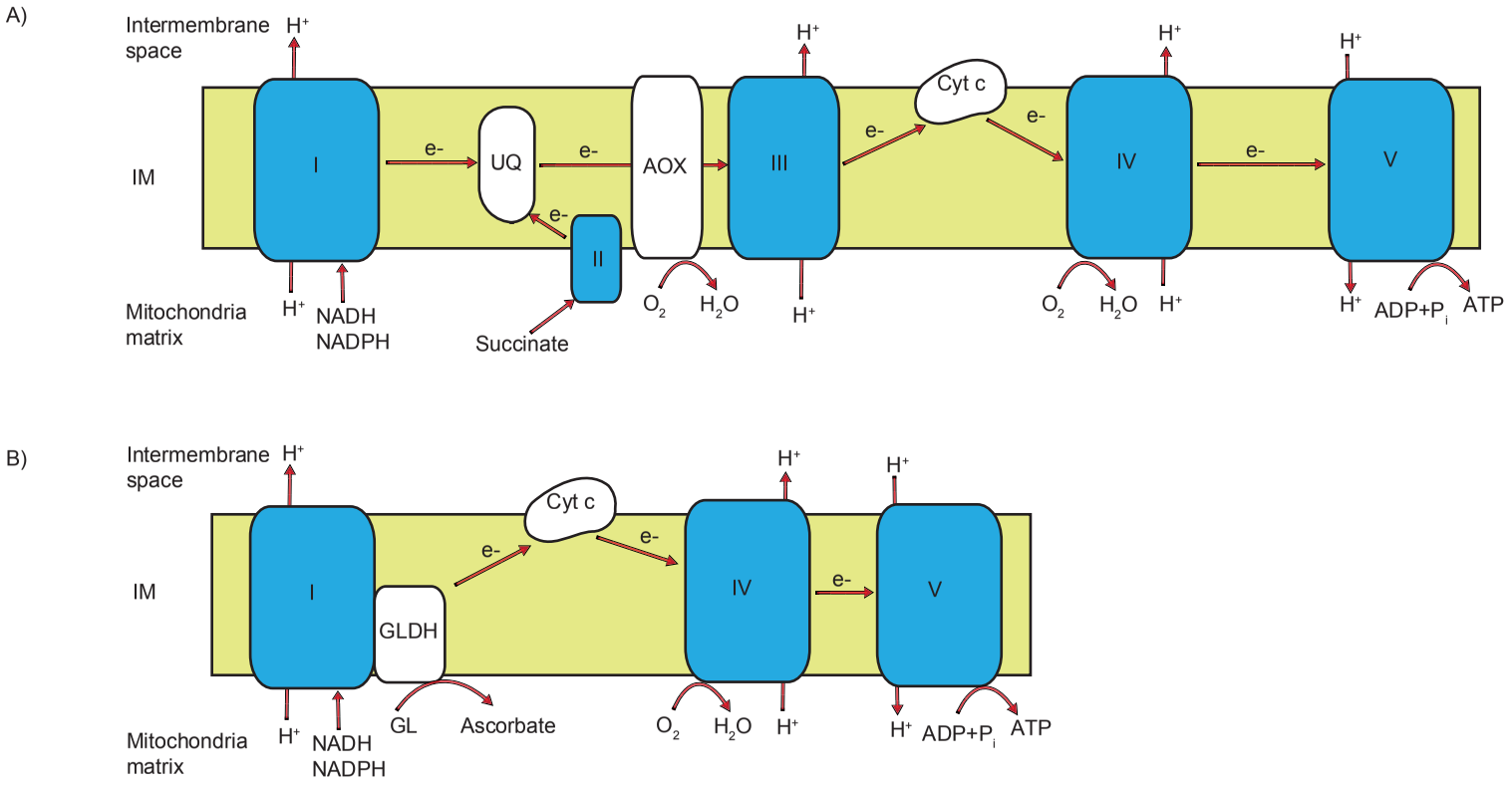

Figure 6.2. Model of plant mitochondrial electron transport chain and the interaction with GLDH. A) The general model of plant mitochondrial eletron transport chain. B) GLDH, the enzyme catalyzing GL into ascorbate, is one of the plant complex I subunits. GLDH feeds electrons into Cyt c, that acts as an electron acceptor, linking complex I and complex IV. Abbreviations, GLDH: galactono-γ-lactone dehydrogenase, UQ: ubiquinone, AOX: alternative oxidase.

References

References

Abe, Y., Shodai, T., Muto, T., Mihara, K., Torii, H., Nishikawa, S., Endo, T., and Kohda, D. (2000). Structural basis of presequence recognition by the mitochondrial protein import receptor Tom20. Cell *100*, 551-560.

Acin-Perez, R., Bayona-Bafaluy, M.P., Fernandez-Silva, P., Moreno-Loshuertos, R., Perez-Martos, A., Bruno, C., MoAcin-Perez, R., Fernandez-Silva, P., Peleato, M.L., Perez-Martos, A., and Enriquez, J.A. (2008). Respiratory active mitochondrial supercomplexes. Mol Cell *32*, 529-539.

Affourtit, C., Krab, K., and Moore, A.L. (2001). Control of plant mitochondrial respiration. Biochim Biophys Acta *1504*, 58-69.

Ahting, U., Thun, C., Hegerl, R., Typke, D., Nargang, F.E., Neupert, W., and Nussberger, S. (1999). The TOM core complex: the general protein import pore of the outer membrane of mitochondria. J Cell Biol *147*, 959-968.

Albrecht, R., Rehling, P., Chacinska, A., Brix, J., Cadamuro, S.A., Volkmer, R., Guiard, B., Pfanner, N., and Zeth, K. (2006). The Tim21 binding domain connects the preprotein translocases of both mitochondrial membranes. EMBO Rep *7*, 1233-1238.

Alcock, F., Clements, A., Webb, C., and Lithgow, T. (2010). Evolution. Tinkering inside the organelle. Science *327*, 649-650.

Alder, N.N., Sutherland, J., Buhring, A.I., Jensen, R.E., and Johnson, A.E. (2008). Quaternary structure of the mitochondrial TIM23 complex reveals dynamic association between Tim23p and other subunits. Mol Biol Cell *19*, 159-170.

Angell, J.E., Lindner, D.J., Shapiro, P.S., Hofmann, E.R., and Kalvakolanu, D.V. (2000). Identification of GRIM-19, a novel cell death-regulatory gene induced by the interferon-beta and retinoic acid combination, using a genetic approach. J Biol Chem *275*, 33416-33426.

Arnold, I., Pfeiffer, K., Neupert, W., Stuart, R.A., and Schagger, H. (1998). Yeast mitochondrial F1F0-ATP synthase exists as a dimer: identification of three dimer-specific subunits. EMBO J *17*, 7170-7178.

Baud, C., de Marcos-Lousa, C., and Tokatlidis, K. (2007). Molecular

interactions of the mitochondrial Tim12 translocase subunit. Protein Pept Lett *14*, 597-600.

Bauer, M.F., Sirrenberg, C., Neupert, W., and Brunner, M. (1996). Role of Tim23 as voltage sensor and presequence receptor in protein import into mitochondria. Cell *87*, 33-41.

Bauwe, H., Hagemann, M., and Fernie, A.R. (2010). Photorespiration: players, partners and origin. Trends Plant Sci *15*, 330-336.

Becker, L., Bannwarth, M., Meisinger, C., Hill, K., Model, K., Krimmer, T., Casadio, R., Truscott, K.N., Schulz, G.E., Pfanner, N.*, et al.* (2005). Preprotein translocase of the outer mitochondrial membrane: reconstituted Tom40 forms a characteristic TOM pore. J Mol Biol *353*, 1011-1020.

Bellomo, F., Piccoli, C., Cocco, T., Scacco, S., Papa, F., Gaballo, A., Boffoli, D., Signorile, A., D'Aprile, A., Scrima, R.*, et al.* (2006). Regulation by the cAMP cascade of oxygen free radical balance in mammalian cells. Antioxid Redox Signal *8*, 495-502.

Berry, E.A., Guergova-Kuras, M., Huang, L.S., and Crofts, A.R. (2000). Structure and function of cytochrome bc complexes. Annu Rev Biochem *69*, 1005-1075.

Berthold, J., Bauer, M.F., Schneider, H.C., Klaus, C., Dietmeier, K., Neupert, W., and Brunner, M. (1995). The MIM complex mediates preprotein translocation across the mitochondrial inner membrane and couples it to the mt-Hsp70/ATP driving system. Cell *81*, 1085-1093.

Boekema, E.J., and Braun, H.P. (2007). Supramolecular structure of the mitochondrial oxidative phosphorylation system. J Biol Chem *282*, 1-4.

Bolliger, L., Deloche, O., Glick, B.S., Georgopoulos, C., Jeno, P., Kronidou, N., Horst, M., Morishima, N., and Schatz, G. (1994). A mitochondrial homolog of bacterial GrpE interacts with mitochondrial hsp70 and is essential for viability. EMBO J *13*, 1998-2006.

Braun, H.P., Emmermann, M., Kruft, V., and Schmitz, U.K. (1992). The general mitochondrial processing peptidase from potato is an integral part of cytochrome c reductase of the respiratory chain. EMBO J *11*, 3219-3227.

Braun, H.P., and Schmitz, U.K. (1997). The mitochondrial processing peptidase. Int J Biochem Cell Biol *29*, 1043-1045.

Brix, J., Dietmeier, K., and Pfanner, N. (1997). Differential recognition of preproteins by the purified cytosolic domains of the mitochondrial import

receptors Tom20, Tom22, and Tom70. J Biol Chem *272*, 20730-20735.

Brix, J., Rudiger, S., Bukau, B., Schneider-Mergener, J., and Pfanner, N. (1999). Distribution of binding sequences for the mitochondrial import receptors Tom20, Tom22, and Tom70 in a presequence-carrying preprotein and a non-cleavable preprotein. J Biol Chem *274*, 16522-16530.

Brix, J., Ziegler, G.A., Dietmeier, K., Schneider-Mergener, J., Schulz, G.E., and Pfanner, N. (2000). The mitochondrial import receptor Tom70: identification of a 25 kDa core domain with a specific binding site for preproteins. J Mol Biol *303*, 479-488.

Budde, S.M., van den Heuvel, L.P., Janssen, A.J., Smeets, R.J., Buskens, C.A., DeMeirleir, L., Van Coster, R., Baethmann, M., Voit, T., Trijbels, J.M.*, et al.* (2000). Combined enzymatic complex I and III deficiency associated with mutations in the nuclear encoded NDUFS4 gene. Biochem Biophys Res Commun *275*, 63-68.

Bukau, B., Weissman, J., and Horwich, A. (2006). Molecular chaperones and protein quality control. Cell *125*, 443-451.

Buschges, R., Bahrenberg, G., Zimmermann, M., and Wolf, K. (1994). NADH: ubiquinone oxidoreductase in obligate aerobic yeasts. Yeast *10*, 475-479.

Cardol, P., Gonzalez-Halphen, D., Reyes-Prieto, A., Baurain, D., Matagne, R.F., and Remacle, C. (2005). The mitochondrial oxidative phosphorylation proteome of Chlamydomonas reinhardtii deduced from the Genome Sequencing Project. Plant Physiol *137*, 447-459.

Carrie, C., Giraud, E., Duncan, O., Xu, L., Wang, Y., Huang, S., Clifton, R., Murcha, M., Filipovska, A., Rackham, O.*, et al.* (2010a). Conserved and novel functions for Arabidopsis thaliana MIA40 in assembly of proteins in mitochondria and peroxisomes. J Biol Chem *285*, 36138-36148.

Carrie, C., Murcha, M.W., and Whelan, J. (2010b). An in silico analysis of the mitochondrial protein import apparatus of plants. BMC Plant Biol *10*, 249.

Cavalier-Smith, T. (2006). Origin of mitochondria by intracellular enslavement of a photosynthetic purple bacterium. Proc Biol Sci *273*, 1943-1952.

Chacinska, A., Koehler, C.M., Milenkovic, D., Lithgow, T., and Pfanner, N. (2009). Importing mitochondrial proteins: machineries and mechanisms. Cell *138*, 628-644.

Chacinska, A., Lind, M., Frazier, A.E., Dudek, J., Meisinger, C., Geissler, A., Sickmann, A., Meyer, H.E., Truscott, K.N., Guiard, B.*, et al.* (2005).

Mitochondrial presequence translocase: switching between TOM tethering and motor recruitment involves Tim21 and Tim17. Cell *120*, 817-829.

Chacinska, A., Pfanner, N., and Meisinger, C. (2002). How mitochondria import hydrophilic and hydrophobic proteins. Trends Cell Biol *12*, 299-303.

Chacinska, A., Pfannschmidt, S., Wiedemann, N., Kozjak, V., Sanjuan Szklarz, L.K., Schulze-Specking, A., Truscott, K.N., Guiard, B., Meisinger, C., and Pfanner, N. (2004). Essential role of Mia40 in import and assembly of mitochondrial intermembrane space proteins. EMBO J *23*, 3735-3746.

Chacinska, A., Rehling, P., Guiard, B., Frazier, A.E., Schulze-Specking, A., Pfanner, N., Voos, W., and Meisinger, C. (2003). Mitochondrial translocation contact sites: separation of dynamic and stabilizing elements in formation of a TOM-TIM-preprotein supercomplex. EMBO J *22*, 5370-5381.

Chacinska, A., van der Laan, M., Mehnert, C.S., Guiard, B., Mick, D.U., Hutu, D.P., Truscott, K.N., Wiedemann, N., Meisinger, C., Pfanner, N.*, et al.* (2010). Distinct forms of mitochondrial TOM-TIM supercomplexes define signal-dependent states of preprotein sorting. Mol Cell Biol *30*, 307-318.

Chan, N.C., Likic, V.A., Waller, R.F., Mulhern, T.D., and Lithgow, T. (2006). The C-terminal TPR domain of Tom70 defines a family of mitochondrial protein import receptors found only in animals and fungi. J Mol Biol *358*, 1010-1022.

Chan, N.C., and Lithgow, T. (2008). The peripheral membrane subunits of the SAM complex function codependently in mitochondrial outer membrane biogenesis. Mol Biol Cell *19*, 126-136.

Chew, O., Rudhe, C., Glaser, E., and Whelan, J. (2003a). Characterization of the targeting signal of dual-targeted pea glutathione reductase. Plant Mol Biol *53*, 341-356.

Chew, O., Whelan, J., and Millar, A.H. (2003b). Molecular definition of the ascorbate-glutathione cycle in Arabidopsis mitochondria reveals dual targeting of antioxidant defenses in plants. J Biol Chem *278*, 46869-46877.

Chupin, V., Leenhouts, J.M., de Kroon, A.I., and de Kruijff, B. (1996). Secondary structure and topology of a mitochondrial presequence peptide associated with negatively charged micelles. A 2D H-NMR study. Biochemistry *35*, 3141-3146.

Clements, A., Bursac, D., Gatsos, X., Perry, A.J., Civciristov, S., Celik, N., Likic, V.A., Poggio, S., Jacobs-Wagner, C., Strugnell, R.A.*, et al.* (2009). The reducible complexity of a mitochondrial molecular machine. Proc Natl Acad Sci U S A *106*, 15791-15795.

Clifton, R., Millar, A.H., and Whelan, J. (2006). Alternative oxidases in Arabidopsis: a comparative analysis of differential expression in the gene family provides new insights into function of non-phosphorylating bypasses. Biochim Biophys Acta *1757*, 730-741.

Conte, L., Trumpower, B.L., and Zara, V. (2011). Bcs1p can rescue a large and productive cytochrome bc(1) complex assembly intermediate in the inner membrane of yeast mitochondria. Biochim Biophys Acta *1813*, 91-101.

Conte, L., and Zara, V. (2011). The Rieske Iron-Sulfur Protein: Import and Assembly into the Cytochrome bc(1) Complex of Yeast Mitochondria. Bioinorg Chem Appl *2011*, 363941.

Crivellone, M.D., Wu, M.A., and Tzagoloff, A. (1988). Assembly of the mitochondrial membrane system. Analysis of structural mutants of the yeast coenzyme QH2-cytochrome c reductase complex. J Biol Chem *263*, 14323-14333.

Cruciat, C.M., Brunner, S., Baumann, F., Neupert, W., and Stuart, R.A. (2000). The cytochrome bc1 and cytochrome c oxidase complexes associate to form a single supracomplex in yeast mitochondria. J Biol Chem *275*, 18093-18098.

Cruciat, C.M., Hell, K., Folsch, H., Neupert, W., and Stuart, R.A. (1999). Bcs1p, an AAA-family member, is a chaperone for the assembly of the cytochrome bc(1) complex. EMBO J *18*, 5226-5233.

Curran, S.P., Leuenberger, D., Oppliger, W., and Koehler, C.M. (2002). The Tim9p-Tim10p complex binds to the transmembrane domains of the ADP/ATP carrier. EMBO J *21*, 942-953.

D'Silva, P.R., Schilke, B., Hayashi, M., and Craig, E.A. (2008). Interaction of the J-protein heterodimer Pam18/Pam16 of the mitochondrial import motor with the translocon of the inner membrane. Mol Biol Cell *19*, 424-432.

Davis, A.J., Alder, N.N., Jensen, R.E., and Johnson, A.E. (2007). The Tim9p/10p and Tim8p/13p complexes bind to specific sites on Tim23p during mitochondrial protein import. Mol Biol Cell *18*, 475-486.

Davis, P.J., and Davis, F.B. (2002). Nongenomic actions of thyroid hormone on the heart. Thyroid *12*, 459-466.

de Duve, C. (2007). The origin of eukaryotes: a reappraisal. Nat Rev Genet *8*, 395-403.

De Vries, S., Van Witzenburg, R., Grivell, L.A., and Marres, C.A. (1992).

Primary structure and import pathway of the rotenone-insensitive NADH-ubiquinone oxidoreductase of mitochondria from Saccharomyces cerevisiae. Eur J Biochem *203*, 587-592.

Dekker, P.J., Keil, P., Rassow, J., Maarse, A.C., Pfanner, N., and Meijer, M. (1993). Identification of MIM23, a putative component of the protein import machinery of the mitochondrial inner membrane. FEBS Lett *330*, 66-70.

Dekker, P.J., Martin, F., Maarse, A.C., Bomer, U., Muller, H., Guiard, B., Meijer, M., Rassow, J., and Pfanner, N. (1997). The Tim core complex defines the number of mitochondrial translocation contact sites and can hold arrested preproteins in the absence of matrix Hsp70-Tim44. EMBO J *16*, 5408-5419.

Dekker, P.J., Ryan, M.T., Brix, J., Muller, H., Honlinger, A., and Pfanner, N. (1998). Preprotein translocase of the outer mitochondrial membrane: molecular dissection and assembly of the general import pore complex. Mol Cell Biol *18*, 6515-6524.

Deponte, M., and Hell, K. (2009). Disulphide bond formation in the intermembrane space of mitochondria. J Biochem *146*, 599-608.

Dessi, P., Smith, M.K., Day, D.A., and Whelan, J. (1996). Characterization of the import pathway of the F(A)d subunit of mitochondrial ATP synthase into isolated plant mitochondria. Arch Biochem Biophys *335*, 358-368.

Dienhart, M.K., and Stuart, R.A. (2008). The yeast Aac2 protein exists in physical association with the cytochrome bc1-COX supercomplex and the TIM23 machinery. Mol Biol Cell *19*, 3934-3943.

Dietmeier, K., Honlinger, A., Bomer, U., Dekker, P.J., Eckerskorn, C., Lottspeich, F., Kubrich, M., and Pfanner, N. (1997). Tom5 functionally links mitochondrial preprotein receptors to the general import pore. Nature *388*, 195-200.

Djafarzadeh, R., Kerscher, S., Zwicker, K., Radermacher, M., Lindahl, M., Schagger, H., and Brandt, U. (2000). Biophysical and structural characterization of proton-translocating NADH-dehydrogenase (complex I) from the strictly aerobic yeast Yarrowia lipolytica. Biochim Biophys Acta *1459*, 230-238.

Dolezal, P., Likic, V., Tachezy, J., and Lithgow, T. (2006). Evolution of the molecular machines for protein import into mitochondria. Science *313*, 314-318.
Donzeau, M., Kaldi, K., Adam, A., Paschen, S., Wanner, G., Guiard, B., Bauer, M.F., Neupert, W., and Brunner, M. (2000). Tim23 links the inner and outer mitochondrial membranes. Cell *101*, 401-412.

Dudkina, N.V., Eubel, H., Keegstra, W., Boekema, E.J., and Braun, H.P. (2005). Structure of a mitochondrial supercomplex formed by respiratory-chain complexes I and III. Proc Natl Acad Sci U S A *102*, 3225-3229.
Dudkina, N.V., Kouril, R., Peters, K., Braun, H.P., and Boekema, E.J. (2010). Structure and function of mitochondrial supercomplexes. Biochim Biophys Acta *1797*, 664-670.

Dutilleul, C., Driscoll, S., Cornic, G., De Paepe, R., Foyer, C.H., and Noctor, G. (2003). Functional mitochondrial complex I is required by tobacco leaves for optimal photosynthetic performance in photorespiratory conditions and during transients. Plant Physiol *131*, 264-275.

Embley, T.M., and Martin, W. (2006). Eukaryotic evolution, changes and challenges. Nature *440*, 623-630.

Emmermann, M., Braun, H.P., Arretz, M., and Schmitz, U.K. (1993). Characterization of the bifunctional cytochrome c reductase-processing peptidase complex from potato mitochondria. J Biol Chem *268*, 18936-18942.

Endo, T., and Yamano, K. (2009). Multiple pathways for mitochondrial protein traffic. Biol Chem *390*, 723-730.

Endo, T., Yamano, K., and Kawano, S. (2010). Structural basis for the disulfide relay system in the mitochondrial intermembrane space. Antioxid Redox Signal *13*, 1359-1373.

Eriksson, A.C., Sjoling, S., and Glaser, E. (1996). Characterization of the bifunctional mitochondrial processing peptidase (MPP)/bc1 complex in Spinacia oleracea. J Bioenerg Biomembr *28*, 285-292.

Esaki, M., Kanamori, T., Nishikawa, S., Shin, I., Schultz, P.G., and Endo, T. (2003). Tom40 protein import channel binds to non-native proteins and prevents their aggregation. Nat Struct Biol *10*, 988-994.

Esaki, M., Shimizu, H., Ono, T., Yamamoto, H., Kanamori, T., Nishikawa, S., and Endo, T. (2004). Mitochondrial protein import. Requirement of presequence elements and tom components for precursor binding to the TOM complex. J Biol Chem *279*, 45701-45707.

Eubel, H., Heinemeyer, J., Sunderhaus, S., and Braun, H.P. (2004). Respiratory chain supercomplexes in plant mitochondria. Plant Physiol Biochem *42*, 937-942.

Eubel, H., Jansch, L., and Braun, H.P. (2003). New insights into the respiratory chain of plant mitochondria. Supercomplexes and a unique composition of complex II. Plant Physiol *133*, 274-286.

Fearnley, I.M., Carroll, J., and Walker, J.E. (2007). Proteomic analysis of the subunit composition of complex I (NADH:ubiquinone oxidoreductase) from bovine heart mitochondria. Methods Mol Biol *357*, 103-125.

Fisher, N., Bourges, I., Hill, P., Brasseur, G., and Meunier, B. (2004). Disruption of the interaction between the Rieske iron-sulfur protein and cytochrome b in the yeast bc1 complex owing to a human disease-associated mutation within cytochrome b. Eur J Biochem *271*, 1292-1298.

Foyer, C.H., and Noctor, G. (2011). Ascorbate and glutathione: the heart of the redox hub. Plant Physiol *155*, 2-18.

Frazier, A.E., Dudek, J., Guiard, B., Voos, W., Li, Y., Lind, M., Meisinger, C., Geissler, A., Sickmann, A., Meyer, H.E.*, et al.* (2004). Pam16 has an essential role in the mitochondrial protein import motor. Nat Struct Mol Biol *11*, 226-233.

Gabriel, K., Egan, B., and Lithgow, T. (2003). Tom40, the import channel of the mitochondrial outer membrane, plays an active role in sorting imported proteins. EMBO J *22*, 2380-2386.

Gebert, N., Chacinska, A., Wagner, K., Guiard, B., Koehler, C.M., Rehling, P., Pfanner, N., and Wiedemann, N. (2008). Assembly of the three small Tim proteins precedes docking to the mitochondrial carrier translocase. EMBO Rep *9*, 548-554.

Geissler, A., Chacinska, A., Truscott, K.N., Wiedemann, N., Brandner, K., Sickmann, A., Meyer, H.E., Meisinger, C., Pfanner, N., and Rehling, P. (2002). The mitochondrial presequence translocase: an essential role of Tim50 in directing preproteins to the import channel. Cell *111*, 507-518.

Geissler, A., Rassow, J., Pfanner, N., and Voos, W. (2001). Mitochondrial import driving forces: enhanced trapping by matrix Hsp70 stimulates translocation and reduces the membrane potential dependence of loosely folded preproteins. Mol Cell Biol *21*, 7097-7104.

Gentle, I., Gabriel, K., Beech, P., Waller, R., and Lithgow, T. (2004). The Omp85 family of proteins is essential for outer membrane biogenesis in mitochondria and bacteria. J Cell Biol *164*, 19-24.

Glaser, E., and Dessi, P. (1999). Integration of the mitochondrial-processing peptidase into the cytochrome bc1 complex in plants. J Bioenerg Biomembr *31*, 259-274.

Glaser, E., Eriksson, A., and Sjoling, S. (1994). Bifunctional role of the bc1 complex in plants. Mitochondrial bc1 complex catalyses both electron transport

and protein processing. FEBS Lett *346*, 83-87.

Glaser, E., Sjoling, S., Tanudji, M., and Whelan, J. (1998). Mitochondrial protein import in plants. Signals, sorting, targeting, processing and regulation. Plant Mol Biol *38*, 311-338.

Gordon, D.M., Kogan, M., Knight, S.A., Dancis, A., and Pain, D. (2001). Distinct roles for two N-terminal cleaved domains in mitochondrial import of the yeast frataxin homolog, Yfh1p. Hum Mol Genet *10*, 259-269.

Gray, M.W., Burger, G., and Lang, B.F. (1999). Mitochondrial evolution. Science (Washington D C) *283*, 1476-1481.

Grigorieff, N. (1998). Three-dimensional structure of bovine NADH:ubiquinone oxidoreductase (complex I) at 22 A in ice. J Mol Biol *277*, 1033-1046.

Guenebaut, V., Vincentelli, R., Mills, D., Weiss, H., and Leonard, K.R. (1997). Three-dimensional structure of NADH-dehydrogenase from Neurospora crassa by electron microscopy and conical tilt reconstruction. J Mol Biol *265*, 409-418.

Gurung, B., Yu, L., Xia, D., and Yu, C.A. (2005). The iron-sulfur cluster of the Rieske iron-sulfur protein functions as a proton-exiting gate in the cytochrome bc(1) complex. J Biol Chem *280*, 24895-24902.

Halbreich, A., Pajot, P., Foucher, M., Grandchamp, C., and Slonimski, P. (1980). A pathway of cytochrome b mRNA processing in yeast mitochondria: specific splicing steps and an intron-derived circular DNA. Cell *19*, 321-329.

Harkness, T.A., Nargang, F.E., van der Klei, I., Neupert, W., and Lill, R. (1994). A crucial role of the mitochondrial protein import receptor MOM19 for the biogenesis of mitochondria. J Cell Biol *124*, 637-648.

Hartl, F.U., and Neupert, W. (1989). Import of proteins into the various submitochondrial compartments. J Cell Sci Suppl *11*, 187-198.

Hase, T., Muller, U., Riezman, H., and Schatz, G. (1984). A 70-kd protein of the yeast mitochondrial outer membrane is targeted and anchored via its extreme amino terminus. EMBO J *3*, 3157-3164.

Hasson, S.A., Damoiseaux, R., Glavin, J.D., Dabir, D.V., Walker, S.S., and Koehler, C.M. (2010). Substrate specificity of the TIM22 mitochondrial import pathway revealed with small molecule inhibitor of protein translocation. Proc Natl Acad Sci U S A *107*, 9578-9583.

Heazlewood, J.L., Howell, K.A., and Millar, A.H. (2003a). Mitochondrial complex I from Arabidopsis and rice: orthologs of mammalian and fungal

components coupled with plant-specific subunits. Biochimica et biophysica acta *1604*, 159-169.

Heazlewood, J.L., Howell, K.A., Whelan, J., and Millar, A.H. (2003b). Towards an analysis of the rice mitochondrial proteome. Plant Physiol *132*, 230-242.

Hell, K. (2008). The Erv1-Mia40 disulfide relay system in the intermembrane space of mitochondria. Biochim Biophys Acta *1783*, 601-609.

Herald, V.L., Heazlewood, J.L., Day, D.A., and Millar, A.H. (2003). Proteomic identification of divalent metal cation binding proteins in plant mitochondria. FEBS Lett *537*, 96-100.

Herrmann, J.M. (2003). Converting bacteria to organelles: evolution of mitochondrial protein sorting. Trends Microbiol *11*, 74-79.

Hill, K., Model, K., Ryan, M.T., Dietmeier, K., Martin, F., Wagner, R., and Pfanner, N. (1998). Tom40 forms the hydrophilic channel of the mitochondrial import pore for preproteins [see comment]. Nature *395*, 516-521.

Hirst, J. (2005). Energy transduction by respiratory complex I--an evaluation of current knowledge. Biochem Soc Trans *33*, 525-529.

Hofhaus, G., Weiss, H., and Leonard, K. (1991). Electron microscopic analysis of the peripheral and membrane parts of mitochondrial NADH dehydrogenase (complex I). J Mol Biol *221*, 1027-1043.

Honlinger, A., Kubrich, M., Moczko, M., Gartner, F., Mallet, L., Bussereau, F., Eckerskorn, C., Lottspeich, F., Dietmeier, K., Jacquet, M.*, et al.* (1995). The mitochondrial receptor complex: Mom22 is essential for cell viability and directly interacts with preproteins. Mol Cell Biol *15*, 3382-3389.

Hoppins, S.C., and Nargang, F.E. (2004). The Tim8-Tim13 complex of Neurospora crassa functions in the assembly of proteins into both mitochondrial membranes. J Biol Chem *279*, 12396-12405.

Hunkapiller, M.W., Lujan, E., Ostrander, F., and Hood, L.E. (1983). Isolation of microgram quantities of proteins from polyacrylamide gels for amino acid sequence analysis. Methods in enzymology *91*, 227-236.

Hunte, C., Koepke, J., Lange, C., Rossmanith, T., and Michel, H. (2000). Structure at 2.3 A resolution of the cytochrome bc(1) complex from the yeast Saccharomyces cerevisiae co-crystallized with an antibody Fv fragment. Structure *8*, 669-684.

Hunte, C., Solmaz, S., Palsdottir, H., and Wenz, T. (2008). A structural

perspective on mechanism and function of the cytochrome bc (1) complex. Results Probl Cell Differ *45*, 253-278.

Hwang, D.K., Claypool, S.M., Leuenberger, D., Tienson, H.L., and Koehler, C.M. (2007). Tim54p connects inner membrane assembly and proteolytic pathways in the mitochondrion. J Cell Biol *178*, 1161-1175.

Iacovino, M., Granycome, C., Sembongi, H., Bokori-Brown, M., Butow, R.A., Holt, I.J., and Bateman, J.M. (2009). The conserved translocase Tim17 prevents mitochondrial DNA loss. Hum Mol Genet *18*, 65-74.

Ishikawa, D., Yamamoto, H., Tamura, Y., Moritoh, K., and Endo, T. (2004). Two novel proteins in the mitochondrial outer membrane mediate beta-barrel protein assembly. J Cell Biol *166*, 621-627.

Ivanova, E., Jowitt, T.A., and Lu, H. (2008). Assembly of the mitochondrial Tim9-Tim10 complex: a multi-step reaction with novel intermediates. J Mol Biol *375*, 229-239.

Iwahashi, J., Yamazaki, S., Komiya, T., Nomura, N., Nishikawa, S., Endo, T., and Mihara, K. (1997). Analysis of the functional domain of the rat liver mitochondrial import receptor Tom20. J Biol Chem *272*, 18467-18472.

Iwata, S. (1998). Structure and function of bacterial cytochrome c oxidase. J Biochem *123*, 369-375.

Jang, B., and Han, S. (2006). Biochemical properties of cytochrome c nitrated by peroxynitrite. Biochimie *88*, 53-58.

Jansch, L., Kruft, V., Schmitz, U.K., and Braun, H.P. (1996). New insights into the composition, molecular mass and stoichiometry of the protein complexes of plant mitochondria. Plant J *9*, 357-368.

Jansch, L., Kruft, V., Schmitz, U.K., and Braun, H.P. (1998a). Unique composition of the preprotein translocase of the outer mitochondrial membrane from plants. J Biol Chem *273*, 17251-17257.

Jansch, L., Kruft, V., Schmitz, U.K., and Braun, H.P. (1998b). Unique composition of the preprotein translocase of the outer mitochondrial membrane from plants. J Biol Chem *273*, 17251-17257.

Jarosch, E., Tuller, G., Daum, G., Waldherr, M., Voskova, A., and Schweyen, R.J. (1996). Mrs5p, an essential protein of the mitochondrial intermembrane space, affects protein import into yeast mitochondria. J Biol Chem *271*, 17219-17225.

Juszczuk, I.M., and Rychter, A.M. (2003). Alternative oxidase in higher plants. Acta Biochim Pol *50*, 1257-1271.

Juszczuk, I.M., Szal, B., and Rychter, A.M. (2011). Oxidation-reduction and reactive oxygen species homeostasis in mutant plants with respiratory chain complex I dysfunction. Plant Cell Environ.

Kühn, K., Carrie, C., Giraud, E., Wang, Y., Meyer, E.H., Narsai, R., Colas des Francs-Small, C., Zhang, B., Murcha, M.W., and Whelan, J. (2011). The RCC1 family protein RUG3 is required for splicing of nad2 and complex I biogenesis in mitochondria of Arabidopsis thaliana. Submitted.

Kaldi, K., Bauer, M.F., Sirrenberg, C., Neupert, W., and Brunner, M. (1998). Biogenesis of Tim23 and Tim17, integral components of the TIM machinery for matrix-targeted preproteins. EMBO J *17*, 1569-1576.

Kanamori, T., Nishikawa, S., Nakai, M., Shin, I., Schultz, P.G., and Endo, T. (1999). Uncoupling of transfer of the presequence and unfolding of the mature domain in precursor translocation across the mitochondrial outer membrane. Proc Natl Acad Sci U S A *96*, 3634-3639.

Kang, P.J., Ostermann, J., Shilling, J., Neupert, W., Craig, E.A., and Pfanner, N. (1990). Requirement for hsp70 in the mitochondrial matrix for translocation and folding of precursor proteins. Nature *348*, 137-143.

Karlberg, O., Canback, B., Kurland, C.G., and Andersson, S.G. (2000). The dual origin of the yeast mitochondrial proteome. Yeast *17*, 170-187.

Kassenbrock, C.K., Cao, W., and Douglas, M.G. (1993). Genetic and biochemical characterization of ISP6, a small mitochondrial outer membrane protein associated with the protein translocation complex. EMBO J *12*, 3023-3034.

Kerscher, O., Holder, J., Srinivasan, M., Leung, R.S., and Jensen, R.E. (1997). The Tim54p-Tim22p complex mediates insertion of proteins into the mitochondrial inner membrane. J Cell Biol *139*, 1663-1675.

Kerscher, O., Sepuri, N.B., and Jensen, R.E. (2000). Tim18p is a new component of the Tim54p-Tim22p translocon in the mitochondrial inner membrane. Mol Biol Cell *11*, 103-116.

Kiebler, M., Keil, P., Schneider, H., van der Klei, I.J., Pfanner, N., and Neupert, W. (1993). The mitochondrial receptor complex: a central role of MOM22 in mediating preprotein transfer from receptors to the general insertion pore. Cell *74*, 483-492.

Klingenberg, M. (2008). The ADP and ATP transport in mitochondria and its carrier. Biochim Biophys Acta *1778*, 1978-2021.

Klodmann, J., and Braun, H.P. (2010). Proteomic approach to characterize mitochondrial complex I from plants. Phytochemistry.

Klodmann, J., and Braun, H.P. (2011). Proteomic approach to characterize mitochondrial complex I from plants. Phytochemistry *72*, 1071-1080.

Klodmann, J., Senkler, M., Rode, C., and Braun, H.P. (2011). Defining the "protein complex proteome" of plant mitochondria. Plant Physiol.

Klodmann, J., Sunderhaus, S., Nimtz, M., Jansch, L., and Braun, H.P. (2010a). Internal architecture of mitochondrial complex I from Arabidopsis thaliana. Plant Cell *22*, 797-810.

Klodmann, J., Sunderhaus, S., Nimtz, M., Jansch, L., and Braun, H.P. (2010b). Internal architecture of mitochondrial complex I from Arabidopsis thaliana. Plant Cell *22*, 797-810.

Kmita, H., and Stobienia, O. (2006). [The VDAC channel as the mitochondria function regulator]. Postepy Biochem *52*, 129-136.

Koehler, C.M. (2004). New developments in mitochondrial assembly. Annu Rev Cell Dev Biol *20*, 309-335.

Koehler, C.M., Murphy, M.P., Bally, N.A., Leuenberger, D., Oppliger, W., Dolfini, L., Junne, T., Schatz, G., and Or, E. (2000). Tim18p, a new subunit of the TIM22 complex that mediates insertion of imported proteins into the yeast mitochondrial inner membrane. Mol Cell Biol *20*, 1187-1193.

Komiya, T., Rospert, S., Koehler, C., Looser, R., Schatz, G., and Mihara, K. (1998). Interaction of mitochondrial targeting signals with acidic receptor domains along the protein import pathway: evidence for the 'acid chain' hypothesis. EMBO J *17*, 3886-3898.

Kovermann, P., Truscott, K.N., Guiard, B., Rehling, P., Sepuri, N.B., Muller, H., Jensen, R.E., Wagner, R., and Pfanner, N. (2002). Tim22, the essential core of the mitochondrial protein insertion complex, forms a voltage-activated and signal-gated channel. Mol Cell *9*, 363-373.

Kozany, C., Mokranjac, D., Sichting, M., Neupert, W., and Hell, K. (2004). The J domain-related cochaperone Tim16 is a constituent of the mitochondrial TIM23 preprotein translocase. Nat Struct Mol Biol *11*, 234-241.

Kozjak, V., Wiedemann, N., Milenkovic, D., Lohaus, C., Meyer, H.E., Guiard, B.,

Meisinger, C., and Pfanner, N. (2003). An essential role of Sam50 in the protein sorting and assembly machinery of the mitochondrial outer membrane. J Biol Chem *278*, 48520-48523.
Krause, F., Reifschneider, N.H., Vocke, D., Seelert, H., Rexroth, S., and Dencher, N.A. (2004). "Respirasome"-like supercomplexes in green leaf mitochondria of spinach. J Biol Chem *279*, 48369-48375.

Krimmer, T., Rapaport, D., Ryan, M.T., Meisinger, C., Kassenbrock, C.K., Blachly-Dyson, E., Forte, M., Douglas, M.G., Neupert, W., Nargang, F.E.*, et al.* (2001). Biogenesis of porin of the outer mitochondrial membrane involves an import pathway via receptors and the general import pore of the TOM complex. J Cell Biol *152*, 289-300.

Kuhn, K., Carrie, C., Giraud, E., Wang, Y., Meyer, E.H., Narsai, R., des Francs-Small, C.C., Zhang, B., Murcha, M.W., and Whelan, J. (2011). The RCC1 family protein RUG3 is required for splicing of nad2 and complex I biogenesis in mitochondria of Arabidopsis thaliana. Plant J.

Kuhn, K., Richter, U., Meyer, E.H., Delannoy, E., de Longevialle, A.F., O'Toole, N., Borner, T., Millar, A.H., Small, I.D., and Whelan, J. (2009). Phage-type RNA polymerase RPOTmp performs gene-specific transcription in mitochondria of Arabidopsis thaliana. Plant Cell *21*, 2762-2779.

Kunkele, K.P., Heins, S., Dembowski, M., Nargang, F.E., Benz, R., Thieffry, M., Walz, J., Lill, R., Nussberger, S., and Neupert, W. (1998a). The preprotein translocation channel of the outer membrane of mitochondria. Cell *93*, 1009-1019.

Kunkele, K.P., Juin, P., Pompa, C., Nargang, F.E., Henry, J.P., Neupert, W., Lill, R., and Thieffry, M. (1998b). The isolated complex of the translocase of the outer membrane of mitochondria. Characterization of the cation-selective and voltage-gated preprotein-conducting pore. J Biol Chem *273*, 31032-31039.

Kurland, C.G., and Andersson, S.G. (2000). Origin and evolution of the mitochondrial proteome. Microbiol Mol Biol Rev *64*, 786-820.

Kutik, S., Stojanovski, D., Becker, L., Becker, T., Meinecke, M., Kruger, V., Prinz, C., Meisinger, C., Guiard, B., Wagner, R.*, et al.* (2008). Dissecting membrane insertion of mitochondrial beta-barrel proteins. Cell *132*, 1011-1024.

Laloi, M. (1999). Plant mitochondrial carriers: an overview. Cell Mol Life Sci *56*, 918-944.

Laloraya, S., Gambill, B.D., and Craig, E.A. (1994). A role for a eukaryotic GrpE-related protein, Mge1p, in protein translocation. Proc Natl Acad Sci U S A *91*, 6481-6485.

Lam, E., Kato, N., and Lawton, M. (2001). Programmed cell death, mitochondria and the plant hypersensitive response. Nature *411*, 848-853.

Lang, B.F. (1999). Mitochondrial genome evolution and the origin of eukaryotes. ANNUAL REVIEW OF GENETICS *CCCP*, 351-397.

Lazarou, M., Thorburn, D.R., Ryan, M.T., and McKenzie, M. (2009). Assembly of mitochondrial complex I and defects in disease. Biochim Biophys Acta *1793*, 78-88.

Lemaire, C., and Dujardin, G. (2008). Preparation of respiratory chain complexes from Saccharomyces cerevisiae wild-type and mutant mitochondria : activity measurement and subunit composition analysis. Methods Mol Biol *432*, 65-81.

Li, Y., Dudek, J., Guiard, B., Pfanner, N., Rehling, P., and Voos, W. (2004). The presequence translocase-associated protein import motor of mitochondria. Pam16 functions in an antagonistic manner to Pam18. J Biol Chem *279*, 38047-38054.

Li, Z., and Xing, D. (2010). Mitochondrial pathway leading to programmed cell death induced by aluminum phytotoxicity in Arabidopsis. Plant Signal Behav *5*, 1660-1662.

Lill, R., Dutkiewicz, R., Elsasser, H.P., Hausmann, A., Netz, D.J., Pierik, A.J., Stehling, O., Urzica, E., and Muhlenhoff, U. (2006). Mechanisms of iron-sulfur protein maturation in mitochondria, cytosol and nucleus of eukaryotes. Biochim Biophys Acta *1763*, 652-667.

Lill, R., and Muhlenhoff, U. (2006). Iron-sulfur protein biogenesis in eukaryotes: components and mechanisms. Annu Rev Cell Dev Biol *22*, 457-486.

Linke, B., and Borner, T. (2005). Mitochondrial effects on flower and pollen development. Mitochondrion *5*, 389-402.

Lionaki, E., de Marcos Lousa, C., Baud, C., Vougioukalaki, M., Panayotou, G., and Tokatlidis, K. (2008). The essential function of Tim12 in vivo is ensured by the assembly interactions of its C-terminal domain. J Biol Chem *283*, 15747-15753.

Lisowsky, T. (1994). ERV1 is involved in the cell-division cycle and the maintenance of mitochondrial genomes in Saccharomyces cerevisiae. Curr Genet *26*, 15-20.

Lister, R., Carrie, C., Duncan, O., Ho, L.H., Howell, K.A., Murcha, M.W., and

Whelan, J. (2007). Functional definition of outer membrane proteins involved in preprotein import into mitochondria. Plant Cell *19*, 3739-3759.

Lister, R., Chew, O., Lee, M.N., Heazlewood, J.L., Clifton, R., Parker, K.L., Millar, A.H., and Whelan, J. (2004). A transcriptomic and proteomic characterization of the Arabidopsis mitochondrial protein import apparatus and its response to mitochondrial dysfunction. Plant Physiol *134*, 777-789.

Lister, R., Mowday, B., Whelan, J., and Millar, A.H. (2002). Zinc-dependent intermembrane space proteins stimulate import of carrier proteins into plant mitochondria. Plant J *30*, 555-566.

Lithgow, T., Junne, T., Suda, K., Gratzer, S., and Schatz, G. (1994). The mitochondrial outer membrane protein Mas22p is essential for protein import and viability of yeast. Proc Natl Acad Sci U S A *91*, 11973-11977.

Lithgow, T., and Schneider, A. (2010). Evolution of macromolecular import pathways in mitochondria, hydrogenosomes and mitosomes. Philos Trans R Soc Lond B Biol Sci *365*, 799-817.

Liu, Q., D'Silva, P., Walter, W., Marszalek, J., and Craig, E.A. (2003). Regulated cycling of mitochondrial Hsp70 at the protein import channel. Science *300*, 139-141.

Liu, S.S. (1999). Cooperation of a "reactive oxygen cycle" with the Q cycle and the proton cycle in the respiratory chain--superoxide generating and cycling mechanisms in mitochondria. J Bioenerg Biomembr *31*, 367-376.

Lu, H., and Cao, X. (2008). GRIM-19 is essential for maintenance of mitochondrial membrane potential. Mol Biol Cell *19*, 1893-1902.

Luttik, M.A., Overkamp, K.M., Kotter, P., de Vries, S., van Dijken, J.P., and Pronk, J.T. (1998). The Saccharomyces cerevisiae NDE1 and NDE2 genes encode separate mitochondrial NADH dehydrogenases catalyzing the oxidation of cytosolic NADH. J Biol Chem *273*, 24529-24534.

Lutz, T., Westermann, B., Neupert, W., and Herrmann, J.M. (2001). The mitochondrial proteins Ssq1 and Jac1 are required for the assembly of iron sulfur clusters in mitochondria. J Mol Biol *307*, 815-825.

Maarse, A.C., Blom, J., Grivell, L.A., and Meijer, M. (1992). MPI1, an essential gene encoding a mitochondrial membrane protein, is possibly involved in protein import into yeast mitochondria. EMBO J *11*, 3619-3628.

Maarse, A.C., Blom, J., Keil, P., Pfanner, N., and Meijer, M. (1994). Identification of the essential yeast protein MIM17, an integral mitochondrial

inner membrane protein involved in protein import. FEBS Lett *349*, 215-221.

Macasev, D., Whelan, J., Newbigin, E., Silva-Filho, M.C., Mulhern, T.D., and Lithgow, T. (2004). Tom22', an 8-kDa trans-site receptor in plants and protozoans, is a conserved feature of the TOM complex that appeared early in the evolution of eukaryotes. Mol Biol Evol *21*, 1557-1564.

Mannella, C.A. (1987). Importance of the mitochondrial outer membrane channel as a model biological channel. Journal of Bioenergetics & Biomembranes *19*, 305-308.

Marienfeld, J. (1999). The mitochondrial genome of Arabidopsis is composed of both native and immigrant information. TRENDS IN PLANT SCIENCE *CCCA CCCP*, 495-502.

Martinez-Caballero, S., Grigoriev, S.M., Herrmann, J.M., Campo, M.L., and Kinnally, K.W. (2007). Tim17p regulates the twin pore structure and voltage gating of the mitochondrial protein import complex TIM23. J Biol Chem *282*, 3584-3593.

Mayer, A., Nargang, F.E., Neupert, W., and Lill, R. (1995). MOM22 is a receptor for mitochondrial targeting sequences and cooperates with MOM19. EMBO J *14*, 4204-4211.

Meier, S., Neupert, W., and Herrmann, J.M. (2005). Conserved N-terminal negative charges in the Tim17 subunit of the TIM23 translocase play a critical role in the import of preproteins into mitochondria. J Biol Chem *280*, 7777-7785.

Meinecke, M., Wagner, R., Kovermann, P., Guiard, B., Mick, D.U., Hutu, D.P., Voos, W., Truscott, K.N., Chacinska, A., Pfanner, N.*, et al.* (2006). Tim50 maintains the permeability barrier of the mitochondrial inner membrane. Science *312*, 1523-1526.

Meisinger, C., Ryan, M.T., Hill, K., Model, K., Lim, J.H., Sickmann, A., Muller, H., Meyer, H.E., Wagner, R., and Pfanner, N. (2001). Protein import channel of the outer mitochondrial membrane: a highly stable Tom40-Tom22 core structure differentially interacts with preproteins, small tom proteins, and import receptors. Mol Cell Biol *21*, 2337-2348.

Melo, A.M., Bandeiras, T.M., and Teixeira, M. (2004a). New insights into type II NAD(P)H:quinone oxidoreductases. Microbiology and molecular biology reviews : MMBR *68*, 603-616.

Meyer, E.H., Taylor, N.L., and Millar, A.H. (2008a). Resolving and identifying protein components of plant mitochondrial respiratory complexes using three dimensions of gel electrophoresis. J Proteome Res *7*, 786-794.

Meyer, E.H., Tomaz, T., Carroll, A.J., Estavillo, G., Delannoy, E., Tanz, S.K., Small, I.D., Pogson, B.J., and Millar, A.H. (2009). Remodeled respiration in ndufs4 with low phosphorylation efficiency suppresses Arabidopsis germination and growth and alters control of metabolism at night. Plant Physiol *151*, 603-619.

Michaud, M., Marechal-Drouard, L., and Duchene, A.M. (2010). RNA trafficking in plant cells: targeting of cytosolic mRNAs to the mitochondrial surface. Plant Mol Biol *73*, 697-704.

Milisav, I., Moro, F., Neupert, W., and Brunner, M. (2001). Modular structure of the TIM23 preprotein translocase of mitochondria. J Biol Chem *276*, 25856-25861.

Millar, A.H., and Heazlewood, J.L. (2003). Genomic and proteomic analysis of mitochondrial carrier proteins in Arabidopsis. Plant Physiol *131*, 443-453.

Millar, A.H., Sweetlove, L.J., Giege, P., and Leaver, C.J. (2001). Analysis of the Arabidopsis mitochondrial proteome. Plant Physiol *127*, 1711-1727.

Mitchell, P. (1961). Coupling of phosphorylation to electron and hydrogen transfer by a chemi-osmotic type of mechanism. Nature *191*, 144-148.

Moczko, M., Bomer, U., Kubrich, M., Zufall, N., Honlinger, A., and Pfanner, N. (1997). The intermembrane space domain of mitochondrial Tom22 functions as a trans binding site for preproteins with N-terminal targeting sequences. Mol Cell Biol *17*, 6574-6584.

Model, K., Meisinger, C., Prinz, T., Wiedemann, N., Truscott, K.N., Pfanner, N., and Ryan, M.T. (2001). Multistep assembly of the protein import channel of the mitochondrial outer membrane. Nat Struct Biol *8*, 361-370.

Model, K., Prinz, T., Ruiz, T., Radermacher, M., Krimmer, T., Kuhlbrandt, W., Pfanner, N., and Meisinger, C. (2002). Protein translocase of the outer mitochondrial membrane: role of import receptors in the structural organization of the TOM complex. J Mol Biol *316*, 657-666.

Mokranjac, D., and Neupert, W. (2009). Thirty years of protein translocation into mitochondria: unexpectedly complex and still puzzling. Biochim Biophys Acta *1793*, 33-41.

Mokranjac, D., and Neupert, W. (2010). The many faces of the mitochondrial TIM23 complex. Biochim Biophys Acta *1797*, 1045-1054.

Mokranjac, D., Paschen, S.A., Kozany, C., Prokisch, H., Hoppins, S.C.,

Nargang, F.E., Neupert, W., and Hell, K. (2003a). Tim50, a novel component of the TIM23 preprotein translocase of mitochondria. EMBO J *22*, 816-825.

Mokranjac, D., Popov-Celeketic, D., Hell, K., and Neupert, W. (2005a). Role of Tim21 in mitochondrial translocation contact sites. J Biol Chem *280*, 23437-23440.

Mokranjac, D., Sichting, M., Neupert, W., and Hell, K. (2003b). Tim14, a novel key component of the import motor of the TIM23 protein translocase of mitochondria. EMBO J *22*, 4945-4956.

Mokranjac, D., Sichting, M., Popov-Celeketic, D., Berg, A., Hell, K., and Neupert, W. (2005b). The import motor of the yeast mitochondrial TIM23 preprotein translocase contains two different J proteins, Tim14 and Mdj2. J Biol Chem *280*, 31608-31614.

Mokranjac, D., Sichting, M., Popov-Celeketic, D., Mapa, K., Gevorkyan-Airapetov, L., Zohary, K., Hell, K., Azem, A., and Neupert, W. (2009a). Role of Tim50 in the transfer of precursor proteins from the outer to the inner membrane of mitochondria. Molecular biology of the cell *20*, 1400-1407.

Mokranjac, D., Sichting, M., Popov-Celeketic, D., Mapa, K., Gevorkyan-Airapetov, L., Zohary, K., Hell, K., Azem, A., and Neupert, W. (2009b). Role of Tim50 in the transfer of precursor proteins from the outer to the inner membrane of mitochondria. Mol Biol Cell *20*, 1400-1407.

Momose, T., Ohshima, C., Maeda, M., and Endo, T. (2007). Structural basis of functional cooperation of Tim15/Zim17 with yeast mitochondrial Hsp70. EMBO Rep *8*, 664-670.

Moro, F., and Muga, A. (2006). Thermal adaptation of the yeast mitochondrial Hsp70 system is regulated by the reversible unfolding of its nucleotide exchange factor. J Mol Biol *358*, 1367-1377.

Moro, F., Sirrenberg, C., Schneider, H.C., Neupert, W., and Brunner, M. (1999). The TIM17.23 preprotein translocase of mitochondria: composition and function in protein transport into the matrix. EMBO J *18*, 3667-3675.

Murcha, M.W., Elhafez, D., Lister, R., Tonti-Filippini, J., Baumgartner, M., Philippar, K., Carrie, C., Mokranjac, D., Soll, J., and Whelan, J. (2007). Characterization of the preprotein and amino acid transporter gene family in Arabidopsis. Plant Physiol *143*, 199-212.

Murcha, M.W., Elhafez, D., Millar, A.H., and Whelan, J. (2004). The N-terminal extension of plant mitochondrial carrier proteins is removed by two-step processing: the first cleavage is by the mitochondrial processing peptidase. J

Mol Biol *344*, 443-454.

Murcha, M.W., Elhafez, D., Millar, A.H., and Whelan, J. (2005a). The C-terminal region of TIM17 links the outer and inner mitochondrial membranes in Arabidopsis and is essential for protein import. J Biol Chem *280*, 16476-16483.
Murcha, M.W., Huang, T., and Whelan, J. (1999). Import of precursor proteins into mitochondria from soybean tissues during development. FEBS Lett *464*, 53-59.

Murcha, M.W., Lister, R., Ho, A.Y., and Whelan, J. (2003). Identification, expression, and import of components 17 and 23 of the inner mitochondrial membrane translocase from Arabidopsis. Plant Physiol *131*, 1737-1747.

Murcha, M.W., Millar, A.H., and Whelan, J. (2005b). The N-terminal cleavable extension of plant carrier proteins is responsible for efficient insertion into the inner mitochondrial membrane. J Mol Biol *351*, 16-25.

Murcha, M.W., Millar, A.H., and Whelan, J. (2005c). The N-terminal cleavable extension of plant carrier proteins is responsible for efficient insertion into the inner mitochondrial membrane. Journal of molecular biology *351*, 16-25.

Muto, T., Obita, T., Abe, Y., Shodai, T., Endo, T., and Kohda, D. (2001). NMR identification of the Tom20 binding segment in mitochondrial presequences. J Mol Biol *306*, 137-143.

Nakai, M., Kato, Y., Ikeda, E., Toh-e, A., and Endo, T. (1994). Yge1p, a eukaryotic Grp-E homolog, is localized in the mitochondrial matrix and interacts with mitochondrial Hsp70. Biochem Biophys Res Commun *200*, 435-442.

Neupert, W. (1997). Protein import into mitochondria. Annu Rev Biochem *66*, 863-917.

Neupert, W., and Herrmann, J.M. (2007). Translocation of proteins into mitochondria. Annu Rev Biochem *76*, 723-749.

Nobrega, F.G., Nobrega, M.P., and Tzagoloff, A. (1992). BCS1, a novel gene required for the expression of functional Rieske iron-sulfur protein in Saccharomyces cerevisiae. EMBO J *11*, 3821-3829.

Noctor, G., De Paepe, R., and Foyer, C.H. (2007). Mitochondrial redox biology and homeostasis in plants. Trends Plant Sci *12*, 125-134.

Noguchi, K., and Yoshida, K. (2008). Interaction between photosynthesis and respiration in illuminated leaves. Mitochondrion *8*, 87-99.

Palmieri, F., Bisaccia, F., Capobianco, L., Dolce, V., Fiermonte, G., Iacobazzi,

V., Indiveri, C., and Palmieri, L. (1996). Mitochondrial metabolite transporters. Biochim Biophys Acta *1275*, 127-132.

Palmisano, G., Sardanelli, A.M., Signorile, A., Papa, S., and Larsen, M.R. (2007). The phosphorylation pattern of bovine heart complex I subunits. Proteomics *7*, 1575-1583.

Papa, S. (2002). The NDUFS4 nuclear gene of complex I of mitochondria and the cAMP cascade. Biochim Biophys Acta *1555*, 147-153.

Papatheodorou, P., Domanska, G., and Rassow, J. (2007). Protein targeting to mitochondria of Saccharomyces cerevisiae and Neurospora crassa: in vitro and in vivo studies. Methods Mol Biol *390*, 151-166.

Paschen, S.A., Waizenegger, T., Stan, T., Preuss, M., Cyrklaff, M., Hell, K., Rapaport, D., and Neupert, W. (2003). Evolutionary conservation of biogenesis of beta-barrel membrane proteins. Nature *426*, 862-866.

Perry, A.J., Hulett, J.M., Likic, V.A., Lithgow, T., and Gooley, P.R. (2006). Convergent evolution of receptors for protein import into mitochondria. Curr Biol *16*, 221-229.

Perry, A.J., Rimmer, K.A., Mertens, H.D., Waller, R.F., Mulhern, T.D., Lithgow, T., and Gooley, P.R. (2008). Structure, topology and function of the translocase of the outer membrane of mitochondria. Plant Physiol Biochem *46*, 265-274.

Petrussa, E., Bertolini, A., Casolo, V., Krajnakova, J., Macri, F., and Vianello, A. (2009). Mitochondrial bioenergetics linked to the manifestation of programmed cell death during somatic embryogenesis of Abies alba. Planta *231*, 93-107.

Pfanner, N., and Geissler, A. (2001). Versatility of the mitochondrial protein import machinery. Nat Rev Mol Cell Biol *2*, 339-349.

Pfanner, N., Hartl, F.U., Guiard, B., and Neupert, W. (1987a). Mitochondrial precursor proteins are imported through a hydrophilic membrane environment. Eur J Biochem *169*, 289-293.

Pfanner, N., Muller, H.K., Harmey, M.A., and Neupert, W. (1987b). Mitochondrial protein import: involvement of the mature part of a cleavable precursor protein in the binding to receptor sites. EMBO J *6*, 3449-3454.

Pfanner, N., and Neupert, W. (1987). Distinct steps in the import of ADP/ATP carrier into mitochondria. J Biol Chem *262*, 7528-7536.

Piccoli, C., Scacco, S., Bellomo, F., Signorile, A., Iuso, A., Boffoli, D., Scrima, R., Capitanio, N., and Papa, S. (2006). cAMP controls oxygen metabolism in

mammalian cells. FEBS Lett *580*, 4539-4543.

Pineau, B., Layoune, O., Danon, A., and De Paepe, R. (2008). L-galactono-1,4-lactone dehydrogenase is required for the accumulation of plant respiratory complex I. J Biol Chem *283*, 32500-32505.

Pla, M., Mathieu, C., De Paepe, R., Chetrit, P., and Vedel, F. (1995). Deletion of the last two exons of the mitochondrial nad7 gene results in lack of the NAD7 polypeptide in a Nicotiana sylvestris CMS mutant. Mol Gen Genet *248*, 79-88.

Popov-Celeketic, D., Mapa, K., Neupert, W., and Mokranjac, D. (2008). Active remodelling of the TIM23 complex during translocation of preproteins into mitochondria. EMBO J *27*, 1469-1480.

Pudelski, B., Kraus, S., Soll, J., and Philippar, K. (2010). The plant PRAT proteins - preprotein and amino acid transport in mitochondria and chloroplasts. Plant Biol (Stuttg) *12 Suppl 1*, 42-55.

Qi, Y., Wang, H., Zou, Y., Liu, C., Liu, Y., Wang, Y., and Zhang, W. (2011). Over-expression of mitochondrial heat shock protein 70 suppresses programmed cell death in rice. FEBS Lett *585*, 231-239.

Rajagukguk, S., Yang, S., Yu, C.A., Yu, L., Durham, B., and Millett, F. (2007). Effect of mutations in the cytochrome b ef loop on the electron-transfer reactions of the Rieske iron-sulfur protein in the cytochrome bc1 complex. Biochemistry *46*, 1791-1798.

Rapaport, D., and Neupert, W. (1999). Biogenesis of Tom40, core component of the TOM complex of mitochondria. J Cell Biol *146*, 321-331.

Rapaport, D., Taylor, R.D., Kaser, M., Langer, T., Neupert, W., and Nargang, F.E. (2001). Structural requirements of Tom40 for assembly into preexisting TOM complexes of mitochondria. Mol Biol Cell *12*, 1189-1198.

Rasmusson, A.G., Soole, K.L., and Elthon, T.E. (2004). Alternative NAD(P)H dehydrogenases of plant mitochondria. Annu Rev Plant Biol *55*, 23-39.

Rassow, J., Dekker, P.J., van Wilpe, S., Meijer, M., and Soll, J. (1999). The preprotein translocase of the mitochondrial inner membrane: function and evolution. J Mol Biol *286*, 105-120.

Reinders, J., Wagner, K., Zahedi, R.P., Stojanovski, D., Eyrich, B., van der Laan, M., Rehling, P., Sickmann, A., Pfanner, N., and Meisinger, C. (2007). Profiling phosphoproteins of yeast mitochondria reveals a role of phosphorylation in assembly of the ATP synthase. Molecular & cellular proteomics : MCP *6*, 1896-1906.

Reisch, A.S., and Elpeleg, O. (2007). Biochemical assays for mitochondrial activity: assays of TCA cycle enzymes and PDHc. Methods Cell Biol *80*, 199-222.

Remacle, C., Barbieri, M.R., Cardol, P., and Hamel, P.P. (2008). Eukaryotic complex I: functional diversity and experimental systems to unravel the assembly process. Mol Genet Genomics *280*, 93-110.

Rigoulet, M., Aguilaniu, H., Averet, N., Bunoust, O., Camougrand, N., Grandier-Vazeille, X., Larsson, C., Pahlman, I.L., Manon, S., and Gustafsson, L. (2004). Organization and regulation of the cytosolic NADH metabolism in the yeast Saccharomyces cerevisiae. Mol Cell Biochem *256-257*, 73-81.

Roise, D., and Schatz, G. (1988). Mitochondrial presequences. J Biol Chem *263*, 4509-4511.

Rowley, N., Prip-Buus, C., Westermann, B., Brown, C., Schwarz, E., Barrell, B., and Neupert, W. (1994). Mdj1p, a novel chaperone of the DnaJ family, is involved in mitochondrial biogenesis and protein folding. Cell *77*, 249-259.

Ryan, K.R., Leung, R.S., and Jensen, R.E. (1998). Characterization of the mitochondrial inner membrane translocase complex: the Tim23p hydrophobic domain interacts with Tim17p but not with other Tim23p molecules. Mol Cell Biol *18*, 178-187.

Ryan, K.R., Menold, M.M., Garrett, S., and Jensen, R.E. (1994). SMS1, a high-copy suppressor of the yeast mas6 mutant, encodes an essential inner membrane protein required for mitochondrial protein import. Mol Biol Cell *5*, 529-538.

Sabar, M., De Paepe, R., and de Kouchkovsky, Y. (2000). Complex I impairment, respiratory compensations, and photosynthetic decrease in nuclear and mitochondrial male sterile mutants of Nicotiana sylvestris. Plant Physiol *124*, 1239-1250.

Saddar, S., Dienhart, M.K., and Stuart, R.A. (2008). The F1F0-ATP synthase complex influences the assembly state of the cytochrome bc1-cytochrome oxidase supercomplex and its association with the TIM23 machinery. J Biol Chem *283*, 6677-6686.

Saitoh, T., Igura, M., Obita, T., Ose, T., Kojima, R., Maenaka, K., Endo, T., and Kohda, D. (2007). Tom20 recognizes mitochondrial presequences through dynamic equilibrium among multiple bound states. EMBO J *26*, 4777-4787.

Saraste, M., and Walker, J.E. (1982). Internal sequence repeats and the path of

polypeptide in mitochondrial ADP/ATP translocase. FEBS Lett *144*, 250-254.

Sardanelli, A.M., Technikova-Dobrova, Z., Scacco, S.C., Speranza, F., and Papa, S. (1995). Characterization of proteins phosphorylated by the cAMP-dependent protein kinase of bovine heart mitochondria. FEBS Lett *377*, 470-474.

Schagger, H. (2002). Respiratory chain supercomplexes of mitochondria and bacteria. Biochim Biophys Acta *1555*, 154-159.

Schagger, H., and Pfeiffer, K. (2000). Supercomplexes in the respiratory chains of yeast and mammalian mitochondria. EMBO J *19*, 1777-1783.

Schatz, G. (1996). The protein import system of mitochondria. J Biol Chem *271*, 31763-31766.

Scherer, P.E., Manning-Krieg, U.C., Jeno, P., Schatz, G., and Horst, M. (1992). Identification of a 45-kDa protein at the protein import site of the yeast mitochondrial inner membrane. Proc Natl Acad Sci U S A *89*, 11930-11934.

Schiller, D., Cheng, Y.C., Liu, Q., Walter, W., and Craig, E.A. (2008). Residues of Tim44 involved in both association with the translocon of the inner mitochondrial membrane and regulation of mitochondrial Hsp70 tethering. Mol Cell Biol *28*, 4424-4433.

Schilling, B., Aggeler, R., Schulenberg, B., Murray, J., Row, R.H., Capaldi, R.A., and Gibson, B.W. (2005). Mass spectrometric identification of a novel phosphorylation site in subunit NDUFA10 of bovine mitochondrial complex I. FEBS Lett *579*, 2485-2490.

Schmidt, O., Pfanner, N., and Meisinger, C. (2010). Mitochondrial protein import: from proteomics to functional mechanisms. Nat Rev Mol Cell Biol *11*, 655-667.

Schmitt, S., Ahting, U., Eichacker, L., Granvogl, B., Go, N.E., Nargang, F.E., Neupert, W., and Nussberger, S. (2005). Role of Tom5 in maintaining the structural stability of the TOM complex of mitochondria. J Biol Chem *280*, 14499-14506.

Schulenberg, B., Aggeler, R., Beechem, J.M., Capaldi, R.A., and Patton, W.F. (2003). Analysis of steady-state protein phosphorylation in mitochondria using a novel fluorescent phosphosensor dye. J Biol Chem *278*, 27251-27255.

Sichting, M., Mokranjac, D., Azem, A., Neupert, W., and Hell, K. (2005). Maintenance of structure and function of mitochondrial Hsp70 chaperones requires the chaperone Hep1. EMBO J *24*, 1046-1056.

Sirrenberg, C., Bauer, M.F., Guiard, B., Neupert, W., and Brunner, M. (1996). Import of carrier proteins into the mitochondrial inner membrane mediated by Tim22. Nature *384*, 582-585.

Sirrenberg, C., Endres, M., Folsch, H., Stuart, R.A., Neupert, W., and Brunner, M. (1998). Carrier protein import into mitochondria mediated by the intermembrane proteins Tim10/Mrs11 and Tim12/Mrs5. Nature *391*, 912-915.

Smith, A.G., Croft, M.T., Moulin, M., and Webb, M.E. (2007). Plants need their vitamins too. Curr Opin Plant Biol *10*, 266-275.

Smith, C., Barthet, M., Melino, V., Smith, P., Day, D., and Soole, K. (2011). Alterations in the Mitochondrial Alternative NAD(P)H Dehydrogenase NDB4 Lead to Changes in Mitochondrial Electron Transport Chain Composition, Plant Growth and Response to Oxidative Stress. Plant Cell Physiol *52*, 1222-1237.

Smith, J.L., Zhang, H., Yan, J., Kurisu, G., and Cramer, W.A. (2004). Cytochrome bc complexes: a common core of structure and function surrounded by diversity in the outlying provinces. Curr Opin Struct Biol *14*, 432-439.

Smith, M.K., Day, D.A., and Whelan, J. (1994). Isolation of a novel soybean gene encoding a mitochondrial ATP synthase subunit. Arch Biochem Biophys *313*, 235-240.

Stepanova, A.N., and Alonso, J.M. (2006). PCR-based screening for insertional mutants. Methods Mol Biol *323*, 163-172.

Stroud, D.A., Becker, T., Qiu, J., Stojanovski, D., Pfannschmidt, S., Wirth, C., Hunte, C., Guiard, B., Meisinger, C., Pfanner, N.*, et al.* (2011). Biogenesis of mitochondrial {beta}-barrel proteins: the POTRA domain is involved in precursor release from the SAM complex. Mol Biol Cell.

Strub, A., Lim, J.H., Pfanner, N., and Voos, W. (2000). The mitochondrial protein import motor. Biol Chem *381*, 943-949.

Stuart, R.A. (2008). Supercomplex organization of the oxidative phosphorylation enzymes in yeast mitochondria. J Bioenerg Biomembr *40*, 411-417.

Suthammarak, W., Morgan, P.G., and Sedensky, M.M. (2010). Mutations in mitochondrial complex III uniquely affect complex I in Caenorhabditis elegans. J Biol Chem *285*, 40724-40731.

Tamura, Y., Harada, Y., Shiota, T., Yamano, K., Watanabe, K., Yokota, M.,

Yamamoto, H., Sesaki, H., and Endo, T. (2009a). Tim23-Tim50 pair coordinates functions of translocators and motor proteins in mitochondrial protein import. The Journal of cell biology *184*, 129-141.

Tamura, Y., Harada, Y., Shiota, T., Yamano, K., Watanabe, K., Yokota, M., Yamamoto, H., Sesaki, H., and Endo, T. (2009b). Tim23-Tim50 pair coordinates functions of translocators and motor proteins in mitochondrial protein import. J Cell Biol *184*, 129-141.

Tanudji, M., Sjoling, S., Glaser, E., and Whelan, J. (1999). Signals required for the import and processing of the alternative oxidase into mitochondria. J Biol Chem *274*, 1286-1293.

Taylor, N.L., and Millar, A.H. (2007). Oxidative stress and plant mitochondria. Methods Mol Biol *372*, 389-403.

Truscott, K.N., Kovermann, P., Geissler, A., Merlin, A., Meijer, M., Driessen, A.J., Rassow, J., Pfanner, N., and Wagner, R. (2001). A presequence- and voltage-sensitive channel of the mitochondrial preprotein translocase formed by Tim23. Nat Struct Biol *8*, 1074-1082.

Ungermann, C., Neupert, W., and Cyr, D.M. (1994). The role of Hsp70 in conferring unidirectionality on protein translocation into mitochondria. Science *266*, 1250-1253.

Vacca, R.A., de Pinto, M.C., Valenti, D., Passarella, S., Marra, E., and De Gara, L. (2004). Production of reactive oxygen species, alteration of cytosolic ascorbate peroxidase, and impairment of mitochondrial metabolism are early events in heat shock-induced programmed cell death in tobacco Bright-Yellow 2 cells. Plant Physiol *134*, 1100-1112.

van der Giezen, M., Sjollema, K.A., Artz, R.R., Alkema, W., and Prins, R.A. (1997). Hydrogenosomes in the anaerobic fungus Neocallimastix frontalis have a double membrane but lack an associated organelle genome. FEBS Lett *408*, 147-150.

van der Laan, M., Chacinska, A., Lind, M., Perschil, I., Sickmann, A., Meyer, H.E., Guiard, B., Meisinger, C., Pfanner, N., and Rehling, P. (2005). Pam17 is required for architecture and translocation activity of the mitochondrial protein import motor. Mol Cell Biol *25*, 7449-7458.

van der Laan, M., Wiedemann, N., Mick, D.U., Guiard, B., Rehling, P., and Pfanner, N. (2006a). A role for Tim21 in membrane-potential-dependent preprotein sorting in mitochondria. Curr Biol *16*, 2271-2276.

van der Laan, M., Wiedemann, N., Mick, D.U., Guiard, B., Rehling, P., and

Pfanner, N. (2006b). A role for Tim21 in membrane-potential-dependent preprotein sorting in mitochondria. Current biology : CB *16*, 2271-2276.

Vanlerberghe, G.C., and McIntosh, L. (1997). ALTERNATIVE OXIDASE: From Gene to Function. Annu Rev Plant Physiol Plant Mol Biol *48*, 703-734.

Vanlerberghe, G.C., Vanlerberghe, A.E., and McIntosh, L. (1997). Molecular Genetic Evidence of the Ability of Alternative Oxidase to Support Respiratory Carbon Metabolism. Plant Physiol *113*, 657-661.

Vercesi, A.E. (2001). The discovery of an uncoupling mitochondrial protein in plants. Biosci Rep *21*, 195-200.

Videira, A., and Duarte, M. (2002). From NADH to ubiquinone in Neurospora mitochondria. Biochim Biophys Acta *1555*, 187-191.

Vogel, R., Nijtmans, L., Ugalde, C., van den Heuvel, L., and Smeitink, J. (2004). Complex I assembly: a puzzling problem. Curr Opin Neurol *17*, 179-186.

Vonck, J., and Schafer, E. (2009). Supramolecular organization of protein complexes in the mitochondrial inner membrane. Biochim Biophys Acta *1793*, 117-124.

Voos, W. (2003). Tom40: more than just a channel. Nat Struct Biol *10*, 981-982.

Voos, W., and Rottgers, K. (2002). Molecular chaperones as essential mediators of mitochondrial biogenesis. Biochim Biophys Acta *1592*, 51-62.

Wabnitz, G.H., Goursot, C., Jahraus, B., Kirchgessner, H., Hellwig, A., Klemke, M., Konstandin, M.H., and Samstag, Y. (2010). Mitochondrial translocation of oxidized cofilin induces caspase-independent necrotic-like programmed cell death of T cells. Cell Death Dis *1*, e58.

Wagner, K., Gebert, N., Guiard, B., Brandner, K., Truscott, K.N., Wiedemann, N., Pfanner, N., and Rehling, P. (2008). The assembly pathway of the mitochondrial carrier translocase involves four preprotein translocases. Mol Cell Biol *28*, 4251-4260.

Walker, J.E., and Dickson, V.K. (2006). The peripheral stalk of the mitochondrial ATP synthase. Biochim Biophys Acta *1757*, 286-296.

Waller, R.F., Jabbour, C., Chan, N.C., Celik, N., Likic, V.A., Mulhern, T.D., and Lithgow, T. (2009). Evidence of a reduced and modified mitochondrial protein import apparatus in microsporidian mitosomes. Eukaryot Cell *8*, 19-26.

Wang, J., Bai, L., Li, J., Sun, C., Zhao, J., Cui, C., Han, K., Liu, Y., Zhuo, X.,

Wang, T.*, et al.* (2009). Proteomic analysis of mitochondria reveals a metabolic switch from fatty acid oxidation to glycolysis in the failing heart. Sci China C Life Sci *52*, 1003-1010.

Weiss, C., Oppliger, W., Vergeres, G., Demel, R., Jeno, P., Horst, M., de Kruijff, B., Schatz, G., and Azem, A. (1999). Domain structure and lipid interaction of recombinant yeast Tim44. Proc Natl Acad Sci U S A *96*, 8890-8894.

Werhahn, W., Niemeyer, A., Jansch, L., Kruft, V., Schmitz, U.K., and Braun, H. (2001). Purification and characterization of the preprotein translocase of the outer mitochondrial membrane from Arabidopsis. Identification of multiple forms of TOM20. Plant Physiol *125*, 943-954.

Whelan, J., Hugosson, M., Glaser, E., and Day, D.A. (1995). Studies on the import and processing of the alternative oxidase precursor by isolated soybean mitochondria. Plant Mol Biol *27*, 769-778.

Whelan, J., Tanudji, M.R., Smith, M.K., and Day, D.A. (1996). Evidence for a link between translocation and processing during protein import into soybean mitochondria. Biochim Biophys Acta *1312*, 48-54.

Wiedemann, N., Kozjak, V., Chacinska, A., Schonfisch, B., Rospert, S., Ryan, M.T., Pfanner, N., and Meisinger, C. (2003). Machinery for protein sorting and assembly in the mitochondrial outer membrane. Nature *424*, 565-571.

Wiedemann, N., Pfanner, N., and Ryan, M.T. (2001). The three modules of ADP/ATP carrier cooperate in receptor recruitment and translocation into mitochondria. EMBO J *20*, 951-960.

Wiedemann, N., Truscott, K.N., Pfannschmidt, S., Guiard, B., Meisinger, C., and Pfanner, N. (2004). Biogenesis of the protein import channel Tom40 of the mitochondrial outer membrane: intermembrane space components are involved in an early stage of the assembly pathway. J Biol Chem *279*, 18188-18194.

Wiedemann, N., van der Laan, M., Hutu, D.P., Rehling, P., and Pfanner, N. (2007). Sorting switch of mitochondrial presequence translocase involves coupling of motor module to respiratory chain. J Cell Biol *179*, 1115-1122.

Wittig, I., and Schagger, H. (2009). Supramolecular organization of ATP synthase and respiratory chain in mitochondrial membranes. Biochim Biophys Acta *1787*, 672-680.

Witzigmann, H., Max, D., Uhlmann, D., Geissler, F., Ludwig, S., Schwarz, R., Krauss, O., Lohmann, T., Keim, V., and Hauss, J. (2002). Quality of life in chronic pancreatitis: a prospective trial comparing classical whipple procedure and duodenum-preserving pancreatic head resection. J Gastrointest Surg *6*,

173-179; discussion 179-180.

Wood, C.K., Dudley, P., Albury, M.S., Affourtit, C., Leach, G.R., Pratt, J.R., Whitehouse, D.G., and Moore, A.L. (1996). Developmental regulation of respiratory activity and protein import in plant mitochondria. Biochem Soc Trans *24*, 746-749.

Wu, Y., and Sha, B. (2006). Crystal structure of yeast mitochondrial outer membrane translocon member Tom70p. Nat Struct Mol Biol *13*, 589-593.

Yamamoto, H., Esaki, M., Kanamori, T., Tamura, Y., Nishikawa, S., and Endo, T. (2002). Tim50 is a subunit of the TIM23 complex that links protein translocation across the outer and inner mitochondrial membranes. Cell *111*, 519-528.

Yamamoto, H., Fukui, K., Takahashi, H., Kitamura, S., Shiota, T., Terao, K., Uchida, M., Esaki, M., Nishikawa, S., Yoshihisa, T.*, et al.* (2009). Roles of Tom70 in import of presequence-containing mitochondrial proteins. J Biol Chem *284*, 31635-31646.

Yamamoto, H., Itoh, N., Kawano, S., Yatsukawa, Y., Momose, T., Makio, T., Matsunaga, M., Yokota, M., Esaki, M., Shodai, T.*, et al.* (2011). Dual role of the receptor Tom20 in specificity and efficiency of protein import into mitochondria. Proc Natl Acad Sci U S A *108*, 91-96.

Yamano, K., Yatsukawa, Y., Esaki, M., Hobbs, A.E., Jensen, R.E., and Endo, T. (2008). Tom20 and Tom22 share the common signal recognition pathway in mitochondrial protein import. J Biol Chem *283*, 3799-3807.

Yao, N., Eisfelder, B.J., Marvin, J., and Greenberg, J.T. (2004). The mitochondrion--an organelle commonly involved in programmed cell death in Arabidopsis thaliana. Plant J *40*, 596-610.

Zara, V., Conte, L., and Trumpower, B.L. (2007). Identification and characterization of cytochrome bc(1) subcomplexes in mitochondria from yeast with single and double deletions of genes encoding cytochrome bc(1) subunits. FEBS J *274*, 4526-4539.

Zara, V., Conte, L., and Trumpower, B.L. (2009a). Biogenesis of the yeast cytochrome bc1 complex. Biochim Biophys Acta *1793*, 89-96.

Zara, V., Conte, L., and Trumpower, B.L. (2009b). Evidence that the assembly of the yeast cytochrome bc1 complex involves the formation of a large core structure in the inner mitochondrial membrane. FEBS J *276*, 1900-1914.

Zerbetto, E., Vergani, L., and Dabbeni-Sala, F. (1997). Quantification of muscle

mitochondrial oxidative phosphorylation enzymes via histochemical staining of blue native polyacrylamide gels. Electrophoresis *18*, 2059-2064.

Zhang, J., Yang, J., Roy, S.K., Tininini, S., Hu, J., Bromberg, J.F., Poli, V., Stark, G.R., and Kalvakolanu, D.V. (2003). The cell death regulator GRIM-19 is an inhibitor of signal transducer and activator of transcription 3. Proc Natl Acad Sci U S A *100*, 9342-9347.

Zickermann, V., Kerscher, S., Zwicker, K., Tocilescu, M.A., Radermacher, M., and Brandt, U. (2009). Architecture of complex I and its implications for electron transfer and proton pumping. Biochim Biophys Acta *1787*, 574-583.

Appendices

Appendix I Media and solutions

1. Genomic DNA extraction buffer

250 mM NaCl, 25 mM EDTA, 0.5% (w/v) SDS, 200 mM Tris-HCl, pH 7.5

2. Arabidopsis mitochondrial isolation media

2.1 Grinding buffer

0.45 M sucrose, 25 mM tetrasodiumpyrophosphate, 1% (w/v) BSA, 1% (w/v) PVP-40, 2 mM EDTA, 10 mM KH_2PO_4. Adjust pH to 8.0 with HCl. Prior to use 20 mM L- cysteine was added.

2.2 2 x Wash buffer

0.6 M sucrose, 20 mM TES, 0.2% (w/v) BSA. Adjust pH to 7.5 with NaOH. Add same volume of SDW to dilute it into 1 x wash buffer.

2.3 Heavy gradient solution

17.5 ml 2 x Wash buffer, 9.8 ml Percoll, 7.7 ml 20% (w/v) PVP-40 for 2 gradient tubes

2.4 Light gradient solution

17.5 ml 2 x Wash buffer, 9.8 ml Percoll, 7.7 ml SDW for 2 gradient tubes

3. *In vitro* transciption/translation reaction master mix (50 µl)

25 µl TNT® rabbit reticulocyte lysate, 4 µl TNT® reaction buffer, 2 µl SP6 or T7 RNA polymerase, 2 µl 1 mM amino acid mixture minus methionine, 2 µl 40 units/µl RNasin® ribonuclease inhibitor (Promega, Melbourne, Australia), 1 µl [35S]-methionine (>1000 Ci/mmol at 10 mCi/ml; Amersham Pharmacia Biotech,

Sydney, Australia).

4. Mitochondrial import solutions

4.1 Import master mix

1 ml 2 x import buffer (Appendix I, 4.3), 2 µl 1 M $MgCl_2$, 20 µl 100 mM methionine, 4 µl 100 mM ADP, 15 µl 100 mM ATP, 20 µl 0.5 M succinate, 20 µl 0.5 M DTT. Made up to 2 ml with SDW.

4.2 2 x Sample buffer

25 ml 10% (w/v) SDS, 10 ml glycerol, made up to 50 ml with stacking buffer (Appendix I, 6.2) and a few grains of bromophenol blue. Before use, 20% (v/v) β-mecaptoethanol was added.

4.3 2 x Mitochondrial import buffer

0.6 M sucrose, 100 mM KCl, 20 mM MOPS, 10 mM KH_2PO_4, 0.2% (w/v) BSA. Adjust

pH to 7.5 with HCl.

5. Agarose gel electrophoresis solutions

5.1 10 x TAE

48.4 g/L Tris, 11.8 ml/l glacial acetic acid, 10 mM EDTA. Diluted 1 in 10 with SDW prior to use.

5.2 5 x loading buffer

30% (v/v) glycerol and a few grains of bromophenol blue. Mixed with a vortex to dissolve.

6. SDS-PAGE solutions

6.1 Separating buffer

1.5 M Tris-Cl, pH 8.8

6.2 Stacking buffer

0.5 M Tris-Cl, pH 6.8

6.3 5 x Running Buffer

15 g/L Tris base, 72 g/L glycine, 5.0 g/L SDS.

Diluted to 1 x Running buffer with 5 volume SDW.

6.4 Coomassie staining buffer

400 ml/l 100% ethanol, 100 ml/l glacial acetic acid, 1 g/L Coomassie Brilliant Blue R-250

6.5 Coomassie destaining buffer

150 ml/l glacial acetic acid, 400 ml/l 100% ethanol, 25 ml/l glycerol

7. Blue Native PAGE

7.1 Digitonin solubilization buffer

30 mM Hepes, 150 mM potassium acetate, 10% (v/v) glycerol, pH 7.4

7.2 Serva Blue G solution

750 mM amino caproic acid, 5% (w/v) Coomassie Brilliant Blue G-250

7.3 Gradient gel

1.5 M amino caproic acid, 150 mM Bis-Tris pH 7.0, 4.5-16% (v/v) acrylamide, 0-87% (v/v) glycerol, 0.05% (w/v) ammonium persulphate (AMPS) and 0.05%

(v/v) TEMED

7.4 Stacking gel

1.5 M amino caproic acid, 150 mM Bis-Tris pH 7.0, 4% (v/v) acrylamide, 0.05% (w/v) ammonium persulphate (AMPS) and 0.05% (v/v) TEMED

7.5 Cathode buffer

50 mM Tricine, 15 mM Bis-Tris, 0.02% (w/v) Coomassie Brilliant Blue G-250, pH 7.0

7.6 Anode buffer

50 mM Bis-Tris, pH 7.0 with HCl

7.7 Fixing buffer

50% (v/v) methanol, 10% (v/v) acetic acid

8. Western blotting solutions

8.1 Transfer buffer

2.93 g/L glycine, 5.81 g/L Tris base, 0.375 g/LSDS, 200 ml/L methanol

8.2 10 x Ponceau stain

2 g/L Ponceau S, 300 g/L trichloroacetic acid, 300 g/L sulfosalicylic acid. Diluted 1 in 10 with SDW before use to 1 x Ponceau stain.

8.3 1 x TBS-Tween

100 ml/L10 x TBS (Appendix I, 8.4), 1 ml/L Tween-20

8.4 10 x TBS

90 g/L NaCl, 12.11 g/L Tris. Adjust pH to 7.4 with HCl.

9. Complex I activity assay solutions

9.1 Complex I activity staining solution

0.1 M Tris pH 7.4, 0.14 mM NADH, 1mg/ml Nitro tetrazolium blue

9.2 Fixing solution

50% (v/v) methanol, 10% (v/v) glacial acetic acid

10. Protein expression and purification buffer

10.1 lysis buffer

6 M urea, 300 mM KCl, 50 mM KH_2PO_4, 5 mM imidaole, pH 8.0

10.2 Denaturing IMAC wash buffer 1

6 M urea, 300 mM KCl, 50 mM KH_2PO_4, 5 mM imidaole, pH 8.0

10.3 Denaturing IMAC wash buffer 2

6 M urea, 300 mM KCl, 50 mM KH_2PO_4, 10 mM imidaole, pH 8.0

10.4 Denaturing IMAC elution buffer

6 M urea, 300 mM KCl, 50 mM KH_2PO_4, 250 mM imidaole, pH 8.0

10.5 Denaturing IMAC cleaning buffer 1

500 mM NaCl, 50 mM Tris, pH 8.0

10.6 Denaturing IMAC cleaning buffer 2

500 mM NaCl, 100 mM NaOAc, pH 4.5

10.7 Storage buffer

2% (w/v) Benzyl alcohol

11. Colloidal Coomassie stain solution

170 g/L $(NH_4)_2SO_4$, 340 ml/L methanol, 36 ml/L ortho-phosphoric acid, 1 g/L Coomassie Brilliant Blue G-250. Stir for 4 h to dissolve.

12. Mass spectrometry solutions

12.1 Destaining buffer

10 mM NH_4CO_3 and 50% (v/v) acetonitrile

12.2 Digestion buffer

10 mM NH_4CO_3 and 12.5 µg/ mL trypsin in 0.01% (v/v) trifluoroacetic acid

12.3 Extraction buffer

50% (v/v) acetonitrile and 5% (v/v) formic acid

12.4 Resuspension buffer

5% (v/v) acetonitrile and 0.1% (v/v) formic acid

Appendix II Primers for T-DNA line screening

Gene	At number	line	Primers 5'-3'
Tim17-1	At1g20350	SALK_092885	RP': TCAAAATCGAAAATCAATGGG
			LP': AAATGGAACCCCAATGACTTC
		SALK_091528	RP: CTGAGGCCATGATGAAGATTC
			LP: AGGAGGAGCATCAAAGCTCTC
Tim17-2	At2g37410	GABI_561E03	RP: TCTATGGTTTGCTTTCGATCG
			LP: GACAAAAAGACGACGAAATGG
Tim17-3	At5g11690	SALK_048425	RP: TATCGGTTATGCATTTGGAGC
			LP: ATCGACATGTAGCAAACCTGG
		SALK_125567	RP': AGCATTGTCAGGAACATGGAC
			LP': GAGATACAAGACCGCTCGTTG
Tim23-1	At1g17530	SALK_030470	RP: TTTTGAATTCGTCTGGTCAGG
			LP: GTTAGCTGACAGGGCACTTTG
		SALK_107963	RP': TTTTGAATTCGTCTGGTCAGG
			LP': ACAGGGCACTTTGTCAATTTG
Tim23-2	At1g72750	SALK_143656	RP': CAATCCAATGATACCAATCCG
			LP': CGTGATTTACCTCGTGCTCTC
		GABI_689C11	RP: ATGGATTGCAATTTTGCAAAG
			LP: CCAATCGGCAAAACATTTAATC
Tim23-3	At3g04800	SALK_129386	RP: GGCGTTGAAGTTATGACCAAG
			LP: CCTCTTTAGTTCTACCGGTTGC
		SAIL_1151_B01	RP': ATGGCAAGCCTTATGTGACTG
			LP': CCTTTTGCTGCTCTTGACTTG

SALK_LBb1.3: ATTTTGCCGATTTCGGAAC

SAIL_LB: GCCTTTTCAGAAATGGATAAATAGCCTTGCTTCC

GABI_LB: GGGAATGGCGAAATCAAGGCATCG

Appendix III Gateway primers for Tim23 antibody production

ATTB1: GGGGACAAGTTTGTACAAAAAAGCAGGCTCCGCGATCAATCGTAGCTCCGAT

B1_Reverse: TACGAATTCCTGAGATTTGATCGGGACCTGGTA

ATTB2: GGGGACCACTTTGTACAAGAAAGCTGGGTCCTAGACAACACTGGTCCA AACATC

B2_Forward: GTAGAATTCTCTGGTCAGGCAGGTCGTACT

ATTB1': GGGGACAAGTTTGTACAAAAAAGCAGGCTCCAACCATAGCACCGGGCATCAA

B1_Reverse': TACGAATTCCTTACGGTACGGAAGATTGACTTGTTG

ATTB2': GGGGACCACTTTGTACAAGAAAGCTGGGTCCTATCTCATATACGTAACACCGCT

B2_Forward': GTAGAATTCTGGGGTTATTGCACTGGATCT

Appendix IV Antibody list

At number	gene	raised to	vector	mitochondrial	2nd Ab	Obtained
At1g72750	Tim23-2	3-32 103-143 aa	pDest17	20 kDa	rabbit	Whelan's lab
At2g37410	Tim17-2	143-243 aa	pDest15	30 kDa	rabbit	Whelan's lab
At3g10110	Tim22	1-50 aa	pDest15	16 kDa	rabbit	Whelan's lab
At5g24650	PRAT member	1-50 aa	pDest17	34 kDa	rabbit	Whelan's lab
At2g42210	PRAT member	1-100 aa	pDest15	20 kDa	rabbit	Whelan's lab
At5g05520	Sam50	1-211 aa	pDest17	60 kDa	rabbit	Whelan's lab
At3g2000	Tom40	1-206 aa	pDest17	37 kDa	rabbit	Whelan's lab
At5g23395	Mia40	full length	pDest17	25 kDa	rabbit	Whelan's lab
At1g49880	Erv1	1-191 aa	pDest17	20 kDa	rabbit	Whelan's lab
At2g19080	Metaxin	1-200 aa	pDest15	30 kDa	rabbit	Whelan's lab
At1g27390	Tom20-2	1-181 aa	pDest15	22 kDa	rabbit	Whelan's lab
At3g27080	Tom20-3	1-161 aa	pDest17	20 kDa	rabbit	Whelan's lab
At5g40930	Tom20-4	1-161 aa	pDest15	20 kDa	rabbit	Whelan's lab
At1g55900	Tim50	110-269 aa	pDest17	42 kDa	rabbit	Whelan's lab
At4g00026	Tim21	160-376 aa	pDest17	45 kDa	rabbit	Whelan's lab
At2g36070	Tim44	100-472 aa	pDest17	47 kDa	rabbit	Whelan's lab
At3g46560	Tim9	1-93 aa	pDest17	10 kDa	rabbit	Whelan's lab
At5g13430	RISP	21-151 aa	pDest17	30 kDa	rabbit	Whelan's lab
Atmg00160	COX II			30 kDa	rabbit	Agrisera
Soybean AOX1/2	AOX			34 kDa	mouse	Agrisera

Manuscript

Interaction between Tim23 and complex I links mitochondrial activity and biogenesis in *Arabidopsis thaliana*.

Yan Wang[1], Chris Carrie[1], Estelle Giraud[1], Dina Elhafez[1], Reena Narsai[2], Owen Duncan[1], James Whelan[1] and Monika W Murcha[1]

[1]ARC Centre of Excellence in Plant Energy Biology, [2]Centre for Computational Systems Biology, Bayliss Building M316 University of Western Australia, 35 Stirling Highway, Crawley 6009, Western Australia, Australia.

Running title : A molecular link between mitochondrial activity and biogenesis

*Corresponding author: Monika Murcha

Email: monika@cyllene.uwa.edu.au

The author responsible for distribution of materials integral to the findings presented in this article in accordance with the policy described in the Instructions for Authors (www.plantcell.org) is: Monika W. Murcha (monika@cyllene.uwa.edu.au).

Abbreviations

ANT	Adenine Nucleotide Translocator
AOX	Alternative Oxidase
BiFC	Biomolecular Fluorescene Complementation
COX	Cytochrome Oxidase
Cyt *c*	Cytochrome C
F_Ad	F_Ad subunit of ATP Synthase
MDHAR	Monodehydroascorbate Reductase
MIC	Mixed Inner membrane Complex
OEP	Outer Envelope Protein
PAM	Presequence translocase Associated Motor
Pic	Phosphate translocator
PRAT	Preprotein and Amino acid Transporter
RISP	Rieske Iron Sulphur cluster Protein
SAM	Sorting and Assembly Machinery
TIM	Translocase of the Inner Membrane
TOM	Translocase of the Outer Membrane
YFP	Yellow Fluorescence Protein
HAP	Heme Activated Proteins

Abstract

Characterisation of the translocase of the inner membrane 17:23 complex (TIM17:23) in mitochondria from *Arabidopsis thaliana* revealed that complete knockout of either component was lethal. However, a subtle two-fold over-expression of Tim23 resulted in a severely retarded growth phenotype. Increased Tim23 protein levels resulted in a severe reduction in the amount of complex I (NADH dehydrogenase) within the mitochondrial respiratory chain. Independent reduction of the amount of complex I resulted in an increase in the amount of Tim23. A physical link between complex I and TIM17:23 was also demonstrated, in that imported Tim23 was incorporated into complex I, could be detected in complex I using antibodies to Tim23 and was shown to interact with complex I subunits using a variety of protein-protein interaction assays. Transcriptome analysis revealed that the increase in Tim23 was accompanied by widespread increases in transcript abundance for transcripts encoding a variety of components required for mitochondrial biogenesis. Taken together these results indicate that the abundance of Tim23 is tightly regulated in Arabidopsis, and via interaction with complex I acts as a sensor for mitochondrial biogenesis,,revealing novel retrograde regulatory pathways from the mitochondrion to the nucleus.

Introduction

The endosymbiotic event that led to the formation of mitochondria is proposed to be a crucial step in the evolution of eukaryotic cells (Lane and Martin, 2010). The production of energy in mitochondria, through the process of oxidative phosphorylation is also well described (Siedow and Day, 2000). However, mitochondria contain many more proteins than those involved in energy metabolism *per se*. Proteome characterisation of mitochondria identified almost 1000 proteins in *Saccharomyces cerevisiae* (yeast) (Sickmann et al., 2003), and experimental approaches have identified just over 1000 and 700 proteins in animal and plant mitochondria respectively (Heazlewood et al., 2007; Calvo and Mootha, 2010). Although often present in lower abundance, a large number of proteins present in mitochondria are required for mitochondrial biogenesis, ranging from proteins involved in DNA replication and transcription (Holt, 2009; Leigh-Brown et al., 2010; Liere et al., 2011), translation of mitochondrial transcripts (Ott and Herrmann, 2010; Watanabe, 2010) and the proteins present in various complexes or translocases that are required for the import of mitochondrial proteins synthesised in the cytosol (Schmidt et al., 2010). Notably, many proteins of the protein import pathway are defined as essential in yeast, due to the importance of mitochondrial biosynthetic function in cell viability (Chacinska et al., 2009).

A variety of multi-subunit protein complexes are present on the outer membrane, (Translocase of the Outer Membrane, TOM; Sorting and Assembly Machinery, SAM) (Stroud et al., 2010), and on the inner membrane, (Translocases of the Inner Membrane 17:23 and 22, TIM17:23 and TIM22) (Rehling et al., 2004; Mokranjac and Neupert, 2010), which together are required to import the wide variety of cytoplasmically synthesised mitochondrial

proteins. While the protein import apparatus is generally well conserved across phylogenetic groups (Hewitt et al., 2011), particularly the pore forming subunits, which display high levels of orthology (Dolezal et al., 2006; Carrie et al., 2010a), significant differences are observed between the outer membrane protein import receptors of plants compared to yeast and mammals (Perry et al., 2006; Lister et al., 2007), and the location of MPP in the cytochrome bc_1 complex (Braun et al., 1992; Glaser et al., 1994). Analysis of the complete genome sequence over a wide variety of organisms indicates that the TIM17:23 translocase is highly conserved between species (Carrie et al., 2010a).

In the last decade, studies have revealed the higher order structure of multi-subunit protein complexes on the mitochondrial inner membrane, in particular the identification of respiratory chain super complexes (Stuart, 2008; Wittig and Schagger, 2009; Dudkina et al., 2010). Super complex structures between complex I and III, complex III and IV, dimeric ATP synthase, and even higher order structures of rows of super complexes have been described (Stuart, 2008; Dudkina et al., 2010; Sunderhaus et al., 2010). The functional significance of these respiratory super complexes is not yet clear; they may enhance electron flow via substrate channelling, prevent production of excess reactive oxygen species or play a role in maintaining the stability of respiratory chain complexes (Dudkina et al., 2010; Sunderhaus et al., 2010). In the case of the ATP synthase complex, the arrangement of such super complexes is proposed to stabilise the cristae structure that is characteristic of the mitochondrial inner membrane (Wittig and Schagger, 2009; Dudkina et al., 2010). In the case of the protein import complexes, the TIM17:23 complex has been reported to be associated with both the TOM complex and the respiratory chain complexes, in addition to the presequence assisted motor complex (PAM)

(Schmidt et al., 2010), that is located on the matrix side of the inner membrane and pulls precursor proteins through the TIM17:23 translocase. Tim21, Tim23 and Tim50 play a role in facilitating interactions with the outer membrane TOM complex to form a dynamic TOM-TIM super complex, and current evidence indicates that Tim21 also mediates the interaction between the TIM17:23 and complex III in yeast (van der Laan et al., 2006). In fact, two distinct forms of TIM17:23 have been identified. TIM17:23^{sort} contains Tim17, 23, 50 and 21, and is involved in the lateral insertion of preproteins into the innermembrane. TIM17:23-PAM translocates protein into the matrix, and does not contain Tim21, but contains the PAM subunits Tim44, HSP70, Mge1, and Pam 16, 17 and 18 (Schmidt et al., 2010).

The TIM17:23 complex appears to be the most highly conserved import complex across the various eukaryotic lineages with respect to composition of the various subunits (Carrie et al., 2010a). Arabidopsis contains seventeen genes encoding proteins that belong to the Preprotein and Amino acid Transport family (PRAT) (Rassow et al., 1999), of which 10 proteins are located in mitochondria, 6 are located in plastids and one protein is dual targeted to mitochondria and plastids (Murcha et al., 2007). The OEP16 subfamily of plastid PRAT proteins has been proposed to be amino acid permeases on the chloroplast outer membrane (Brautigam and Weber, 2009; Pudelski et al., 2010). In order to further characterise the interactions of TIM17:23 with other components in mitochondria, we used knock-out and over-expression approaches. We uncovered substantial evidence indicating that over-expression of Tim23 results in a dramatic reduction in complex I (NADH: ubiquinone oxidoreductase). Independent reduction of complex I by genetic approaches results in an up-regulation of Tim23, and, in both cases, reduced

complex I is accompanied by an up-regulation of many of the components required for active mitochondrial biogenesis. It was demonstrated that Tim23 associated with the monomeric form of complex I. These results suggest that, in addition to its role as a translocase, Tim23 interacts with complex I and affects signals relating to mitochondrial biogenesis.

Results

Over-expression of Tim23 results in growth retardation

Several attempts to over-express tagged or un-tagged Tim17 (At1g20350 Tim17-1; At2g37410 Tim17-2; At5g11690 Tim17-3) and Tim23 (At1g17530 Tim23-1; At1g72750 Tim23-2; At3g04800 Tim23-3) proteins in Arabidopsis yielded no transgenic plants where over-expressed protein could be detected. Therefore, to characterise the role of the three isoforms encoding either Tim23 or Tim17 in Arabidopsis (Murcha et al., 2003). T-DNA insertion lines for each of the genes were obtained. With the exception of *tim17-2,* all T-DNA insertion lines were viable (data not shown). Crossing the single *tim23* T-DNA insertion lines revealed that various combinations of knocking out two *tim23* genes were also lethal (data not shown). As *tim17* and *tim23* are essential genes in yeast, it is not unexpected that a similar situation was observed in Arabidopsis (Dekker et al., 1993; Maarse et al., 1994). Notably, for Arabidopsis, there is additional complexity in that for Tim23*,* some redundancy is observed; while for Tim17, *tim17-2* is essential and neither *tim17-1* nor *tim17-3* can compensate for its loss at a functional level or at a regulatory level. Almost all viable single T-DNA lines displayed no altered phenotype, however, for *tim23*-2, one T-DNA line (SALK_143656*),* displayed retarded growth compared to wild-type (Col-0), whilst another T-DNA line (GABI_689C11) displayed a normal growth

phenotype (Figure 1A). Thus, both T-DNA lines for *tim23-2* were further investigated.

The retarded growth phenotype of the T-DNA line SALK_143656 for *tim23* was confirmed after several backcrosses and was evident throughout the plants' lifecycle (Figure 1A). Mapping and sequencing of the T-DNA insertion in both lines revealed that while one line (GABI_689C11) represented an insertion in the gene at position 43 bp 3' of the translational start site, the insertion for the other line (SALK_143656) was in fact located 135 bp 5' of the translational start site (Figure 1B). To determine the effect of both insertions on the abundance of Tim23-2 protein, antibodies raised against Tim23-2 were used in western blot analysis of mitochondria isolated from each line (Figure 1C). In the T-DNA insertion line, SALK_143656, where the T-DNA was inserted 135 bp upstream of the translation start site and exhibited a retarded growth phenotype (Figure 1A and B), there was a ~2 fold increase in abundance of the protein detected (Figure 1C). In contrast, immunodetection of the T-DNA insertion line GABI_689C11, where the T-DNA insert is located at a position 43 bp 5' of the gene, resulted in no Tim23-2 protein detected with an apparent mol mass of 20 kDa (Figure 1C). Thus, these lines are referred to as knock-out (*tim23* KO) for GABI_689C11 and over-expresser (*tim23* OE) for SALK_143656.

The specificity of the Tim23-2 antibody, which was raised against Tim23-2 amino acid regions 3-32 and 103-143, was verified using full-length over-expressed protein for all three Tim23 proteins (Supplementary Figure 1A). The Tim23-2 antibody cross-reacted with both recombinant Tim23-1 and Tim23-2, (Supplementary Figure 1A). Thus, it was not possible to distinguish between Tim23-1 and Tim23-2 using the Tim23-2 antibody alone. An antibody to Tim23-3, which was raised against the amino acids 6-32 and 64-132, detected both

recombinant Tim23-1 and Tim23-3 proteins, but not Tim23-2 (Supplementary Figure 1A). Using the Tim23-3 antibody, no signal was detected in western blot analysis for mitochondria isolated from Col-0 plants (Supplementary Figure 1A), or any of the T-DNA lines for Tim23 (data not shown), thus implying that both Tim23-1 and Tim23-3 are not present in mitochondria in detectable amounts under the conditions tested in this study.

Notably, probing mitochondria isolated from the *tim23-2* KO line with the Tim23-2 antibody detected a weak band, corresponding to a smaller protein of approximately 18 kDa in size, which is not evident in Col-0 or *tim23* OE blots (Supplementary Figure 1A and Figure 1C). Analysis of the transcript abundance for *Tim23-1* and *Tim23-2* revealed that for the *tim23* KO line, the T-DNA insertion at position 43 bp results in elevated amounts of transcript missing the first part of the *Tim23-2* transcript upstream of the T-DNA. This is also in agreement with the western blot analysis of a smaller protein, outlined above that is likely to represent a truncated form of Tim23-2, translated downstream of the T-DNA insert (Figure 1B, Supplementary Figure 1B). In the case of the *tim23* OE line, while *Tim23-2* transcript abundance was not elevated, and was somewhat reduced in amount (Supplementary Figure 1B), protein abundance was increased (Figure 1C, see below). Thus, the amount of Tim23 in the *tim23* OE line appears to be regulated by translational control, which may be due to insertion of the T-DNA in the 5' UTR.

Over-expression of Tim23-2 results in elevated levels of protein import via the general import pathway

As Tim23 is the channel forming subunit in the TIM17:23 translocase in yeast (Truscott et al., 2001), we investigated whether protein import was

affected in the *tim23* KO and OE lines. Three proteins that contain N-terminal cleavable targeting signals, imported via the general import pathway were used, Alternative oxidase (AOX) (Whelan et al., 1995), the F_Ad subunit of ATP synthase (F_Ad) (Smith et al., 1994), and the dual targeted protein monodehydroascorbate reductase (MDHAR) (Chew et al., 2003). Protein import via the carrier import pathway was also tested, using the adenine nucleotide carrier (ANT) and the phosphate carrier (Pic) (Murcha et al., 2005b). The increase in Tim23 protein resulted in almost double the rates of import for AOX, F_Ad and MDHAR, while mitochondria isolated from KO plants displayed reduced rates of protein import of these three precursor proteins (Figure 1D). The effect of altered Tim23 levels was specific to proteins imported via the general import pathway, as no differences were observed with the import of ANT or Pic into mitochondria isolated from Col-0 compared to *tim23* OE or KO lines (Figure 1D). Thus, while over-expression of Tim23 resulted in a doubling of the rate of protein import via the general import pathway, it is not clear why this should result in severely retarded plant growth.

Over-expression of Tim23-2 results in a reduction of complex I

Mitochondria from Col-0, *tim23* OE and KO lines were analysed by BN-PAGE in order to further investigate possible reasons for the growth defect of *tim23 OE* plants. Analysis of the Coomassie stained gel showed that there was a difference in the banding pattern observed for Col-0, *tim23* OE and *tim23* KO mitochondria. Mitochondria from Col-0 plants contained the characteristic pattern of the respiratory chain complexes, with both the monomeric complexes I and III and the super complex I+III evident (Figure 2A). The monomeric form of complex I appeared to be totally absent in the *tim23* OE line, while the super

complex I+III was greatly reduced in intensity. An additional band, between the super complex I+III and complex I was observed (Figure 2A, black square). The pattern of protein complexes from *tim23* KO plants were similar to Col-0 plants, except that the monomeric form of complex I appeared slightly diffused (Figure 2A). An activity stain for complex I, analysed by BN-PAGE, confirmed the dramatic reduction of complex I, although it is notable that some activity is still present, especially at the super complex I+III. Western blotting confirmed that complex I was severely reduced in mitochondria from *tim23* OE lines (Figure 2A, Ndufs4), but that the mobility and amount of other respiratory chain components were essentially unchanged, as seen with complex III (RISP) and complex IV (COXII) or even increased, as seen with complex V (α–subunit of ATP synthase) (Figure 2A).

A Reduction in Complex I Results in an Increase in Tim23

The *tim23* OE line resulted from a T-DNA insertion upstream of the protein coding sequence, and thus, represents a single line that cannot be biologically replicated in order to verify a direct connection between the amount of Tim23 and the amount of complex I. Also, previous attempts to over-express Tim23 have been unsuccessful. Therefore, to verify the connection between Tim23 and complex I, we characterised a mutant where complex I activity had been dramatically reduced in a similar manner to the *tim23* OE line, and investigated the level of Tim23 and import capacity. We choose a mutant (*rug*) that has a specific defect in splicing the mitochondrial transcript *nad2,* displays a similar growth phenotype to the *tim23* OE line and has complex I levels that are similarly reduced by approximately 90% (Figure 2B) (Kühn et al., 2011).

Note that this line does not display the extra complex band evident in the *tim23* OE line (Figure 2B).

Characterisation of the import capacity of mitochondria isolated from the *rug* mutant line revealed increased import rates of all proteins tested, via both the general import pathway (AOX, F_Ad, MDHAR) and the carrier import pathway (ANT and Pic) (Figure 2C i and ii). The latter differs from the *tim23* OE line, that showed no increase in import rates of carrier pathway proteins (Figure 1D, ANT and Pic panels verse Figure 2C, ANT and Pic panels).

In order to further investigate the similarities between *tim23* OE and *rug* plants, mitochondria were isolated from Col-0, *tim23* KO, *tim23* OE and *rug* plants and probed with a series of antibodies against mitochondrial PRAT proteins (Murcha et al., 2007), respiratory chain components, proteins involved in protein import and mitochondrial proteins that are normally increased in abundance under various stresses (Giraud et al., 2011) (Figure 3). In the case of mitochondrial PRAT proteins, it was evident that an increase or decrease in the amount of Tim23 resulted in an increase or decrease in Tim17-2 protein abundance. A protein encoded by At3g10110 or At1g18320 (two genes which have 100% identity), which has been shown to complement a yeast *tim22* deletion mutant (Murcha et al., 2007), was also increased in the *tim23* OE and *rug* lines (Figure 3A). In contrast, a PRAT protein of unknown function (At3g25120) was decreased in the *tim23* OE and *rug* lines, but increased in the *tim23* KO line (Figure 3A). Finally, At2g42210, that encodes a PRAT protein previously identified as a subunit of complex I in two independent studies (Meyer et al., 2008; Klodmann et al., 2010), was shown to decrease in protein abundance in the *tim23* KO line and remained relatively unchanged in the *tim23* OE line (Figure 3A), but decreased in the *rug* line (Figure 3A).

In the case of a variety of other respiratory chain components, the most notable effect observed was a > 80% reduction of Ndufs4 in the *tim23* OE and *rug* lines (Figure 3A), as previously reported for mitochondria from *rug* lines (Kühn et al., 2011). This is a complex I subunit proposed to be present in the peripheral portion of complex I (Klodmann and Braun, 2010; Klodmann et al., 2010). Notably, Nad9, a mitochondrial encoded complex I component, present in the matrix arm, Q module (Klodmann and Braun, 2010; Klodmann et al., 2010) was also slightly decreased (Figure 3A), but not to the same extent as the Ndufs4 protein. A variety of other respiratory chain components decreased to some extent in both the *tim23* OE and KO lines, and in the *rug* line, thus COXII decreased by approximately 50% in these three lines and the β-subunit of the ATP synthase complex decreased by 30% to 40% (Figure 3A). In contrast the α-subunit of ATP synthase complex and the Rieske FeS protein of the cytochrome bc_1 complex increased by 50% in the *rug* and *tim23* OE lines (Figure 3A). Thus, analysis by BN-PAGE banding pattern, activity staining for complex I and western blot analysis of SDS-PAGE separated proteins reveal a reduction in the activity and amount of complex I in *tim23* OE and *rug* lines.

Analysis of a variety of proteins involved in protein import revealed that in the *tim23* OE and *rug* line there was an increase in all three Tom20 isoforms (Lister et al., 2007), with Tom20-4 and Tom20-2 showing increases of greater than two-fold (Figure 3A). Increases were also observed in Tim50, Tim21 and Tim9 (Figure 3A). Both the *tim23* OE and KO lines resulted in an induction of the Alternative Oxidase (AOX), a marker of the mitochondrial retrograde response in Arabidopsis (Figure 3A (Clifton et al., 2005; Rhoads and Subbaiah, 2007; Giraud et al., 2008). No change was observed in porin, a marker used to verify equal loading on a total mitochondrial protein basis (Figure 3A).

Additional complex I mutants analysed included plants in which one of the RNA polymerases targeted to mitochondria is inactivated, *rpotmp* (Kühn et al., 2009) and a knock-out of a complex I subunit, *ndusf4* (Meyer et al., 2009). Analysis of the abundance of Tim23-2 and Tim17-2 in these mutant backgrounds that show a reduction in the abundance of complex I reveal a similar pattern, in that both Tim23-2 and Tim17-2 are also increased by greater than 2-fold in these lines (Figure 3B). Analysis of *in vitro* import into mitochondria from both *rpotmp* and *ndusf4* lines also revealed an increase in import, as observed for mitochondria isolated from the *tim23* OE and *rug* lines (Figure 3C). Thus in a variety of independent genetic backgrounds there is a correlation between an increase in Tim23, a reduction of complex I and an increase in the rate of protein import.

Mitochondria from tim23 OE Do Not Assemble Complex I

The decrease in the abundance of complex I in *tim23* OE plants could be due to either failure to assemble the complex or instability of the complex. It was notable that while mitochondria from *tim23* OE plants had much reduced levels of complex I and the super complex I+III on BN-PAGE, an additional complex was also present (Figure 2A and B), labelled as MIC (mixed inner membrane complex). This band was observed in all preparations of mitochondria from *tim23* OE plants, irrespective of growth conditions. This band was gel excised, purified and analysed by SDS-PAGE, and proteins then identified by mass spectrometry. This complex contained a number of proteins from complex I (At2g42210, At4g16450, At5g63510), complex III (At3g52730, At4g32470, At1g51980), complex V (AtMg01190, At5g08670), prohibitin (At1g03680, At5g40770) as well as proteins of unknown function (At2g33220)

(Supplementary Figure 2A, Supplementary Table 1). Thus, this complex is not a complex I assembly intermediate with another complex, neither is it predominantly comprised of complex I subunits, rather it is a mixture of different proteins from various inner membrane complexes and is thus will be referred to as the Mixed Inner membrane Complex (MIC). Note, the presence of the protein encoded by At2g42210 in this complex can account for the presence of this protein in *tim23* OE plants, even though complex I has diminished, compared with the *rug* plants which do not contain MIC and display reduced amounts of this component (Figure 3A). Also, western blot analysis with the antibody to the complex III protein RISP detects this MIC (Figure 2A), further showing that it appears to be a hybrid complex. A variety of proteins in this complex were assembled into this complex upon import (Supplementary Figure 2C).

A molecular connection between complex I and Tim23

Import of Tim23 into isolated mitochondria and analysis by BN-PAGE revealed that it is predominantly incorporated into two complexes of ~100 kDa and ~200 kDa, compared to complex sizes of 90, 140 and 240 kDa when yeast Tim23 is imported into yeast mitochondria in a similar manner (Dekker et al., 1993). Tim23 was also incorporated into complex I (Figure 4A). This incorporation into complex I increased over time from 5 to 40 min and notably Tim23 was not incorporated into the super complex I+III (Figure 4B). No incorporation of Tim17-2 into complex I was observed, despite heavy labelling into the TIM17:23 complex (Figure 4A and B). *In vitro* import assays with the complex I subunit At2g42210 displayed incorporation only into complex I (Figure 4A and B), while the complex I subunit encoded by At1g47620 was

incorporated into complex I, and the super complex I+III (Figure 4A and B). Import of the complex III protein MPPα, (At1g51980), revealed that it was imported into complex III and the super complex I+III (Figure 4A).

A similar assay into mitochondria from *tim23* OE and KO mitochondria revealed that incorporation of Tim23 into complex I was reduced in mitochondria from the *tim23* OE line, compared to mitochondria from Col-0 or *tim23* KO plants (Figure 4C). Western blot analysis revealed that Tim23 was only present in complex I in mitochondria from Col-0 plants (Figure 4D). Import of Tim17-2 into mitochondria from the *tim23* OE and KO lines showed no incorporation into complex I (Figure 4C), and antibodies to Tim17-2 did not cross react with any product that was related to complex I (Figure 4D). On the basis of these results, it was concluded that Tim23 alone can interact and be incorporated into complex I.

The interaction of Tim23 with complex I was further confirmed by immunoprecipitation, yeast-2-hybrid interactions and bimolecular fluorescence complementation (BiFC) (Figure 5). Mitochondria isolated from Col-0 plants were lysed and immunoprecipitation was carried out with antibodies raised against Tim23-2. In addition to Tim23 being detected in the precipitated products (Figure 5A), the complex I subunit Ndufs4 was also detected, while cytochrome c was not, therefore indicating that antibodies to Tim23 can specifically pull-down complex I subunits (Figure 5A). Using a split YFP BiFC assay, the interaction of Tim23 with Tim17-2 and the complex I component encoded by At2g42210 could be demonstrated (Figure 5B), again no interaction was observed with a variety of negative control proteins (data not shown).

Protein-protein interactions were also tested using yeast two-hybrid assays. Proteins known to interact with Tim23; Tim23, Tim17-2 and Tim50, displayed

positive interactions as expected. The complex I subunit encoded by PRAT family member At2g42210, was also tested, and displayed a positive interaction (Figure 5C). A variety of other respiratory proteins and the empty vector alone showed no growth on selective media, indicating that the growth observed was due to specific interactions of Tim23 with partner proteins.

Analysis of global transcriptional changes in Tim23 mutant plants

tim23 OE lines displayed extensive transcriptional reprogramming, with a total of 1645 transcripts significantly altered with respect to Col-0 seedlings (861 transcripts up-regulated and 784 transcripts down-regulated greater than 1.5 fold, after False Discovery Rate (FDR) correction ($p<0.05$, PPDE(<p)>0.95)). *tim23* KO lines displayed fewer significant changes, with 525 and 466 transcripts significantly down and up-regulated greater than 1.5 fold, respectively, after FDR correction. Comparison of transcript responses between *tim23* OE and *rug* showed significant overlap, not only in the specific genes altered, but also the direction and magnitude of the responses. Significantly more transcripts were co-expressed between *rug* and *tim23* OE than would be expected by random chance, shown by # ($p<0.001$, chi-squared test) (Figure 6A). This indicates the transcriptional responses of *rug* and *tim23* OE show significant similarity on a genome wide scale. Transcript abundance changes for components specifically related to mitochondrial import functions were examined in the two mutant lines. For both lines, transcripts encoding mitochondrial intermembrane space chaperones, and factors associated with folding in the matrix were all consistently up-regulated (Supplementary Table 2, Figure 6B).

To further investigate changes in the *tim23* OE mutants in relation to mitochondrial function and regulation, significant changes were visualized on a custom MapMan image displaying diverse facets of mitochondrial function and biogenesis (Figure 6B). Over-expression of Tim23, and the associated complex I defect, appears to induce a substantial response within the mitochondrion, including the up-regulation of numerous nuclear encoded and organelle encoded components of all five cytochrome respiratory pathway complexes (Figure 6B). This is accompanied by an up-regulation, at the transcript level, of nuclear encoded mitochondrial transcription/translation machinery, mitochondrial import components, and a specific up-regulation of ROS/REDOX scavenging systems within the mitochondria, most likely due to an increase in potential for ROS production due to respiratory chain dysfunction (Figure 6B). Furthermore, steady state mitochondrial transcript levels were measured by QRT-PCR and a 4-10 fold increase was observed for almost all transcripts encoded by the mitochondrial genome (Figure 6B and C). This increase in mitochondrial transcription was also accompanied by an increase in the rates of mitochondrial translation, evident with a number of mitochondrial encoded proteins (Figure 6C). Together, these results suggest that over-expression of Tim23 results in instability of the mitochondrial respiratory chain complex I, and signals a mitochondrial biogenesis response to induce transcription/translation of all components necessary to build a functional organelle.

This potential regulation of Tim23 with mitochondrial biogenesis is further supported by genome wide analysis of the local co-expression environment of *Tim23-2*. The top 50 co-expressed Arabidopsis genes with *Tim23-2* (based on r values across >300 public microarray datasets) from the BAR expression Angler and the ACT

(http://www.arabidopsis.leeds.ac.uk/act/coexpanalyser.php) were combined, leaving a list of 76 unique genes (Supplementary Table 3). Figure 6D shows a functional categorization of this list, compared to the whole genome, these genes are significantly ($p<0.0001$) over represented in the functional categories of protein synthesis (15.8% versus 2.6%), development (11.8% versus 2.8%), protein targeting (6.6% versus 1.1%), RNA binding (6.6% versus 0.7%), RNA processing (6.6% versus 1.1%), cell division (2.6% versus 0.4%) and protein folding (2.6% versus 0.3%). Notably, *Tim23-1* and *Tim23-2* are highly co-expressed with each other, shown by the relatively tight grouping of gene expression r values along a line close to 45 degrees (Figure 6D) and thus, genes that are highly co-expressed with *Tim23-2* are also co-expressed with *Tim23-1*.

Discussion

Here, we showed that in Arabidopsis there is an interaction between complex I of the respiratory chain and the mitochondrial import component Tim23. Furthermore, an increase in Tim23 abundance causes a decrease in complex I, and a decrease in complex I causes an increase in Tim23. Previously, in yeast, it has been demonstrated that the TIM17:23 complex interacts with a variety of other protein complexes, such as the TOM complex to form a dynamic TOM-TIM super complex (Geissler et al., 2002; Yamamoto et al., 2002; Mokranjac et al., 2009; Tamura et al., 2009), the PAM complex to form TIM17:23-PAM super complex (Chacinska et al., 2005; Chacinska et al., 2010) and with complex III to form the TIM17:23^{sort} super complex (van der Laan et al., 2006). However, as yeast lacks complex I, and instead contains a

simple type II NADH dehydrogenase (Melo et al., 2004), this interaction with complex I has not been previously detected.

Attempts to over-express Tim23 (and Tim17) in our hands have been unsuccessful, and thus we investigated the affects of T-DNA insertional inactivation, in an effort to functionally characterise this complex. These proteins were presumed to be essential in Arabidopsis, as they are in yeast, and as both Tim23 and Tim17 are encoded by small gene families, it was reasoned that inactivation of single genes may result in altered amounts of the TIM17:23 complex. However, surprisingly it was the over-expression of Tim23 that resulted in an altered phenotype. Notably, Tim23 over-expression of just two-fold at a protein level yielded dramatic effects within the mitochondrial respiratory chain, with greater than an 80% reduction in complex I. Given the nature of this *tim23* OE line, it was not possible to 'complement' this mutant. Therefore, to verify the findings that an increase in Tim23 resulted in a reduction of complex I, we investigated a number of additional mutants which also exhibit over 80% reduction in complex I activity, including the *rug* mutant, a *nad2* splicing mutant (Kühn et al., 2011), the *rpotmp* mutant (Kühn et al., 2009) and the *ndufs4* mutant (Meyer et al., 2009); and in all cases, a reduction in complex I activity resulted in significantly increased amounts of Tim23. Thus, overall the amount of complex I and Tim23 appears to be linked in Arabidopsis.

The increased abundance of Tim23 in the *tim23* OE line was accompanied by additional changes that together can be grouped into the process of mitochondrial biogenesis. It was notable that transcripts encoding many of the components of the mitochondrial respiratory chain were up regulated in abundance in the *tim23* OE line. An analysis of a variety of transcriptome datasets reveals that this up-regulation of respiratory chain

components is quite unique (Giraud et al., 2011), as generally transcripts encoding respiratory chain components are stable under a variety of stresses (Clifton et al., 2005) or even in knock-outs of complex I components (Meyer et al., 2009). In addition, an increase in the amount of the alternative oxidase (AOX) was observed at the transcript and protein level. While it is common for AOX to be increased under conditions where complex I activity is perturbed (Giraud et al., 2011), it has not been previously observed that both AOX and the cytochrome electron transport chain are up-regulated simultaneously. This suggests that a variety of retrograde signals are produced in the *tim23* OE line that result in an activation of several signal transduction pathways.

There are two additional features of the response to *tim23* OE that are worth noting; a comparison of the protein changes observed with western blotting reveals that the increase in Tom20-2 and Tom20-4 at a protein level is not accompanied by an increase in the transcripts of genes encoding these proteins. This suggests that post-transcriptional regulation of the abundance of these proteins occurs. In a previous study when any one or two of the Tom20 isoforms in Arabidopsis were inactivated, an increase in the other isoforms was observed, again without any change in transcript abundance (Lister et al., 2007). Secondly, while there is a significant overlap in the transcriptome response between the *tim23* OE line and the *rug* line, there are also responses that are unique to both (Figure 6A). While both mutations display many common features; such as a > 80% reduction in complex I activity, an increase in Tim23 and various other proteins of the protein import apparatus, and many common changes in the transcriptome; they differ in that mitochondria from the *rug* mutant also display an increase in the rate of protein imported via the carrier import pathway and transcripts encoding components of the

mitochondrial respiratory chain are not up-regulated, with the exception of AOX. One possibility for the difference in the responses observed is that the *rug* and *rpotmp* mutants are compromised in organelle transcripts, for *nad2* and several *nad* genes, respectively (Kühn et al., 2009; Kühn et al., 2011). This suggests that effective organelle transcription and/or translation may be required as a feedback signal to trigger the response observed in the *tim23* OE line, and this response cannot be fully executed in the *rug* and *rpotmp* mutants, due to the defect in organelle transcript production. Previously, studies investigating the effect of mutations in a gene encoding a dual-targeted protein, Prolyl-tRNA synthetase1, that is required for translation in mitochondria and plastids, demonstrated an important role for organelle translation in retrograde signalling (Pesaresi et al., 2006). Finally, the expression of Tim23 has been altered previously, in order to characterise the TIM17:23 translocase in yeast, with no detrimental effects reported. This may be due to the fact that as yeast is a facultative anaerobic organism and the expression of the respiratory chain components and mitochondrial biogenesis are not necessarily coupled. Rather, in yeast, the expression of mitochondrial respiratory chain components is under the control of heme activated proteins (HAP), that are in turn regulated by the availability of oxygen (Kwast et al., 1998).

In addition to the interaction of Tim23 with complex I, we also observed that Tim23 interacted with complex III via Tim21 (Supplementary Figure 3), as has been previously demonstrated in yeast (van der Laan et al., 2006; Schmidt et al., 2010). Thus, in Arabidopsis it appears that subunits of the TIM17:23 complex interact with both complex I and III, and the latter two form a super complex structure of I+III, as is regularly observed on BN-PAGE. Notably,

Tim23 and Tim21 were not observed in the super complex I+III (Figure 4 and Supplementary Figure 3). As the amount of Tim23 is several fold less abundant compared to complex I (and complex III), the interaction of Tim23 with complex I is likely to be dynamic in nature, as observed with the interaction of TIM23 complex with TOM, PAM and complex III in yeast. Notably, the decrease in the amount of Tim23 in the *tim23* KO line, has little or no effect on the abundance of complex I or the super complex I+III, except that complex I does appear more diffuse when observed on BN-PAGE.

The TIM17:23 complex exists as a modular complex of TIM17:23^{sort} and TIM17:23-PAM complex (Schmidt et al., 2010). A model for the novel interaction of Tim23 with complex I based on the evidence presented in the current work is proposed in Figure 7. Briefly, the over-expression of Tim23 results in an increase in the amount of TIM17:23^{sort}, this is consistent with the increase in Tim50 and Tim21 observed (Figure 3). An increase in the amount of TIM17:23^{sort} results in instability of complex I or an inability to assemble complex I, due to the interaction of Tim23 with complex I subunits, possibly via the complex I PRAT protein At2g42210. An analysis of the import of complex I subunits in the *tim23 OE* lines suggests that it is an inability to assemble complex I, while assembly of subunits into other complexes is not affected (Figure 7). This model is also consistent with the presence of the MIC complex in the *tim23* OE line (Figure 2), as there is an increase in transcripts encoding complex I and several other respiratory chain components (Figure 6), the increase in TIM17:23^{sort} results in them being imported and laterally inserted into the membrane. The reason that the MIC complex may not be observed in the *rug* line is simply that there is no up-regulation of transcript abundance for

these proteins as observed in the *tim23* OE line, and thus this complex does not accumulate.

Finally the results presented here suggest that, in addition to being a subunit of the TIM17:23 translocase, the amount of Tim23 in Arabidopsis is finely regulated with complex I. This provides for an elegant system for retrograde signalling to control the expression of nuclear encoded genes required for mitochondrial biogenesis and respiratory chain activity. Any decrease in the amount of complex I, due to oxidative damage or increased respiratory demand will result in signals that increase the amount of Tim23 and activate mitochondrial biogenesis.

EXPERIMENTAL PROCEDURES

Gene identification

The Mitochondrial Protein Import Components database (MPRIC) (Lister et al., 2003) was used to identify genes used in this study.

Plant material and culture conditions

The SALK T-DNA insertion lines were obtained from the ABRC seed stock centre (Alonso et al., 2003), and GABI lines were obtained from GABI-Kat (Rosso et al., 2003). Lines were screened for homozygosity of the T-DNA insert using primers listed in the Extended Experimental Procedures, as previously outlined (Carrie et al., 2010b; Kühn et al., 2011).

DNA and PCR

Genomic DNA was isolated from 14-day-old plants and PCR was carried out using the REDExtract-N-Amp^{TM} Plant PCR Kit (Sigma Aldrich, Sydney) according to the manufacturer's instructions. Cloning from cDNA was carried out as previously described (Murcha et al., 2003).

Isolation of mitochondria from Arabidopsis plants

For the isolation of mitochondria from water cultured plants, mutant and Col-0 seeds were sterilized and inoculated in half-strength Murashige and Skoog media, containing 0.5 X Gamborgs B5 salts, 3% (w/v) sucrose, 50 µg/ml cefotaxime, 2 mM MES KOH pH 5.7, 0.75% (w/v) agar. Plants were grown for 2

weeks as described above, and the mitochondria isolated as described previously (Lister et al., 2007).

Blue-Native PAGE (BN-PAGE) and immunodetection of protein complexes

BN-PAGE was performed according to (Jänsch et al., 1996) as described in (Meyer et al., 2009). Following separation, gels were stained with Coomassie, and either subjected to an in-gel complex I activity assay or protein complexes were blotted to PVDF membrane and immunodetected with a selection of antibodies as described below. *In vitro* uptake of proteins into mitochondria, followed by BN-PAGE, was assessed by drying gels and exposing them to a BAS TR2040 phosphor-imaging plate (Fuji) for 24 h. The exposed plate was visualized using the BAS 2500 Bio Imaging Analyser (Fuji).

In-gel complex I activity assay

The assay was performed according to (Zerbetto et al., 1997).

Western blot analysis

30 μg of mitochondrial protein was separated by SDS-PAGE, transferred to Hybond-C extra nitrocellulose membrane (GE Healthcare**)** Immunodetection of proteins was carried out as described previously (Murcha et al., 2005a). Antibodies used were raised against Tim17-2 (Murcha et al., 2005a), Tom20-2, 20-3, 20-4, Metaxin (Lister et al., 2007), Tom40, RISP, Sam50, Mia40, Erv1 (Carrie et al., 2010b), AOX, ATP α-subunit of ATP synthase and Porin (Elthon et al., 1989), Nad9 (Lamattina et al., 1993) , COXII, Cytochrome c and β-subunit of ATP synthase (Agrisera) and Ndufs4 (Meyer et al., 2009). For the remaining antibodies, recombinant proteins for Tim9 (At3g46560 amino acids 1-93),

Tim50 (At1g55900 amino acids 110-269), Tim44-2 (At2g36070 amino acids 100-472), Tim21 (At4g00026 amino acids 160-376), Tim23-2 (At1g72750 amino acids 3-32 and 103-143), Tim23-3 (At3g04800 amino acids 6-32 and 64-132), At3g25120 (amino acids 89-189), were expressed and purified as outlined previously (Carrie et al., 2010b). For antibodies raised against At5g24650 (amino acids1-50), At2g42210 (amino acids 1-100) and At3g10110/At1g18320 (amino acids 1-50), cDNA was cloned into pdest15 using Gateway technology, GST tagged recombinant proteins were expressed, bound to GST-Sepharose (Scientifix) and electroeluted. Recombinant proteins where confirmed by mass spectrometry prior to inoculation into rabbits (Cooper and Paterson, 2009).

In vitro import studies

Mitochondria for *in vitro* import experiments were prepared from 14 day old Arabidopsis seedlings grown in liquid culture, as previously described (Lister et al., 2007). [^{35}S]-Met labelled precursor proteins of AOX (X68702) (Whelan et al., 1995), F_Ad subunit of ATP synthase (X74296) (Smith et al., 1994), ANT (X57556) and Pic (AB016063) (Murcha et al., 2005a) and MDHAR (At3g09940) (Chew et al., 2003) were used in import assays. Precursor proteins were synthesized using the rabbit reticulocyte T_NT *in vitro* transcription/translation lysate (Promega). Time course analysis of precursor protein import into mitochondria was carried out as previously described (Lister et al., 2007) at 5, 10, 15 and 20 min time points. Proteinase K protected, mature, radiolabelled imported proteins were quantified at each time point and normalised to highest time point for wild-type which was set to 1 (Lister et al., 2007).

BN-PAGE import studies

Imports analysed by BN-PAGE were performed as previously described (Carrie et al., 2010b). [^{35}S]-Met labelled precursor proteins of Tim17-2 (At2g37410), Tim23-2 (At1g72750) (Murcha et al., 2005a), Tim21 (At4g00026) At1g47260 and MPPa (At1g51980) (Kühn et al., 2011), At2g42210 (Murcha et al., 2007) and cytochrome c_1 subunit of ubiquinone cytochrome c reductase (At4g32470) were generated from Arabidopsis cDNA cloned into pDest14 using Gateway technology (Invitrogen) and used in import assays. Precursor proteins were synthesized using rabbit reticulocyte T_NT *In vitro* transcription/translation lysate (Promega). Imports were carried out in the same manner as those analysed by SDS-PAGE, except that 250 μg of mitochondrial protein was used per time point. After import, mitochondria were pelleted at 20 000 x *g* for 5 min and subjected to BN-PAGE as detailed above. BN-PAGE gels were then fixed in 40% methanol *(v/v)* and 10% acetic acid *(v/v)* and visualized by autoradiography, as described above.

RNA isolation and Global transcript analysis

Analysis of the changes in transcript abundance between Col-0, *tim23 OE* and *tim23 KO* lines was performed using Affymetrix GeneChip™ Arabidopsis ATH1 Genome Arrays (Affymetrix). Green tissue from several seedlings was pooled for each biological replicate; Col-0 and mutant tissue samples were collected in biological triplicate. For each replicate, total RNA was isolated and microarrays were carried out as described in (Kühn et al., 2011).

Quantitative RT-PCR

RNA, isolated as described above, from Col-0, *tim23-2 OE* and *tim23-2 KO* plants was subjected to two consecutive treatments with TURBO DNase

(Ambion), confirmed by PCR to be free of detectable amounts of DNA and reverse-transcribed exactly as described (Kühn et al., 2009). Quantitative RT-PCR on the mitochondrial transcriptome was performed using the LightCycler 480 SYBR Green I Master Mix (Roche Applied Science) using the PCR programme, primer pairs and analysed as described (Kühn et al., 2009).

Statistical analysis

Microarray data quality was assessed using GCOS 1.4 before CEL files were exported into AVADIS Prophetic (Version 4.3, Strand Genomics) and Partek Genomics Suite software, version 6.3 (Partek), for further analysis. (.CEL files for microarray analyses performed are available at Array Express (http://www.ebi.ac.uk/arrayexpress/) under the accession E-MEXP-3309). Public array data for the *rug* mutant (Kühn et al., 2011) was also independently analysed and included.

***In organello* protein synthesis assays**

Mitochondria was isolated as described above and protein synthesis reactions were carried out as previously described (Giege et al., 2005).

Yeast-2-Hybrid Protein Interactions

Yeast-2-Hybrid interactions were carried out as described (Giraud et al., 2010). AH109 cells transformed with pGAD Tim23-2 were mated with Y187 cells transformed with pGBK Tim17-2, pGBK Tim23-2, pGBK Tim50, pGBK At2g42210 and empty pGBK. Positive interactors growing on auxothrophic selection media where re-streaked on selection plates DDO (SD –Trp –Leu) for

diploid selection, and (QDO) SD –Trp –Leu -Ade –His, and QDO with X-α-D-galactoside X to confirm interactions.

Immunoprecipitations

200 *µ*g of mitochondria was solubilised in digitonin buffer consisting of 30 mM Hepes KOH pH 7.4, 150 mM potassium acetate, 10% *(v/v)* glycerol and 1 mg digitonin and placed on ice for 20 min. 100 *µ*l of Protein A Sepharose and 10 *µ*l of antibody was added with solubilisation buffer without digitonin, including 0.5% *(w/v)* BSA and Complete Protease inhibitor (Roche) and incubated for 3 h at 4°C. Beads were washed and samples resolved by SDS-PAGE, transferred to nitrocellulose membrane and immunodetected with antibodies indicated.

Biomolecular fluorescence complementation

Biomolecular fluorescence complementation (BiFC) was carried out as outlined previously (Citovsky et al., 2008), testing the interactions of At2g42210, Tim23-2 and Tim17-2.

Blue native elution and in gel digestion

The complex of interest was excised from Blue native gels and proteins extracted by electroelution. Gel slices were minced by passing back and forth between two syringes and added to the H shaped eluter vessel of a CBS scientific electroeluter (CBS scientific). Proteins were eluted according to the technique detailed previously (Hunkapiller et al., 1983). Proteins were separated by SDS-PAGE. In gel digestion and protein identification by ESI MS/MS were performed as per (Meyer et al., 2007).

Supplementary Figure 1. Expression of Tim23 at a protein and transcript level in the *tim23* mutants lines.

Supplementary Figure 2. Identification of the Mixed Inner membrane Complex (MIC) in the Tim23 overexpresser (OE) line

Supplementary Figure 3. Interaction of Arabidopsis Tim21 with complex III.

Supplementary Table 1. Mass spectrometry based identification of subunits of the Mixed Intermediate Complex (MIC).

Supplementary Table 2. Summary of changes in transcript abundance for nuclear genes encoding mitochondrial import and assembly components.

Supplementary Table 3. Summary of 76 transcripts defined as being highly co-expressed with *tim23-2* across public Arabidopsis microarray datasets.

References

Alonso, J.M., Stepanova, A.N., Leisse, T.J., Kim, C.J., Chen, H., Shinn, P., Stevenson, D.K., Zimmerman, J., Barajas, P., Cheuk, R., Gadrinab, C., Heller, C., Jeske, A., Koesema, E., Meyers, C.C., Parker, H., Prednis, L., Ansari, Y., Choy, N., Deen, H., Geralt, M., Hazari, N., Hom, E., Karnes, M., Mulholland, C., Ndubaku, R., Schmidt, I., Guzman, P., Aguilar-Henonin, L., Schmid, M., Weigel, D., Carter, D.E., Marchand, T., Risseeuw, E., Brogden, D., Zeko, A., Crosby, W.L., Berry, C.C., and Ecker, J.R. (2003). Genome-wide insertional mutagenesis of Arabidopsis thaliana. Science **301,** 653-657.

Braun, H.P., Emmermann, M., Kruft, V., and Schmitz, U.K. (1992). The general mitochondrial processing peptidase from potato is an integral part of cytochrome c reductase of the respiratory chain. Embo J **11,** 3219-3227.

Brautigam, A., and Weber, A.P. (2009). Proteomic analysis of the proplastid envelope membrane provides novel insights into small molecule and protein transport across proplastid membranes. Mol Plant **2,** 1247-1261.

Calvo, S.E., and Mootha, V.K. (2010). The mitochondrial proteome and human disease. Annu Rev Genomics Hum Genet **11,** 25-44.

Carrie, C., Murcha, M.W., and Whelan, J. (2010a). An in silico analysis of the mitochondrial protein import apparatus of plants. BMC Plant Biol **10,** 249.

Carrie, C., Giraud, E., Duncan, O., Xu, L., Wang, Y., Huang, S., Clifton, R., Murcha, M., Filipovska, A., Rackham, O., Vrielink, A., and Whelan, J. (2010b). Conserved and novel functions for Arabidopsis thaliana MIA40 in assembly of proteins in mitochondria and peroxisomes. J Biol Chem **285,** 36138-36148.

Chacinska, A., Koehler, C.M., Milenkovic, D., Lithgow, T., and Pfanner, N. (2009). Importing mitochondrial proteins: machineries and mechanisms. Cell **138,** 628-644.

Chacinska, A., van der Laan, M., Mehnert, C.S., Guiard, B., Mick, D.U., Hutu, D.P., Truscott, K.N., Wiedemann, N., Meisinger, C., Pfanner, N., and Rehling, P. (2010). Distinct forms of mitochondrial TOM-TIM supercomplexes define signal-dependent states of preprotein sorting. Mol Cell Biol **30,** 307-318.

Chacinska, A., Lind, M., Frazier, A.E., Dudek, J., Meisinger, C., Geissler, A., Sickmann, A., Meyer, H.E., Truscott, K.N., Guiard, B., Pfanner, N., and Rehling, P. (2005). Mitochondrial presequence translocase: switching between TOM tethering and motor recruitment involves Tim21 and Tim17. Cell **120,** 817-829.

Chew, O., Whelan, J., and Millar, A.H. (2003). Molecular definition of the ascorbate-glutathione cycle in Arabidopsis mitochondria reveals dual targeting of antioxidant defenses in plants. J Biol Chem **278,** 46869-46877.

Citovsky, V., Gafni, Y., and Tzfira, T. (2008). Localizing protein-protein interactions by bimolecular fluorescence complementation in planta. Methods **45,** 196-206.

Clifton, R., Lister, R., Parker, K.L., Sappl, P.G., Elhafez, D., Millar, A.H., Day, D.A., and Whelan, J. (2005). Stress-induced co-expression of alternative respiratory chain components in Arabidopsis thaliana. Plant Mol Biol **58,** 193-212.

Cooper, H.M., and Paterson, Y. (2009). Production of polyclonal antisera. Curr Protoc Neurosci **Chapter 5,** Unit 5 5.

Dekker, P.J., Keil, P., Rassow, J., Maarse, A.C., Pfanner, N., and Meijer, M. (1993). Identification of MIM23, a putative component of the protein import machinery of the mitochondrial inner membrane. FEBS Lett **330,** 66-70.

Dolezal, P., Likic, V., Tachezy, J., and Lithgow, T. (2006). Evolution of the molecular machines for protein import into mitochondria. Science **313,** 314-318.

Dudkina, N.V., Kouril, R., Peters, K., Braun, H.P., and Boekema, E.J. (2010). Structure and function of mitochondrial supercomplexes. Biochim Biophys Acta **1797,** 664-670.

Elthon, T.E., R.L., N., and McIntosh, L. (1989). Monoclonal Antibodies to the Alternative Oxidase of Higher Plant Mitochondria. Plant Physiol **89,** 1311-1317.

Geissler, A., Chacinska, A., Truscott, K.N., Wiedemann, N., Brandner, K., Sickmann, A., Meyer, H.E., Meisinger, C., Pfanner, N., and Rehling, P. (2002). The mitochondrial presequence translocase: an essential role of Tim50 in directing preproteins to the import channel. Cell **111,** 507-518.

Giege, P., Sweetlove, L.J., Cognat, V., and Leaver, C.J. (2005). Coordination of nuclear and mitochondrial genome expression during mitochondrial biogenesis in Arabidopsis. The Plant Cell **17,** 1497-1512.

Giraud, E., Van Aken, O., Uggalla, V., and Whelan, J. (2011). REDOX regulation of mitochondrial function in plants. Plant, Cell & Environment **doi: 10.1111/j.1365-3040.2011.02293.x**.

Giraud, E., Ng, S., Carrie, C., Duncan, O., Low, J., Lee, C.P., Van Aken, O., Millar, A.H., Murcha, M., and Whelan, J. (2010). TCP transcription factors link the regulation of genes encoding mitochondrial proteins with the circadian clock in Arabidopsis thaliana. The Plant Cell **22,** 3921-3934.

Giraud, E., Ho, L.H., Clifton, R., Carroll, A., Estavillo, G., Tan, Y.F., Howell, K.A., Ivanova, A., Pogson, B.J., Millar, A.H., and Whelan, J. (2008). The absence of ALTERNATIVE OXIDASE1a in Arabidopsis results in acute sensitivity to combined light and drought stress. Plant Physiology **147,** 595-610.

Glaser, E., Eriksson, A., and Sjoling, S. (1994). Bifunctional role of the bc1 complex in plants. Mitochondrial bc1 complex catalyses both electron transport and protein processing. FEBS Lett **346,** 83-87.

Heazlewood, J.L., Verboom, R.E., Tonti-Filippini, J., Small, I., and Millar, A.H. (2007). SUBA: the Arabidopsis Subcellular Database. Nucleic Acids Res **35,** D213-218.

Hewitt, V., Alcock, F., and Lithgow, T. (2011). Minor modifications and major adaptations: The evolution of molecular machines driving mitochondrial protein import. Biochim Biophys Acta **1808,** 947-954.

Holt, I.J. (2009). Mitochondrial DNA replication and repair: all a flap. Trends Biochem Sci **34,** 358-365.

Hunkapiller, M.W., Lujan, E., Ostrander, F., and Hood, L.E. (1983). Isolation of microgram quantities of proteins from polyacrylamide gels for amino acid sequence analysis. Methods in enzymology **91,** 227-236.

Jänsch, L., Kruft, V., Schmitz, U.K., and Braun, H.P. (1996). New insights into the composition, molecular mass and stoichiometry of the protein complexes of plant mitochondria. Plant J **9,** 357-368.

Klodmann, J., and Braun, H.P. (2010). Proteomic approach to characterize mitochondrial complex I from plants. Phytochemistry **72,** 1071-1080.

Klodmann, J., Sunderhaus, S., Nimtz, M., Jansch, L., and Braun, H.P. (2010). Internal architecture of mitochondrial complex I from Arabidopsis thaliana. Plant Cell **22,** 797-810.

Kühn, K., Richter, U., Meyer, E.H., Delannoy, E., de Longevialle, A.F., O'Toole, N., Borner, T., Millar, A.H., Small, I.D., and Whelan, J. (2009). Phage-type RNA polymerase RPOTmp performs gene-specific transcription in mitochondria of Arabidopsis thaliana. The Plant Cell **21,** 2762-2779.

Kühn, K., Carrie, C., Giraud, E., Wang, Y., Meyer, E.H., Narsai, R., Colas des Francs-Small, C., Zhang, B., Murcha, M.W., and Whelan, J. (2011). The RCC1 family protein RUG3 is required for splicing of nad2 and complex I biogenesis in mitochondria of Arabidopsis thaliana. doi: 10.1111/j.1365-313X.2011.04658.

Kwast, K.E., Burke, P.V., and Poyton, R.O. (1998). Oxygen sensing and the transcriptional regulation of oxygen-responsive genes in yeast. The Journal of experimental biology **201,** 1177-1195.

Lamattina, L., Gonzalez, D., Gualberto, J., and Grienenberger, J.M. (1993). Higher plant mitochondria encode an homologue of the nuclear-encoded 30-kDa subunit of bovine mitochondrial complex I. Eur J Biochem **217,** 831-838.

Lane, N., and Martin, W. (2010). The energetics of genome complexity. Nature **467,** 929-934.

Leigh-Brown, S., Enriquez, J.A., and Odom, D.T. (2010). Nuclear transcription factors in mammalian mitochondria. Genome Biol **11,** 215.

Liere, K., Weihe, A., and Borner, T. (2011). The transcription machineries of plant mitochondria and chloroplasts: Composition, function, and regulation. J Plant Physiol **168,** 1345-1360.

Lister, R., Murcha, M.W., and Whelan, J. (2003). The Mitochondrial Protein Import Machinery of Plants (MPIMP) database. Nucleic acids research **31,** 325-327.

Lister, R., Carrie, C., Duncan, O., Ho, L.H., Howell, K.A., Murcha, M.W., and Whelan, J. (2007). Functional definition of outer membrane proteins involved in preprotein import into mitochondria. The Plant Cell **19,** 3739-3759.

Maarse, A.C., Blom, J., Keil, P., Pfanner, N., and Meijer, M. (1994). Identification of the essential yeast protein MIM17, an integral mitochondrial inner membrane protein involved in protein import. FEBS Lett **349,** 215-221.

Melo, A.M., Bandeiras, T.M., and Teixeira, M. (2004). New insights into type II NAD(P)H:quinone oxidoreductases. Microbiology and molecular biology reviews : MMBR **68,** 603-616.

Meyer, E.H., Heazlewood, J.L., and Millar, A.H. (2007). Mitochondrial acyl carrier proteins in Arabidopsis thaliana are predominantly soluble matrix proteins and none can be confirmed as subunits of respiratory Complex I. Plant Mol Biol **64,** 319-327.

Meyer, E.H., Taylor, N.L., and Millar, A.H. (2008). Resolving and identifying protein components of plant mitochondrial respiratory complexes using three dimensions of gel electrophoresis. J Proteome Res **7,** 786-794.

Meyer, E.H., Tomaz, T., Carroll, A.J., Estavillo, G., Delannoy, E., Tanz, S.K., Small, I.D., Pogson, B.J., and Millar, A.H. (2009). Remodeled respiration in ndufs4 with low phosphorylation efficiency suppresses Arabidopsis germination and growth and alters control of metabolism at night. Plant Physiol **151,** 603-619.

Mokranjac, D., and Neupert, W. (2010). The many faces of the mitochondrial TIM23 complex. Biochim Biophys Acta **1797,** 1045-1054.

Mokranjac, D., Sichting, M., Popov-Celeketic, D., Mapa, K., Gevorkyan-Airapetov, L., Zohary, K., Hell, K., Azem, A., and Neupert, W. (2009). Role of Tim50 in the transfer of precursor proteins from the outer to the inner membrane of mitochondria. Molecular biology of the cell **20,** 1400-1407.

Murcha, M.W., Millar, A.H., and Whelan, J. (2005a). The N-terminal cleavable extension of plant carrier proteins is responsible for efficient insertion into the inner mitochondrial membrane. J Mol Biol **351,** 16-25.

Murcha, M.W., Lister, R., Ho, A.Y., and Whelan, J. (2003). Identification, expression, and import of components 17 and 23 of the inner mitochondrial membrane translocase from Arabidopsis. Plant physiology **131,** 1737-1747.

Murcha, M.W., Elhafez, D., Millar, A.H., and Whelan, J. (2005b). The C-terminal region of TIM17 links the outer and inner mitochondrial membranes in Arabidopsis and is essential for protein import. J Biol Chem **280,** 16476-16483.

Murcha, M.W., Elhafez, D., Lister, R., Tonti-Filippini, J., Baumgartner, M., Philippar, K., Carrie, C., Mokranjac, D., Soll, J., and Whelan, J. (2007). Characterization of the preprotein and amino acid transporter gene family in Arabidopsis. Plant Physiol **143,** 199-212.

Ott, M., and Herrmann, J.M. (2010). Co-translational membrane insertion of mitochondrially encoded proteins. Biochim Biophys Acta **1803,** 767-775.

Perry, A.J., Hulett, J.M., Likic, V.A., Lithgow, T., and Gooley, P.R. (2006). Convergent evolution of receptors for protein import into mitochondria. Curr Biol **16,** 221-229.

Pesaresi, P., Masiero, S., Eubel, H., Braun, H.P., Bhushan, S., Glaser, E., Salamini, F., and Leister, D. (2006). Nuclear photosynthetic gene expression is synergistically modulated by rates of protein synthesis in chloroplasts and mitochondria. The Plant Cell **18,** 970-991.

Pudelski, B., Kraus, S., Soll, J., and Philippar, K. (2010). The plant PRAT proteins - preprotein and amino acid transport in mitochondria and chloroplasts. Plant Biol (Stuttg) **12 Suppl 1,** 42-55.

Rassow, J., Dekker, P.J., van Wilpe, S., Meijer, M., and Soll, J. (1999). The preprotein translocase of the mitochondrial inner membrane: function and evolution. J Mol Biol **286,** 105-120.

Rehling, P., Brandner, K., and Pfanner, N. (2004). Mitochondrial import and the twin-pore translocase. Nat Rev Mol Cell Biol **5,** 519-530.

Rhoads, D.M., and Subbaiah, C.C. (2007). Mitochondrial retrograde regulation in plants. Mitochondrion **7,** 177-194.

Rosso, M.G., Li, Y., Strizhov, N., Reiss, B., Dekker, K., and Weisshaar, B. (2003). An Arabidopsis thaliana T-DNA mutagenized population (GABI-Kat) for flanking sequence tag-based reverse genetics. Plant Mol Biol **53,** 247-259.

Schmidt, O., Pfanner, N., and Meisinger, C. (2010). Mitochondrial protein import: from proteomics to functional mechanisms. Nat Rev Mol Cell Biol **11,** 655-667.

Sickmann, A., Reinders, J., Wagner, Y., Joppich, C., Zahedi, R., Meyer, H.E., Schonfisch, B., Perschil, I., Chacinska, A., Guiard, B., Rehling, P., Pfanner, N., and Meisinger, C. (2003). The proteome of Saccharomyces cerevisiae mitochondria. Proc Natl Acad Sci U S A **100,** 13207-13212.

Siedow, J.N., and Day, D.A. (2000). Respiration and photorespiration. In Biochemistry and Molecular Biology of Plants, B.B. Buchanan, W. Guissem, and R.L. Jones, eds (Rockville, MD: Am. Soc. Plant Physiol), pp. 676–728.

Smith, M.K., Day, D.A., and Whelan, J. (1994). Isolation of a novel soybean gene encoding a mitochondrial ATP synthase subunit. Arch Biochem Biophys **313,** 235-240.

Stroud, D.A., Meisinger, C., Pfanner, N., and Wiedemann, N. (2010). Biochemistry. Assembling the outer membrane. Science **328,** 831-832.

Stuart, R.A. (2008). Supercomplex organization of the oxidative phosphorylation enzymes in yeast mitochondria. J Bioenerg Biomembr **40,** 411-417.

Sunderhaus, S., Klodmann, J., Lenz, C., and Braun, H.P. (2010). Supramolecular structure of the OXPHOS system in highly thermogenic tissue of Arum maculatum. Plant Physiol Biochem **48,** 265-272.

Tamura, Y., Harada, Y., Shiota, T., Yamano, K., Watanabe, K., Yokota, M., Yamamoto, H., Sesaki, H., and Endo, T. (2009). Tim23-Tim50 pair coordinates functions of translocators and motor proteins in mitochondrial protein import. The Journal of cell biology **184,** 129-141.

Truscott, K.N., Kovermann, P., Geissler, A., Merlin, A., Meijer, M., Driessen, A.J., Rassow, J., Pfanner, N., and Wagner, R. (2001). A presequence- and voltage-sensitive channel of the mitochondrial preprotein translocase formed by Tim23. Nature structural biology **8,** 1074-1082.

van der Laan, M., Wiedemann, N., Mick, D.U., Guiard, B., Rehling, P., and Pfanner, N. (2006). A role for Tim21 in membrane-potential-dependent preprotein sorting in mitochondria. Current biology : CB **16,** 2271-2276.

Watanabe, K. (2010). Unique features of animal mitochondrial translation systems. The non-universal genetic code, unusual features of the translational apparatus and their relevance to human mitochondrial diseases. Proc Jpn Acad Ser B Phys Biol Sci **86,** 11-39.

Whelan, J., Hugosson, M., Glaser, E., and Day, D.A. (1995). Studies on the import and processing of the alternative oxidase precursor by isolated soybean mitochondria. Plant Mol Biol **27,** 769-778.

Wittig, I., and Schagger, H. (2009). Supramolecular organization of ATP synthase and respiratory chain in mitochondrial membranes. Biochim Biophys Acta **1787,** 672-680.

Yamamoto, H., Esaki, M., Kanamori, T., Tamura, Y., Nishikawa, S., and Endo, T. (2002). Tim50 is a subunit of the TIM23 complex that links protein translocation across the outer and inner mitochondrial membranes. Cell **111,** 519-528.

Zerbetto, E., Vergani, L., and Dabbeni-Sala, F. (1997). Quantification of muscle mitochondrial oxidative phosphorylation enzymes via histochemical staining of blue native polyacrylamide gels. Electrophoresis **18,** 2059-2064.

Acknowledgments

This work was supported by the University of Western Australia SIRF grant to Y.W, an Australian Research Council APD grant to M.W.M and Australian Research Council Centre of Excellence Program CEO561495.

Author Contributions

JW and MWM designed the experiments and wrote the manuscript. YW, CC, EG, DE, OD, RN and MWM performed the experimental procedures and carried out the data analysis.

Figure 1. Over-expression of Tim23 results in a retarded growth phenotype and increased rates of protein uptake in isolated mitochondria **A)** Growth phenotypes for Arabidopsis plants that contain T-DNA insertions annotated to be located in *Tim23-2* (At1g72760) at 2 and 6 weeks old. **B)** The positions of the T-DNA inserts in SALK_143656 and GABI_689C11 lines. **C)** Mitochondria isolated from wild-type (Col-0), SALK_143656 (*tim23* OE) (over-expresser) and GABI_689C11 (*tim23* KO) (knock-out) were subjected to SDS-PAGE and probed with antibodies raised against Tim23-2 (see also Supplementary Figure 1). The apparent mol mass of the protein detected is indicated. The 20 kDa band is consistent with previous analysis of *in vitro* synthesised and imported Tim23 (Murcha et al., 2005b)**. D)** *In vitro* uptake assays into mitochondria isolated from Col-0, *tim23* OE and *tim23* KO lines. Import of [^{35}S] Met-radiolabelled Alternative Oxidase (AOX), F_Ad subunit of ATP synthase (F_Ad), Monodehydroascorbate reductase (MDHAR), Adenine Nucleotide Translocator (ANT) and Phosphate Translocator (Pic) into isolated mitochondria. Aliquots where removed at 5, 10 15 and 20 min time points and Proteinase K (PK) treated. The precursor (p) and mature (m) form are indicated. PK protected mature bands were quantified for all precursor proteins, at all time points and normalized to Col-0 at 20 min for each replicate experiment ($n \geq 3 \pm$ SE).

Figure 2. Similarity in phenotype and protein import between complex I (*rug*) and *tim23* OE mutants. A) Complex I is reduced in *tim23* OE (over-expresser) mitochondria. Mitochondria was isolated from Col-0 (wild-type), *tim23* OE and *tim23* KO (knock-out) lines and resolved by one-dimensional BN-PAGE, stained with Coomassie and analysed for complex I activity. The bands

corresponding to the super complex I+III, complex I, complex V, complex III and complex IV are indicated. The gel was transferred to a PVDF membrane and immunodetected with antibodies against complex I subunit Ndufs4, complex V α–subunit of ATP synthase, complex III subunit, Rieske iron-sulfur protein (RISP) and complex IV subunit, COXII. The presence of an additional complex in the *tim23* OE line termed, Mixed Intermediate Complex (MIC), was also detected by Coomassie stain and the RISP antibody as indicated with a ■. **B)** A comparison between Col-0, *tim23* KO, *tim23* OE and *rug* (a complex I deficient mutant, (Kühn et al., 2011)), indicates that *tim23* OE and *rug* plants display the same retarded growth phenotype. Mitochondria isolated from Col-0, *rug* and *tim23* OE, resolved by BN-PAGE, stained with Coomassie and tested for complex I activity. The almost total absence of complex I is evident for both lines. The presence of an additional complex termed Mixed Intermediate Complex (MIC) in the *tim23* OE line is indicated by ■. **C)** *In vitro* protein uptake assays into mitochondria isolated from the *rug* mutant. **i)** Import of [^{35}S] Met-radiolabelled Alternative Oxidase (AOX), F_Ad subunit of ATP synthase (F_Ad), Monodehydroascorbate reductase (MDHAR), Adenine Nucleotide Translocator (ANT) and Phosphate Translocator (Pic) into isolated mitochondria. Aliquots where removed at 5, 10 15 and 20 min time points and Proteinase K (PK) treated. The precursor (p) and mature (m) form are indicated. **ii)** The rate of import of all PK protected proteins was quantitated at all time points and normalized to Col-0 (wild-type) at 20 min for each replicate experiment ($n \geq 3 \pm$ SE).

Figure 3. The abundance of a variety of proteins as determined by western blot analysis of mitochondria isolated from Col-0 (wild-type),

***tim23* OE (over-expresser), *tim23* KO (knock-out) and *rug* lines. A)** PRAT Family - Immunodetection with antibodies raised against various proteins that belong to the mitochondrial Preprotein and amino acid transporters (PRAT) family. Note that the protein encoded by gene At2g42210 is classified as being a member of the PRAT family (Rassow et al., 1999) and is also identified as a subunit of complex I (Meyer et al., 2008; Klodmann et al., 2010). Immunodetection assays were also completed with antibodies raised against various respiratory chain proteins, components of the mitochondrial protein import apparatus and with antibodies raised against mitochondrial Alternative oxidase (AOX) that is induced upon stress (Clifton et al., 2005). Porin was used as a loading control for total protein abundance. Values in black next to the western blots represent the average relative abundance ratios of proteins present in the 3 mutants, respectively, compared to Col-0 mitochondria ($n \geq 3 \pm$ SE). Standard errors for these average ratios are indicated below in grey. **B)** The abundance of Tim17-2 and Tim23-2 in mitochondria from various complex I mutant lines, *rug* (Kühn et al., 2011)*, ndufs4* (Meyer et al., 2009) *and rpotmp* (Kühn et al., 2009). **C)** *In vitro* protein uptake assays into mitochondria isolated from complex I mutants *ndufs4* and *rpotmp* lines. Imports carried out as described for Figure 3, except that 3, 6 and 12 minute time points were used.

Figure 4. Tim23 is assembled into complex I upon import and interacts with complex I. A) *In vitro* protein uptake assays of radiolabelled Tim23-2, Tim17-2, At2g42210, At1g47260 and MPPα into mitochondria isolated from Col-0 (wild-type). After the import assay was carried out mitochondrial proteins were resolved by one-dimensional BN-PAGE. The positions of the super complex I+III, complex I, complex V, complex III, complex IV and the TIM17:23

complex are indicated. Incorporation of Tim23-2 into complex I and complex III is indicated with ⇒. **B)** Time course analysis of radiolabelled Tim23-2, Tim17-2, At2g42210 and At1g47260 import and assembly into complex I. **C)** *In vitro* protein uptake assays of radiolabelled Tim23-2, Tim17-2 and At2g42210 into mitochondria isolated from Col-0, *tim23-2* OE and *tim23-2 KO* plants. The position of Tim23 in complex I is indicated with ⇒. **D)** Mitochondria isolated from Col-0, *tim23* OE and *tim23* KO plants were resolved by one dimensional BN-PAGE, and immunodetection of the immobilised proteins was carried out with antibodies raised against Tim23-2, Tim17-2, At2g42210 and complex I subunit Nad9. The location of Tim23 in Complex I is indicated with ⇒.

Figure 5. Tim23 interacts with complex I components. A) Mitochondria isolated from Col-0 (wild-type) plants were incubated with or without antibodies raised against Tim23-2 and Protein A-Sepharose. The wash and pellet fractions were resolved by SDS-PAGE and immunodetected with antibodies against Tim23-2, complex I subunit Ndufs4 and cytochrome c. **B)** Interaction of Tim23-2 with Tim17-2 and At2g42210 as determined by bimolecular fluorescence complementation (BiFC). **C)** Yeast-2-Hybrid interaction assays indicate a positive interaction of Tim23-2 with complex I subunit At2g42210. The yeast strain AH109, transformed with pGADT7-Tim23-2, was mated with yeast strain Y187, transformed with either pGBKT7 Tim17-2, Tim23-2, Tim50, At2g42210 or empty vector. Diploid yeast growth on Double Drop Out (DDO) SD –Trp –Leu media indicates successful mating. Growth on Quadruple Drop Out (QDO) SD –Trp –Leu –Ade –His and QDO with X-α-GAL indicates specific protein-protein interactions.

Figure 6. Global analysis of transcript abundance changes in *tim23-2* OE and KO lines with other mutants affecting complex I. A) Venn diagrams showing the overlap of significantly changing genes at a fold change cut-off of 1.5 fold for *rug* mutants (Kühn et al., 2011) and *tim23 OE* lines. Red indicates induced transcripts and blue indicates down regulated transcripts. **B)** Overview of significant changes (FDR corrected $p<0.05$) in transcript abundance, in response to over-expression of Tim23, for transcripts associated with mitochondrial function and organelle biogenesis. Red boxes indicate transcripts that are induced in *tim23* OE lines and blue boxes show transcripts, which are down regulated. Colour scale is shown as $\log_2$ fold change. **C)** *Left panel* **-** qRT-PCR was performed to compare the abundances of mitochondrial transcripts in *tim23* OE and KO seedlings compared to Col-0 seedlings. Transcript levels are depicted as log2 of the ratio of values determined in mutant versus Col-0 samples for each transcript on the mitochondrial genome. Three technical replicates of three independent biological repeats were performed and averaged per genotype; standard errors are indicated. *Nuclear 18S* (used as a normalization control) along with *ACT2* and *UBC* transcripts were included as controls. *Right panel* - In organellar translations in mitochondria isolated from Col-0, *tim23* OE and KO lines. Equal amounts of mitochondria were used in assays and the incorporation of [^{35}S]-methionine was monitored into proteins over time. **D)** Pearson co-correlation co-expression plot between *tim23-1* and *tim23-2* across all NASC public microarray experiments (http://www.arabidopsis.leeds.ac.uk/act/coexpanalyser.php#CO2). A straight line at 45° indicates a perfect correlation between the two isoforms (r value between genes =1). 76 genes defined as highly co-expressed with *tim23-2* are highlighted in red and this set of genes is further characterized by functional

categorization (left panel pie chart); to determine over or under-represented groups compared to the whole genome. Categories shown in bold red and blue indicate significantly ($p<0.0001$, chi-squared test) over and under-represented categories, respectively, compared to the whole genome. Percentages shown in brackets indicate the relevant percentage observed for a whole genome categorization. (See also Supplementary Table 2 and 3).

Figure 7. Diagrammatic representation of the interaction of Tim23 with complex I in mitochondria from Arabidopsis. The top left panel – Static – represents the complexes as defined by biochemical and genetic studies. Only the subunits that change and are referred to are indicated and labelled for clarity. The bottom left panel – Dynamic- represents the interactions between the complexes, and Tim21 and Tim23 that were determined in this study. Imported Tim23 is incorporated into complex I and imported Tim21 is incorporated into complex III. However, as most of the Tim23 and Tim21 are present in the TIM17:23 complex, and the respiratory complexes are more abundant than TIM17:23, the association of Tim23 and Tim21 with complex I and complex III is not in stoichiometric levels, and thus indicated in blue. A supercomplex of complex I+III is indicated, that does not contain Tim23, Tim21 or another PRAT protein encoded by At2g42210. The right panel shows the situation when an increase in Tim23 or decrease in complex I occurs. There is an increase in the Tom20 receptors proteins and proteins of the TIM17:23^{sort} complex, indicated in red. Monomeric complex I is almost completely absent, as indicated by open blue symbols, and the super complex I+III is reduced in abundance, indicated in blue. In addition there is global changes in the transcriptome, some of which appears to require mitochondrial transcription

and/or translation, as all the changes observed in the *tim23* OE line are not observed in the *rug* line.

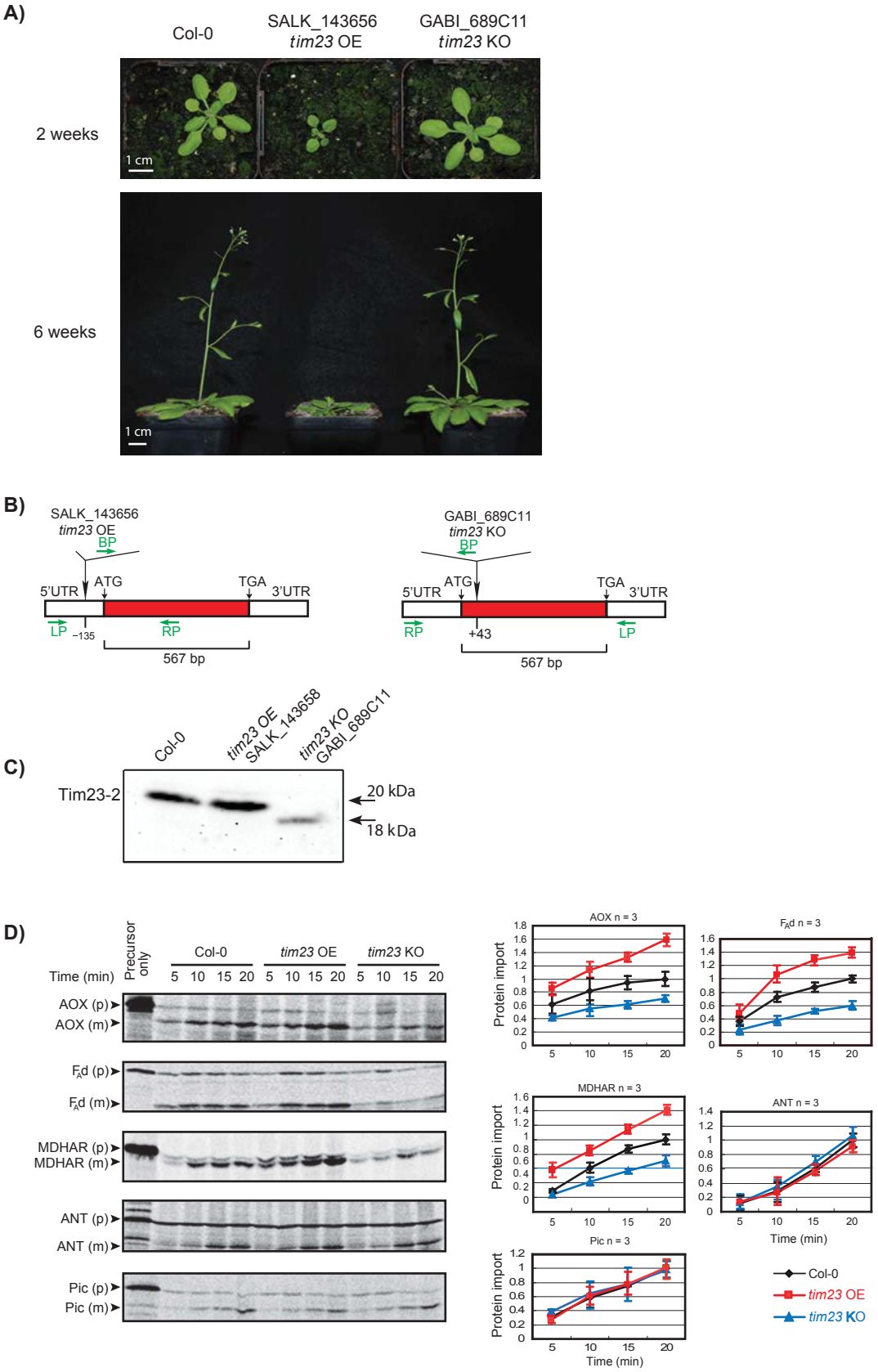
A)
Col-0
SALK_143656
tim23 OE
GABI_689C11
tim23 KO
2 weeks
6 weeks
1 cm
1 cm
B)
SALK_143656
tim23 OE
BP
5'UTR
ATG
TGA
3'UTR
LP
−135
RP
567 bp
GABI_689C11
tim23 KO
BP
5'UTR
ATG
TGA
3'UTR
RP
+43
LP
567 bp
C)
Col-0
tim23 OE
SALK_143658
tim23 KO
GABI_689C11
Tim23-2
20 kDa
18 kDa
D)
Precursor only
Col-0
tim23 OE
tim23 KO
Time (min)
5 10 15 20 5 10 15 20 5 10 15 20
AOX (p)
AOX (m)
FAd (p)
FAd (m)
MDHAR (p)
MDHAR (m)
ANT (p)
ANT (m)
Pic (p)
Pic (m)
AOX n = 3
FAd n = 3
MDHAR n = 3
ANT n = 3
Pic n = 3
Protein import
Time (min)
Col-0
tim23 OE
tim23 KO

Figure 1

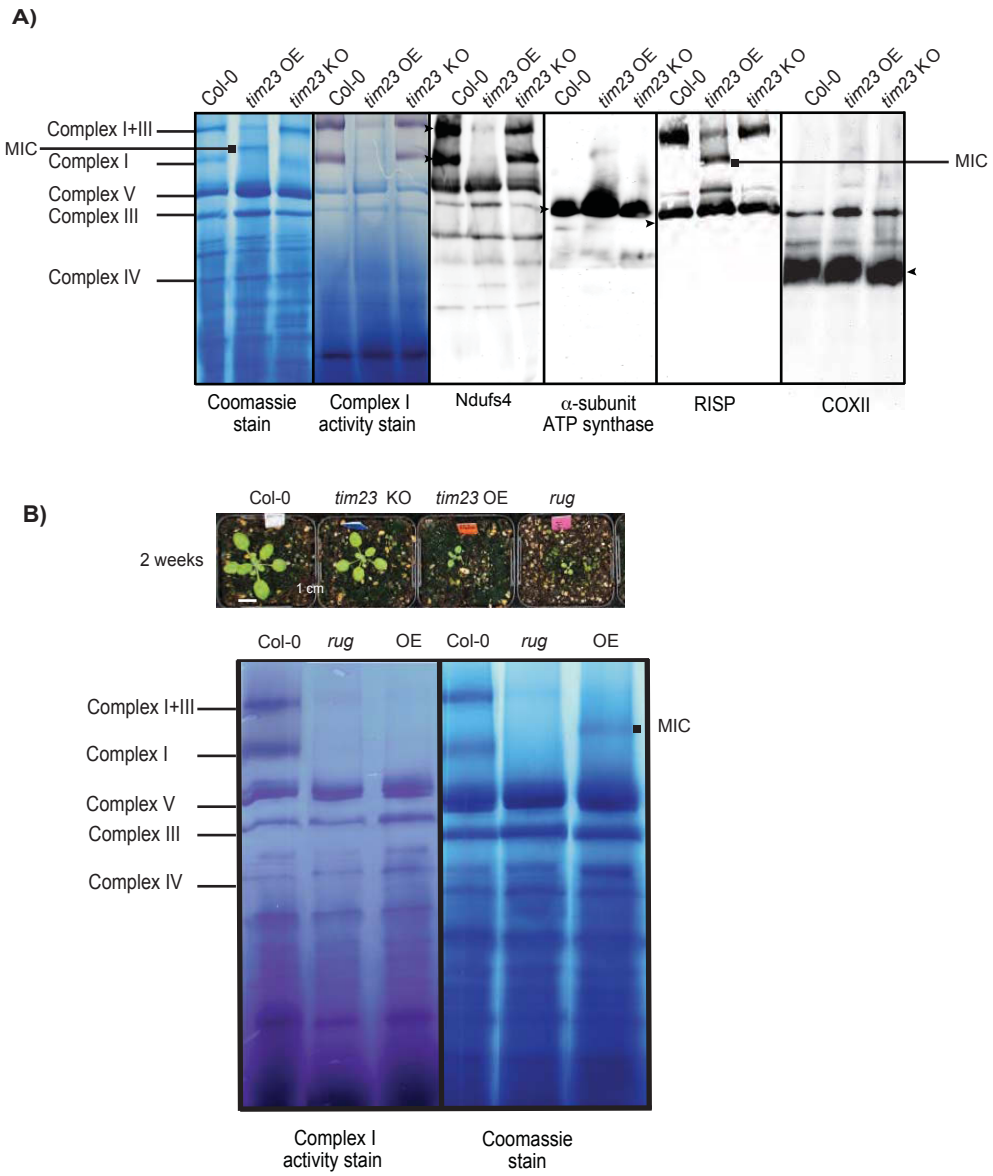
A)
Col-0
tim23 OE
tim23 KO
Complex I+III
MIC
Complex I
Complex V
Complex III
Complex IV
MIC
Coomassie stain
Complex I activity stain
Ndufs4
α-subunit ATP synthase
RISP
COXII
B)
Col-0
tim23 KO
tim23 OE
rug
2 weeks
1 cm
Col-0
rug
OE
Complex I+III
Complex I
Complex V
Complex III
Complex IV
MIC
Complex I activity stain
Coomassie stain
C) i
Precursor only
Col-0
rug
Time (min)
5 10 15 20 5 10 15 20
AOX (p)
AOX (m)
FAd (p)
FAd (m)
MDHAR (p)
MDHAR (m)
ANT (p)
ANT (m)
Pic (m)
Pic (p)
C) ii
AOX n=3
FAd n=3
MDHAR n=3
ANT n=3
Pic n=3
Protein import
Time (min)
Col-0
rug

Figure 2

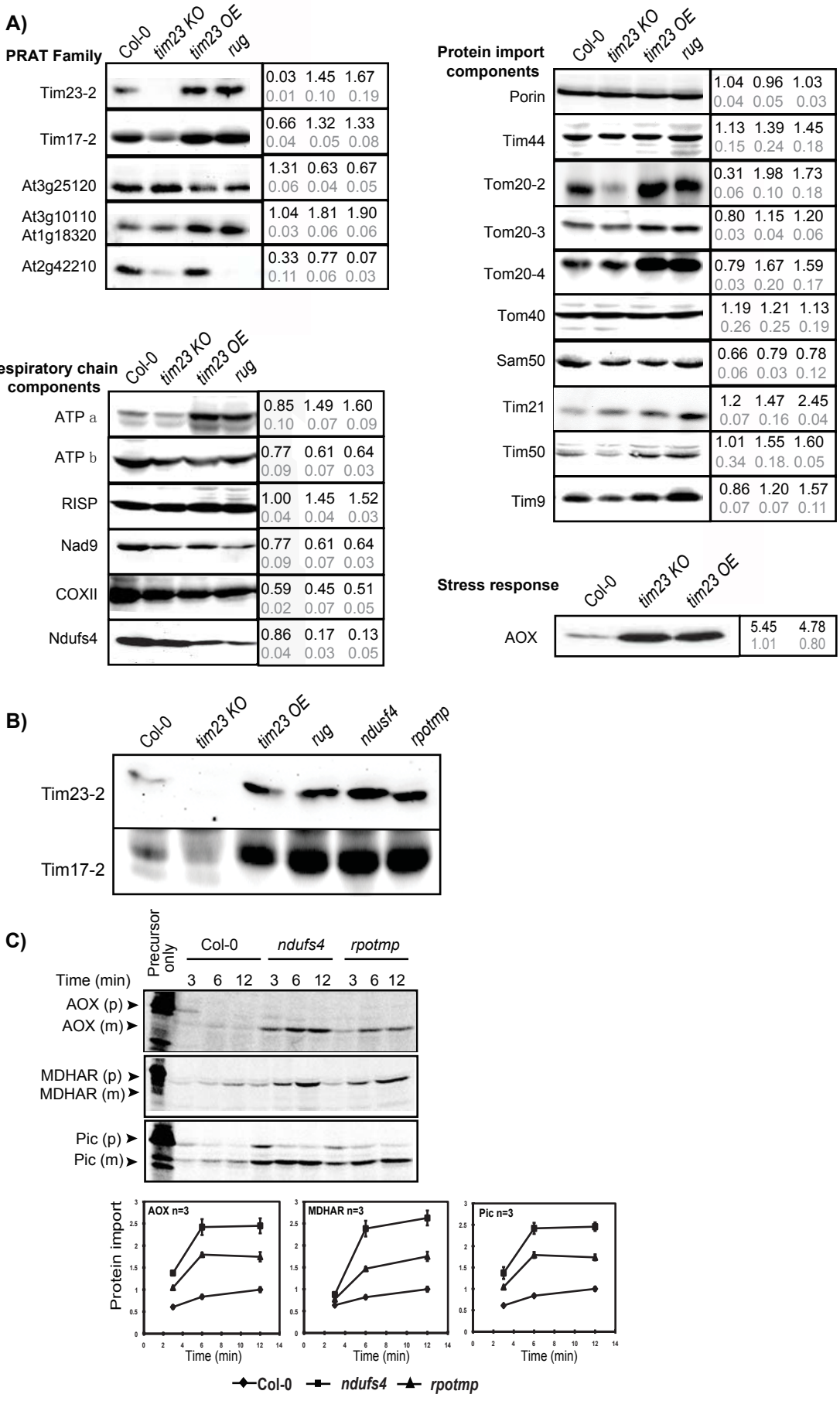
A)
PRAT Family
Col-0
tim23 KO
tim23 OE
rug
Tim23-2
0.03 1.45 1.67
0.01 0.10 0.19
Tim17-2
0.66 1.32 1.33
0.04 0.05 0.08
At3g25120
1.31 0.63 0.67
0.06 0.04 0.05
At3g10110
At1g18320
1.04 1.81 1.90
0.03 0.06 0.06
At2g42210
0.33 0.77 0.07
0.11 0.06 0.03
Respiratory chain components
ATP a
0.85 1.49 1.60
0.10 0.07 0.09
ATP b
0.77 0.61 0.64
0.09 0.07 0.03
RISP
1.00 1.45 1.52
0.04 0.04 0.03
Nad9
0.77 0.61 0.64
0.09 0.07 0.03
COXII
0.59 0.45 0.51
0.02 0.07 0.05
Ndufs4
0.86 0.17 0.13
0.04 0.03 0.05
Protein import components
Porin
1.04 0.96 1.03
0.04 0.05 0.03
Tim44
1.13 1.39 1.45
0.15 0.24 0.18
Tom20-2
0.31 1.98 1.73
0.06 0.10 0.18
Tom20-3
0.80 1.15 1.20
0.03 0.04 0.06
Tom20-4
0.79 1.67 1.59
0.03 0.20 0.17
Tom40
1.19 1.21 1.13
0.26 0.25 0.19
Sam50
0.66 0.79 0.78
0.06 0.03 0.12
Tim21
1.2 1.47 2.45
0.07 0.16 0.04
Tim50
1.01 1.55 1.60
0.34 0.18. 0.05
Tim9
0.86 1.20 1.57
0.07 0.07 0.11
Stress response
AOX
5.45 4.78
1.01 0.80
B)
rug
ndusf4
rpotmp
Tim23-2
Tim17-2
C)
Precursor only
Col-0
ndufs4
rpotmp
Time (min)
3 6 12 3 6 12 3 6 12
AOX (p)
AOX (m)
MDHAR (p)
MDHAR (m)
Pic (p)
Pic (m)
Protein import
AOX n=3
MDHAR n=3
Pic n=3
Time (min)
Col-0
ndufs4
rpotmp

Figure 3

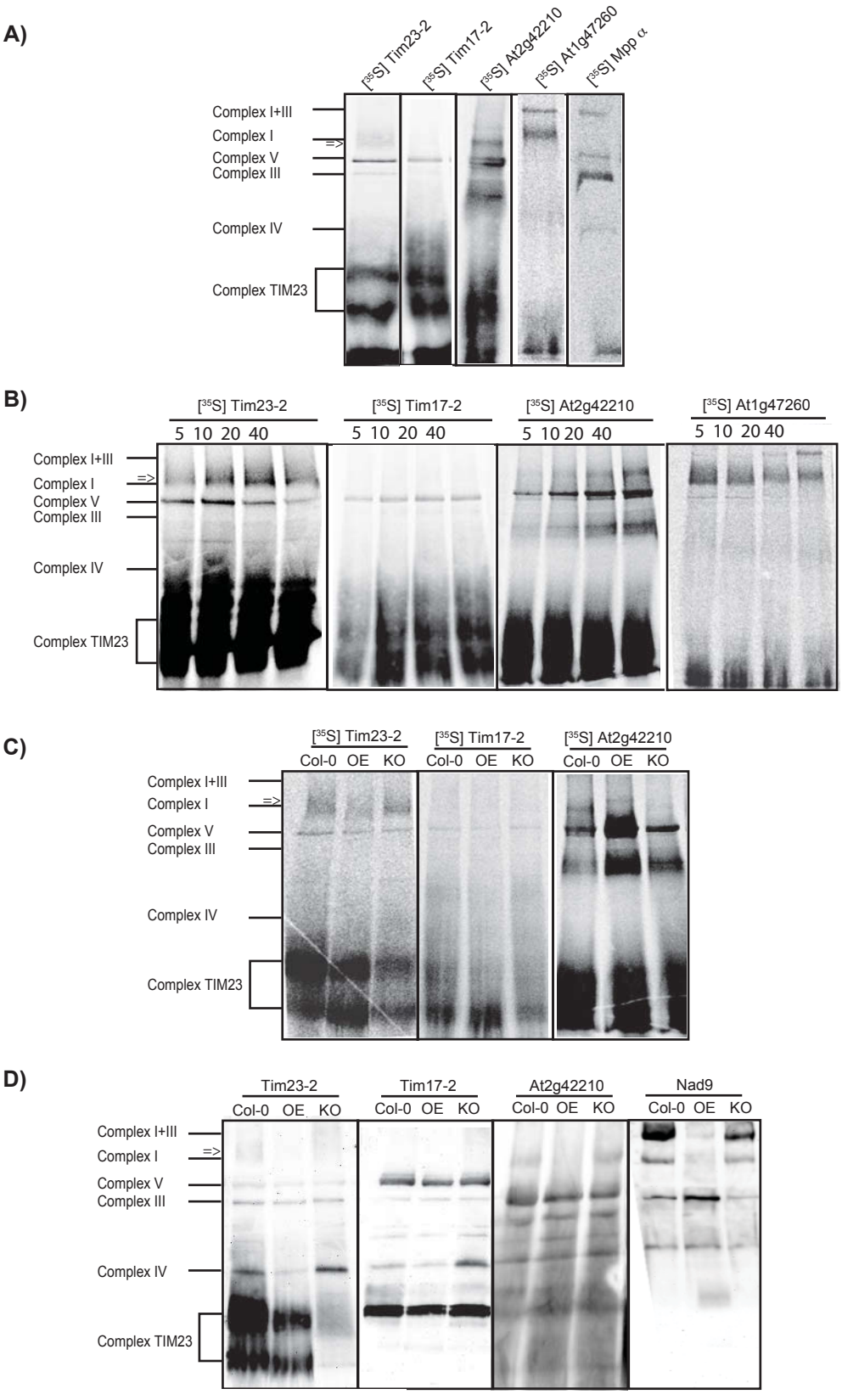
A)
[35S] Tim23-2
[35S] Tim17-2
[35S] At2g42210
[35S] At1g47260
[35S] Mpp α
Complex I+III
Complex I
=>
Complex V
Complex III
Complex IV
Complex TIM23
B)
[35S] Tim23-2
[35S] Tim17-2
[35S] At2g42210
[35S] At1g47260
5 10 20 40
Complex I+III
Complex I
=>
Complex V
Complex III
Complex IV
Complex TIM23
C)
[35S] Tim23-2
[35S] Tim17-2
[35S] At2g42210
Col-0 OE KO
Complex I+III
Complex I
=>
Complex V
Complex III
Complex IV
Complex TIM23
D)
Tim23-2
Tim17-2
At2g42210
Nad9
Col-0 OE KO
Complex I+III
Complex I
=>
Complex V
Complex III
Complex IV
Complex TIM23

Figure 4

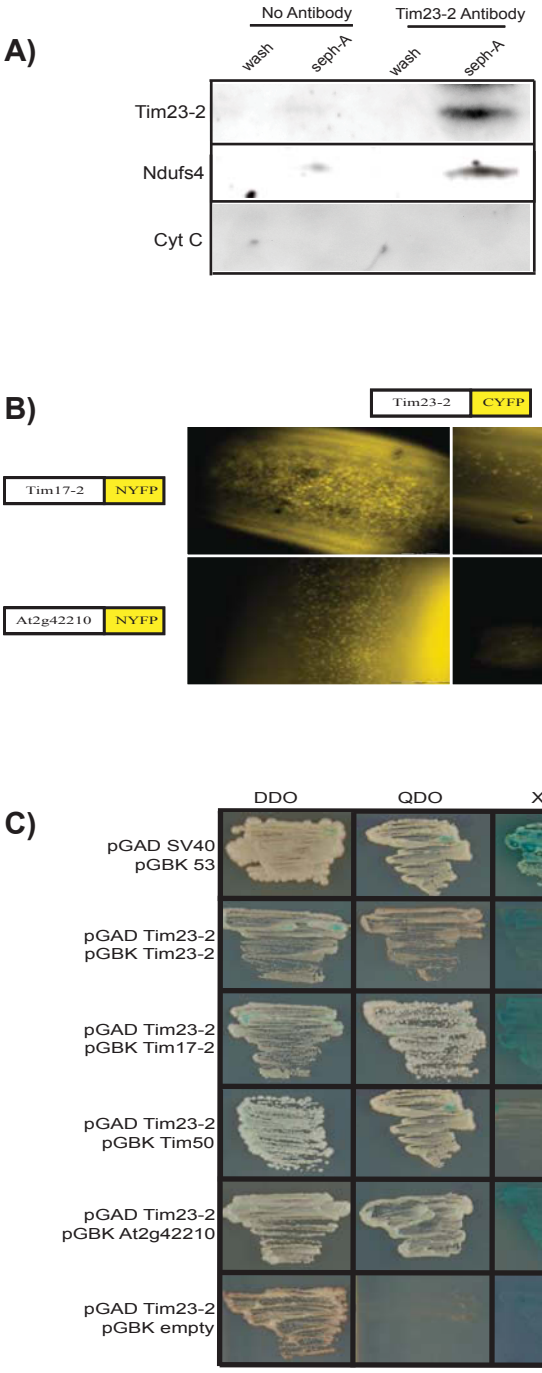
A)
No Antibody
Tim23-2 Antibody
wash
seph-A
wash
seph-A
Tim23-2
Ndufs4
Cyt C
B)
Tim23-2
CYFP
Tim17-2
NYFP
At2g42210
NYFP
C)
DDO
QDO
X-a-GAL
pGAD SV40
pGBK 53
pGAD Tim23-2
pGBK Tim23-2
pGAD Tim23-2
pGBK Tim17-2
pGAD Tim23-2
pGBK Tim50
pGAD Tim23-2
pGBK At2g42210
pGAD Tim23-2
pGBK empty

Figure 5

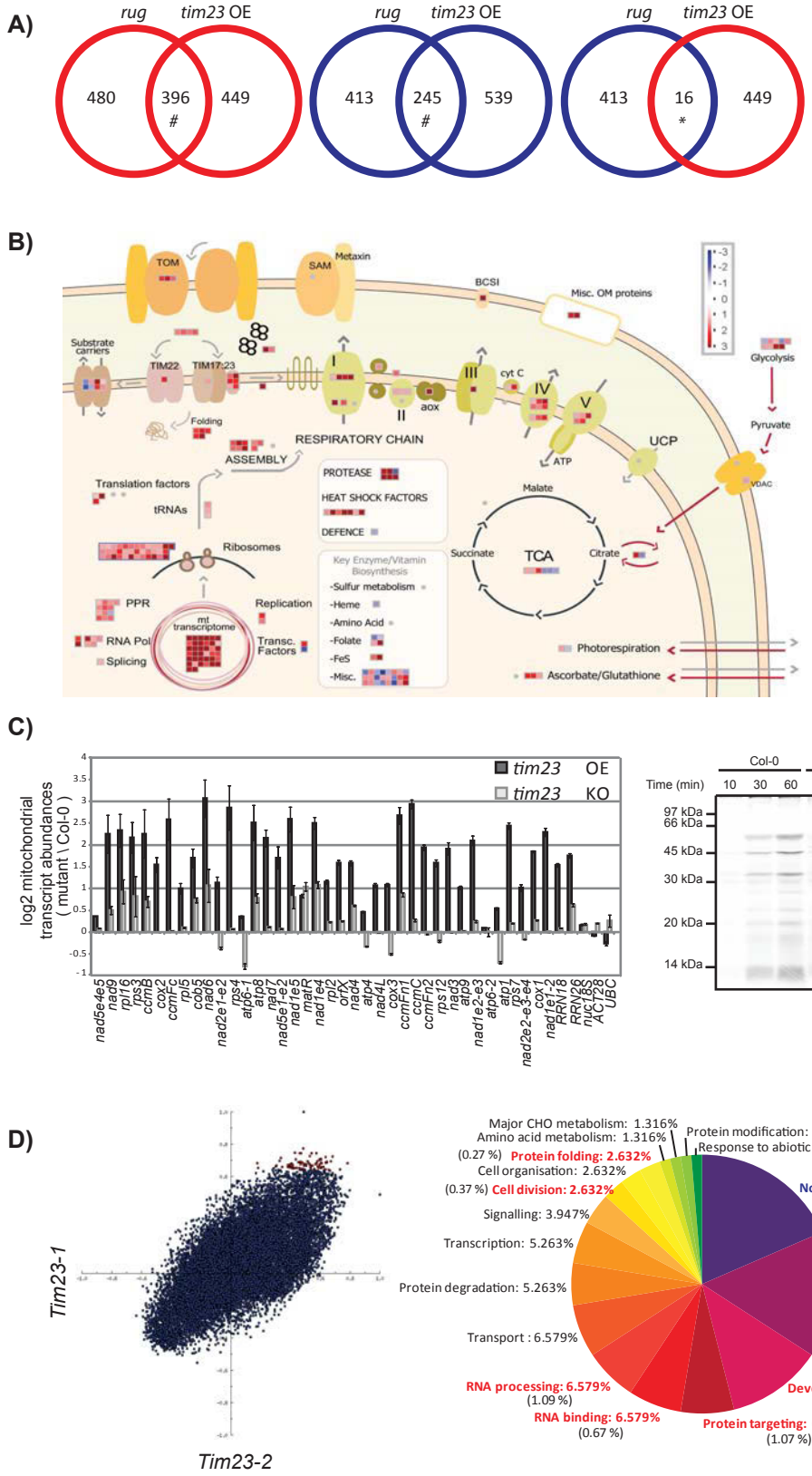
A)
rug
tim23 OE
480
396
#
449
413
245
#
539
413
16
*
449
B)
TOM
SAM
Metaxin
BCSI
Misc. OM proteins
Substrate carriers
TIM22
TIM17:23
Folding
ASSEMBLY
RESPIRATORY CHAIN
I
II
III
cyt C
IV
V
aox
ATP
UCP
Glycolysis
Pyruvate
VDAC
Translation factors
tRNAs
Ribosomes
PROTEASE
HEAT SHOCK FACTORS
DEFENCE
Malate
Succinate
TCA
Citrate
Key Enzyme/Vitamin Biosynthesis
-Sulfur metabolism
-Heme
-Amino Acid
-Folate
-FeS
-Misc.
PPR
RNA Pol
Splicing
mt transcriptome
Replication
Transc. Factors
Photorespiration
Ascorbate/Glutathione
C)
log2 mitochondrial transcript abundances (mutant \ Col-0)
tim23 OE
tim23 KO
nad5e4e5
nad9
rpl16
rps3
ccmB
cox2
ccmFc
rpl5
cob
nad6
nad2e1-e2
rps4
atp6-1
atp8
nad7
nad5e1-e2
nad1e5
matR
nad1e4
rpl2
orfX
nad4
atp4
nad4L
cox3
ccmFn1
ccmC
ccmFn2
rps12
nad3
atp9
nad1e2-e3
atp6-2
atp1
rps1
nad2e2-e3-e4
cox1
nad1e1-2
RRN18
RRN26
nuc18S
ACT28
UBC
Col-0
tim23 OE
tim23 KO
Time (min)
10 30 60 10 30 60 10 30 60
97 kDa
66 kDa
45 kDa
30 kDa
20 kDa
14 kDa
atp1
cob
cox2
nad9
nad6
atp9
D)
Tim23-1
Tim23-2
Major CHO metabolism: 1.316%
Amino acid metabolism: 1.316%
Protein modification: 1.316%
Response to abiotic stress: 1.316%
(0.27 %) Protein folding: 2.632%
Cell organisation: 2.632%
(0.37 %) Cell division: 2.632%
Signalling: 3.947%
Transcription: 5.263%
Protein degradation: 5.263%
Transport : 6.579%
RNA processing: 6.579%
(1.09 %)
RNA binding: 6.579%
(0.67 %)
Protein targeting: 6.579%
(1.07 %)
Development: 11.842%
(2.83 %)
Protein synthesis: 15.789%
(2.57 %)
Not assigned: 18.421%
(28.84 %)

Figure 6

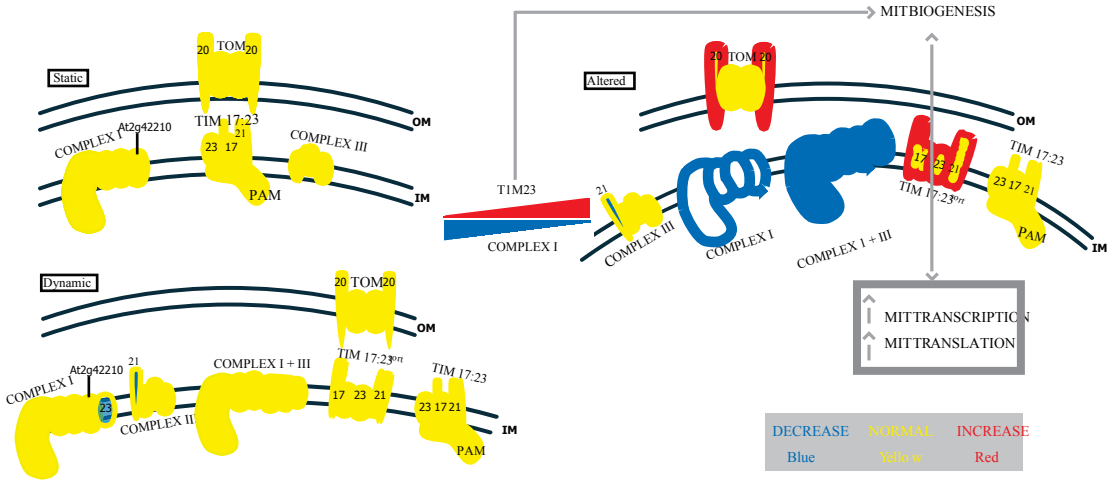
Static
20 TOM 20
OM
COMPLEX I
At2g42210
TIM 17:23
21
23 17
COMPLEX III
PAM
IM
Dynamic
20 TOM20
OM
COMPLEX I
At2g42210
21
23
COMPLEX II
COMPLEX I + III
TIM 17:23 pm
17 23 21
TIM 17:23
23 17 21
PAM
IM
MITBIOGENESIS
T1M23
COMPLEX I
Altered
20 TOM 20
OM
21
COMPLEX III
COMPLEX I
COMPLEX I + III
17 23 21
TIM 17:23 pm
TIM 17:23
23 17 21
PAM
IM
MITTRANSCRIPTION
MITTRANSLATION
DECREASE
Blue
NORMAL
Yellow
INCREASE
Red

Figure 7